

DOT/FAA/PM-87-20

Program Engineering
and Maintenance Service
Washington, D.C. 20591

Theoretical Model for Stabilization of Clay-Silt Airport Pavement Subgrade Systems

Phase I-Laboratory Investigation
Phase II-Rutting Tests

AD-A211 182

DTIC
ELECTE
AUG 14 1989
S D

William A. Grissom, Ph.D., P.E.
Abayomi J. Ajayi-Majebi, Ph.D., P.E.
L. Shelbert Smith, Ph.D.
Carl L. White
Mahmoud A. Abd-Allah, Ph.d.

Manufacturing Engineering Department
Central State University
Wilberforce, Ohio 45384

Eugene E. Jones, Ph.D.

Tractell, Inc.
4490 Needmore Road
Dayton, Ohio 45424

May 1989

Final Report

DISTRIBUTION STATEMENT A
Approved for public release
Distribution Unlimited

This document is available to the public
through the National Technical Information
Service, Springfield, Virginia 22161.

89



US Department
of Transportation
Federal Aviation
Administration

NOTICE

This document is disseminated under the sponsorship of the Department of Transportation in the interest of information exchange. The United States Government assumes no liability for its contents or use thereof.

1. Report No. DOT/FAA/PM-87/20	2. Government Accession No.	3. Recipient's Catalog No.
4. Title and Subtitle THEORETICAL MODEL FOR STABILIZATION OF CLAY-SILT AIRPORT PAVEMENT SUBGRADE SYSTEMS Phase I - Laboratory Investigation Phase II - Rutting Tests	5. Report Date MAY 1989 August 31, 1988	6. Performing Organization Code
7. Author(s) Dr. William A. Grissom, P.E., Dr. Abayomi Ajayi-Majebi, P.E., Dr. L. Shelbert Smith, Mr. Carl L. White, Dr. Mahmoud A. Abd-Allah, and Dr. Eugene F. Jones.	8. Performing Organization Report No.	10. Work Unit No. (TRAIS)
9. Performing Organization Name and Address Central State University Manufacturing Engineering Department Wilberforce, Ohio 45384	11. Contract or Grant No. DOT/FAA-DTFA01-84-C-00023	13. Type of Report and Period Covered Final Report (Phases I & II)
12. Sponsoring Agency Name and Address U.S. Department of Transportation Federal Aviation Administration Program Engineering and Maintenance Services Washington, D.C. 20591	14. Sponsoring Agency Code APM - 740	
15. Supplementary Notes Prepared under DOT/FAA Research Contract No. DTAF01-84-00023 Aircraft, Interfacility and Safety Branch, Washington, D.C. 20591		
16. Abstract The results of a research effort executed at Central State University, Manufacturing Engineering Department on the development of theoretical models for low-volume airport pavement stabilization of clay-silt systems are documented. This study is considered very significant because it identifies a non-traditional method of soil stabilization for improving the subgrade strength of poorly graded clay-silt, considered one of the most difficult soil types to stabilize. The research (Phase I) focuses on: (1) Identification of a chemical additive capable of increasing the load bearing strength of clay-silt soil; (2) Additive application to a clay-silt soil system leading to increased bearing strength; (3) Development of mathematical models for soil strength prediction, and; (4) In Phase II, field validation of the test results through studies of pavement rutting. Literature review suggests that little or no work has been done previously using organic additives in stabilization of clay-silt soil systems; however, many inorganic additives such as cement, lime, fly ash, and phosphoric acid have been satisfactorily tested on soils with good particle size distributions. Among several effective non-traditional organic additives tested in this research, the two-part Epoxy system, Bisphenol A/Epichlorohydrin resin plus a Polyamide hardener gave the best result as measured by the dry CBR test. The choice of the dry CBR test performed to ASTM specification was motivated by a need to capture optimum moisture content as a variable in addition to percent additive, clay-silt ratio, temperature and dry density, using a full factorial experimental design. The statistical regression models developed support the Hypothesis that only additive percentage, moisture content and temperature are significant variables influencing the strength of the clay-silt soil system tested. The nomograph developed for CBR prediction enables quick estimates of dry CBR. The marginal increase in CBR values due to a percent increase in Epoxy resin application is 11.1 and the marginal degradation of CBR due to a percent increase in moisture level is 5.6. In Phase II the rutting validation study confirmed the effectiveness of the chemical stabilizing agent identified for strengthening a clay-silt soil at the 4% level of additive application. Based on the results of the rutting test conducted on a Tire Force Machine (TFM) at Wright-Patterson Air Force Base (WPAFB) in Dayton, Ohio the stabilized pavement will sustain an aircraft load of 10,000 lbs applied through 1000 wheel load passes while meeting the $\frac{1}{2}$ " rutting criteria.		
17. Key Words Soil Stabilization, Clay-Silt, Moisture, Temperature, Dry Density, California Bearing Ratio, Dry CBR, Chemical Additive, Epoxy Resin, Theoretical, Mathematical, Statistical Models, Automated Data Collection, Low-Duty Airports, Rutting Test, Rut Depth, Tire Force Machine (TFM).	18. Distribution Statement Distribution is available to the public through the National Technical Information Service, Springfield, VA 22151	
19. Security Classification (of this report) Unclassified	20. Security Classification (of this page) Unclassified	21. No. of Pages 325
		22. Price

PREFACE

This study was conducted by the Central State University, Manufacturing Engineering Department, Wilberforce, Ohio. Funding was provided by the Federal Aviation Administration, Systems Technology Division under DOT/FAA Contract No. DTFA01-84-C-00023.

Dr. William A. Grissom was Principal Investigator. As the research progressed, Dr. Abayomi J. Ajayi-Majebi assumed a role as Co-Principal Investigator through the leadership and expertise which he brought to the project. Other faculty and staff members who participated as research associates included Mr. Carl L. White, Dr. Mahmoud A. Abd-Allah, Mr. Clark E. Beck, Dr. Bryant Crawford, Jr., Mr. Donald Stewart, Mr. John Sassen and Mr. LaRue Turner.

Dr. Shelbert Smith of the Central State University Department of Chemistry served as chemical consultant and guided research efforts in the search for suitable and effective additives.

Ms. Lynn Adams, Mr. Richard Carter, Mr. Anthony Collett, Mr. David Hines, Mr. Kirk Johnson, Mr. William Middleton III, Mr. Troy Neal, Mr. Oghogho Obasuyi, Mr. Terence Pettus, Mr. Marvin Scott, Mr. David Thompson, Mr. Laurence Weir, Mr. Bryan White and Mr. J. Kevin Wiggins, all Manufacturing Engineering students served as research assistants on various aspects of this study. The work of Mr. Laurence Weir in data collection and computer-graphics generation is specially acknowledged.

The effort of Mr. Tony Schooler, an undergraduate research assistant from the Department of Mathematics and Computer Science in coding the software for driving the data collection system is appreciated.

Dr. Eugene E. Jones, President of Tractell, Inc., in Dayton, Ohio, served as consultant. His contributions and comments are reflected in the body of this report; in addition Mr. John Biernacki of Tractell played an important role in selecting and fabricating some essential components of the automated CBR data collection system.

We gratefully appreciate the assistance of the Landing Gear Test facility (LGTF) of the Wright Patterson Air Force Base (WPAFB) in providing the Tire-Force Machine (TFM) and vital instrumentation and computer support services. Special thanks to Mr. Igors Skriblis, Bob Jenkins, Ben Noble, and all other staff at the base who contributed to the success of Phase II of this research effort. We are grateful to all at the Marmac Co. in particular Mr. Bob McCreery and Mr. Lechner who enabled and expedited the procurement and fabrication of the test-bed component.

Dr. Mark T. Bowers of the University of Cincinnati, Department of Civil and Environmental Engineering, and Mr. Jim Fletcher, Materials Engineer with Bowser and Marner, soil testing consultants, Dayton, Ohio are recognized for their assistance in providing the additional CBR test equipment used for this soil stabilization research.

Most importantly, during the entire span of this research, Dr. Aston L. McLaughlin, served as FAA Technical Officer. We strongly and gratefully acknowledge the guidance and direction he gave to this study. His invaluable assistance was vital to the execution of this research.



Accession For	
NTIS CRA&I	<input checked="" type="checkbox"/>
DTIC TAB	<input type="checkbox"/>
Unannounced	<input type="checkbox"/>
Justification	
By	
Distribution /	
Availability Codes	
Dist	Avail and/or Special
A-1	

TABLE OF CONTENTS

	Page
Preface	iii
List of Figures	x
List of Tables	xvi
Conversion Table	xviii
Definitions	xix
Introduction	1
1.1 Background	1
1.2 Problem Statement	1
1.3 Objectives	2
1.4 Scope of Work	2
Literature Review	4
2.1 Introduction	4
2.2 Low Duty Airports	6
2.3 Soil Stabilization	6
2.4 Stabilization Materials	8
2.5 Physico-Chemical Behavior	9
2.6 Expansive Soil Characterization Study	10
2.7 Soil Classification	13
Research Methodology	15
3.1 General Overview/CBR Rationale	15
3.1.1 Dry CBR Test	15
3.1.2 CBR Test Overview	16
3.2 Experimental Design	18
3.2.1 Variables Specification	18
3.2.2 Crack Pattern Specification	19
3.2.3 Factorial Design Specification	19
3.2.4 Levels of Variables	20
3.3 Testing Procedure	21
3.4 Automated Data Collection System	35

3.4.1	LVDT Overview	40
3.4.2	LVDT Mode of Operation	41
3.4.3	Signal Conditioner	42
3.4.4	Functional Aspects of Signal Conditioning	43
3.4.5	Data Acquisition and Reduction Software	44
3.4.6	DT/Notebook Software	48
3.4.7	Basic Operation	48
3.4.8	Complementary Data Collection Software	49
3.4.9	Data Collection Accuracy	50
Material Selection		58
4.1	Aggregate Selection - Soil Classification.	58
4.1.1	Clay-Silt Soil Classification	59
4.1.1.1	Unified Soil Classification Specification (Corps of Engineers)	59
4.1.1.2	AASHTO Soil Classification Specification	61
4.1.2	Summary of Physical Properties of Soil	61
4.2	Additive Selection	64
4.2.1	General Overview	64
4.2.2	Screened Additive Materials	65
4.2.2.1	High Density Polyethylene.	65
4.2.2.2	Polystyrene.	66
4.2.2.3	Urea Formaldehyde.	66
4.2.2.4	Polypropylene.	66
4.2.2.5	Polyvinyl Chloride	67
4.2.2.6	Phenolic Resin	67
4.2.2.7	Polyurethane.	67
4.2.2.8	Polyester Resin.	68
4.2.3	Tested Pilot Additive Materials	68
4.2.4	Tested Preliminary Additive Materials	71
4.2.5	Final Test Additive Selection Process	75
4.2.5.1	Additional Investigations and Inquiries	75
4.2.5.2	New Additive Case Analysis	75
4.2.6	Epoxy Resin/Hardener Specification	78
4.2.7	Experimental CBR Data Collected	80
4.2.8	Epoxy Resin Cost vs. Effectiveness Tradeoff	80

Mathematical Analysis	98
5.1 General Discussion	98
5.2 Regression Model Form Specification	99
5.3 Regression Analysis	100
5.3.1 Additive Treatment Statistical Analysis (No Interaction Effects)	104
5.3.2 Additive Treatment Statistical Analysis (With Interaction Effects)	109
5.3.3 Control Case Statistical Analysis (No Additive Treatment).	110
5.3.3.1 Model Specifications	115
5.3.3.2 Model Refinement	117
5.3.4 Additive Treatment Effectiveness Analysis	117
5.4 MANOVA Analysis	122
5.4.1 Four-Factor Full $3^3 \times 4$ Factorial Model Analyses	122
5.4.2 MANOVA Analysis Result	127
5.4.2.1 Additive Treatment Case	127
5.4.2.2 Additive Effectiveness Case	130
5.5 Complementary Regression Modelling	132
5.5.1 Composite Regression Modelling (No Stratification)	132
5.5.2 Stratified Regression Modelling (By Temperature)	137
5.5.3 Stratified Regression Modelling (By Clay-Silt Ratio)	145
5.6 Soaked Test CBR Analysis	150
5.6.1 General Discussion	150
5.6.2 Soaked CBR Model (Molding Moisture Content Specification)	150
5.6.3 Soaked CBR Model (Final Saturated Moisture Content Specification)	151
Discussion/Conclusions	153
6.1 General Discussion	153
6.2 Control Case Clay-Silt System Results	153
6.3 Additive Clay-Silt System Results	159

6.4	Validation/Correlation Follow-Up Study	165
6.5	Conclusions	167

VALIDATION STUDY VIA RUTTING TEST

PHASE II

	Page
Introduction	172
7.1 Background	172
7.2 Scope.	172
7.3 Rutting Definition	173
7.4 Objectives	173
Review of Literature on Pavement Rutting	175
8.1 Introduction	175
8.2 Pavement Simulation Analysis	176
8.3 Clay/Silt Soil Rheology	179
8.4 Models Predicting Permanent Strain	182
8.5 Rutting Prediction Models.	183
Methodology	192
9.1 Rationale	192
9.2 Experimental Design	193
9.2.1 Test-Bed Experimental Arrangement	194
Experimental Investigation	195
10.1 Tire Force Machine (TFM)	195
10.2 Test-Bed Design & Construction	200
10.3 Tire Footprint / Justification of Test bed	
Structural Dimensions	206
10.4 Soil Sample Preparation	208
10.4.1 General.	208
10.4.2 Mixing Specification	208
10.4.3 Compaction Specification.	210
10.4.4 Asphalt Surfacing	212
10.5 Environmental Condition of Testing	214
Rut Test Results and Analysis	219
11.1 Test Information Specification	219
11.1.1 Experimental Testing Progress Photograph	219
11.1.2 Rutting Data	229
11.1.3 CBR Test / Cone Penetrometer Results	234

11.1.4	Rutting profile of Clay-Silt Soil Matrix vs Wheel Load Passes	237
11.1.5	Tire Load Response Profile for Six Soil Sample Matrices	248
11.1.6	Rutting Response Surface Analysis	248
	Computer Modelling of Rut Depth.	251
12.1	The Waterways Experiment Station (WES, MI) Rut Depth Prediction Model	251
12.2	CSU Modified (WES) Rut Depth Prediction Model . .	253
12.3	Comparison of Actual vs Predicted Rut Depth . .	256
	Discussion & Summary	257
	Conclusions/Recommendations	261
	References	264
	Appendices	267
A	Clay-Silt Batching and Data Reduction Programs	267
A-1	Formulae for Batching Clay-Silt Mixtures .	268
A-2	Computer Program for Batching Clay-Silt Mixtures	270
A-3	Computer Program Output for Batching Clay-Silt Mixture Treated with Epoxy Resin	273
A-4	Computer Program Code and Output for Transforming Load Penetration and Mold Indices Into CBR and Dry Density Values. .	277
B	Rut Depth Prediction Model (Four Pavement Types). .	281
B-1	Modified Rutting Model (CSU/WES) Waterways Experiment Station Model.	283
B-2	Rutting Model Typical Input Data	294
B-3	Rutting Model Typical Output Data.	298
C	Technical Data for BOMAG Compactor Used for Test Sample Compaction.	302

LIST OF FIGURES

<u>FIGURE</u>	<u>DESCRIPTION</u>	<u>PAGE</u>
2.1	ODOT Classification of Soils	14
3.1	Dry density vs. moisture content by temperature by clay-silt ratio	22
3.2	Dry density vs. moisture content by clay-silt ratio by temperature	23
3.3	Fine grained clay(L) and silt(R) soil samples . .	25
3.4	Various additives screened or tested for stabilization effectiveness	26
3.5	General view of soil-stabilization laboratory . .	27
3.6	View of automated compaction equipment, additive drum rack and epoxy-resin stabilized samples . .	27
3.7	CBR test specimens in thermal chamber	28
3.8	Close-up view of soil stabilization research laboratory	29
3.9	Stabilized clay-silt soil already tested for CBR strength	30
3.10	Close-up view of epoxy-resin stabilized clay-silt soil showing assorted crack patterns	30
3.11	Storage rack supporting tested epoxy-resin stabilized soil samples	31
3.12	General view of the automated data collection system	32
3.13	View of tested chemicals plus stabilized and tested clay-silt samples with and without aluminum lining	33
3.14	Close-up view of the CBR and automated data collection equipment showing penetration gauge adjustment	34
3.15	Close-up view of the CBR test equipment and LVDT attachment	37
3.16	Schematic of automated CBR data collection and display system	38

LIST OF FIGURES (CONT'D)

<u>FIGURE</u>	<u>DESCRIPTION</u>	<u>PAGE</u>
3.17	Graphic display of automated data collection and display system.	39
3.18	Automated plot of load vs penetration data and resulting CBR values	51
4.1	Clay-silt particle size distribution chart	60
4.2	Approximate interrelationships of soil classification and bearing values	63
4.3	Pilot test samples (substandard) for additive effectiveness screening	76
5.1	CBR vs. moisture content by additive at 3 levels of clay-silt ratio. (Temperature = 40°F)	101
5.2	CBR vs. moisture content by additive at 3 levels of clay-silt ratio. (Temperature = 65°F)	102
5.3	CBR vs. moisture content by additive at 3 levels of clay-silt ratio. (Temperature = 90°F)	103
5.4	Nomograph for clay-silt system CBR prediction (stabilizing agent - Epoxy Resin)	106
5.5	CBR vs. moisture content by clay-silt ratio (Unstabilized clay-silt system, temperature = 40°F)	111
5.6	CBR vs. moisture content by clay-silt ratio (Unstabilized clay-silt system, temperature = 65°F)	112
5.7	CBR vs. moisture content by clay-silt ratio and temperature (Unstabilized clay-silt system)	113
5.8	CBR differential vs. moisture content by additive at 3 levels of clay-silt ratio (Temperature = 40°F)	119
5.9	CBR differential vs. moisture content by additive at 3 levels of clay-silt ratio (Temperature = 65°F)	120
5.10	CBR differential vs. moisture content by additive at 3 levels of clay-silt ratio (Temperature = 90°F)	121

LIST OF FIGURES (CONT'D)

<u>FIGURE</u>	<u>DESCRIPTION</u>	<u>PAGE</u>
5.11	Predicted CBR vs. moisture (Temperature = 40°F, C/S = 0.4)	133
5.12	Predicted CBR vs. moisture (Temperature = 65°F, C/S = 0.4)	134
5.13	Predicted CBR vs. moisture (Temperature = 65°F, C/S = 0.5)	135
5.14	Predicted CBR vs. moisture (Temperature = 90°F, C/S = 0.6)	136
5.15	Predicted CBR vs. moisture (Temperature = 40°F, C/S = 0.4)	140
5.16	Predicted CBR vs. moisture (Temperature = 40°F, C/S = 0.5)	141
5.17	Predicted CBR vs. moisture (Temperature = 40°F, C/S = 0.6)	142
5.18	Predicted CBR vs. moisture (Temperature = 65°F, C/S = n/a)	143
5.19	Predicted CBR vs. moisture (Temperature = 90°F, C/S = n/a)	144
5.20	Predicted CBR vs. moisture (Temperature = n/a, C/S = 0.4)	146
5.21	Predicted CBR vs. moisture (Temperature = n/a, C/S = 0.5)	147
5.22	Predicted CBR vs. moisture (Temperature = n/a, C/S = 0.6)	148
6.1	Dry density vs. moisture content by clay-silt ratio by temperature	156
6.2	Dry density vs. moisture content by temperature by clay-silt ratio	157
6.3	CBR vs. moisture content at various levels of all independent variables	161
6.4	CBR differential vs. moisture content at various levels of all independent variables	162
6.5	Nomograph for clay-silt system CBR prediction (stabilizing agent--Epoxy Resin)	166

LIST OF FIGURES (CONT'D)

PHASE II

<u>FIGURE</u>	<u>DESCRIPTION</u>	<u>PAGE</u>
8.1	Strain vs Time Dependency.176
8.2	Permissible Stress/CBR Versus Number of Loads.178
8.3	Arrangement of Atoms in Clay Minerals.180
8.4	Structure of Clay Minerals181
8.5	Procedure for Computing Permanent Deformation of . . . Subgrade.185
8.6- 8.9	Comparison of OSU and FHWA Rutting Models.190
9.1	Test-Bed Experimental Arrangement.194
10.1	Flat Surface Tire-Force Machine (TFM).196
10.2	Schematic Representation of Vector Forces and Moments Acting on Test Tire197
10.3	Front View of Unloaded Tire-Force Machine (TFM).198
10.4	Rear View of Tire Force Machine (TFM) Showing Unbalanced Hydraulic System198
10.5	Rear View of TFM Showing V-Shaped Bearing Assembly on Which the Test Platform Moves201
10.6	Close-Up View of TFM Bearing Assembly Supporting Test-Bed.201
10.7	3-D View of Two (2) Identical Test-Beds Constructed at CSU.202
10.8	Two (2) Identical Test Bed Construction in Process Showing Magnetic Base Drill, Clamps, etc.205
10.9	One (1) Test-Bed Unit After Construction and Finishing.205
10.10	YF-16 Tire Footprint for 5000 lbs Rated Load.207
10.11	Sample Preparation Under Tent Using 6 cu.ft. Mortar Mixer.211

10.12	Test-Bed Samples Compacted to AASHTO Specification Using the BOMAG Compactor.	211
10.13	Close-Up View of Resonating BOMAG Compactor.	213
10.14	BOMAG Compactor in Action.	213
10.15	11" Thickness of Compacted Soil Sample Showing 10" Wide Cutout Plates Removed from Transverse Partition.	215
10.16	Close-Up View of a Single Test-Bed Section Showing Loading Platform in Rear.	215
10.17	Compaction of ASPHALT Surfacing Using a 250 lb Roller.	216
10.18	Two Test-Bed Units Treated with 1" Asphalt Surfacing.	216
10.19	Side View of the Tire Force Machine with Tire at Start Position; in Foreground, Control Station with Operator.	217
10.20	Bird's Eye View of Test Setup Showing Test Pavement Channelization and Rutting.	217
11.1	Tire Force Machine (TFM) Loaded with Test-Beds Ready for Rutting Test.	220
11.2	YF-16 Aircraft Tire 25.5" x 8.0" at 200 PSI Tire Pressure.	220
11.3	Rutting Test in Progress Showing Tire Imprint on Loading Platform.	221
11.4	Rutting Test Showing Video-Tape of Testing During Forward Motion of Table at Speed of 0.17 Knots.	221
11.5	Rut Depth Indication for A=4%, M=17% Experimental Point After 100 Passes.	222
11.6	Rut Depth Indication for A=4%, M=17% Experimental Point After 100 Passes.	222
11.7	Rut Depth Indictaion for A=4%, M=14% Experimental Point After 20 Passes.	224
11.8	Rut Depth Indication for A=4%, M=14% Experimental Point After 100 Passes.	224
11.9	Rut Depth Indication (7" Including Heave) After 40 Passes (A=0%, M=17%, Control).	225

11.10	Rut Depth Indication (8" Including Heave) After 150 Passes (A=0%, M=17%, Control).	225
11.11	Rut Depth Profile After 300 Passes.	226
11.12	Rut Depth Indication After 250 Passes (A=4%, M=14%). .226	
11.13	Rut Depth Indication After 450 Passes (A=4%, M=14%). .227	
11.14	Rut Depth Indication After 450 Passes (A=2%, M=14%). .227	
11.15	Rut Depth Indication After 450 Passes (A=0%, M=14%). .228	
11.16	Rut Depth Indication After 450 Passes (A=2%, M=17%). .228	
11.17	Automated Data Acquisition Interface Showing: Load Cell Calibration Switches, Signal Conditioners, Control Panel and PDP-11 Computers and Terminals. . .233	
11.18	Rut Depth Profile After 650 Passes.	233
11.19	Cone Penetrometer (Maximum Gage - 300 Psi).	235
11.20	Plot of Horizontal Table Position (Inches) vs Time. . .238	
11.21-	Plots of Vertical Ram Position (Clay-Silt Surface	
11.30	Profile) for Six Samples, by Passes.	239
11.31	Unfiltered Surface Profile Reading vs Testing for Passes = 2, 3, 4.	244
11.32	Surface Profile vs Test-Bed Position for Passes = 2, 3, 6, 7, 9, 10, 15, 20.	245
11.33	Applied Wheel Load Variation vs Time (Mean Load 5000 lbs).	246
11.34	Applied Wheel Load Profile (Filtered) vs Time for Passes = 2, 6, 10, 15, 20.	247
11.35	Surface Plot of Rut Depth vs Passes and Additive (Moisture Content = 14%, C/S = 0.5).	249
11.36	Surface Plot of Rut Depth vs Passes and Additive (Moisture Content = 17%, C/S = 0.5).	250

LIST OF TABLES

<u>TABLE</u>	<u>DESCRIPTION</u>	<u>PAGE</u>
4.1	Physical Properties of Clay-Silt System.	62
4.2	Unconfined Compressive Strength of Stabilized Clay-Silt Samples	69
4.3	Soil Test Data For Unconfined Compression Test . .	70
4.4	Stabilization Effectiveness of Latex at Optimum Moisture Content	72
4.5	Stabilization Effectiveness of H-SPAN at Optimum Moisture Content	73
4.6	Comparison of Actual and "Pseudo-CBR" values for tested Clay-Silt Samples.	77
4.7	Full Factorial CBR Experimental Design Data Matrix (All Combinations)	81
4.8	Full Factorial CBR Additive Effectiveness Matrix (All Combinations)	82
4.9 -4.11	CBR Values for Stabilized Clay-Silt System (Temperature = 90°F)	83
4.12-4.14	CBR Values for Stabilized Clay-Silt System (Temperature = 65°F)	86
4.15-4.17	CBR Values for Stabilized Clay-Silt System (Temperature = 40°F)	89
4.18	CBR Values for Unstabilized Clay-Silt System (Temperature = 90°F)	92
4.19	CBR Values for Unstabilized Clay-Silt System (Temperature = 65°F)	93
4.20	CBR Values for Unstabilized Clay-Silt System (Temperature = 40°F)	94
4.21	Soaked CBR Values for Stabilized Clay-Silt System	95
5.1	MANOVA Analysis of Main and Interaction Effects for CBR Data	128
5.2	MANOVA Analysis of Main and Interaction Effects for CBR Differential Data	129

LIST OF TABLES (CONT'D)

<u>TABLE</u>	<u>DESCRIPTION</u>	<u>PAGE</u>
5.3	Predicted CBR Values for Specified Levels of Independent Variables	138
5.4	Predicted CBR Values for Specified Levels of Independent Variables (Stratified by Temperature)	139
5.5	Predicted CBR Values for Specified Levels of Independent Variables (Stratified by C/S Ratio) .	149
10.1	Mean Daily Temperature and Humidity	214
11.1	Rutting Test Data Using Factorial Experimental Design with wheel load Passes As A Correlated Variable	230
11.2	CBR values for Clay-Silt Specimens Sampled from Test Beds.	236
12.1	Comparison of Actual vs Predicted Rut-Depth for Stabilized Clay-Silt (Moisture Level = 14%). . .	254
12.2	Comparison of Actual vs Predicted Rut-Depth for Stabilized Clay-Silt (Moisture Level = 17%). . .	255

METRIC CONVERSION FACTORS

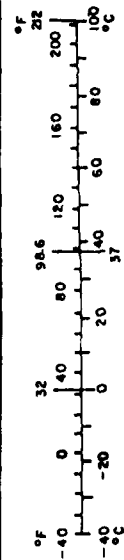
Approximate Conversions to Metric Measures

Symbol	When You Know	Multiply by	To Find	Symbol
LENGTH				
in	inches	2.5	centimeters	cm
ft	feet	30	meters	m
yd	yards	0.9	kilometers	km
mi	miles	1.6		
AREA				
in ²	square inches	6.5	square centimeters	cm ²
ft ²	square feet	0.09	square meters	m ²
yd ²	square yards	0.8	square meters	m ²
mi ²	square miles	2.6	square kilometers	km ²
	acres	0.4	hectares	ha
MASS (weight)				
oz	ounces	28	grams	g
lb	pounds	0.45	kilograms	kg
	short tons (2000 lb)	0.9	tonnes	t
VOLUME				
tsp	teaspoons	5	milliliters	ml
Tbsp	tablespoons	15	milliliters	ml
fl oz	fluid ounces	30	milliliters	ml
c	cups	0.24	liters	l
pt	pints	0.47	liters	l
qt	quarts	0.95	liters	l
gal	gallons	3.8	liters	l
ft ³	cubic feet	0.03	cubic meters	m ³
yd ³	cubic yards	0.76	cubic meters	m ³
TEMPERATURE (exact)				
°F	Fahrenheit temperature	5/9 (after subtracting 32)	Celsius temperature	°C

* 1 in x 2.54 (exactly). For other exact conversions and more detailed tables, see NBS Misc. Publ. 286, Units of Weights and Measures, Price \$2.75. SO Catalog No. C13.10.286.

Approximate Conversions from Metric Measures

Symbol	When You Know	Multiply by	To Find	Symbol
LENGTH				
mm	millimeters	0.04	inches	in
cm	centimeters	0.4	inches	in
m	meters	3.3	feet	ft
m	meters	1.1	yards	yd
km	kilometers	0.6	miles	mi
AREA				
cm ²	square centimeters	0.16	square inches	in ²
m ²	square meters	1.2	square yards	yd ²
km ²	square kilometers	0.4	square miles	mi ²
ha	hectares (10,000 m ²)	2.5	acres	ac
MASS (weight)				
g	grams	0.035	ounces	oz
kg	kilograms	2.2	pounds	lb
t	tonnes (1000 kg)	1.1	short tons	ton
VOLUME				
ml	milliliters	0.03	fluid ounces	fl oz
l	liters	2.1	pints	pt
l	liters	1.06	quarts	qt
l	liters	0.26	gallons	gal
m ³	cubic meters	35	cubic feet	ft ³
m ³	cubic meters	1.3	cubic yards	yd ³
TEMPERATURE (exact)				
°C	Celsius temperature	9/5 (then add 32)	Fahrenheit temperature	°F



DEFINITIONS

To assure clarity of meaning and uniformity of understanding, the following definitions are provided:

Soil (earth) - Sediments or other unconsolidated accumulations of solid particles produced by the physical and chemical disintegration of rocks, and which may or may not contain organic matter. They are naturally occurring materials that are used for the construction of all except the surface layers of pavements and that are subject to classification tests to provide a general concept of their engineering characteristics. Also included are the materials normally used for base courses, subbase courses, select material layers, and subgrades.

Stabilization - Stabilization is the process of blending and mixing materials with a soil to improve the pertinent properties of the soil through any process either natural, such as compaction, or artificial, such as chemical. The process may include the blending of soils to achieve a desired gradation or the mixing of commercially available material that may alter the gradation, change certain properties, or act as a binder for the solid. There are broadly two types--chemical or mechanical treatment designed to increase or

maintain the stability of a mass of soil, its resistance to deformation or otherwise to improve its engineering properties. The effectiveness of stabilization is dependent upon the ability to obtain uniformity in blending the various materials. Mixing in a stationary or traveling plant is preferred; however, other means of mixing, such as scarifiers, plows, disks, graders, and rotary mixers, have been satisfactory.

Additives - "Additives" refers to a manufactured generic or proprietary commercial product that, when added to the soil in the proper quantities, will improve the quality of the soil layer. The use of such traditionally well-accepted additives as Portland Cement, lime, lime-cement, fly ash, and bitumen, alone or in combination, as additives to stabilize soils is well documented.

Chemical Stabilization - The altering of soil properties by use of certain chemical additives, which when mixed into a soil often change the surface molecular properties of the soil grains and, in some cases, cement the grains together resulting in strength increases.

Mechanical Stabilization - Mechanical stabilization is accomplished by mixing or blending soils of two or more gradations to obtain a material meeting the required specification. The soil blending may take

place at the construction site, at a central plant, or at a borrow pit area. The blended material is then spread and compacted to required densities by conventional means.

Additive Stabilization - Two types of additive stabilization are chemical and bituminous. Chemical stabilization is achieved by the addition of proper percentages of cement, lime, fly ash, or combinations of these or other materials to the soil. Bituminous stabilization is achieved by the addition of proper percentages of bituminous material to the soil. The selection and determination of the percentage of additive to be added is dependent upon the soil classification and the degree of improvement in soil quality desired. Generally, smaller amounts of additives are required when it is simply desired to alter soil properties, such as gradation, workability, and plasticity than when it is desired to improve the strength and durability sufficiently to permit a reduction in design thickness. After the additive has been mixed with the soil, spreading and compaction are achieved by conventional means.

Aggregate - A granular material of mineral composition such as sand, gravel, shell, slag, or crushed stone, used with a cementing medium to form mortars of cement, or alone as in base courses, railroad ballasts, etc.

- Clay - A solid particle colloid produced by the physical and chemical decomposition of rocks, which may or may not contain organic matter, but which passes through sieves finer than No. 200 (0.074mm) and has both plasticity and high dry strength, i.e., a hard dry clod of this material will not crumble easily, is broken only with great effort and does not exhibit a glassy appearance upon shaking.
- Silt - A solid particle produced by mechanical weathering or the physical decomposition of rocks which may or may not contain organic matter but which passes through sieves finer than No. 200 (0.074mm) and has low dry strength. In the presence of water, silt becomes shiny when gently shaken in the hand but loses its glassy appearance when squeezed gently in the hand.

INTRODUCTION

1.1 Background:

Materials engineers are frequently confronted with the problem of improving the bearing strength of unsuitable soils through methods and techniques of soil stabilization. The Federal Aviation Administration (FAA) provides guidance to airport owners, operators, and designers on methods to increase the load bearing capabilities of subgrades in order to support aircraft loads. Existing methods include the application of various combination of cement, lime, and fly ash to native materials or as an extreme measure, replacing unsuitable material with improved, higher quality material.

1.2 Problem Statement

In small remote airports serviced by light aircraft such as some on the north slopes of Alaska, major portions of Florida and also in other areas where unsuitable subgrade conditions exist due to poor soil conditions, the difficulty in obtaining native stabilizers such as cement and fly ash for standard methods of soil stabilization is evident. Even where standards exist in the technology of soil stabilization for airport pavements, design and construction methods are only empirically-based and the analytical foundation for the criteria is minimal.

The need exists to quantify the manner in which various substances interact to increase the stability of subgrade material. An analytic investigation must necessarily include a screening of suitable yet untested compounds and agents,

identification of subsoil types yielding the worst type of soil system requiring stabilization, geo-climatic factors, soil forming process variables and subsoil loading factors. These soil stabilization process variables are more representative than exclusive and some of these variables may not be as significant as others.

1.3 Objectives:

This research is concerned with the formulation of a mathematical/statistically-based model for airport pavement subgrade stabilization through the use of stabilization agents applied to yielding native subgrade material. This model will link the characteristic of the soil support system with load handling parameters and will be applicable, at the very least, to a variety of potentially low-volume airport sites. The use of this model will enable the airport pavement designer to predict expected soil strength and effect design under a wide range of feasible combination of these variables.

The most significant variables influencing the resistance to deformation of both stabilized and unstabilized clay-silt soils will be identified by statistical techniques. Research on the performance of various rationally and judiciously selected stabilizing agents applied to a clay-silt subgrade will be examined through experimental test measurements.

1.4 Scope of Work:

The research scope includes a state-of-the-art investigation, automated data collection, and analysis of full-scale laboratory

data and formulation of a statistically-based model for soil stabilization of airport pavement subgrades. The work will, at final stages, include site investigations and the development and verification of criteria through application on a special test bed constructed for this purpose on or near the Central State University campus. This research is aimed at altering the engineering properties of a clay-silt system by use of certain non-traditional chemical additives which when mixed uniformly into the soil system changes the surface molecular properties of the soil grains and, in most cases, cement the grains together resulting in strength increases. The use of mechanical stabilization techniques on the clay-silt system being studied is precluded in this research effort.

LITERATURE REVIEW

2.1 INTRODUCTION

Soil improvement or modification through the use of stabilization techniques using lime or pozzolans, has been practiced as far back into antiquity as 5000 years. Though the process of enhancing the engineering properties of soils has been around for thousands of years, it was only after World War II that it gained acceptance in the USA as a means of improving the quality of roads and air fields and reducing the thickness of pavements (1).

A reason for the increased acceptance of this technique in design and construction has been the growing shortage of conventional aggregates due to economic, political and geographic factors. For example, environmental and zoning regulations and land use patterns that preclude mining and production of aggregates, in addition to the dwindling supply of aggregates, have combined to increase the cost of aggregates. Consequently the need for more economical, effective and practical sources of aggregate substitutes has been explored.

Currently, the use of marginally unacceptable but stabilizable engineering materials is being accepted as effective replacements for airfield and roadway construction.

The use of soil stabilization techniques (1) provides the following engineering qualities that are sometimes better realized in stabilized soils as compared to conventional unstabilized construction materials:

1. Function as an all-weather working platform (for construction operation expediency)

2. Reduce dusting
3. Water-proof the soil
4. Upgrade marginal materials
5. Improve strength
6. Improve durability
7. Control volume change of soils
8. Improve workability of soil
9. Drying of wet soils
10. Reduce pavement thickness requirements
11. Conserve aggregate materials
12. Reduce cost
13. Conserve energy
14. Provide a temporary or permanent wearing surface.

The most common quality improvement in soil through soil stabilization or modification includes better soil gradation, reduced plasticity and swelling potential, and increased strength and durability. Such material characterization properties as tensile strength and stiffness of a soil layer can be improved through the use of chemical stabilization thereby permitting, after a successful test of durability, a reduction in the thickness of the stabilized layer and overlying layers within the pavement system.

Pavement design is based on the premise that an adequate strength can be obtained for the pavement layers resting on the subgrade. Any improvement therefore in the subgrade quality and strength correspondingly increases the strength and durability of the pavement. Soil stabilization therefore becomes an important factor in designing and utilizing pavements for

numerous applications.

2.2 LIGHT AIRCRAFT PAVEMENTS

The current FAA research on clay-silt soil stabilization is directed at light aircraft pavements. These pavements are defined as "landing facilities to accommodate personal aircraft or other small aircraft engaged in nonscheduled activities as agricultural, industrial, executive, or industrial flying." Such pavements will not be required to handle aircraft exceeding a gross weight of 30,000 pounds. It has been suggested by Horonjeff (2) that many secondary airports may not require any pavement at all, a turf surface may be adequate. On the other hand, when pavements are required, they usually consist of thin bituminous surfaces placed on base courses. This assumes a stable subgrade. For yielding subgrades, such as found in a clay-silt soil system, stabilization using tested and effective additives to achieve the required pavement strength and ensure safe operation is necessary.

The total depth of pavements for light airport pavements rarely exceeds 22 inches (2) corresponding to soils with very low California Bearing Ratio (CBR), typically 3-4.

2.3 SOIL STABILIZATION

A study by McLaughlin (3) suggested that engineers will be more inclined to use stabilization techniques to strengthen pavement structures in the wake of such factors as increasing aircraft payloads, traffic frequency, scarcity of sites with good

subgrade bearing values, and the dwindling supply of conventional aggregates.

The research examined the application of lime, cement, and fly ash base courses. With reference to clay stabilization with lime cement or fly ash (LCF) McLaughlin submitted that very complex and long-term chemical reactions calls for a thorough study and extensive soil analyses before a mix is selected. The studies and tests should include particle size, gradation, reactivity, plasticity index, pH concentration, degree of drainage, ratio of calcium to magnesium ions, ratio of silica to sesquioxides, presence of organic material, sulfates and carbonates and general clay mineralogy.

This study reviewed the experiences of soils engineers and the performance of airport pavements in different parts of the US and found that soil mixtures with lime, cement, and fly ash base courses have been used occasionally, and in this regard, complex long-lasting chemical reactions produce a material with acceptable mechanical properties under the right conditions of temperature and moisture. However, certain insitu pavement conditions, if allowed, could lead to a weak pavement system due to infiltration of sulfate and carbonate bearing moisture or a strong acidic ground water condition, i.e., ground water condition with low pH.

Engineers at airports where LCF systems are in place are aware of these potential eventualities and have put in place preventive programs of monitoring, coring, and non-destructive testing to extend the LCF pavement service lives. The study listed recommendations which include further study of the effects

of deleterious substances that degrade LCF pavement materials, the changes in properties or cross section, and the crack propagation modes that may occur.

2.4 STABILIZATION MATERIALS

Report No. FHWA-RD-75-17 (4) documents the results of 20 years cooperative effort between the Federal Highway Administration (FHWA) and the chemical industry to investigate and develop specific compounds or combinations thereof, industrial products and wastes, for the purpose of soil stabilization or compaction aids, or both. About 50 chemicals and proprietary products were tested. With a few exceptions, such as phosphoric acid, the chemicals were mixtures of various chemicals rather than specific compounds. Most of the items had trade names, some were waste products and many were proprietary. The best of stabilizers include Quaternary amines, AM-9 chemical grout, phosphoric acid, lignin and cellulose derivatives, sodium chloride, and hydraulic lime. The best of compaction aids include Earth-pack, Terraformer, Roadpacker, Paczme, and others. The study concluded that no single chemical or combination of chemicals has been found acceptably effective as a major soil stabilizer.

Report No. FHWA-RD-75-32 (5) documents the test done on two proprietary materials Paczyme and Reynolds Road Packer as compaction aids and soil stabilizers. Extensive tests using these additives against a placebo of water showed that neither of the two materials significantly improved the engineering characteristics of the four soils tested. The test conducted

includes 1) Unconfined compressive strength test, 2) CBR, R-value and Tri-axial tests, 3) Plasticity, 4) Permeability and capillarity, 5) Water Penetration resistance, 6) Optimum moisture-maximum density compactive effort.

2.5 PHYSICO-CHEMICAL BEHAVIOR

Carpenter and Lytton (6) examined the physico-chemical behavior of a clay-silt soil and confirmed their thermal susceptibility which indicates that clay-silt systems will experience a volumetric contraction on freezing in a condition of constant moisture content. The measure of thermal susceptibility is the freeze coefficient of the material which is defined as linear coefficient of thermal contraction for temperature changes below freezing (strain per degree centigrade). Scanning electron microscopy confirmed that clay minerals, attapulgite and montmorillonite, when mixed with silt, combine to form an interconnecting clay-silt structure which upon freezing and thawing undergo reorientation. The contraction is controlled by the properties of the clay minerals and the unique, membrane-like clay particle structure they form around the larger silt particles. The freezing process forces the clay particles to reorientate leading to volumetric contraction as registered on the scanning electron micrographs.

The significance of this research lies in the aid provided in quantifying the magnitude of the freeze coefficient to be used in pavement design under frost conditions and damage assessment.

2.6 EXPANSIVE SOIL CHARACTERIZATION STUDY

McKeen and Nielson (7) studied various methods of assessing the swell potential of soils which can be used in preliminary investigations to determine whether soils present sufficient potential for damage to warrant special precautions. This study characterized the compressibility of an expansive soil due to suction and load, and ultimately the differential heave predictable under these conditions. Expansive soils are those that cause early pavement distress due to swelling or shrinkage of the subgrade in response to internal or external forces. The Atterberg limit tests were confirmed to be the best available general indicators of potential expansion and the plasticity index for such soils may vary between 22 and 65 for expansive soils. The factors that affect the expansive behavior of soils include the clay composition of the soil by type, amount and density, the nature of the initial and final moisture (measure of soil suction) and load condition. The clay content from samples with pronounced heave activity in the form of fissures and slickensides, etc., ranged from 40% to 70%. A clay content between 25% and 70% was observed in samples not exhibiting evidence of this pronounced activity.

McKeen (8) followed upon the characterization study in 1978 to develop design criteria for pavements to be built on expansive soils. Characterization of the suction and the in-situ differential movement likely to occur under the pavement are key inputs into the design criteria. The study stressed the importance of adherence to procedures designed to protect the

subgrade from moisture variations that occur with climatic changes.

Edris and Lytton (9) characterized the performance-related characteristics of fine-grained subgrade soils. Using fine grained soil with clay content ranging from 20% to 70%, they developed statistical models for resilient modulus, resilient strain relations, and permanent deformation per unit length or residual strain. The research demonstrated that dynamic properties of fine-grained soil such as modulus of resilience depend strongly on traffic volume (measured by load cycles), climatic factors (measured by soil suction and temperature), and soil composition. Soil suction is the energy with which water is attracted to soil and is measured by the work required to move this water from its existing state to a pressure free, distilled state.

A significant finding is that if the temperature is high enough, 95°F (35°C), for clay contents above 70% at moisture contents in excess of 32%, then periods of heavy traffic under this condition can lead to accelerated pavement rutting indicative of progressively increasing permanent strain with each load cycle. This situation is avertable in warmer climates by providing a thick pavement to reduce traffic stresses in the subgrade and provide thermal insulation to keep the subgrade from distress.

Chou (10) investigated the marginal effect of the variability of design variables in the CBR equation on pavement performance. The research provided insights into the degree of variation in the variables that affect pavement integrity significantly and

which should therefore be subject to greater control. These are variations of pavement thickness, variations of wheel loads and variation of subgrade CBR. Variations of tire contact area had the least influence on pavement performance.

It was recommended that strict quality control should be exercised during construction to reduce variations of pavement thickness and subgrade CBR. The tire contact area was insignificant in the analysis of flexible pavements and can therefore be discarded as a design parameter.

Brabston (11) investigated the FAA soil compaction criteria for airport pavement subgrades using laboratory compaction and tri-axial tests to determine resilient and permanent axial strain. Three soil types compacted to densities at or below current FAA compaction criteria were subjected to repeated axial loading in a tri-axial test chamber. The FAA compaction criteria for fill sections of an airport pavement for cohesive soils is, for flexible pavement, a minimum dry density of 95% for the top 9" and 90% of the ASTM D 1557 maximum dry density for the remainder of the fill. For rigid pavements, it is 90% of the recommended maximum dry density. The compaction is required to be at the optimum moisture content to prevent the development of excessive pore water pressures and subsequent shear failure that might result from soil suction.

The stringent density values required and their necessity for the full depth of the fill have sometimes been questioned. Undoubtedly, compaction or the densification of subgrades reduce compressibility, increase strength, control volume change characteristics, decrease permeability, control resilience

properties and reduce frost susceptibility.






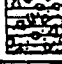


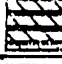




A statistical model developed by Brabston (11) for prediction of permanent soil strain based on such soil properties as density, clay content, compaction characteristics and shear strength was used to calculate permanent soil deformation at the surface of the subgrade for various levels of soil density. The wide variation in soil permanent strain for the three materials tested strengthened the need to uphold the rather stringent compaction criteria.

2.7 SOIL CLASSIFICATION
















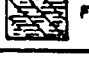





The State of Ohio Department of Transportation (12) has developed a soil classification specification for subsurface investigations which parallels the AASHTO specification. The classification of a soil is found by the process of elimination. Using the required test data, the soil analyst proceeds from the top of the chart Figure 2.1. The first classification that lists the test is the correct classification.

The clay-silt soil data analyzed by Lamb and Ritchie (13) confirm the results of the laboratory tests done to determine the Atterberg limit parameters of the clay-silt tested for the Central State University (CSU) soil stabilization research. In particular, the specific gravity for the clay-silt samples tested ranged from 2.67-2.72, the liquid limit and plastic limit of 28-32 and 11-14 respectively for the first researchers and 27-83 and 0-55 respectively for the second researchers. The shear strength values obtained by Lamb, et al., (13) ranging from 89 - 356 psi agree with the test results obtained in this research report.

FIGURE 2.1 CLASSIFICATION OF SOILS ^a

SYMBOL	DESCRIPTION	Classification		% Pass #10	% Pass #40	% Pass #200	Liquid Limit (LL)	Plasticity Index (PI)	Group Index Max.	REMARKS
		AASHTO	ON10							
	Gravel and /or Stone Fragments	A-1-a		50 Max.	30 Max.	15 Max.		6 Max.	0	
	Gravel and /or Stone Fragments with Sand	A-1-b			50 Max.	25 Max.		6 Max.	0	
	Fine Sand	A-3			51 Min.	10 Max.	NON-PLASTIC		0	
	Coarse and Fine Sand	—	A-3a			35 Max.		6 Max.	0	Min. of 50% combined coarse and fine sand sizes
	Gravel and/or Stone Fragments with Sand and Silt	A-2-4				35 Max.	40 Max.	10 Max.	0	
		A-2-5					41 Min.			
	Gravel and/or Stone Fragments with Sand, Silt and Clay	A-2-6				35 Max.	40 Max.	11 Min.	4	
		A-2-7					41 Min.			
	Sandy Silt	A-4	A-4a			36 Min.	40 Max.	10 Max.	8	Less than 50% silt sizes
	Silt	A-4	A-4b			50 Min.	40 Max.	10 Max.	8	50% or more silt sizes
	Elastic Silt and Clay	A-5				36 Min.	41 Min.	10 Max.	12	
	Silt and Clay	A-6	A-6a			36 Min.	40 Max.	11-15	10	
	Silty Clay	A-6	A-6b			36 Min.	40 Max.	16 Min.	16	
	Elastic Clay	A-7-5				36 Min.	41 Min.	≤ LL-30	20	
	Clay	A-7-6				36 Min.	41 Min.	> LL-30	20	

* The classification of a soil is found by the process of elimination. Using the required test data, proceed from the top of the chart. The first classification the test data fits is the correct classification.

MATERIAL CLASSIFIED BY VISUAL INSPECTION					
	Sod and/or Topsoil		Coal		Shale
	Berm Material		Coal Blossom		Weathered Shale
	Peat - S-Sedimentary W-Woody F-Fibrous L-Loamy M-Mariy &c		Claystone		Sandstone
	Random Fill		Mudstone		Weathered Sandstone
	Bouldery Zone		Weathered Mudstone		Siltstone
	Fire Clay or Underclay				Limestone
					Leached Limestone
					Dolomite
					Leached Dolomite
					Various Other Materials

^a Courtesy, Ohio Department of Transportation (1984)

RESEARCH METHODOLOGY

3.1 GENERAL OVERVIEW/CBR RATIONALE

The enhancement of soil properties of a clay-silt system through soil stabilization requires a method of testing that guarantees 1) simple and consistent technique for determining the strength of the subgrade and pavement components, 2) a generally accepted, reliable and representative strength measurement approach, 3) applicability to airport pavement design methodology in a reasonable period of time and with minimal outlay of resources. These requirements are met by the CBR pavement material testing and design method.

The California Bearing Ratio (CBR) method of design developed by the California Division of Highways in 1928 meets the above criteria. Application of the widely used CBR design method allows the design engineer to proportion the thickness of subbase, base, and surface course by entering a set of design curves with the results of a comparatively simple soil test, which measures the index of shearing strength or resistance of a soil to penetration, expressed as a percentage of the resistance for a standard crushed stone.

3.1.1 DRY CBR TEST

The choice between using a dry CBR test and a wet one is influenced by many factors chiefly the condition of the soil system in the field on a short-term and long-term basis. If there is reason to believe that the moisture content of a soil

will be reasonably constant and not approach that of the worst condition as simulated by a soaked test, then a dry test can be used, otherwise the wet test is used representing the worst possible condition. The Dry CBR test was adopted because it allowed the specification of clay-silt soil optimum moisture content as an experimental variable for analysis (See Section 3.3).

To gain control over the various factors that influence field CBR, representative ranges of all hypothesized variables were tested and analyzed for CBR response as explained in the previous sections. One of the important considerations was the specification of the range of applicable moisture content for the experimentation. Based on the results obtained from the curves of maximum dry density versus moisture content under standard compaction (AASHO) for the control case there emerged a range of values for moisture content within which the maximum dry density and optimum moisture content lie for all the various combinations of temperature and clay-silt ratio. This band was between 13% and 21% and since moisture content was set at three levels in the factorial experimentation, moisture content at 13%, 17%, and 21% were selected as representing the range of optimum moisture content for the clay-silt system.

3.1.2 CBR TEST OVERVIEW

The CBR test involves several steps including the compaction of at least 10 pounds of a soil sample in a 6-inch diameter CBR mold in five layers using a standard 10 pound compaction rammer

raised 18 inches each blow. Each layer receives a prespecified 55 standard blows (AASHTO compaction effort). The last layer after compaction receives a surcharge weight to simulate the weight of the overlying pavement the soil would typically support and the entire sample, if a soaked CBR test is employed, is then immersed in water for four days. The four-day period was chosen because many soils approach complete saturation in this time period within the depth affected by the piston. A shorter time could be used if experience suggests a faster rate of saturation attainment for the particular soil being considered. The soaked soil sample therefore represents the worst possible condition of the soil regarding its ability to support a pavement structure. It is important to note that soaking of the sample is not required where it can be conclusively shown that moisture will not ingress into the pavement structure.

The CBR test is valid if the major portion of the piston's penetration is caused by shear deformation. Since the CBR is a percent of a standard load, it is possible in some cases to measure CBR values in excess of 100 percent. Generally the CBR at 0.1 inch penetration is used in design. However, if the bearing ratio at 0.2 inch penetration is still greater, this value is used after the experiment has been repeated. As a general rule, the CBR will decrease as the penetration value increases. In spite of its arbitrary nature, the CBR test has most widely been used with considerable satisfaction by engineers. Provided that standard procedures are followed throughout in such details as size of compacted sample, rate of

loading (0.05 inch/minute), piston size (3 square inches) and prespecified level of compaction, the results provided can be very reliable.

The tradeoffs in CBR procedures are governed by test material types. Considering granular materials, surcharge weights are not very significant during the soaking test because granular materials are not greatly affected by swelling. In contrast, claylike materials which are greatly affected by swelling pressures will yield CBR values depending on the weight of the surcharges used during the soaking period.

During the penetration testing portion surcharge weights are extremely important for granular materials but not too significant for the fine-grained soils.

The choice of the CBR method for this research stems not only from the widespread usage it has enjoyed, but also its reliability, simplicity, and generality to a variety of soil types and its correlation to several airport design parameters.

3.2 EXPERIMENTAL DESIGN

3.2.1 Variables Specification

Several variables were hypothesized as influencing the resistance of a clay-silt soil to deformation as measured by the CBR. These are:

- Additive Content (%)
- Moisture Content (%)
- Clay-silt Ratio
- Curing Temperature (°F)
- Soil Density (dry)

These variables conversely affect the pattern of cracks obtained in the soil testing phase.

3.2.2 Crack Pattern Specification

The crack patterns observed during CBR testing exhibited soil-strength dependency and included:

- Cylindrical cracks
- Radial cracks
- Cylindrical and radial (combination) cracks
- Irregular cracks
- No cracks

Soil samples with CBR less than five generally exhibited no cracks.

3.2.3 Factorial Design Specification

One of the basic problems of experimental design is deciding what pattern of design points will best reveal important aspects of the yet unknown situation under study, in this case CBR response to the hypothesized variables.

In exploring a functional mathematical relationship, it might appear reasonable on first impression to adopt a comprehensive approach in which the entire range of every factor is investigated. Such a design would invariably contain all combinations of several levels of all factors as hypothesized. A better and more efficient approach would involve the use of a sequential approach to the experimental investigations.

Guided by the 25% rule of experimental design which states

that not more than one quarter of the experimental effort (budget) should be invested in a first design, the control experimentation in which no additive treatment was applied was run, representing about 25% of the experimental effort. The behavior of CBR with such variables as moisture content, clay-silt ratios, and temperature was better understood from this partial set of experimental runs.

The experimental design was fashioned to fit a factorial design matrix. Factorial designs facilitate the visualization and comprehension of similarities and simplifications in the experimental process and thus assist the task of model building and the estimation of main effects and interactions arising as a result of changes in the model experimental variables.

For the first four hypothesized experimental variables, i.e. additive, moisture, clay-silt ratio, and temperature, a $4 \times 3 \times 3 \times 3$ factorial design requiring 108 experimental runs was effected. Added to the 38 control runs described previously with no additive treatment, a total of 146 data points was obtained.

3.2.4 Levels of Variables:

The levels of various variables hypothesized as affecting CBR were specified as follows:

<u>Experimental Variable</u>	<u>Factorial Design Levels</u>
Additive Percentage (%)	0, 1/2, 1, 4 (4 levels)
Moisture Percentage (%)	13, 17, 21, (3 levels)
Clay-silt ratio	0.4, 0.5, 0.6
Curing Temperature (°F)	40, 65, 90

Each experimental point in the factorial design matrix generated a value for the dry-density of the soil hence its exclusion from specification in the design levels.

One of the important considerations was the specification of the range of applicable moisture content for the experimentation. The choice of the levels of moisture content fixed at 13%, 17% and 21% was based on earlier control case test results obtained from the curves of maximum dry density versus moisture content under standard compaction (AASHO). The curves similar to Figures 3.1 and 3.2 showed that maximum dry densities obtained corresponded to moisture contents between 13% and 21% and since moisture content was set at three levels in the factorial experimentation, 13%, 17%, and 21% were selected as representing the range of optimum moisture content and optimum dry density variations for the clay-silt system.

The four levels of additives were set based on economics of additive cost, the results of pilot tests, and the need to obtain reasonable values of CBR. During earlier pilot tests, 10% and 30% epoxy-resin additive levels had yielded CBR's of 168 and 683 respectively.

The three temperature levels were set based on the prevailing temperatures in the regions most likely to benefit from this research effort.

3.3 Testing Procedure

The ASTM D 1883-73 provides step by step procedures for CBR testing which were followed in conducting the experiments to

FIGURE 3.1 DRY DENSITY VS. MOISTURE CONTENT BY TEMPERATURE BY CLAY-SILT RATIO

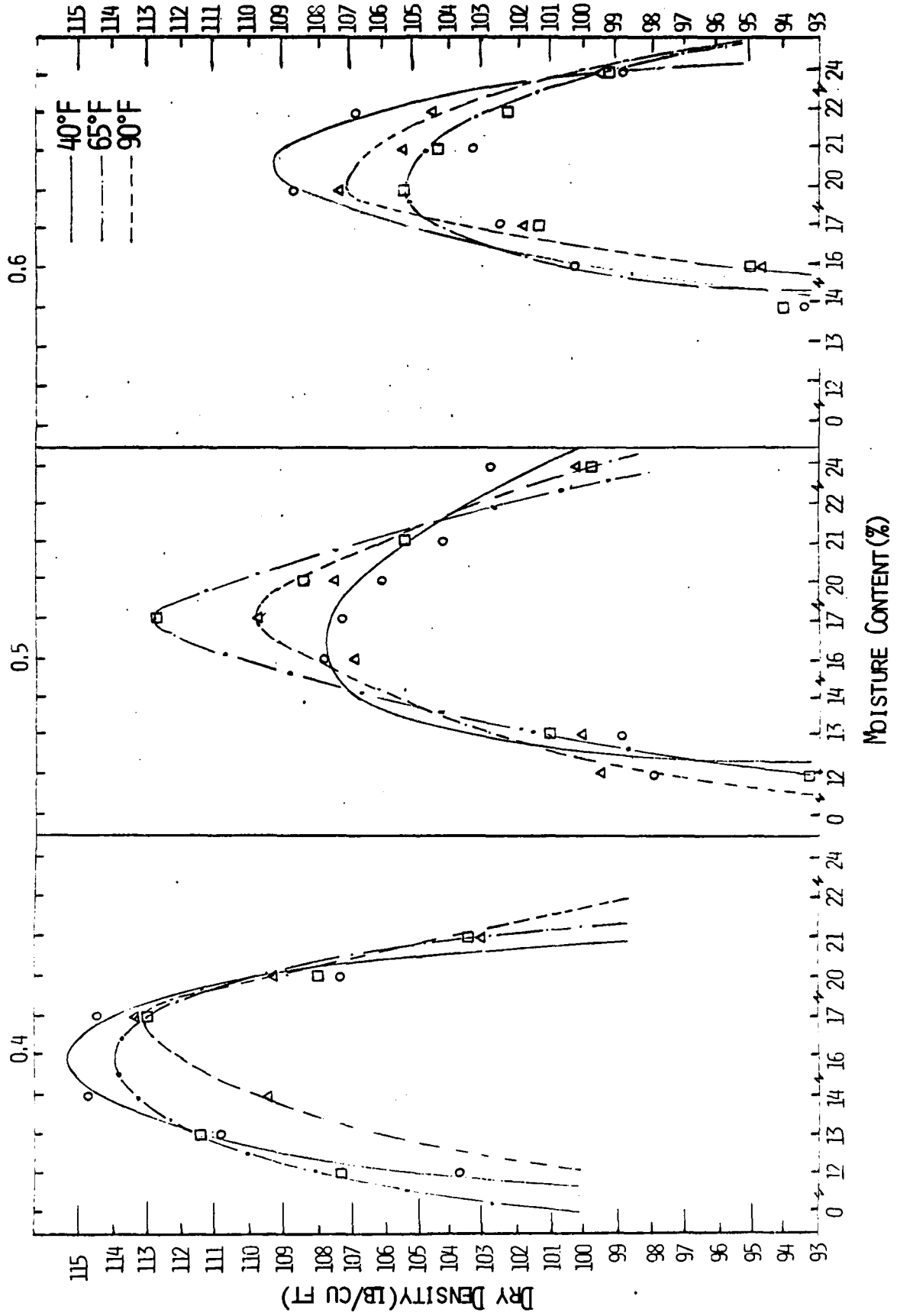
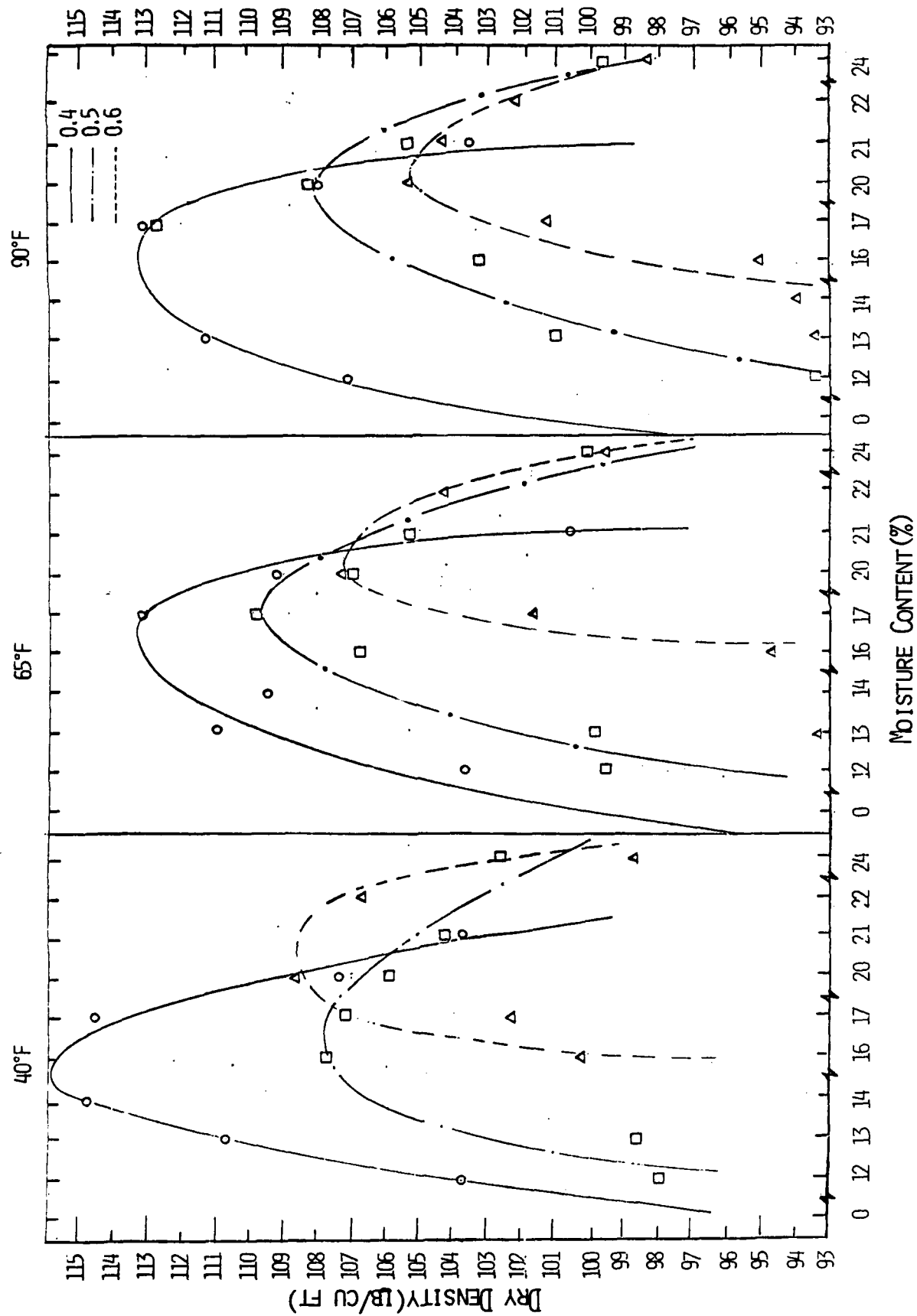


FIGURE 3.2 DRY DENSITY VS. MOISTURE CONTENT BY CLAY-SILT RATIO BY TEMPERATURE



determine the strength of a clay-silt soil system. The soil specimen may be tested unsoaked or soaked. The limited number of soaked tests performed were effected by immersing the specimen in water for about four days in order to simulate very poor soil conditions.

The clay and silt (Figure 3.3) samples were prepared in a manner closely following the ASTM method D 1557. The majority of the testings were on unsoaked samples because the clay-silt optimum moisture content was specified as an experimental variable.

The batching of various ratios of clay to silt by weight was made and resulted in a representative clay-silt sample over 12 pounds to which was added the required amount of water. The sample was mixed to a uniform consistency. Various additives (Figure 3.4) were applied to the wet sample and mixed uniformly and manually to an even texture.

The samples treated with epoxy resin were compacted in the standard CBR molds specially lined with aluminum foil to preserve the molds and reduce demolding efforts. Figures 3.5 and 3.6 show the motorized compaction equipment used in the research.

The compacted specimens were trimmed to specification and covered with nylon wrappers for moisture preservation before being thermally soaked in a specially prepared curing chamber for three days. Three days were considered enough time for the registration of steady state conditions. Sideviews of the thermal chamber interior are shown in Figures 3.7 and 3.8.

CBR testing of the thermally cured clay-silt stabilized

FIGURE 3.3 FINE GRAINED CLAY (L) AND SILT (R) SOIL SAMPLES



FIGURE 3.4 VARIOUS ADDITIVES SCREENED OR TESTED FOR STABILIZATION EFFECTIVENESS



FIGURE 3.5 GENERAL VIEW OF SOIL STABILIZATION LABORATORY

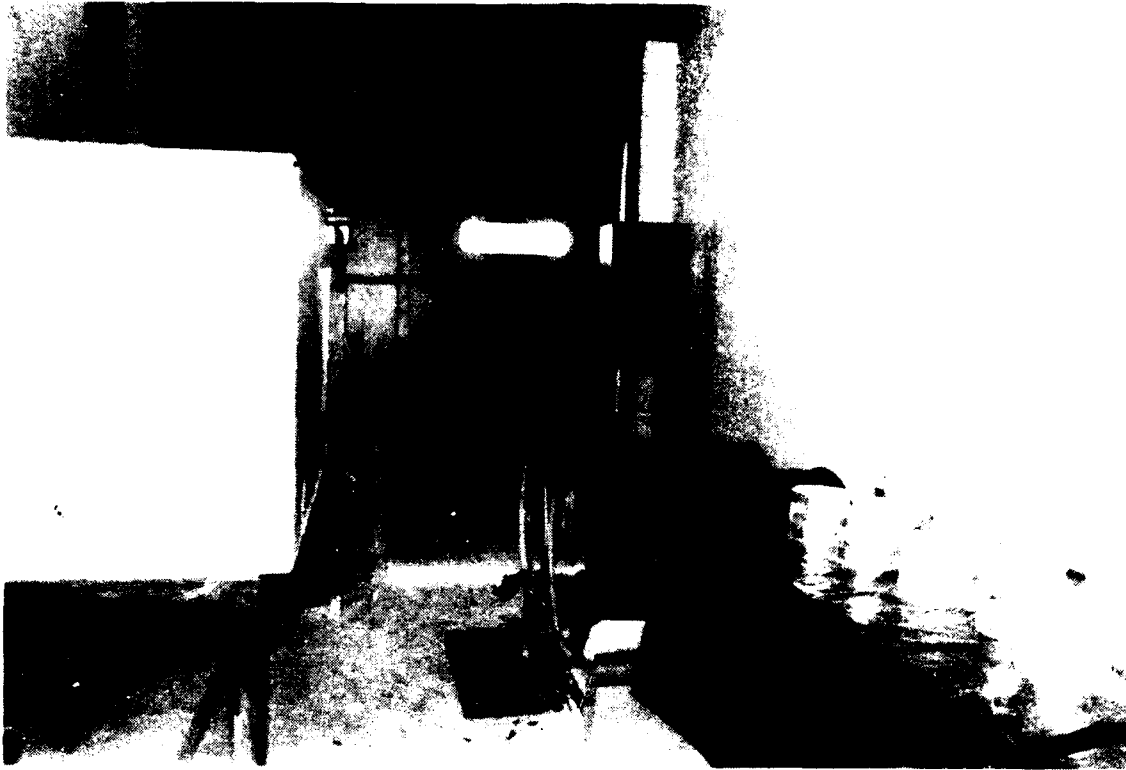


FIGURE 3.6 VIEW OF AUTOMATED COMPACTION EQUIPMENT, ADDITIVE DRUM RACK AND EPOXY RESIN STABILIZED SAMPLES



FIGURE 3.7 CBR TEST SPECIMENS IN THERMAL CHAMBER



FIGURE 3.8 CLOSE-UP VIEW OF SOIL STABILIZATION RESEARCH LABORATORY

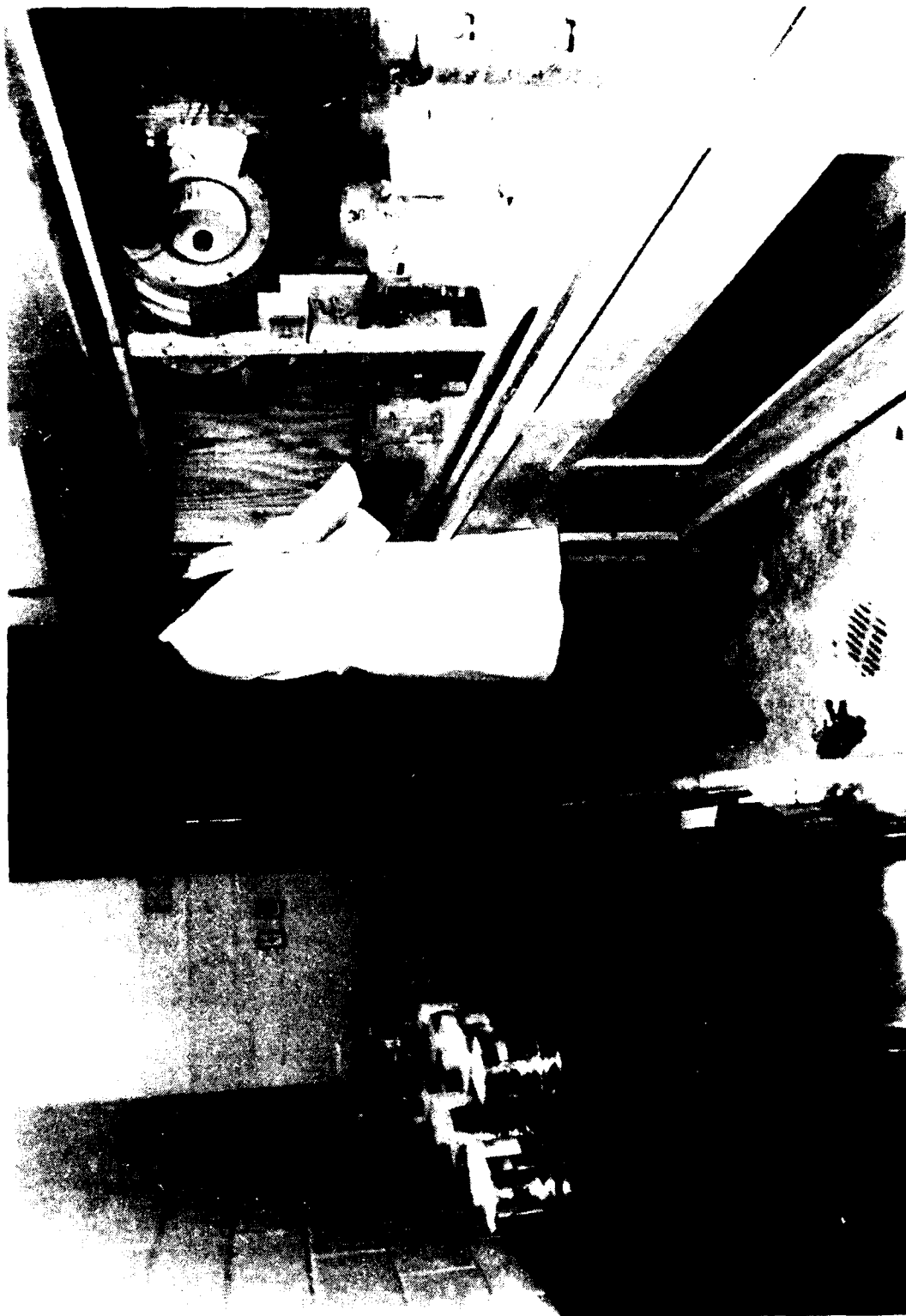


FIGURE 3.9 STABILIZED CLAY-SILT SOIL ALREADY TESTED FOR CBR STRENGTH



FIGURE 3.10 CLOSE-UP VIEW OF EPOXY RESIN STABILIZED CLAY-SILT SHOWING ASSORTED CRACK PATTERNS



FIGURE 3.11 STORAGE RACK SUPPORTING TESTED EPOXY-RESIN STABILIZED SOIL SAMPLES



FIGURE 3.12 GENERAL VIEW OF THE AUTOMATED DATA COLLECTION EQUIPMENT

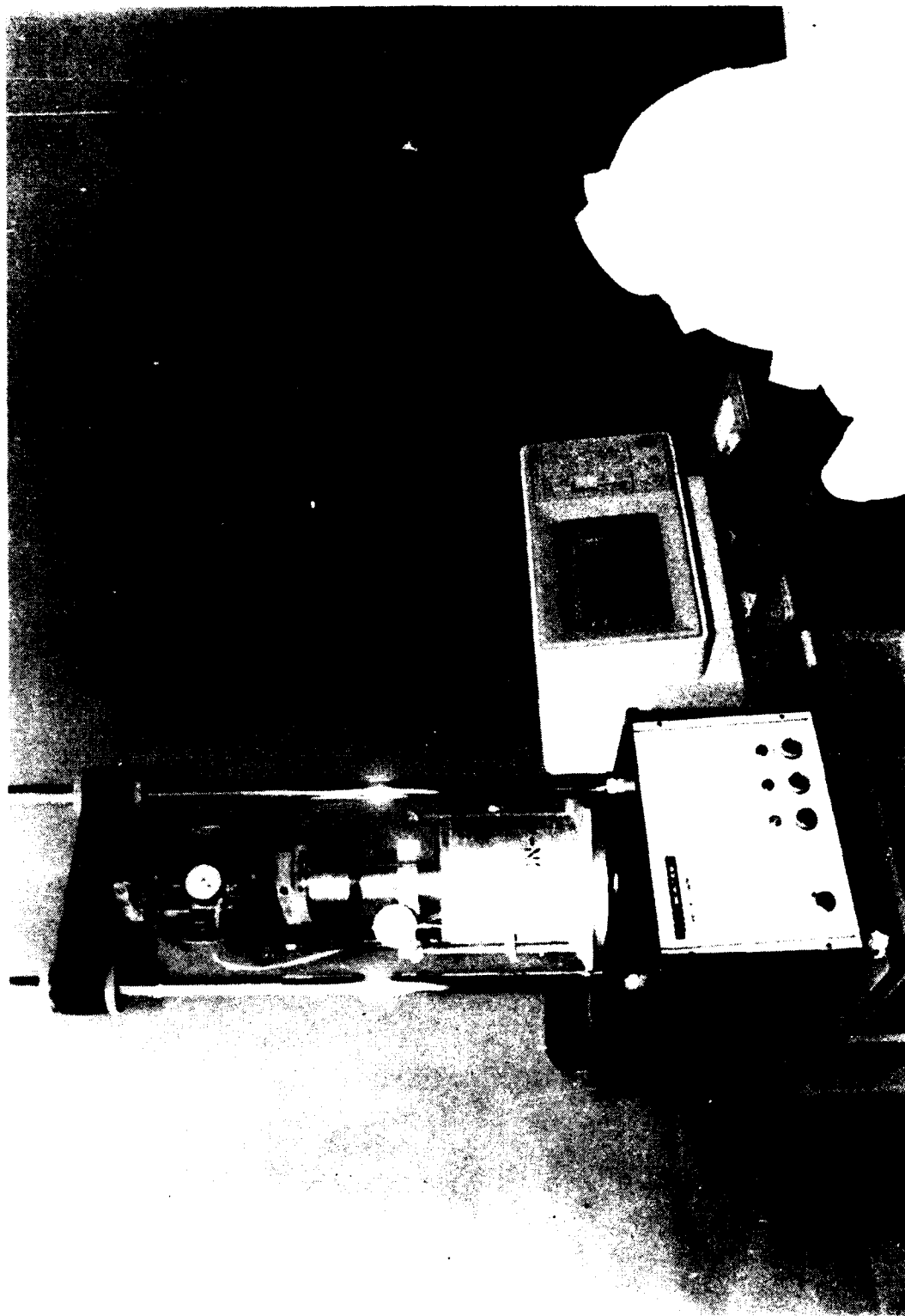
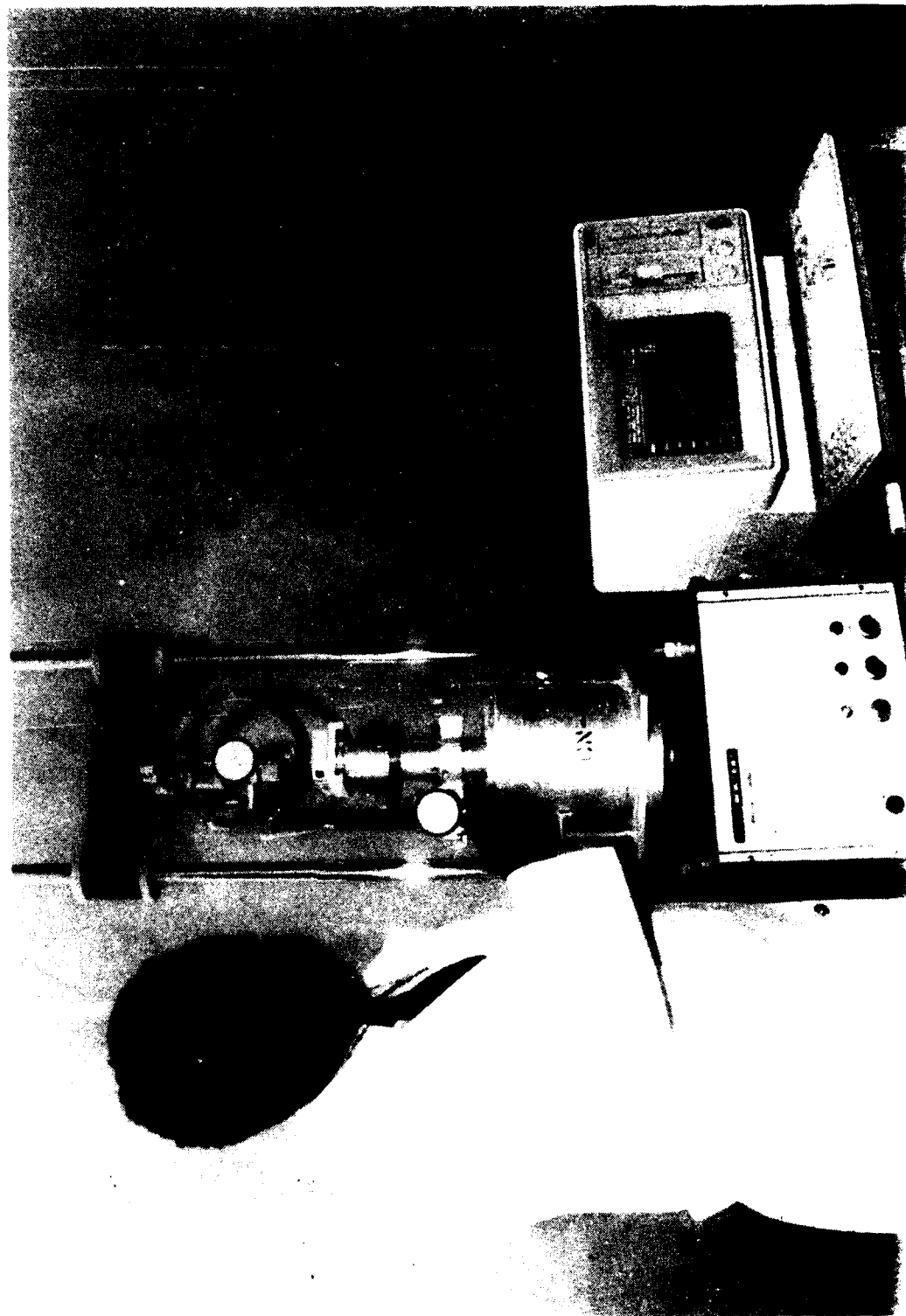


FIGURE 3.13 VIEW OF TESTED CHEMICALS PLUS STABILIZED AND TESTED CLAY-SILT SAMPLES
WITH AND WITHOUT ALUMINUM LINING



FIGURE 3.14 CLOSE-UP VIEW OF THE CBR AND AUTOMATED DATA COLLECTION EQUIPMENT



samples was effected using the soil test CBR testing equipment shown in Figures 3.12 and 3.14 through 3.17. Both a general and close view of the already tested samples bearing the cylindrical plunger impressions are shown in Figures 3.9 and 3.10. A collection of the samples tested is shelved on the rack shown in Figure 3.11. The samples are shown still wrapped in their aluminum linings.

3.4 Automated Data Collection System

To facilitate the acquisition and reduction of the CBR test data, a microcomputer-based automatic data collection system was devised (Figure 3.12).

The data collection system consisted of (1) The motorized SOILTEST CBR testing equipment complete with a loading platform, plunger, proving rings, force and displacement dial indicators and other attached accessories, (2) Linear Variable Differential Transformer (LVDT) displacement transducer, (3) Signal conditioner, 4) Digital display, (5) Screw terminal boards (panels) and (6) Personal computer.

The objective of the automated data collection system is the automatic recording and analysis of the displacement and resistance to deformation of clay-silt samples prepared and compacted to standard specifications after thermal soaking in a temperature controlled chamber. Occasional manual checks on the collected data were effected for correlation and calibration purposes.

The cylindrical molds used for forming these specimens

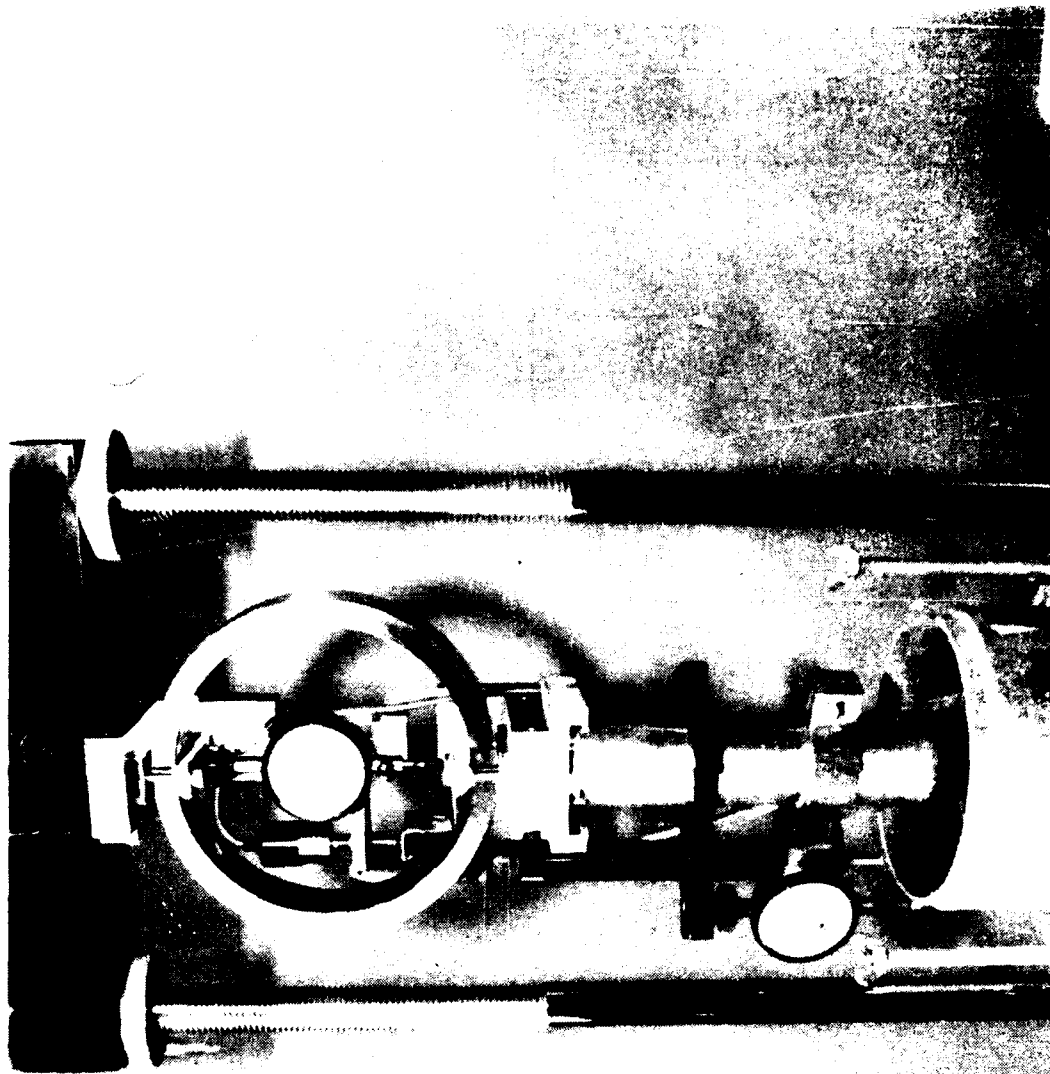
generally had an inside diameter of 6 ± 0.005 inches (152 ± 0.13 mm) and a height of 7 ± 0.005 inches (177.8 ± 0.13 mm) to which was attached a metal extension collar 2.0 inches (50.8 mm) in height and a perforated base plate $3/8$ inch (9.53 mm) in height. The mechanical compaction of soil in this mold was followed, after thermal curing, with testing on the Versa-Loader.

The vertical force on the sample in the mold was applied via a static plunger, as the versa-loading machine, with a proving ring capacity of at least 10,000 pounds, moved its platform at a uniform (non-pulsating) rate of 0.05 inch (1.27 mm) per minute. Automated measurement of the vertical force was effected through an LVDT securely and properly positioned about two inches to the left of the vertical axis of symmetry of the proving ring. The LVDT measured the vertical deflection of the proving ring which is directly proportional to the vertical load. Manual readouts of the force was made by dial gauges.

The vertical deformation of the sample was measured by attaching a second LVDT and a dial gauge to the stem of the plunger (Figure 3.15). The load readings at penetration of 0.1 inch and 0.2 inch were used to determine the appropriate CBR values which characteristically are referenced to the strength of standard crushed gravel.

Figure 3.16 shows a schematic of the automated data collection and display system used, with annotation of the various components.

FIGURE 3.15 CLOSE-UP VIEW OF THE CBR TEST EQUIPMENT AND LVDT ATTACHMENTS



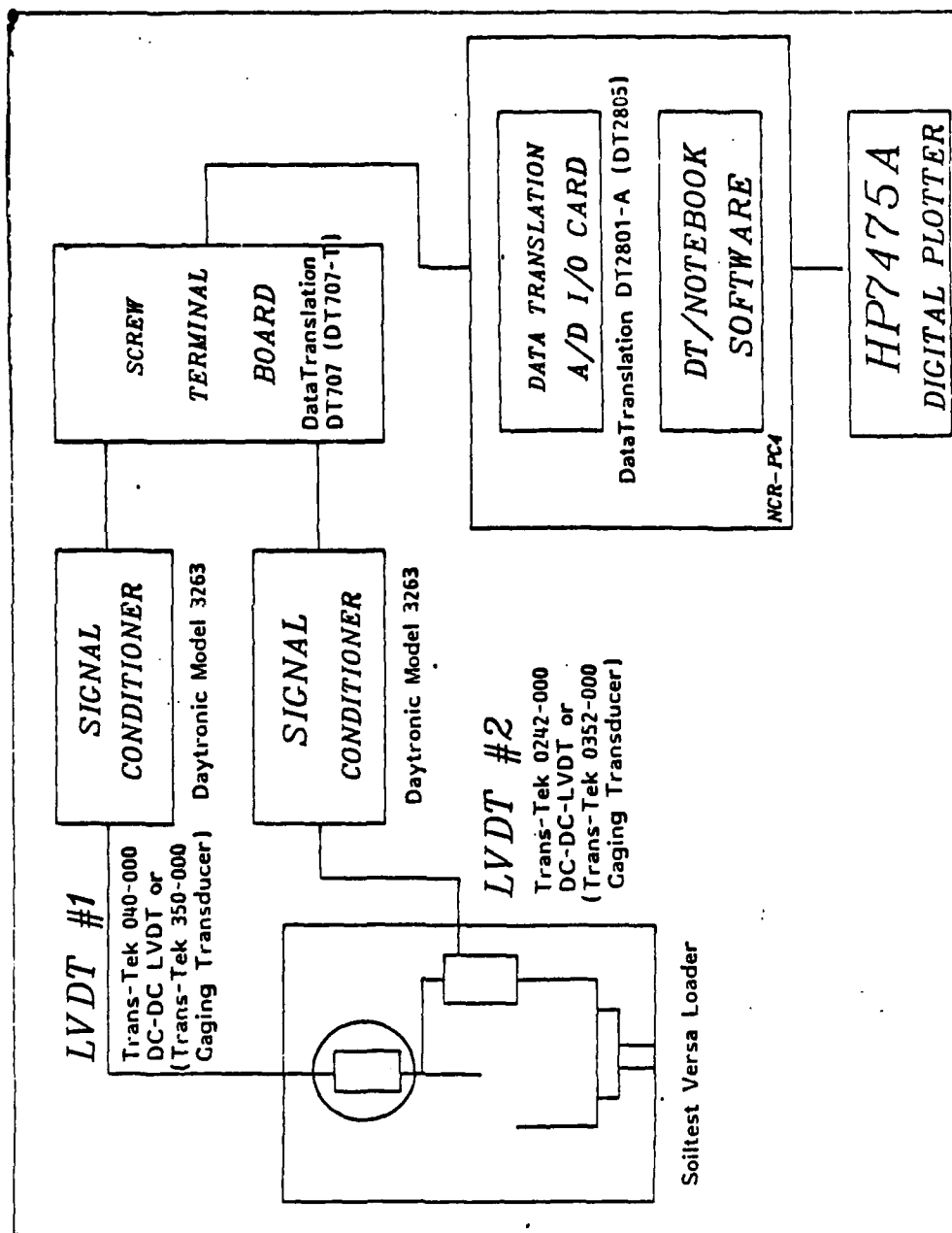


FIGURE 3.16 SCHEMATIC OF AUTOMATED DATA COLLECTION AND DISPLAY SYSTEM

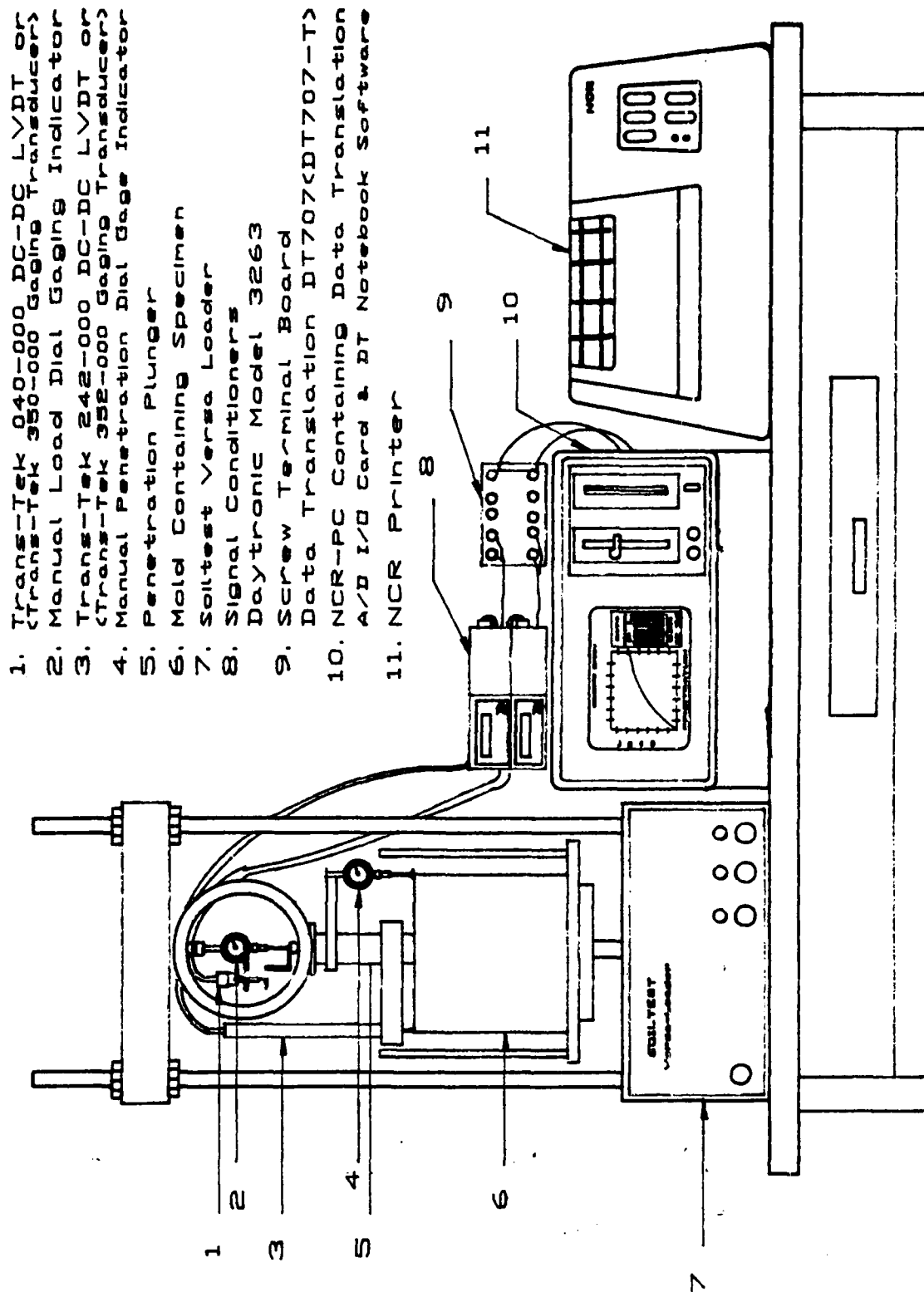


FIGURE 3.17.
AUTOMATED DATA COLLECTION AND DISPLAY SYSTEM

3.4.1 LVDT Overview

The LVDT is an electromechanical transducer that produces an electrical output proportional to the displacement of a separate moveable core. It consists of a primary coil and two secondary coils symmetrically spaced in a cylindrical form.

There exists a wide variety of LVDT units featured in different shapes, sizes, types, ranges and physical configurations. A very important LVDT design consideration is the determination of the combination of windings which produces excellent linearity without compromising other desirable performance characteristics. Therefore, the materials are usually carefully selected to achieve optimum performance. The stainless steel housing, coil assembly, oscillator-demodulator, and Teflon-insulated leads are carefully encapsulated in epoxy-resin. Oscillator-demodulator components are individually selected to assure accuracy and reliability.

The reason for using the LVDT in this research is to detect changes in physical parameters (stress and strain or deformation resistance) of the soil specimens measured during the CBR soil testing procedures. The response of soil specimens to these changes is, in this situation, a voltage variation with respect to their generally constant input or excitation voltages. Devices such as the LVDT and electronic dial gages are used to measure directly deformation or any other physical parameter which can be translated into a linear displacement value. This is effected by the measurement of force with a proving ring and a displacement transducer. Clearly, both the proving ring "spring" constant

(usually given in lb/in) and the displacement transducer calibration constant (usually given in Volt/in) are needed in the determination of the force applied to the testing specimen.

3.4.2 LVDT Mode of Operation

The mode of operation of the LVDT is analogous to an elastic member which can be loaded in either tension and/or compression. This leads to deflection in either direction, depending on the type of load applied. The bi-directional nature of the displacement characteristic of an LVDT perfectly parallels the bi-directional deflection of an elastic member.

A free-moving rod-shaped magnetic core inside the coil assembly provides a path for the magnetic flux linking the coils together. When the primary coil is energized by an external source, voltages are induced in the two secondary coils. These are connected in opposing series so the two voltages are of opposite polarity. Therefore, the net output of the transducer is the difference between these voltages, which is zero when the core is at the center or the null position. When the core is moved from the null position, the induced voltage in the coil towards which the core is moved increases, while the induced voltage in the opposite coil decreases. This action produces a differential voltage output that varies linearly with changes in core positioning. The phase of this output voltage changes suddenly by 180-degrees as the core is moved from one side of the null position to the other.

3.4.3 Signal Conditioner

The signal conditioning equipment performs many functions. It provides the input or excitation voltage to passive transducers. It also provides any necessary impedance matching or transmission compensation for the output signal from the transducer. Once the signal is properly matched, the signal conditioning equipment fulfills the requirements for amplification or attenuation, demodulation, filtering, or other signal processing.

The signal conditioner will be called upon to modify the output signal. This modification will include producing a digital signal from an analog signal or vice-versa, changing the form of the output from voltage to frequency or from voltage to current, or compressing the data by a linear-to-logarithmic conversion.

The signal conditioner selected was the Daytronic Model 3263 Signal Conditioner because a signal conditioner with a digital indicator and DC Volts/Millivolts and DC-to-DC LVDT's/Potentiometer signal sources was required. This unit was considered the best selection for this research because of its overall effectiveness.

Whatever form the output of the signal conditioner takes, quantitative information from that signal is required and is provided by a digital display readout. A readout consists of an information recording system, an information display system, or a combination of both systems. This can be analog, such as an indicating meter, or digital using an LED display. A recording

oscillograph or chart recorder is a combination of an analog display and recording device. Digital recording is commonly done on wide-band magnetic tape but these readouts will be fed to a screw terminal board that will be interfaced with a data acquisition and reduction system.

3.4.4 Functional Aspects of Signal Conditioning

The specific functions of signal conditioning are:

1. Carrier Generation - for an LVDT which is a passive transducer requiring AC excitation at a voltage and frequency not directly available.
2. Demodulation and Filtering - for practically all readouts, records, meters, and analog controlled devices that are DC-input devices. This means that AC-output of an LVDT must eventually be converted into filtered DC-outputs before being applied to the readouts.
3. Amplification - for the typical readout used with an LVDT which requires a higher input voltage and power supply than is directly available from the LVDT.
4. DC-operating Power - means that all of the electronic circuitry requires stable DC voltages for proper operation.
5. Temperature Compensation (LVDT) - to electronically compensate for a decrease in primary current with increasing temperature.

These functions are not necessarily the only characteristics

demand of the signal conditioning equipment, but it does represent those ordinarily required for the majority of LVDT measurement systems.

3.4.5 Data Acquisition and Reduction Software

The DT2801 Series is a high performance analog to digital (A/D) input/output (I/O) board. This series consists of the DT2801-A, DT2801, DT2801/5716, DT2805, and the DT2805/5716. In this project, it was decided to order the DT2801-A and the DT2805 as a backup unit but not the DT2801. The DT2801-A was chosen over the DT2805 because it has a higher conversion throughput of 27.5KHz as compared to the 13.7KHz of the DT2801. The DT2805 was selected because it has a pre-amplification voltage gain of up to 500 which is very useful for the pickup of small signals. An example of such a case is the signal produced by a weak and slushy clay-silt mixture. The DT2805 is capable of a throughput of 13.7KHz using one of the preprogrammed 1 or 10 voltage gain.

Two separate screw terminal boards (panels) were obtained and used in combination with the DT2801-A and the DT2805. The DT707 screw terminal will work with the DT2801-A, while the DT707-T will accommodate the DT2805. These terminals are discussed later. The DT2801-A and the DT2805 boards can be plugged into one of the system expansion slots of the NCR-PC computer backplane. The board can be programmed from the NCR-PC but for ease of programming it was decided to order the DT-notebook software which will also be discussed later.

The DT2801-A and the DT2805 are identical for the most part except for the on-board clock of the DT2801-A. The DT2801-A/2805 also includes two 12-bit digital to analog (D/A) converters.

These D/A converters can provide either sequential outputs or simultaneous outputs. In addition, the DT2801-A/2805 also feature two 8-bit digital I/O ports which can be used separately to read or write 8-bit transfers or 16-bit transfers. The boards also contain an on-board programmable clock, which can be used to provide clock pulses to control the operations of the board's A/D and D/A subsystems.

An on-board microprocessor acts as the interfacing between the I/O board and the NCR-PC. The microprocessor controls all on-board operations and simplifies program control by the host NCR-PC. Tasks such as A/D converter sequencing and error checking are carried out by the I/O boards and on-board microprocessor which simplifies the work done by the NCR-PC. The circuitry is simplified to allow the analog and digital I/O boards to plug into a single expansion slot of the NCR-PC.

The on-board programmable clock's function is to initiate repetitive data conversion events on the DT2801-A/2805 boards. The boards internal clock is programmable for periods ranging from five microseconds to 0.1638 seconds in increments of 2.5 microseconds and can be used for internal clocking of A/D and D/A converters. Another feature of the DT2801-A/2805 boards is their external triggers. An external trigger is a user supplied pulse used to specify the exact time at which an A/D, D/A, or a digital I/O command begins execution. An external trigger input enables the synchronizing of I/O event with an external event by deferring the command execution until an external trigger pulse is received. The on-board power converter generates all of the

needed supply voltages from the +5 volts provided on the NCR-PC and provides high noise isolation from the computer system's power supplies.

The A/D system of the DT2801 series boards has 12 or 16 bits of resolution. However, the DT2801-A/2805 uses a 12-bit A/D converter. The incoming analog signal is converted into a binary number. In the DT2801-A/2805, the binary number is 12 bits long and can assume 4,096 different states. This 12-bit converter can therefore resolve differences on an analog input as small as .024%. In the DT2801-A/2805 A/D system, the A/D conversion happens as follows:

1. The analog multiplexer chooses one input channel from those connected to the board.
2. The programmable gain amplifier buffers the analog input. Since the analog input signal from the transducer may only be +1.25V at its maximum, an amplifier is used to boost the signal's voltage between the 0 through +10V level required by the board's A/D converter.
3. A sample and hold circuit acquires the selected analog signal from the multiplexer and stores it on a capacitor, keeping the signal's voltage constant so an accurate A/D conversion can be made.
4. Finally, the A/D converter translates the analog signal held by the sample and holds it into a digital code.

The DT2801-A/2805 board's D/A system contains two 12-bit digital to analog converters (DAC0 and DAC1) which may be operated in any of three modes, as determined by the DAC select parameter. When the DAC select equals 0 data is written to the DAC0 only, and when the DAC select equals 1 data is written to the DAC1 only, but when the DAC select equals 2 data is written to both of the DAC (0 and 1 simultaneously).

The digital I/O subsystem of the DT2801-A/2805 permits the NCR-PC to be used with peripherals which accept or supply parallel digital data. On the DT2801-A/2805 boards, a total of 16 digital I/O lines are provided. The 16 lines are divided into two ports of eight lines each. Either port can be used for writing data out of the DT2801-A/2805 board (digital output) or reading data into the DT2801-A/2805 board (digital input). All connections for the 16 digital I/O lines are made on the DT707/DT707-T screw terminal board (panel).

The DT707 screw terminal panel is an accessory product which permits all user connections (A/D, D/A, Digital I/O, External Trigger, and External Clock) to the DT2801-A board to be made on screw terminals. Screw terminal connections are solderless connections. The DT707 plugs into connector J1 on the DT2801-A board via an integral one meter ribbon cable. Each screw terminal panel has rubber feet for horizontal table-top mounting. The DT707-T plugs into the DT2805 board and is equipped with a thermocouple cold-junction compensation circuit by which a user can determine the temperature of the screw terminal panel.

The screw terminal panel consists of 80 barrier strip connections in four sections of 20 connections each. The

connections for the D/A, Digital I/O, External Clock subsystems, and those for the External Trigger are simply the DT2801-A/2805 board's J1 pins brought out to screw terminal connectors. The function of each screw terminal on the DT707 is indicated directly on the board's silkscreen.

3.4.6 DT/Notebook Software

The DT/Notebook is an integrated, general-purpose software package for real-time data acquisition and control. It supports the A/D, D/A, digital I/O, and clock functions of data translations. It replaces the lab notebook and requires no software skills on the part of the user. The DT/Notebook is menu driven, easy to learn, and it is also easy to use. The existing conditions which define the current data to be collected are displayed on the screen and can be easily modified. The DT/Notebook can reduce complicated data acquisition and control procedures to single-key operations so repetitive tests are simplified.

3.4.7 Basic Operation

Once the data acquisition problem has been defined and analyzed, the notebook can be put to good use. First, the setup function is selected from the main menu; the setup menu will appear offering five different choices.

The setup function is divided into three parts represented by the first three choices in the setup menu, which are channels, files, and displays. Channels define the transfer data between

the hardware interface and the notebook. "Files" is used to set up the transfer of data from the notebook to the disk storage file. Display controls the real-time display. Secondly, channels are selected and a lower level menu appears offering two choices: normal and high. An option table appears on the screen which can be modified to suit this particular problem.

"Files" is now selected and another option table appears. This table contains setup conditions which will control the storage of data on a floppy disk.

The display function is now selected and a lower level menu appears offering two selections: windows or traces. Each command corresponds to an option table. The windows option table determines the size, number, and color of the graphs to be displayed on the screen during the data acquisition run. "Traces" is used to set up the data traces which will be drawn in the windows. Data changes in these tables can be accommodated to meet stated needs.

3.4.8 Complementary Data Collection Software

The software developed for the automated data collection process was modified in view of the difficulties associated with probe setup and initialization. Therefore it was decided to incorporate a self calibrating procedure preparatory to data collection.

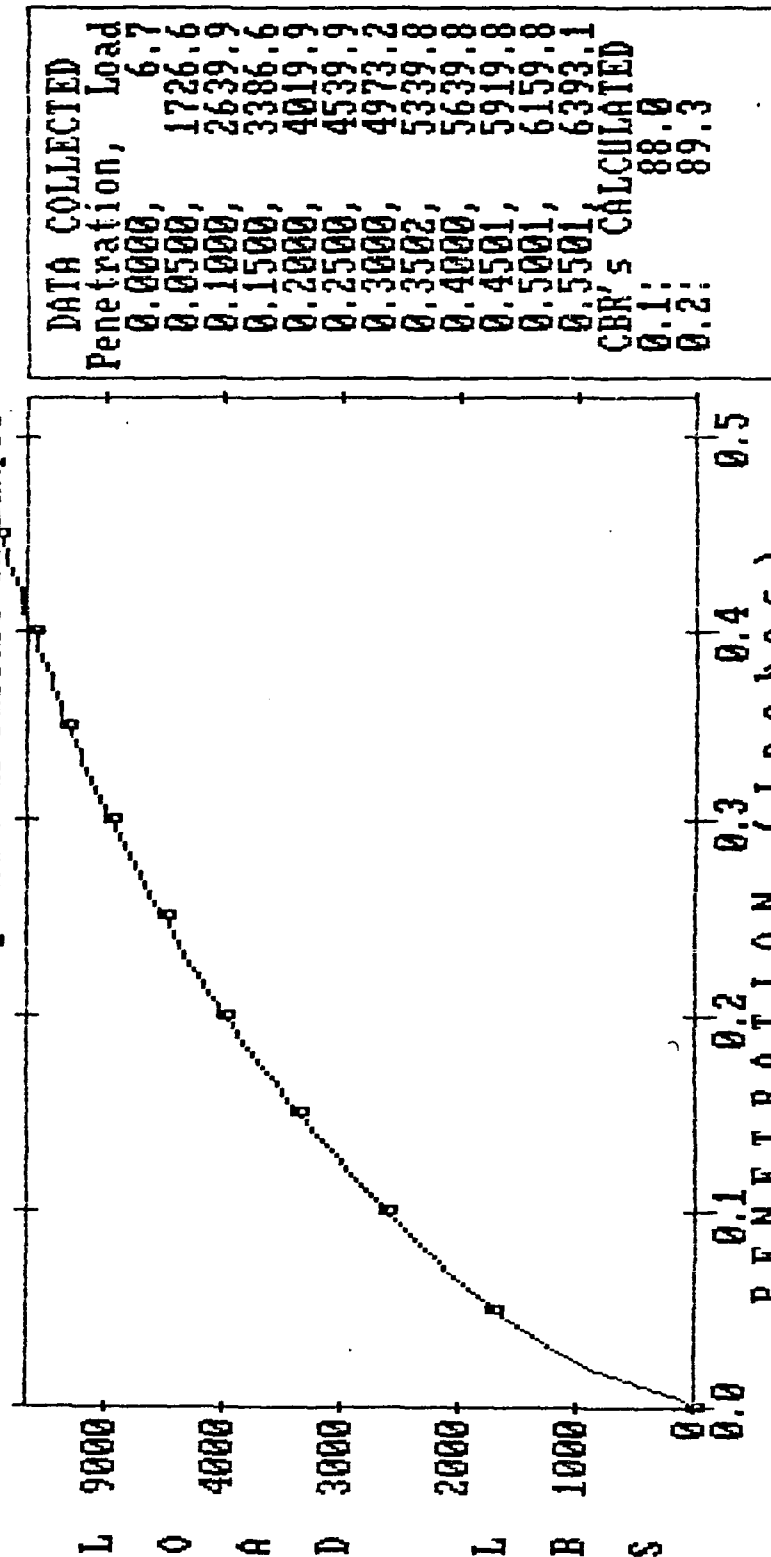
The program written in Turbo Pascal to achieve this objective features the One Touch Menu System and Fill Screen Data Entry System for ease of use. The One Touch Menu System enables the

user to touch only one key to select the needed option. The Fill Field Screen Data Entry System allows the user to type in the requested data and advance easily from one field to the next until all the requested data is correctly entered. The automated system is ready for data gathering after the space bar is depressed. Figures 3.18(1) to 3.18(7) show sample plots of the penetration in inches and load in pound force from the automated data collection system which also calculates and displays the CBR values corresponding to the observed data.

3.4.9 Data Collection Accuracy

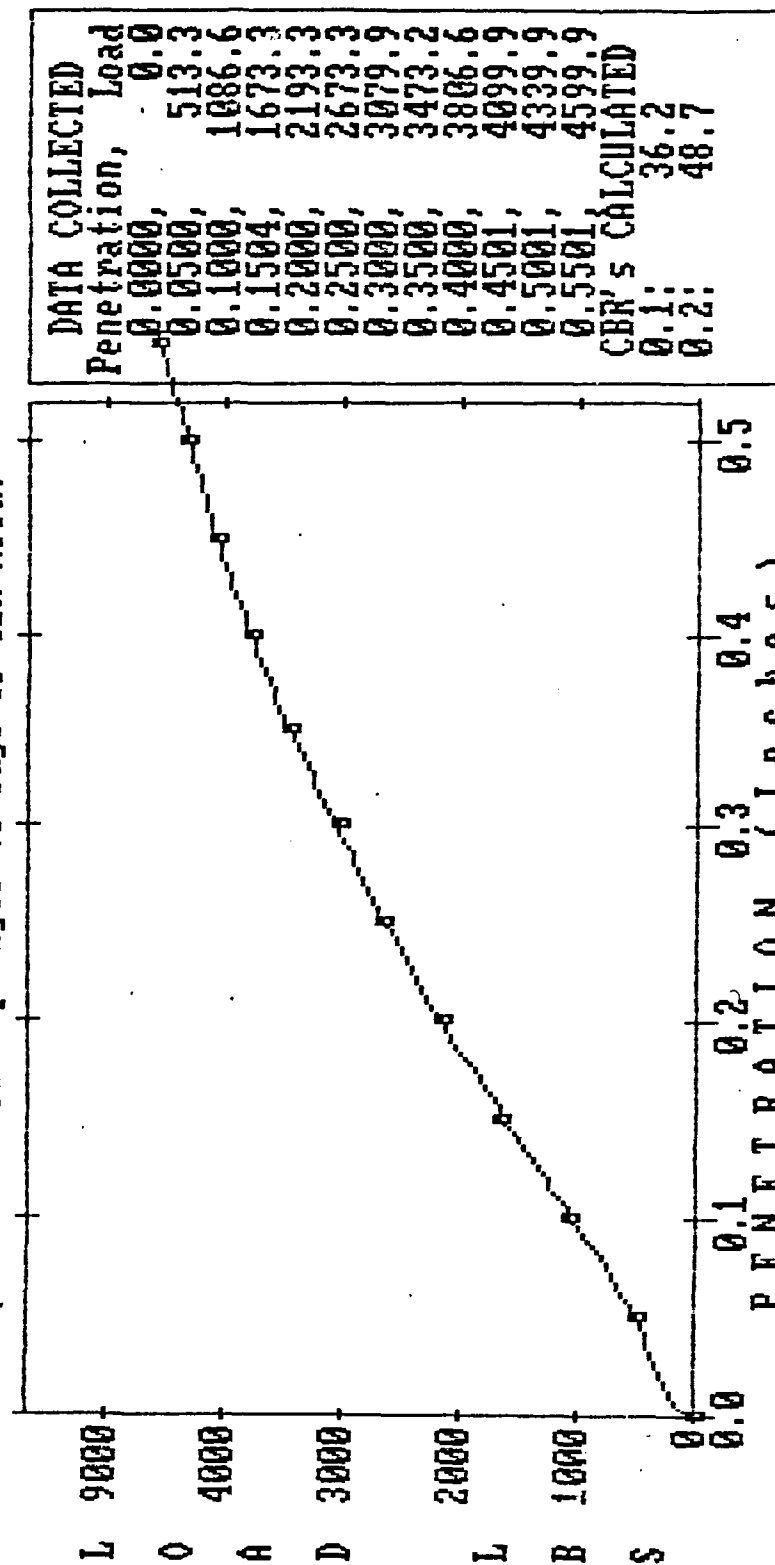
The accuracy of the test results depends on the careful calibration of the data acquisition system components. Electronic measuring devices must be calibrated at their excitation voltage after which their linear working range is determined. Careful positioning of the LVDT's core is required so that the expected specimen and proving ring deformation occur within the linear range throughout the test. Load cells could replace the LVDT-proving ring combination to measure force but since the main advantages of the LVDTs are their self-contained design and their need for a single calibration constant, usually given in lb/Volt, this replacement is unnecessary.

FIGURE 3.18(1) GENERIC EPOXY #7
 Additive Ratio= 4.0%, Moisture= 13.0%, Clay Silt Ratio=0.6, Temperature= 40.0F
 Half quadrant of sample experienced 3/4 inch heave failure
 Microcrack cylindrical failure in sample



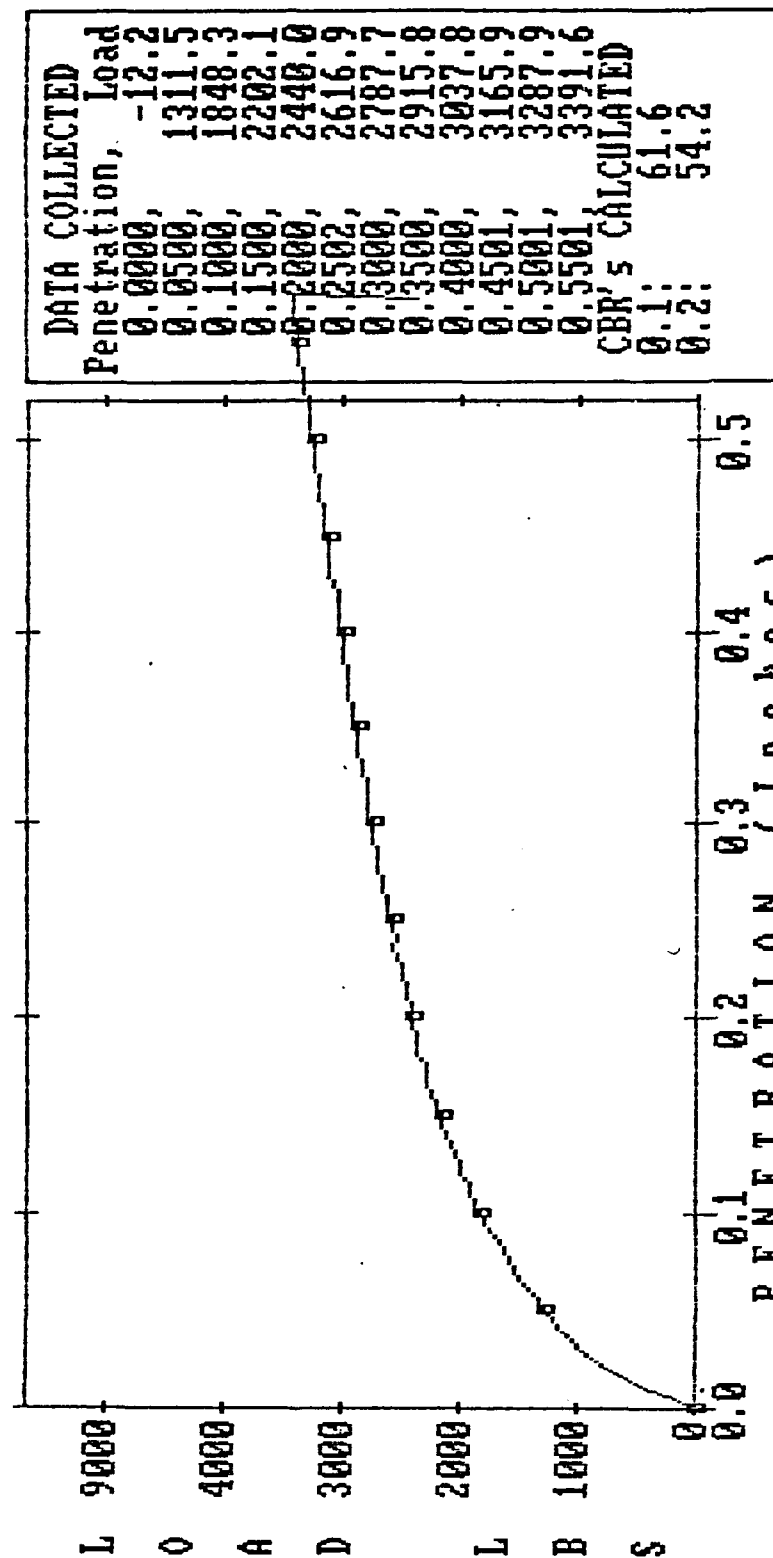
View Menu: F)first, L)ast, N)ext, P)revious, G)oto, E)dit, D)delete, Q)uit?

FIGURE 3.18(2) Generic Epoxy #10
 Additive Ratio= 4.0%, Moisture= 21.0%, Clay Silt Ratio=0.4, Temperature= 40.0F
 No visible crack. Sample surface glossy. Elastic deformation
 from plunger to edge of CBR mold.



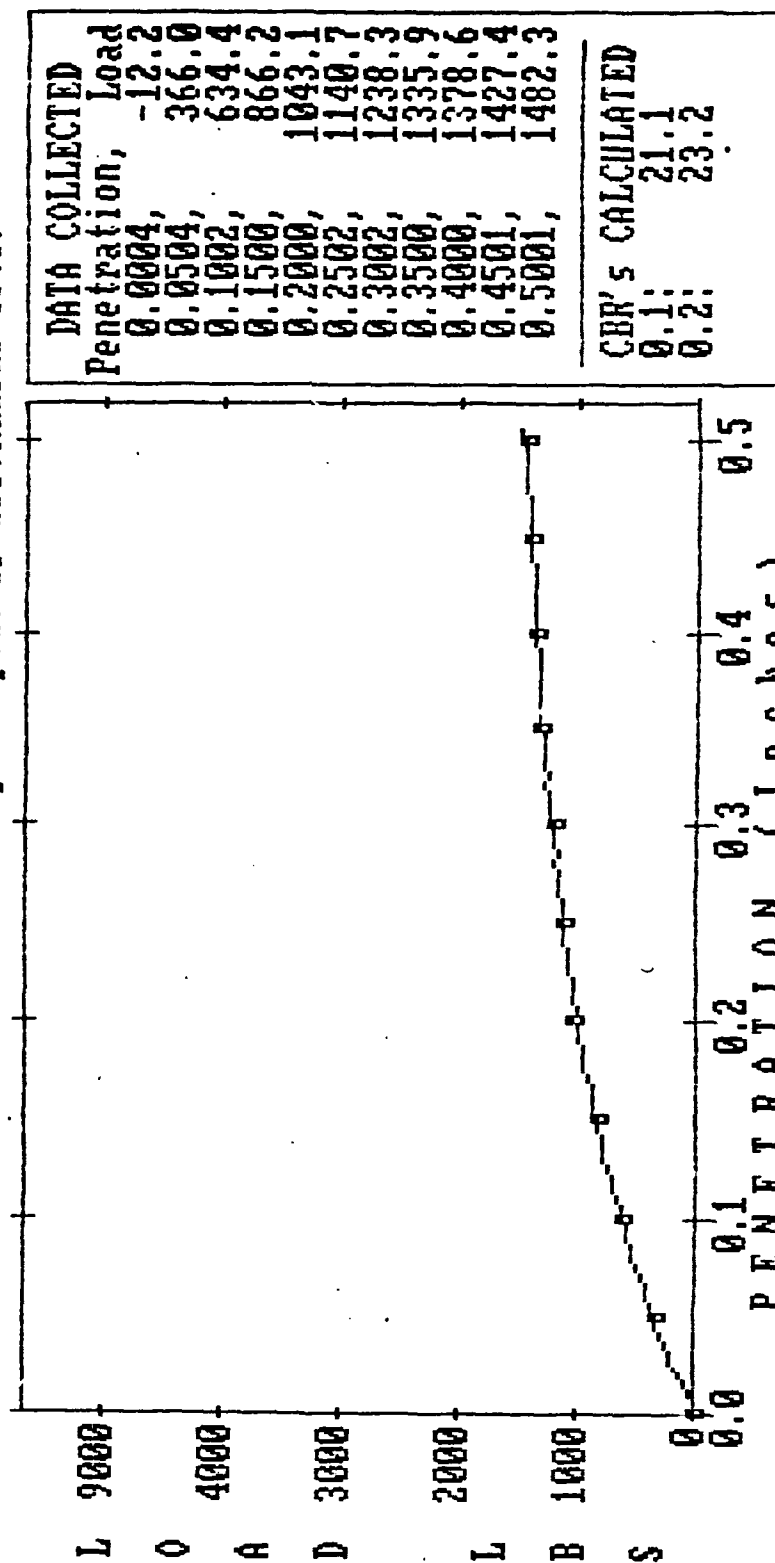
View Menu: F)First, L)ast, N)ext, P)revious, G)oto, E)dit, D)etele, Q)uit?

FIGURE 3.18(3) Generic Epoxy #16
 Additive Ratio= 1.0%, Moisture= 13.0%, Clay Silt Ratio=0.5, Temperature= 40.0F
 Cylindrical cracks near circumference of mold. Repeat of #15



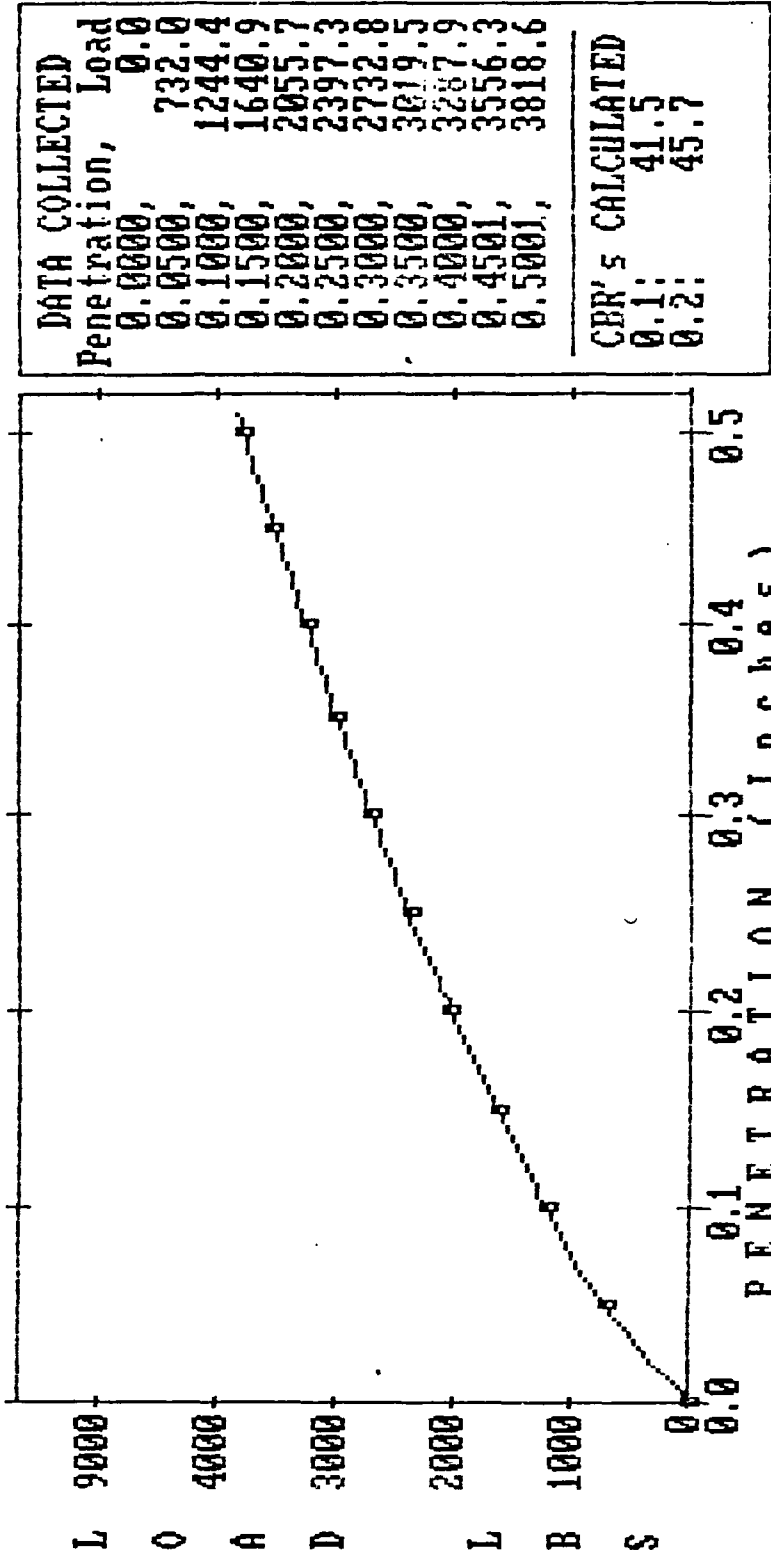
View Menu: F)First, L)ast, N)ext, P)revious, G)oto, E)dit, D)delete, Q)uit?

FIGURE 3.18(4) Generic Epoxy #69
 Additive Ratio= 0.3%, Moisture= 17.0%, Clay Silt Ratio=0.5, Temperature= 90.0F
 Complete heave failure. Top of sample tested at 11.45pm on
 1/19/87. Made 1/16/87 at 2.45pm. Repeat of #68. Radial cr(5)



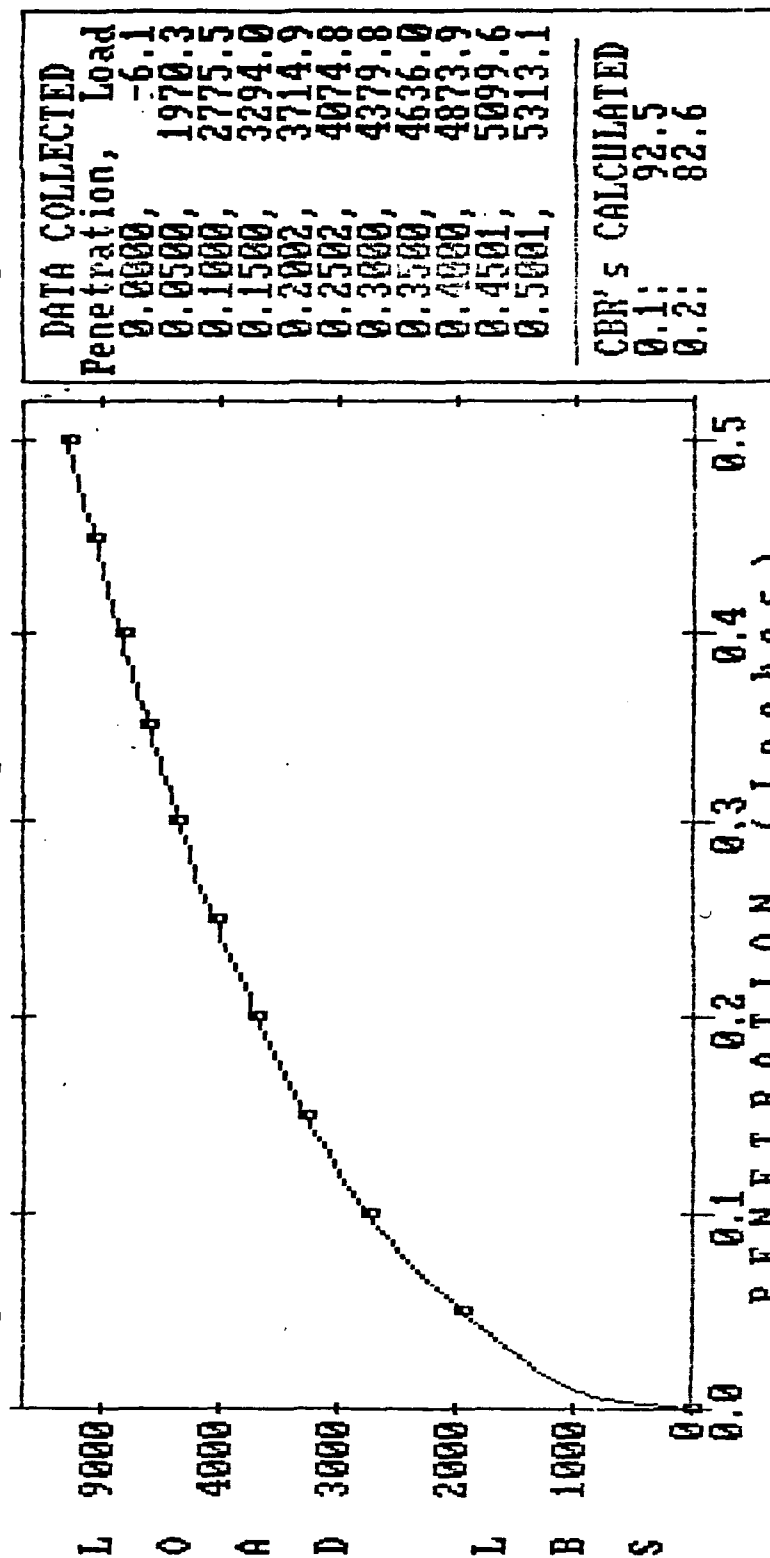
View Menu: F)irst, L)ast, N)ext, P)revious, G)oto, E)dit, D)delete, Q)uit?

FIGURE 3.18(5) Generic Epoxy #70
 Additive Ratio= 4.0%, Moisture= 17.0%, Clay Silt Ratio=0.4, Temperature= 90.0F
 Cylindrical microcracks. Top of sample tested on 1/20/87.
 Sample made on 1/17/87 at 11.30am. Tested at 11.20am



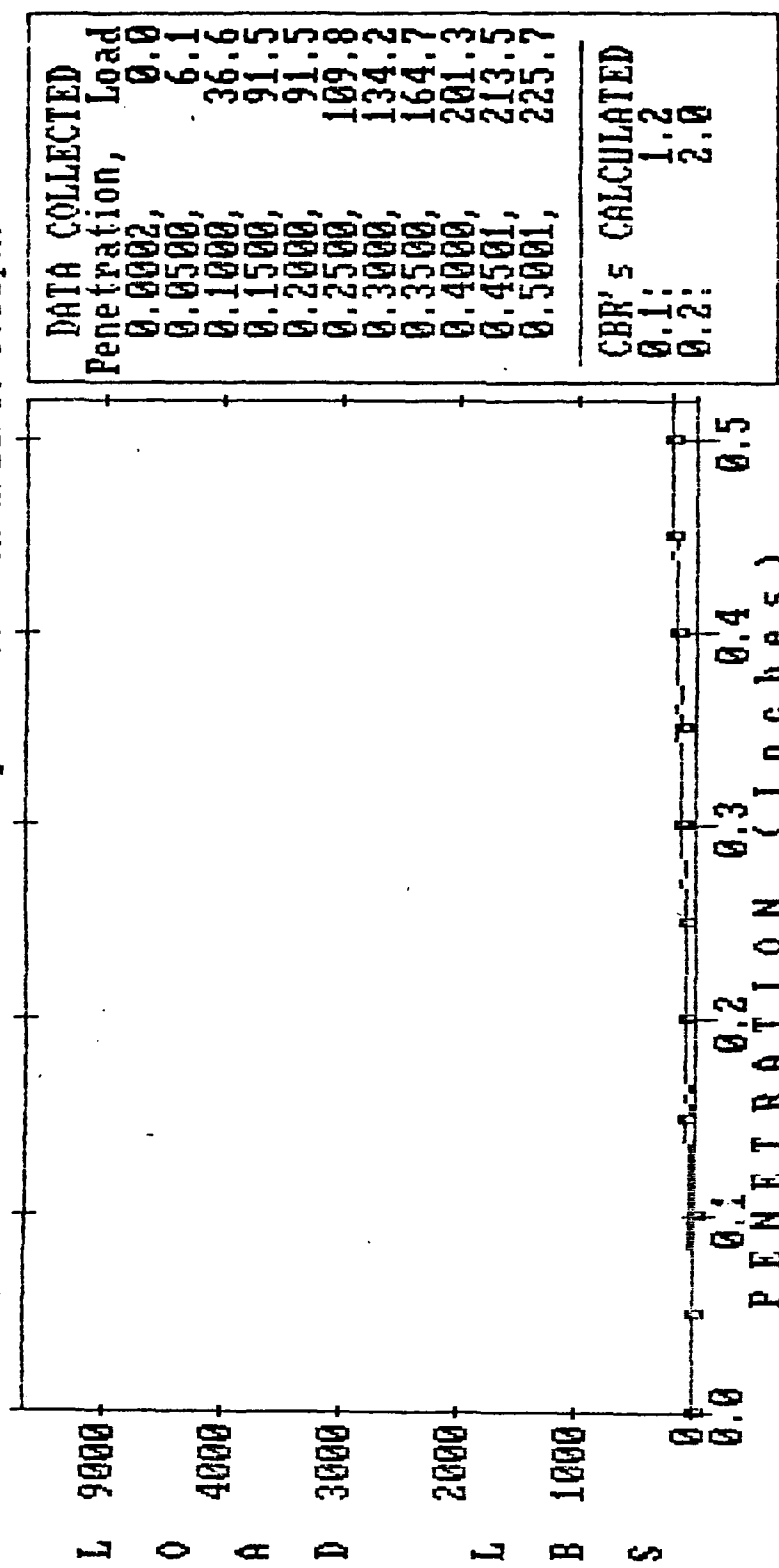
View Menu: F)First, L)ast, N)ext, P)revious, G)oto, E)dit, D)elete, Q)uit?

FIGURE 3.18(6) Generic Epoxy #72
 Additive Ratio= 4.0%, Moisture= 17.0%, Clay Silt Ratio=0.6, Temperature= 90.0F
 Cylindrical cracks near mold surface. Top tested.
 Sample made on 1/17/87 at 12.55pm. Tested on 1/20/87 2.25pm.



View Menu: F)First, L)ast, N)ext, P)revious, G)oto, E)dit, D)delete, Q)uit?

FIGURE 3.18(7) Generic Epoxy #73
 Additive Ratio= 0.0%, Moisture= 17.0%, Clay Silt Ratio=0.4, Temperature= 90.0F
 Short disjointed cylindrical cracks. Top tested-soft.
 Sample made on 1/17/87 at 1.15pm. Tested on 1/20/87 3.00pm.



View Menu: F)first, L)ast, N)ext, P)revious, G)oto, E)dit, D)delete, Q)uit?

MATERIAL SELECTION

4.1 AGGREGATE SELECTION - SOIL CLASSIFICATION

Minimum requirements have evolved over the years for the classification of soil samples. Such requirements include the identification of the potential uses to which the soil will be subjected, the molding strength of the soil in either the insitu or disturbed condition, its plasticity, sensitivity, consistency, soil structure, alkalinity, grain size, and plant growth supporting ability.

For engineering purposes, however, soil classification efforts include a qualitative visual description of the relative compactness, relative moisture, color consistency, as well as pertinent geological descriptors. Such descriptive information as previously provided are very useful preliminary classification criteria which are followed by more quantitative standard soil classification tests such as the Atterberg limits tests, plasticity tests, sieve analysis tests, and natural moisture content tests.

Systems of soil classification depend to a considerable extent upon the distribution of various-sized particles in a soil. The nature, composition and distribution of soil particles vary widely but are determinable through standard tests. Course-grained particle size distribution can be ascertained through sieve analysis, while for finer particles such as clay and silt, sieve analysis in conjunction with a method of measuring the rate of settlement in a dispersing medium is typically used. For this study the particle size distribution test result for the fine

particle was provided by the silt test sample suppliers (Figure 4.1).

4.1.1 Clay-Silt Soil Classification

The theory of fine analysis is usually based on Stoke's law of particle settlement in a dispersing medium such as water, i.e., small approximately spherical particles in a liquid settle at different rates according to the size of the spheres whose diameters are approximated by an effective diameter defined as the diameter of an imaginary sphere of the same material which would sink in water with the same velocity as the irregular particle in question.

The typical method used is either the pipette method or the hydrometer method. The tests are performed by first pre-treating the fine soil to remove organic matter, then applying a dispersing agent to prevent flocculation. The coarse particles are then removed by washing through a sieve of size $63\mu\text{m}$ and the pipette or hydrometer test is then performed to determine the effective diameter and the percent of particles less than the specified diameter. Generally silt particles range in size from $2 - 6\mu\text{m}$ for fine silt, $6 - 20\mu\text{m}$ for medium silt and $20-60\mu\text{m}$ for coarse silt fractions. Clay particles have sizes typically less than $2\mu\text{m}$.

4.1.1.1 Unified Soil Classification Specification

Using the Corps of Engineers unified soil classification system Technical Memorandum 3-357, the clay-silt system was of the CL soil classification extraction for the clay-silt sample

U.S. STANDARD SIEVE OPENING IN INCHES

U.S. STANDARD SIEVE NUMBER

PER CENT FINER BY WEIGHT

GRAIN SIZE IN MILLIMETERS

GRAIN SIZE IN MILLIMETERS	PER CENT FINER BY WEIGHT
0.075	100
0.15	100
0.3	100
0.6	100
1.2	100
2.5	100
5.0	100
10.0	100
20.0	100
40.0	100
60.0	100
80.0	100
100.0	100
150.0	100
200.0	0

with ratio 0.5 and 0.6 and the ML soil classification extraction for the 0.4 clay-silt ratio sample.

Soils of the ML and CS characteristics are generally susceptible to frost action, have medium compressibility and expansion with fair to poor or sometimes impervious drainage characteristics. The typical soaked CBR values they encounter are 5-10 at optimum moisture content, and dry density ranges from 100-125 pcf. They are generally unsuitable as a base under a wearing surface.

4.1.1.2 AASHTO Soil Classification Specification

From the AASHTO soil classification scheme, the selected soil types ranged from A-7 for the clay sample tested to A-4 for the silt sample. The clay-silt system ranged from A-5 through A-7 suggesting a silty-clayey soil with a fair to poor subgrade rating (Figure 2.1).

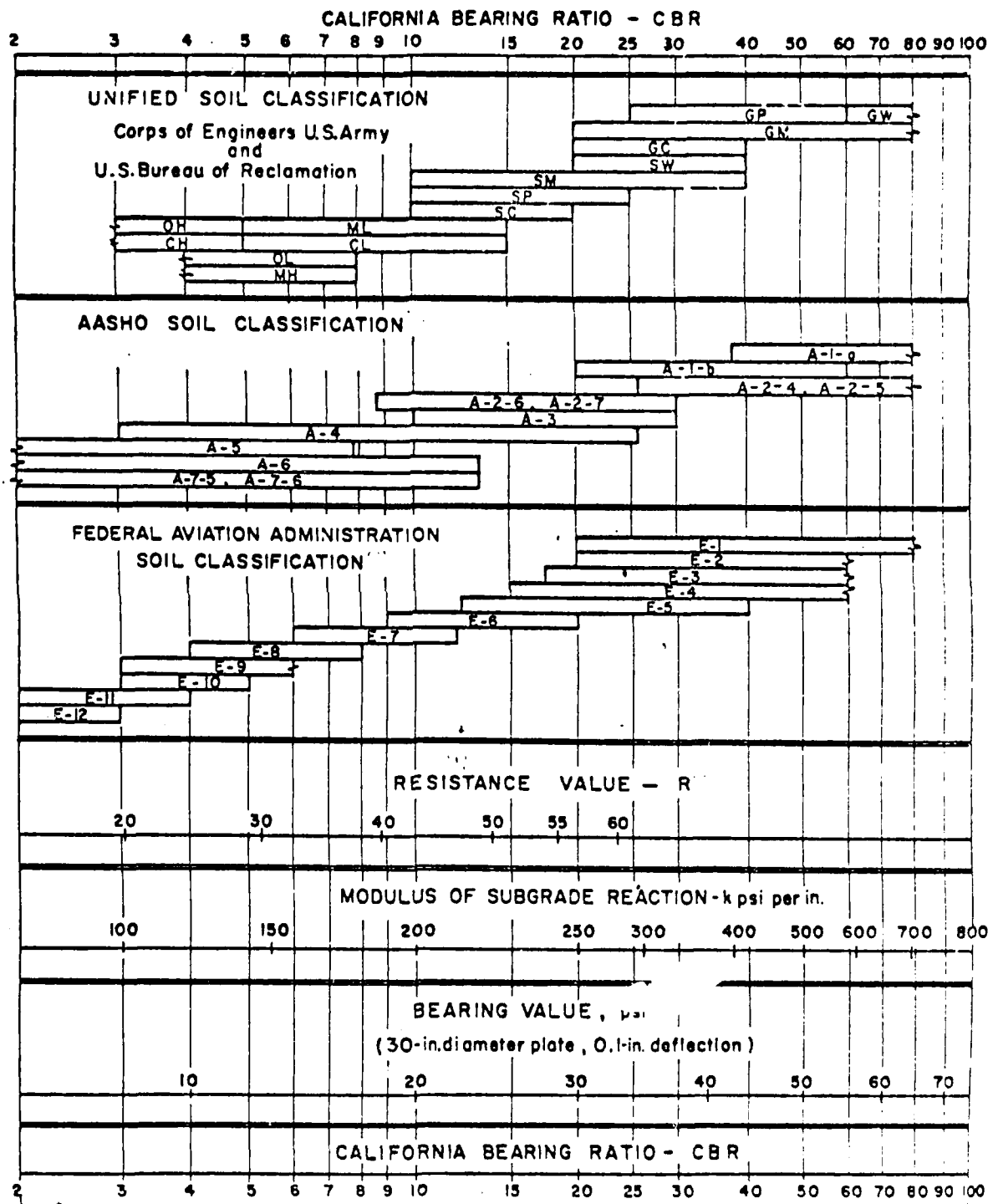
4.1.2 Summary of Physical Properties of Soil

The physical properties of the clay and silt samples are shown in Table 4.1 below. Corresponding to the various soil classification scheme for soil analysis, the typical California Bearing Ratio values obtained in practice are shown in Figure 4.2. For example, using the current Federal Aviation Administration (FAA) soil classification system which is based on ASTM D 2487, commonly known as the "Unified Soil Classification System," for the clay-silt system used in this research, the E-7 classification commands an expected CBR between 6 and 12 in the unstabilized state.

TABLE 4.1: Physical Properties of Clay & Silt

<u>Properties</u>	<u>Clay</u>	<u>SOIL TYPES</u>	
		<u>Silt</u>	<u>Clay-Silt Systems</u>
1. Liquid limit, %	60	22	37 - 45
2. Plastic limit, %	32	19	24 - 27
3. Plasticity index, %	28	3	13 - 18
4. Optimum moisture content, %	-	-	13 - 21
5. Absorbed moisture, %	1.5	0.5	1.0
6. Soil classification:			
a) Unified system	CL	ML	CL/ML
b) AASHO	A-7	A-4	A-5 to A-7
7. Specific gravity	2.63	1.84	2.33
8. Percent passing No. 200 sieve	100%	55%	73 - 82
9. pH, dry clay at 20% solids, airfloated	3.5-5.0	--	--
10. Clay fraction	1.0	0.0	0.4 to 0.6

FIGURE 4.2 APPROXIMATE INTERRELATIONSHIPS OF SOIL CLASSIFICATIONS AND BEARING VALUES^a



^aCourtesy of Thompson M.R., Journal of Materials vol 4, no 4 (ASTM) 1969

4.2 ADDITIVE SELECTION

4.2.1 General Overview

In considering possible materials for the stabilization of the clay-silt system being studied, the applicability of conventional methods was examined bearing in mind the economic ramifications, i.e. the need to use locally available material that exists in large quantities procurable at inexpensive costs. Also considered was the real possibility of merely increasing compaction requirements.

Conventional methods considered include, (1) The use of cementing agents such as Portland cement, lime, fly ash, or lime/fly ash combination to improve soil strength through hydration. According to Yoder, et. al. (14) the quantity of cement needed may be up to 20% by weight for lean clays. This method is not advisable for soils with organic components. (2) Improvement of soil plasticity by modification of clay minerals using lime modifiers. Use of up to 4% of such modifiers on silt-clay systems is not guaranteed to yield appreciable increase in soil strength. (3) Use of water retaining agents such as Calcium or Sodium Chloride that lowers the freezing point and possesses deliquescent properties. Application of up to 1 1/2% of these materials to clay-silt systems leads to little or no strength gain except the slight alteration of mechanical properties. (4) Use of organic cationic compounds such as emulsions to clay-silt systems results in little strength gain and construction difficulties. The advantage seems to lie in the alteration of the clay minerals to act as a hydrophobic agent; however, mixing small quantities may be difficult.

Most of the above materials will not impart sufficient strength to the clay-silt system under study to meet FAA requirements because of the poor clay-silt system particle size distribution and accompanying loss of frictional strength component, coupled with the degradation of cohesive strength that could quickly result with the infiltration of moisture. The results of CBR test on the untreated (control) clay-silt system support the position that little reliance should be placed solely on the effect of compaction and plasticity enhancement as a means of soil stabilization of clay-silt systems. The combined effect of additive application, effective construction practices, provision of adequate roadway drainage and ditches, in addition to good compaction and plasticity enhancement techniques, are equally vital.

The search for effective additives that could adequately meet flexible pavement design requirements for low-duty airport pavements was focussed on organic materials and polymers. A move to screen candidate materials was effected through survey of chemical companies, materials testing laboratories, in-house (CSU) materials testing, and personal contact.

4.2.2 SCREENED ADDITIVE MATERIALS:

4.2.2.1 HIGH DENSITY POLYETHYLENE

High density polyethylene was considered as a stabilizing agent. It exists in solid pellet form and possesses excellent molding qualities. It is several times as expensive as cement at \$0.35 per pound. The molding temperature of 300°F it requires makes it unattractive as a stabilizing agent. The fumes that are

given off at its glass transition temperature further affect its rating.

4.2.2.2 POLYSTYRENE

Polystyrene as a polymerized hydrocarbon in its unfilled or fibre filled state (30/35%) exists in a solid pellet form and has good molding qualities. It is about 10 times as expensive as lime/cement and possesses high compressive strength of 10-20 ksi. It is physically stable and has a melting temperature of 360-440°F implying higher than average construction requirements. At the construction temperatures required for mixing with silt-clay, the fumes it gives off would precipitate adverse environmental impacts. It burns on the application of temperature but slowly changes color slightly in the presence of sunlight, is not affected by weak acids, is attacked by oxidizing acids and is not affected by strong or weak alkalies. It is soluble in aromatic and chlorinated hydrocarbons, a strong negative factor to be considered in its candidacy as a stabilizing agent.

4.2.2.3 UREA FORMALDEHYDE

Urea formaldehyde as a thermoplastic was considered because of its good corrosion resistance and excellent molding properties. Its heat distortion temperature of 270-280°F could lead to higher than average construction difficulties inspite of its good tensile and compressive strength.

4.2.2.4 POLYPROPYLENE

Polypropylene, a polymer used as a Geo-Textile material, exists in the solid pellet form. It was considered unsuitable as a stabilizing agent for clay-silt systems in view of its high melting temperature of 335°F. Although it is physically stable,

it has adverse environmental impacts at its high melting temperatures.

4.2.2.5 POLYVINYL CHLORIDE

Polyvinyl Chloride exists as a polymer in either a solid or powdery form. In its solid form, it has compressive strength of 12,000 psi and costs between \$0.35 to \$0.60 per pound. It was considered unsuitable as a stabilizing agent because of its chemical instability--at high temperatures it decomposes and gives off hydrochloric acid, a highly toxic gas.

4.2.2.6 PHENOLIC RESIN

Phenolic resin of the type used in foundry castings was considered as a clay-silt stabilizer. This additive has been used successfully to impart high compressive strength (7,000-8,000 psi) and impact resistance to clean fine sand. As a polymer existing in liquid form, it is used effectively as a three component system for foundry purposes. It has very high resistance to temperature but darkens in the presence of sunlight, it is attacked by strong acids and alkalies and is relatively unaffected by organic solvents. Its hydrophobic characteristics and cost of \$1.80 per pound limit its use as a stabilizing agent.

4.2.2.7 POLYURETHANE

Polyurethane has compressive strength that varies (55-1000 psi) with density. Formed as a multi-component system (resin and catalyst with fillers) it is liquid in physical appearance and has poor physical stability under heat and sunlight. At a cost of \$0.90 per pound, and due to substandard stability, this polymer was not tested.

4.2.2.8 POLYESTER RESIN

Polyester resin of the thixotropic laminating resin type exists in the liquid form and in the cast form has high resistance to temperature, sunlight, and strong acids and alkalies. It attains high compressive strengths of up to 10,500 psi. Organic solvents especially ketones and chlorinated solvents attack the resin. Costs range from \$0.65 - \$1.71 per pound of resin and it has a few adverse chemical effects upon the application of temperature. Therefore, this additive was tested based on its thixotropic behavior and other desirable properties.

4.2.3 TESTED PILOT ADDITIVE MATERIALS

Most of the screened materials described above were not tested considering such factors as material costs, chemical stability, resistance to attacks by acids and alkalies, and their adverse effects at elevated temperatures.

The pilot additive materials selected for this study were chosen based on information in the literature documenting their use in other soil stabilization efforts and also based on their perceived potential as clay/silt stabilization agents. To test their effectiveness, unconfined compression tests were executed.

Typical unconfined compressive strength values obtained for untreated silty-clay ranged from 30 - 150 psi depending on the relative properties of the clay-silt mixture and the associated amount of organic matter.

Table 4.2 shows the summary experimental result of the unconfined compressive strength tests obtained for a subset of the selected additives at various levels of additive and

TABLE 4.2
UNCONFINED COMPRESSIVE STRENGTH OF STABILIZED CLAY-SILT SAMPLES

<u>Additive</u>	<u>Unconfined Compressive</u>
<u>Material</u>	<u>Strength Range</u>
	<u>(psi)</u>
1. Control (untreated soil)	32
2. Polystyrene	56
3. Saturated starch	102
4. Latex	20-135
5. Starch Polymer	62
6. Syloid	10-168
7. Fly ash	7-304
8. Fly ash/Acrylic latex	109
9. Gelatin and Alumina	63
10. Magnesium Chloride	28-109

Table 4.3

SOIL TEST DATA FOR UNCONFINED COMPRESSION TESTS

<u>Additive</u>	<u>%Add</u>	<u>% H₂O</u>	<u>Max Load (LBF)</u>	<u>Stress (PSI)</u>	<u>(In/In X 100) %Elongation</u>
Flyash	5%	10%	75.00	36.78	3.94
Flyash/Acrylic					
Latex	10%/10%	10%	221.10	108.45	4.50
Flyash	5%	6%	621.00	304.56	4.00
Flyash	5%	6%	279.00	136.83	4.27
Flyash	5%	10%	85.00	41.69	4.35
Flyash	5%	14%	18.30	8.98	8.05
Flyash	5%	14%	15.02	7.36	8.759
Flyash	20%	6%	224.00	109.86	4.023
Flyash	20%	6%	193.00	96.13	3.47
Flyash	20%	10%	115.00	56.40	3.45
Flyash	20%	10%	30.04	14.73	1.827
Flyash	20%	10%	191.00	93.67	4.949
Flyash	20%	14%	47.40	23.24	3.80
Flyash	20%	14%	20.18	9.90	3.964
Flyash	20%	14%	30.98	15.19	6.313
Syloid	5%	6%	157.00	77.00	2.36
Syloid	5%	22%	71.00	34.82	4.87
Syloid	5%	18%	-		
Syloid	5%	12%	342.00	167.73	3.03
Syloid	20%	10%	64.00	31.49	3.27
Syloid	20%	6%	20.65	10.13	2.86
Syloid	18.1%	29.2%	111.26	54.57	4.14
M.Chloride	1.4/1.4	9.1	56.00	27.46	7.901
Latex					
M.Chloride	1.4/1.4	9.1	221.12	108.45	4.65
Latex	10%	6%	251.64	123.41	5.54
Latex	10%	6%	277.00	135.85	7.472
Latex	10%	10%	58.00	28.45	17.65
Latex	10%	10%	41.30	20.25	10.65
Latex	10%	14%			
Latex	20%	6%	119.50	56.17	10.49
Latex	20%	10%	32.85	16.11	12.18
Gelatin & Alumina	10%	10%	129.00	63.27	2.30
Starch (Sat'd)	10.5%	10%	207.00	101.52	4.162
Polystyrene	5%	10%	113.00	55.92	3.287
Starch Polymer	5%	10%	127.00	62.29	9.853
(None)	0%	10%	65.00	31.88	5.844

moisture concentrations. The results are shown in Table 4.3

The results of these limited preliminary unconfined compression tests showed that some increases in compressive strength values were secured, though some of these increases were not sufficient to warrant the use of some of the materials as effective stabilizers of a poorly graded clay-silt soil system.

A switch to the CBR testing procedure was made after these preliminary tests since this test is generally regarded as the most reliable laboratory test for predicting subgrade performance in commercial construction industries as well as by the FAA.

4.2.4 TESTED PRELIMINARY ADDITIVE MATERIALS

The following additives were tested as candidate materials for the clay-silt soil stabilization research effort based on additional information gathered:

- Natural Latex
- H-Span
- Polymer Starch
- Sodium Silicate
- Epoxy Resin (and Five Star Epoxy Resin)
- Polyester Resin
- Phosphoric Acid
- Latex

LATEX:

Low-ammonia natural latex (Hartex 102) was identified for testing on the basis of preliminary unconfined compression tests conducted. Such factors as cost and availability weighed in the decision process. Hartex 102 is a uniform, high quality, centrifuged, natural latex to which has been added Sodium Pentachlorophenate (0.22%) and a low concentration of ammonia to greatly extend the storage life. The low-ammonia content makes it possible to use this latex without a de-ammoniation step. The natural latex consists of 62% solids, predominantly rubber (60%). The water content is 38% (approx.).

The optimum moisture content for the latex specimens was between 22% and 28%. At 28% moisture content and a clay-silt ratio of 0.5 the specimen was plastic and difficult to handle, at a temperature of 75°F and across all clay-silt ratios, the CBR value was zero.

TABLE 4.4
STABILIZATION EFFECTIVENESS OF LATEX AT OPTIMUM MOISTURE
CONTENT

<u>Clay-Silt</u>	<u>Percent</u>	<u>Optimum</u>	<u>Unsoaked</u>
<u>Ratio</u>	<u>Additive</u>	<u>Moisture Content</u>	<u>CBR</u>
0.4	5%	19%	0.0
0.5	10%	27%	0.0
0.6	15%	25%	0.0

The above results established the unsuitability of LATEX as a soil-stabilization agent.

H-SPAN:

H-SPAN (STA-WET) - Hydrolized starch poly acrylo-nitryl, supposed to be the most absorbent material known, is claimed to absorb 200 - 300 times its weight of water. It finds application in agricultural research and in numerous other areas where the presence of water is undesirable.

It was conjectured that the reduction of moisture in the clay-silt system using H-SPAN could lead to the development of enhanced compressive strength and corresponding resistance to deformation.

The test results obtained so far have not confirmed this hypothesis, rather the opposite effect was obtained. The CBR values obtained at various optimum moisture contents are shown:

TABLE 4.5
STABILIZATION EFFECTIVENESS OF H-SPAN AT OPTIMUM MOISTURE CONTENT

<u>Clay-Silt</u>	<u>Percent</u>	<u>Optimum</u>	<u>Unsoaked</u>
<u>Ratio (R)</u>	<u>Additive (%)</u>	<u>Moisture</u>	<u>CBR</u>
		<u>Content (%)</u>	
0.4	5%	22%	1
0.5	10%	28%	0
0.6	15%	26%	0

For a given quantity of H-SPAN added to the clay-silt soil, the progressive addition of water resulted in a color change and an increasingly sticky and bouncy mass with decreasing resistance to deformation and progressively reduced workability.

To test the absorption characteristic of the soil treated with H-SPAN, a soaked sample was obtained. After an elapsed time of approximately 12 hours, the treated soil had expanded considerably out of the mold; taking on the appearance of a flocculated, spongy mass.

Further tests suggested that H-SPAN had the opposite characteristics to that desired in a soil-stabilization agent.

POLYMER STARCH

This material was tested on the basis of unconfined compression tests that yielded a value of 62.3 psi. Test on this material yielded results similar to the latex additive, in addition to a slightly offensive odor.

SODIUM SILICATE

This material has been successfully used in grouting operations for highway construction, and was considered because it is cheaply available at a cost of \$6/100 pounds.

Grade 40 Sodium Silicate (containing 38.3% solids) was mixed with water in equal proportions with 3% calcium chloride and 5% Ethyl Acetate as accelerators. A whitish corrosive precipitate resulted which cured several days slower than expected. The stipulated strength of 2000 - 6000 psi for the dilute straight gel as claimed was not realized.

4.2.5 FINAL TEST ADDITIVE SELECTION PROCESS:

4.2.5.1 Additional Investigations and Inquiries

The search for suitable additives involved additional review of various literature, telephone surveys, and personal contacts. Some of these efforts resulted in the procurement of small test samples from manufacturers. As a result of tests on these samples, new promising additives were identified.

4.2.5.2 New Additive Case Analysis

Further experimental work (Figure 4.3, Table 4.6) identified the two part Epoxy Resin as the most suitable material to be tested among the class of all candidate materials tested. The four additives (mainly polymers) isolated for further study are the two part Epoxy Resin, Polyester Resin, Five-Star Epoxy Resin, and Phosphoric Acid. Inorganic additives that have proven effectiveness and have been traditionally in use for soil-stabilization such as cement, lime-fly ash were specifically excluded from the research effort.

Due to the limited quantity of test sample sent by manufacturers, small scale pilot tests of the four additives were effected to monitor their clay-silt stabilization properties. These tests unavoidably had to be performed on substandard specimens (Figure 4.3); the intent of the experiments was to ascertain the relative performance of the four additives identified and to provide new directions for the research.

The derived values of the resistance to deformation of these materials, as measured by the standard CBR equipment were termed Pseudo-CBR's.

FIGURE 4.3 PILOT TEST SAMPLE (SUBSTANDARD) FOR ADDITIVE EFFECTIVENESS SCREENING



TABLE 4.6 COMPARISON OF ACTUAL & "PSEUDO-CBR" VALUES FOR TESTED CLAY-SILT SAMPLES

Material	Percent Additive	Percent Water	Clay/Silt Ratio	Temp of	Actual CBR	"Pseudo-CBR" Replicates			Strength Factor
						(1)	(2)	(3)	
EPOXY RESIN	10%	16%	0.4	65	44.6	28.7	26.0	32.1	1.54
	5%	12%	0.5	65	105.4	47.0	32.5	43.9	2.56
POLYESTER RESIN	20%	12%	0.5	65	187.3	139.1	159.4	127.3	1.32

A correlation of actual CBR values and the "Pseudo-CBR" values was effected for two of the additives. This was done by mixing enough samples and subjecting all the samples to identical three days curing conditions and final testing. The results of the experiment suggest that the standard mold CBR values are consistently higher than the Pseudo-CBR values on the sample by average factors ranging from 1.3 through 2.5 (Table 4.6).

Among the set of surviving candidate stabilization materials considered, the two part Epoxy Resin was selected because of (1) the higher strength factor it delivered compared to the other stabilizers tested (Table 4.6), (2) Epoxy Resin is relatively odorless compared to Polyester Resin.

4.2.6 EPOXY RESIN/HARDENER SPECIFICATION

The stabilization additive selected consisted of a two part Epoxy Resin system. The first part is a Bis-phenol A/Epichlorohydrin resin of the epoxy resin family. This resin which has negligible solubility in water is a very viscous liquid, very light yellow in color with a specific gravity of 1.17. Though a very stable material, in the presence of a strong mineral or acid, or a strong oxidizing agent, the epoxy resin can react vigorously to release considerable heat but hazardous polymerization will not occur. The heat release during the use of the resin in this research was very minimal and generally unnoticeable at the 1/4% - 4% threshold additive level. Preliminary pilot tests at higher concentrations of epoxy resin, say, 10% and above, released a noticeable amount of heat.

The second of the two part epoxy resin system, a curing

agent, is a viscuous water insoluble polyamide, tan in color, with a specific gravity of 0.97. In the presence of a strong oxidizing agent, it could react to form nitrogen oxides, carbon monoxide or release free polyamides which are deleterious to health.

Epoxy resin is an organic chemical group composed of polymerized molecules consisting of split oxygen molecules bonded with two carbon atoms already united in some way. Epoxy resin is an amorphous, natural organic substance which could be of plant origin or synthesized by, for example, the dehydrohalogenation of the chlorohydrin prepared by the reaction of epichlorohydrin with a suitable di- or polyhydroxyl substance or other active-hydrogen-containing molecule. Numerous types of epoxy resin are possible (over 20 types) and resin formulation to suit particular application is almost always necessary. For the achievement of high strength, the use of a hardener or setting or curing agent is always essential for cross linking between the epoxy resin and hardener molecule. The mix of epoxy resin and curing agent used in all the tests was 1:1 by weight.

Though epoxy resin hardens through exothermic reactions, the quantities needed for stabilization, generally 4% or less, would not generate heat and stress that could lead to cracks and other imperfections. The addition of clay and silt as fillers for the epoxy resin system act as heat sinks and the release of the generated heat can be controlled through choice of hardeners or variation of hardener concentration to control the length of time the hardening requires. Though epoxy resins can set in as short

as 20 minutes, they can be designed to set in 3 hours thereby easing and making flexible the time required for construction procedures preparatory to stabilization and subsequent construction equipment cleanup.

A very important strength delivery factor in epoxy resin application is the mixing quality. Thorough mixing of the two part system for a length of time until mixing resistance drops off noticeably is imperative for effective crosslinking and strength development.

4.2.7 EXPERIMENTAL CBR DATA COLLECTED:-

The results of CBR experimentation is shown in Tables 4.7 through 4.21. Table 4.7 contains all the CBR values associated with the full factorial design data matrix for the stabilized clay-silt system. Table 4.8 shows the CBR effectiveness of additive application over the control or zero additive application case.

The data in Tables 4.9 through 4.17 compose the data points represented in Table 4.7. The data obtained from the soaked CBR test is shown in Table 4.21.

The analysis of these data is detailed in Section 5.

4.2.8 EPOXY RESIN COST VS. EFFECTIVENESS TRADEOFF

The cost of Epoxy resin varies depending on the type and application. The Epoxy - Bisphenol A/Epichlorohydrin resin costs about \$1.60/lb and the polyamide hardener used for crosslinking with the epoxy costs about \$1.90/lb. These costs are much higher than those associated with traditionally used additives such as

TABLE 4.7
CBR Values for Stabilized Clay-Silt System
Full Factorial Experimental Design Data Matrix
Additive: Epoxy Resin
Cure Period: 3-Days

C/S = 0.4					C/S = 0.5					C/S = 0.6					T (°F)
SM	%A				%A				%A						
	0	.25	1	4	0	.25	1	4	0	.25	1	4			
13	(2) 61.2	(2) 55.8	(1) 71.0	(2) 86.2	(1) 68.3	(2) 50.15	(2) 62.9	(1) 84.2	(3) 37.7	(2) 44.9	(2) 48.8	(1) 89.6	40		
17	(1) 3.9	(1) 16.2	(1) 19.1	(1) 42.5	(2) 19.9	(1) 37.4	(2) 31.45	(1) 44.3	(2) 35.0	(1) 60.6	(2) 53.86	(1) 66.4			
21	(1) 0.8	(1) 4.2	(3) 14.5	(3) 47.0	(1) 1.5	(1) 8.2	(1) 9.3	(3) 23.2	(1) 3.9	(2) 11.3	(1) 18.6	(2) 25.0			
13	(1) 39.6	(1) 44.6	(1) 68.3	(1) 103.7	(1) 24.6	(1) 41.2	(1) 71.9	(1) 100.6	(1) 22.7	(1) 38.0	(1) 52.0	(1) 96.2	65		
17	(1) 4.4	(1) 10.0	(1) 24.8	(1) 47.0	(1) 21.7	(1) 36.0	(1) 42.6	(2) 60.5	(1) 34.2	(1) 55.7	(1) 62.0	(1) 93.4			
21	(1) 1.2	(1) 4.4	(1) 20.9	(1) 64.0	(1) 2.4	(1) 7.1	(1) 14.7	(1) 40.0	(1) 5.0	(1) 17.8	(1) 31.7	(1) 39.3			
13	(2) 82.0	(2) 89.5	(1) 45.6	(1) 135.4	(2) 67.2	(2) 52.3	(1) 86.4	(2) 134.2	(2) 26.9	(1) 33.9	(1) 51.3	(2) 115.9	90		
17	(2) 3.5	(2) 6.8	(1) 28.5	(1) 47.38	(2) 13.7	(2) 26.6	(2) 36.6	(1) 70.05	(1) 45.7	(1) 59.0	(1) 64.15	(1) 93.52			
21	(1) 0.7	(1) 9.5	(1) 27.2	(5) 87.1	(1) 1.4	(1) 14.1	(3) 20.0	(3) 48.7	(1) 6.1	(1) 6.7	(1) 44.7	(1) 33.8			

* Connnotes number of CBR values averaged to obtain indicated CBR

TABLE 4.8
CBR Additive Effectiveness Relative to Unstabilized Points
Clay-Silt Soil Stabilization Full Factorial Design Matrix
Additive: Epoxy Resin
Cure Period: 3-Day

C/S = 0.4					C/S = 0.5					C/S = 0.6					T (°F)
%M	%A				%A				%A						
	0	.25	1	4	0	.25	1	4	0	.25	1	4			
13	0	-5.4	9.8	25.0	0	-18.1	-5.4	15.9	0	7.2	11.1	51.9	40		
17	0	12.3	15.2	38.6	0	17.5	11.6	24.4	0	25.6	18.9	31.4			
21	0	3.4	13.7	4.2	0	6.7	7.8	21.3	0	7.4	14.7	21.1			
13	0	5.0	28.7	64.1	0	16.6	47.3	76.0	0	15.3	29.3	3.9	65		
17	0	5.6	20.4	42.6	0	14.2	20.9	38.8	0	21.5	27.8	59.2			
21	0	3.2	19.7	62.4	0	4.7	12.3	37.6	0	12.8	26.7	34.3			
13	0	27.5	-16.4	73.4	0	-14.9	19.2	67.0	0	7.0	24.4	89.0	90		
17	0	3.3	25.0	43.6	0	12.9	22.9	56.4	0	13.3	18.5	79.8			
21	0	8.6	26.5	86.4	0	12.7	18.6	37.3	0	6.7	38.6	27.7			

TABLE 4.9
CBR Values for Stabilized Clay-Silt System
Full Factorial Experimental Design Data Matrix
Additive: Epoxy Resin
Cure Period: 3-Days
Cure Temperature: 90°F

Experimental Run	Percent Additive (%)	Percent Moisture (%)	Clay/Silt Ratio	Temperature (°F)	Bulk Density (lb/ft ³)	Dry Density (lb/ft ³)	CBR
79	4	13	0.4	90	125.0	110.6	135.4(2)
80,93	4	13	0.5	90	121.5	107.5	134.2(4)
78,81	4	13	0.6	90	113.3	98.5	115.9(4)
83	1	13	0.4	90	108.4	95.9	45.6(2)
114	1	13	0.5	90	113.2	100.2	86.4(1)
92,109	1	13	0.6	90	104.9	92.8	51.3(4)
94,110	$\frac{1}{2}$	13	0.4	90	123.9	109.6	89.4(4)
95	$\frac{1}{2}$	13	0.5	90	111.2	98.4	52.3(2)
116	$\frac{1}{2}$	13	0.6	90	105.1	93.0	33.9(2)
101,102	0	13	0.4	90	125.9	111.4	82.0(4)
103,104	0	13	0.5	90	114.1	101.0	67.2(4)
82	0	13	0.6	90	98.1	86.8	26.9(2)

TABLE 4.10
CBR Values for Stabilized Clay-Silt System
Full Factorial Experimental Design Data Matrix

Additive: Epoxy Resin
Cure Period: 3-Days
Cure Temperature: 90°F

Experimental Run	Percent Additive (%)	Percent Moisture (%)	Clay/Silt Ratio	Temperature (°F)	Bulk Density (lb/ft ³)	Dry Density (lb/ft ³)	CBR
66	4	17	0.4	90	119.9	102.5	47.38(4)
71	4	17	0.5	90	125.2	107.0	70.05(2)
72	4	17	0.6	90	119.4	102.0	93.52(2)
60	1	17	0.4	90	127.4	108.9	28.5(2)
61, 62	1	17	0.5	90	127.8	109.2	36.6(4)
63	1	17	0.6	90	118.5	101.3	64.15(2)
64, 65	$\frac{1}{2}$	17	0.4	90	133.9	114.4	6.8(4)
68, 69	$\frac{1}{2}$	17	0.5	90	125.7	107.5	26.6(4)
67	$\frac{1}{2}$	17	0.6	90	116.4	99.5	59.0(2)
73, 74	0	17	0.4	90	132.2	113.0	3.5(2)
76, 77	0	17	0.5	90	131.9	112.8	13.7(4)
75	0	17	0.6	90	118.4	101.2	45.7(2)

TABLE 4.11
CBR Values for Stabilized Clay-Silt System
Full Factorial Experimental Design Data Matrix

Additive: Epoxy Resin
Cure Period: 3-Days
Cure Temperature: 90°F

Experimental Run	Percent Additive (%)	Percent Moisture (%)	Clay/Silt Ratio	Temperature (°F)	Bulk Density (lb/ft ³)	Dry Density (lb/ft ³)	CBR
84, 87, 105, 106, 111	4	21	0.4	90	116.6	96.4	87.1(7)
85, 112, 113	4	21	0.5	90	116.8	96.5	48.7(5)
86	4	21	0.6	90	113.4	93.7	33.8(2)
91	1	21	0.4	90	125.3	103.5	27.2(2)
90, 107, 108	1	21	0.5	90	124.2	102.7	20.0(4)
89	1	21	0.6	90	124.6	103.0	44.7(2)
97	$\frac{1}{2}$	21	0.4	90	128.1	105.9	9.5(2)
88	$\frac{1}{4}$	21	0.5	90	130.3	107.7	14.1(2)
117	$\frac{1}{4}$	21	0.6	90	126.2	104.3	6.7(2)
99	0	21	0.4	90	125.4	103.7	0.7(2)
100	0	21	0.5	90	127.4	105.3	1.4(2)
98	0	21	0.6	90	126.3	104.4	6.1(2)

TABLE 4.12

CBR Values for Stabilized Clay-Silt System
Full Factorial Experimental Design Data Matrix

Additive: Epoxy Resin

Cure Period: 3-Days

Cure Temperature: 65°F

Experimental Run	Percent Additive (%)	Percent Moisture (%)	Clay/Silt Ratio	Temperature (°F)	Bulk Density (lb/ft ³)	Dry Density (lb/ft ³)	CBR
123	4	13	0.4	65	124.0	109.7	103.7(1)
125	4	13	0.5	65	119.8	106.1	100.6(1)
124	4	13	0.6	65	111.9	99.0	96.2(1)
127	1	13	0.4	65	115.8	102.5	68.3(2)
128	1	13	0.5	65	112.2	99.3	71.9(1)
126	1	13	0.6	65	102.1	90.4	52.0(1)
135	$\frac{1}{2}$	13	0.4	65	114.4	101.2	44.6(1)
149	$\frac{1}{2}$	13	0.5	65	107.8	95.4	41.2(1)
137	$\frac{1}{2}$	13	0.6	65	104.2	92.2	38.0
136	0	13	0.4	65	125.4	111.0	39.6(2)
140	0	13	0.5	65	113.0	100.0	24.6(2)
141	0	13	0.6	65	104.4	92.3	22.7(2)

TABLE 4.13
CBR Values for Stabilized Clay-Silt System
Full Factorial Experimental Design Data Matrix

Additive: Epoxy Resin
Cure Period: 3-Days
Cure Temperature: 65°F

Experimental Run	Percent Additive (%)	Percent Moisture (%)	Clay/Silt Ratio	Temperature (°F)	Bulk Density (lb/ft ³)	Dry Density (lb/ft ³)	CBR
120	4	17	0.4	65	121.3	103.7	47.0(1)
118,119	4	17	0.5	65	123.8	105.8	60.5(4)
121	4	17	0.6	65	119.3	102	93.4(2)
122	1	17	0.4	65	128.6	109.9	24.8(2)
133	1	17	0.5	65	127.1	108.6	42.6(2)
130	1	17	0.6	65	117.8	100.7	62.0(2)
129	1	17	0.4	65	134.5	114.9	10.0(2)
132	1	17	0.5	65	125.2	107.0	36.0(1)
131	1	17	0.6	65	113.6	97.1	55.7(2)
139	0	17	0.4	65	132.7	113.4	4.4(2)
138	0	17	0.5	65	128.6	109.9	21.7(2)
134	0	17	0.6	65	119.2	101.8	34.2(2)

TABLE 4.14
CBR Values for Stabilized Clay-Silt System
Full Factorial Experimental Design Data Matrix
Additive: Epoxy Resin
Cure Period: 3-Days
Cure Temperature: 65°F

Experimental Run	Percent Additive (%)	Percent Moisture (%)	Clay/Silt Ratio	Temperature (°F)	Bulk Density (lb/ft ³)	Dry Density (lb/ft ³)	CBR
146	4	21	0.4	65	115.0	95.1	64.0
145	4	21	0.5	65	118.8	98.2	40.0
144	4	21	0.6	65	118.3	97.7	39.3(2)
153	1	21	0.4	65	122.9	101.5	20.9
154	1	21	0.5	65	123.9	102.4	14.7
152	1	21	0.6	65	124.7	103.1	31.7
147	$\frac{1}{2}$	21	0.4	65	126.8	104.8	4.4(1)
150	$\frac{1}{2}$	21	0.5	65	127.7	105.6	7.1(1)
148	$\frac{1}{2}$	21	0.6	65	124.8	103.1	17.8(2)
142	0	21	0.4	65	122	100.8	1.2(1)
143	0	21	0.5	65	127.6	105.4	2.4(1)
151	0	21	0.6	65	126.1	103.8	5.0(1)

TABLE 4.15
CBR Values for Stabilized Clay-Silt System
Full Factorial Experimental Design Data Matrix

Additive: Epoxy Resin
Cure Period: 3-Days
Cure Temperature: 40°F

Experimental Run	Percent Additive (%)	Percent Moisture (%)	Clay/Silt Ratio	Temperature (°F)	Bulk Density (lb/ft ³)	Dry Density (lb/ft ³)	CBR
1,2	4	13	0.4	40	126.9	112.3	86.2(4)
3	4	13	0.5	40	118.2	104.6	84.2(2)
7	4	13	0.6	40	113.9	100.8	89.6(2)
14	1	13	0.4	40	123.6	109.3	71.0(2)
15,16	1	13	0.5	40	111.2	98.4	62.9(4)
17,19	1	13	0.6	40	102.2	90.5	48.8(4)
39,44	$\frac{1}{4}$	13	0.4	40	113.1	100.1	55.8(4)
40,43	$\frac{1}{4}$	13	0.5	40	104.3	92.3	50.15(4)
41,51	$\frac{1}{4}$	13	0.6	40	103.3	91.4	44.9(4)
28,29	0	13	0.4	40	125.1	110.7	61.21
31	0	13	0.5	40	111.8	98.9	68.3
27,30,57	0	13	0.6	40	102.9	91.3	37.7

TABLE 4.16
CBR Values for Stabilized Clay-Silt System
Full Factorial Experimental Design Data Matrix
Additive: Epoxy Resin
Cure Period: 3-Days
Cure Temperature: 40°F

Experimental Run	Percent Additive (%)	Percent Moisture (%)	Clay/Silt Ratio	Temperature (°F)	Bulk Density (lb/ft ³)	Dry Density (lb/ft ³)	CBR
4	4	17	0.4	40	120.6	103.1	42.5
5	4	17	0.5	40	122.4	104.6	44.3
6	4	17	0.6	40	119.3	102.0	66.4
20	1	17	0.4	40	129.7	110.8	19.1
22,42	1	17	0.5	40	126.3	108.0	31.45
18,21	1	17	0.6	40	116.4	99.5	53.86
50	$\frac{1}{2}$	17	0.4	40	129.6	110.8	16.2
54	$\frac{1}{2}$	17	0.5	40	125.8	107.5	37.4
48	$\frac{1}{2}$	17	0.6	40	112.6	96.2	60.6
32	0	17	0.4	40	134.1	114.6	3.9
34,59	0	17	0.5	40	125.3	107.1	19.9
35,58	0	17	0.6	40	119.9	102.4	35.0

TABLE 4.17
CBR Values for Stabilized Clay-Silt System
Full Factorial Experimental Design Data Matrix
Additive: Epoxy Resin
Cure Period: 3-Days
Cure Temperature: 40°F

Experimental Run	Percent Additive (%)	Percent Moisture (%)	Clay/Silt Ratio	Temperature (°F)	Bulk Density (lb/ft ³)	Dry Density (lb/ft ³)	CBR
10, 11, 44	4	21	0.4	40	118.5	97.9	47.0
8, 12, 46	4	21	0.5	40	117.2	96.8	23.2
9, 13	4	21	0.6	40	117.9	97.4	25.0
23, 24, 47	1	21	0.4	40	123.1	102.0	14.5
25	1	21	0.5	40	122.1	100.9	9.3
26	1	21	0.6	40	124.8	103.1	18.6
49	$\frac{1}{2}$	21	0.4	40	125.4	103.6	4.2
56	$\frac{1}{2}$	21	0.5	40	125.9	104.1	8.2
33, 55	$\frac{1}{2}$	21	0.6	40	121.5	100.4	11.3(4)
36	0	21	0.4	40	125.5	103.7	0.8
38	0	21	0.5	40	126.0	104.1	1.5
37	0	21	0.6	40	125.9	103.2	3.9

TABLE 4.18
CBR Values for Unstabilized Clay-Silt System
Experimental Design Data Matrix

Additive: None
Cure Period: 1-Day
Cure Temperature: 90°F

Experimental Run	Percent Additive (%)	Percent Moisture (%)	Clay/Silt Ratio	Temperature (°F)	Bulk Density (lb/ft ³)	Dry Density (lb/ft ³)	CBR
9	0	12	0.4	90	119.9	107.1	62.8
11	0	14	0.4	90	120.1	105.4	42.2
12	0	16	0.4	90	113.3	96.0	3.4
13	0	20	0.4	90	129.5	108.0	1.3
5	0	12	0.5	90	103.1	92.1	52.0
6	0	16	0.5	90	119.9	103.4	42.2
7	0	20	0.5	90	130.0	108.4	2.8
8	0	24	0.5	90	123.7	99.8	1.0
1	0	14	0.6	90	107.8	94.0	46.6
10	0	16	0.6	90	110.2	95.0	48.7
2	0	20	0.6	90	126.3	105.3	12.2
3	0	22	0.6	90	124.6	102.2	3.8
4	0	24	0.6	90	123.2	99.4	1.7

TABLE 4.19
CBR Values for Unstabilized Clay-Silt System
Experimental Design Data Matrix

Additive: None
Cure Period: 1-Day
Cure Temperature: 65°F

Experimental Run	Percent Additive (%)	Percent Moisture (%)	Clay/Silt Ratio	Temperature (°F)	Bulk Density (lb/ft ³)	Dry Density (lb/ft ³)	CBR
5	0	12	0.4	65	115.8	103.4	58.8
13	0	14	0.4	65	124.8	109.5	33.1
10	0	16	0.4	65	133.9	115.4	6.1
15	0	20	0.4	65	131.8	109.8	4.1
2	0	12	0.5	65	111.6	99.6	55.7
9	0	16	0.5	65	124.0	106.9	39.5
11	0	20	0.5	65	128.9	107.4	4.1
14	0	24	0.5	65	124.3	100.2	3.4
1	0	16	0.6	65	109.9	94.7	34.0
4	0	20	0.6	65	128.7	107.3	12.5
12	0	22	0.6	65	127.5	104.5	3.1
7	0	24	0.6	65	123.4	99.5	1.7

TABLE 4.20
CBR Values for Unstabilized Clay-Silt System
Experimental Design Data Matrix

Additive: None
Cure Period: 1-Day
Cure Temperature: 40°F

Experimental Run	Percent Additive (%)	Percent Moisture (%)	Clay/Silt Ratio	Temperature (°F)	Bulk Density (lb/ft ³)	Dry Density (lb/ft ³)	CBR
10	0	12	0.4	40	116.0	103.6	67.9
11	0	14	0.4	40	130.9	114.8	28.4
12	0	16	0.4	40	130.2	112.2	4.8
13	0	20	0.4	40	128.8	107.3	1.1
6	0	12	0.5	40	109.8	98.0	57.4
7	0	16	0.5	40	125.2	107.9	42.6
8	0	20	0.5	40	127.2	106.0	2.1
9	0	24	0.5	40	127.3	102.7	2.4
1	0	14	0.6	40	106.5	93.4	60.8
2	0	16	0.6	40	116.2	100.2	59.0
3	0	20	0.6	40	130.4	108.7	9.5
4	0	22	0.6	40	130.3	106.8	4.8
5	0	24	0.6	40	122.6	98.9	1.4

TABLE 4.2]
Soaked CBR Values for Stabilized Clay-Silt System
Partial Experimental Data Matrix

Additive: Epoxy Resin
Water Temperature: 63°F

		C/S = 0.5					C/S = 0.6						
%M		%A					%A					Soak Duration	
		0	.25	1	4		0	.25	1	4			
13		---	---	---	---	---	---	1.8	---		4 Days		
17		---	---	---	50.6	---	---	0.9	---				
21		---	---	---	---	---	---	---	---				
13		---	---	4.3	69.7	---	---	---	27.2		5 Days		
17		---	---	5.9	---	---	---	---	67.6				
21		---	---	---	---	---	---	---	---				
13		---	---	2.9	37.2	---	---	1.8	26.3		7 Days		
17		---	---	6.8	43.2	---	---	1.8	59.3				
21		---	---	---	---	---	---	---	---				

cement. With the advent of high technology epoxy application techniques since the 1970's, the total cost advantages of using epoxy resins in engineering construction is beginning to compare favorably with such conventional materials as concrete when such costs as labor, materials and other indirect cost factors are considered.

The advantages of epoxy resin include: i) reduction in direct cost of repairs by substituting high technology application techniques for costly manual labor; ii) introduction of improved consistency and quality leading to savings in terms of reduced deterioration, because of the strength and durability of epoxy-treated materials; iii) accelerated strength attainment within a few hours due to the formation of a solid, dense material capable of withstanding inclement weather, heavy traffic and chemical attack. The strength of epoxies is borne out by the fact that broken chunks of concrete bonded together by epoxy resin become stronger than before disintegration; iv) reduction in indirect cost of repairs, such as delayed air traffic, can be very substantial in addition to the reduction in the frustration of aircraft and vehicular operators due to these unwelcome delays.

Through use of the very rapid setting properties of epoxy resins, runway closure resulting in delay and disruption of air traffic operations could be reduced from a time span of months to hours or minutes because of the significant engineering properties of epoxy resins.

Large scale epoxy resin based applications have gained considerable acceptance in the construction industry. In

Philadelphia, for example, use of over 10,000 gallons of epoxy resin was reported in the construction of the city's Schuylkill Expressway (Compressed Air Magazine, July & September 1986), as follows:

"The surface of the 1.3-mile-long expressway had become heavily worn and pitted. One way to have repaired it would have been to tear it out and replace it. However, to minimize disruption to traffic and still assure a long lasting repair, engineers chose to glue fresh wet concrete to a web of reinforcing bars placed over the old surface."

"After preparing the surface and placing the rebars, 53,000 square yards of roadway surface were coated, section by section, with more than 10,000 gallons of epoxy. As soon as each section was covered with epoxy, trucks dumped fresh concrete to a depth of 6 inches on top. The glue is designed to stick equally well to all concrete, fresh and wet or old and dry. The result was a sturdy, completely new roadway surface. The expressway was reopened far sooner and at a lower total cost than might have been expected of alternative methods."

MATHEMATICAL ANALYSIS

5.1 GENERAL DISCUSSION

The results of the $3 \times 3 \times 3 \times 4$ full factorial design ($3^3 \times 4$) experiment in temperature (TEMP), clay-silt ratio (CS), moisture percentage (PM) and additive percentage (PA) respectively, were subjected to descriptive and inferential statistical analysis. These analyses yielded estimates of the effects of the various independent variables on CBR the dependent variable.

There are several advantages to studying the effects of several independent variables on a dependent variable, say CBR, using factorial designs. First, and most significantly, it is possible to determine whether the experimental independent variables interact in their effect on the dependent variable. While an independent variable may capture a relatively small proportion of the variance of a dependent variable, its interactions with other independent variables may capture a large proportion of the variance, which cannot otherwise be captured by the study of the independent variables in isolation.

Second, factorial designs afford the researcher greater statistical control, and therefore more discriminatory statistical tests than those tests typically associated with single variables. The use of a single variable leads to a lumping of the variances not explained by the variable into the error term which results in a less sensitive model and statistical testing. Consequently, reduction of the magnitude of the error term is possible through the specification of several independent variables to increase the sources of systematic

variance of the dependent variable.

Factorial experiments allow the testing of the separate and combined effects of several variables using the same or lesser number of experimental runs as would have been the case for several single factor experiments. Another appeal of factorial designs is that the effect of a variable is studied across different conditions of other experiments, therefore generalizations from factorial experiments are broader than generalizations from single variable experiments.

5.2 REGRESSION MODEL FORM SPECIFICATION

The results of the $3^3 \times 4$ factorial design experiments for both the treatment (additive case) and the control (no treatment case) were subjected to regression analysis. These regression analyses were performed to determine the form of the statistical models suitable for predicting the CBR of a clay-silt system when stabilized at various levels of the independent variables.

The comprehensive second order multiple linear regression relation of the form below was used for some of the analyses:

$$y = \beta_0 + \sum_{i=1}^k \beta_i x_i + \sum_{i=1}^k \beta_{ii} x_i^2 + \sum_{i < j}^k \beta_{ij} x_i x_j \quad (5.1)$$

where:

y is the CBR value (the dependent variable)

$\beta_0, \beta_1, \beta_{11}, \dots$ are multiple regression coefficients
 x_1, x_2, \dots, x_k are independent variables
 $i, j = 1, 2, \dots, k$ - number of independent variables

The regression was performed through use of a stepwise multiple regression program contained within the Statistical Package for the Social Science (SPSS) library. The key feature of this program is that a number of intermediate regression models are obtained, adding one variable at a time. The variable added is that which makes the greatest improvement in the "goodness-of-fit." The significance level for staying in the model was set at 0.05 and for exiting 0.10.

5.3 REGRESSION ANALYSIS

The full factorial CBR data incorporating as design variables, moisture content, clay-silt ratio, temperature, all at four levels of additive, were analyzed. A graphical display of the CBR data is provided in Figures 5.1, 5.2, and 5.3. The figures all show a striking and similar CBR response of the clay-silt system to additive treatment at the three temperatures tested 40°F, 65°F, and 90°F. The CBR degrading influence of moisture in clay-silt soil system is generally emphasized by all the plots and particularly by the evenly split clay-silt mixture (C/S = 0.5).

Regression analysis enabled the quantification of the influences of the experimental independent variables and the identification of their levels of significance using all the full

FIGURE 5.1 CBR vs Moisture Content by Additive at 3 Levels of Clay-Silt Ratio

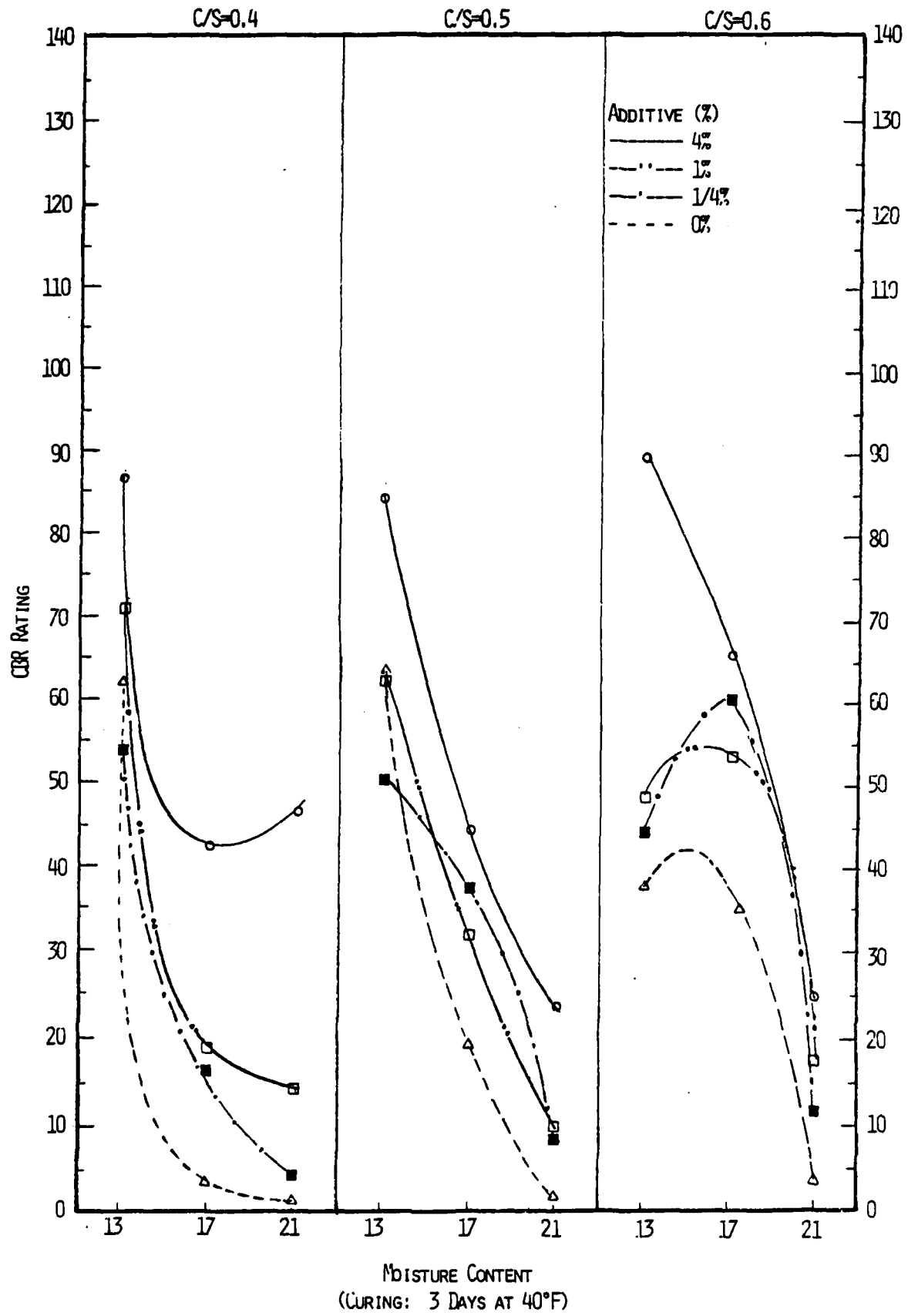


FIGURE 5.2 CBR vs Moisture Content by Additive at 3 Levels of Clay-Silt Ratio

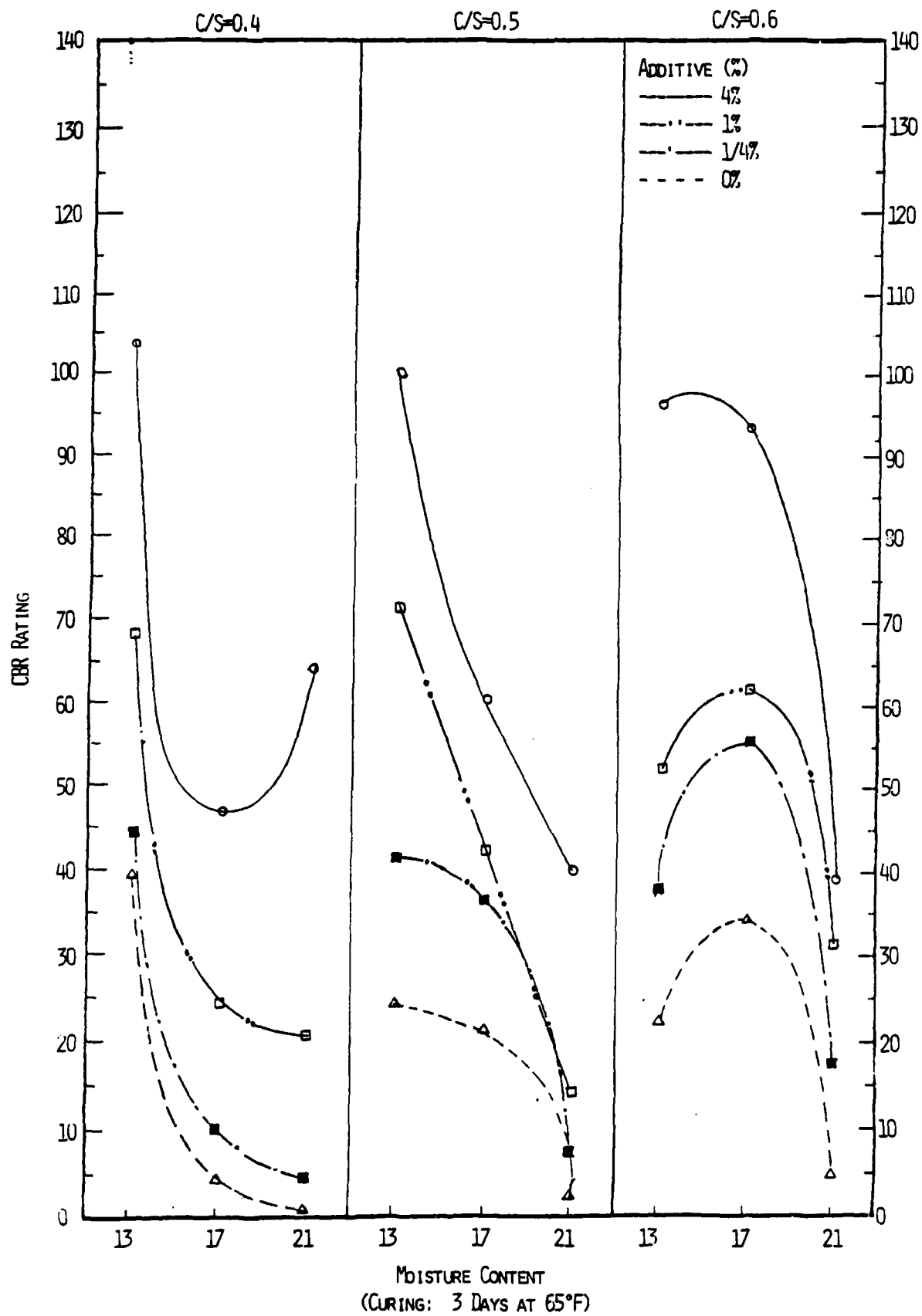
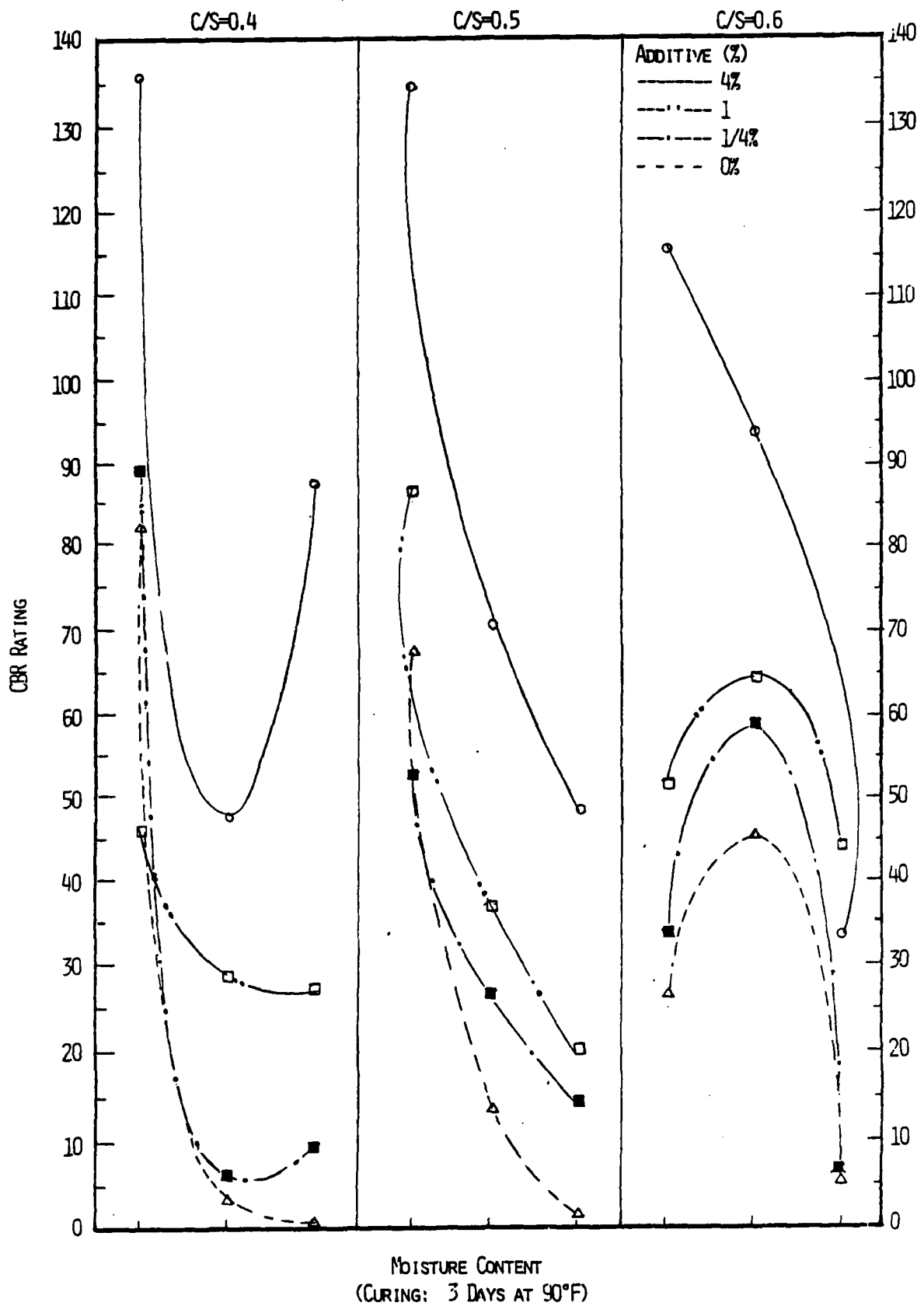


FIGURE 5.3 CBR VS MOISTURE CONTENT BY ADDITIVE AT 3 LEVELS OF CLAY-SILT RATIO



factorial data for analysis.

5.3.1 ADDITIVE TREATMENT STATISTICAL ANALYSIS (No Interaction Effects)

The main regression model to be used in the prediction of clay-silt system soil strength was obtained by pooling all of the experimental data. The result obtained using the stepwise regression procedure involving first order terms only is:

$$\text{CBR} = 91.69 + 11.07(\text{PA}) - 5.62(\text{PM}) + 44.97(\text{CS}) + 0.14(\text{TEMP})$$
$$(R^2 = 0.76) \quad (5.2)$$

where:

PA is Epoxy Resin additive level in percent (%)

PM is moisture content level in percent (%)

CS is clay-silt ratio as a decimal

TEMP is temperature of curing in degrees F

All the regression coefficients were significant at even the 3% level, the model therefore supports the hypothesis that increased moisture content leads to a degradation of CBR values by its reduction of the cohesive and frictional strength of the soil particles. Since the CBR test measures the shear resistance of a soil to deformation under applied loads and since a clay-silt system is being tested, then applying Coulomb's law of shear resistance, increases in the clay content of a clay-silt soil leads to increased cohesive strength and an overall increase in the shear strength and consequently the CBR. The marginal increase in the clay-silt CBR values due to a unit percent

increase in additive content was 11.07 CBR units. The temperature component of the CBR model with a positive coefficient supports the hypothesis that increased temperature leads to increased strength formation with the use of epoxy-resin. A nomograph for clay-silt soil system CBR prediction using epoxy resin as the stabilizing agent is shown in Figure 5.4 and is based on equation 5.1

An alternative model was specified using a two-step regression method as suggested by Edris and Lytton (9). In the first step a linear multiple regression analysis of the logarithms of the dependent and independent variables is obtained. Taking the antilog of the coefficients specifies the best linear unbiased estimator of the powers of the independent variables. For the second step, a linear multiple regression of the independent variables raised to the powers determined in the first step is effected. The appeal of this approach is that there is no predetermined polynomial form, rational function, or power law expression for the model, and it is reported that this method produces a consistently higher coefficient of determination (R^2), (9).

The results obtained from the two-step procedure are:

STEP-1

$$\begin{aligned} \ln \text{ CBR} = & 16.102 + 0.040 \ln(\text{PA}) - 4.257 \ln(\text{PM}) + 1.511 \ln(\text{CS}) \\ & + 0.139 \ln(\text{TEMP}) \end{aligned}$$

$$(R^2 = 0.71) \quad (5.3)$$

NOMOGRAPH FOR CLAY-SILT SYSTEM CBR PREDICTION

(STABILIZING AGENT - EPOXY RESIN)

$$CBR = 91.69 + 11.07(PA) - 5.62(PM) + 44.97(CS) + 0.14(TEMP) \quad (R^2 = 0.78)$$

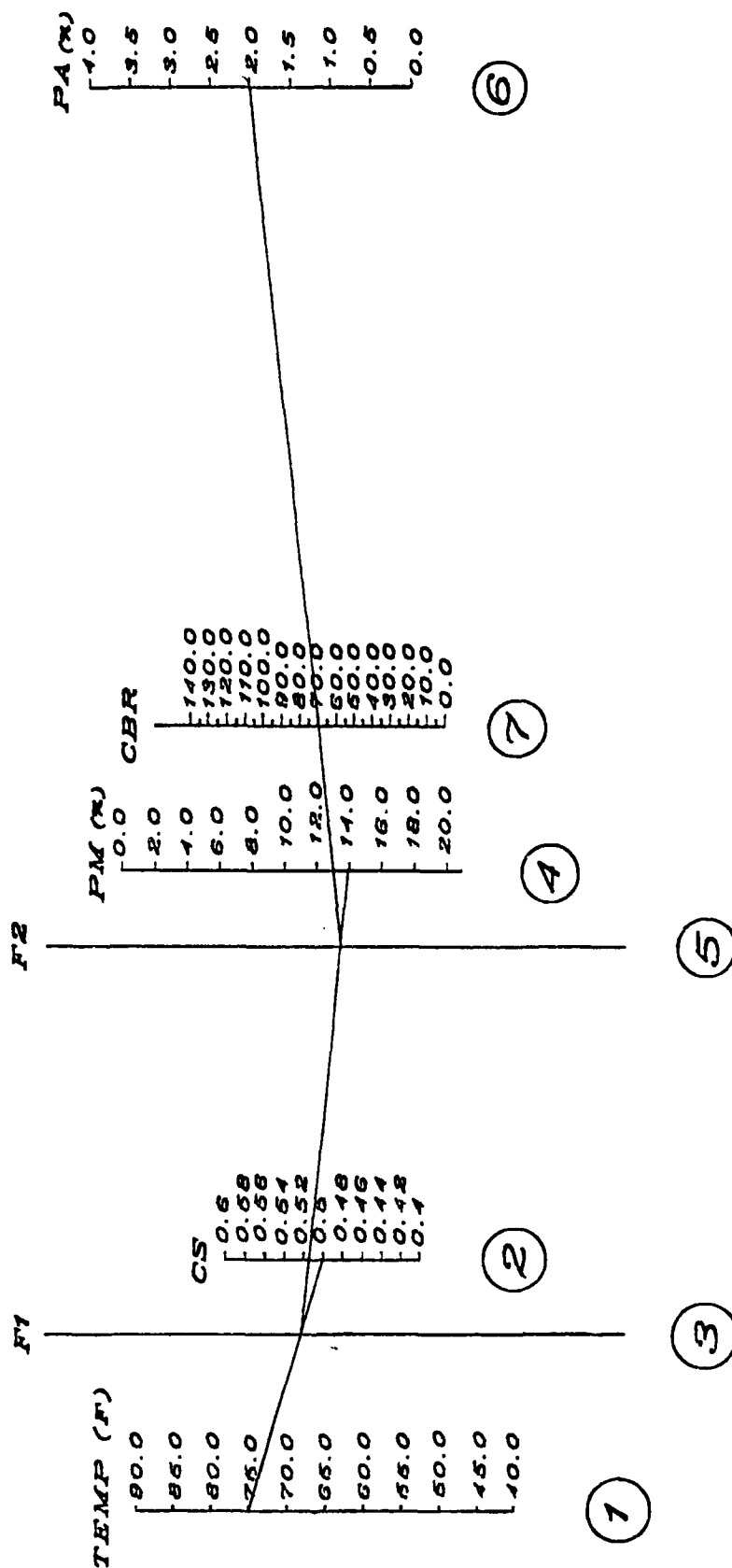


FIGURE 5.4

STEP-2

$$\begin{aligned} \text{CBR} = & 6708.25 + 10.58(\text{PA})^{1.041} - 6431.74(\text{PM})^{0.0142} \\ & + 106.80(\text{CS})^{4.532} + 0.06(\text{TEMP})^{1.149} \end{aligned}$$

($R^2 = 0.77$) (5.4)

A casewise multiple linear regression analysis of the data at fixed levels of selected independent variables was performed. The results for fixed levels of additive, clay-silt ratio and temperature are as provided below:

FIXED ADDITIVE LEVEL

Additive level = 4%

$$\text{CBR} = 160.87 - 7.47(\text{PM}) + 0.57(\text{TEMP}) \quad (R^2 = 0.75) \quad (5.5)$$

Additive level = 1%

$$\text{CBR} = 125.78 - 4.95(\text{PM}) \quad (R^2 = 0.61) \quad (5.6)$$

Additive level = 1/4%

$$\text{CBR} = 117.85 - 5.10(\text{PM}) \quad (R^2 = 0.56) \quad (5.7)$$

Additive level = 0%

$$\text{CBR} = 90.50 - 5.43(\text{PM}) + 56.00(\text{CS}) \quad (R^2 = 0.70) \quad (5.8)$$

FIXED CLAY-SILT LEVEL

Clay-silt level = 40%

$$\begin{aligned} \text{CBR} = & - 423.20 + 13.38(\text{PA}) + 5164.62(\text{PM}) \\ & + 0.39(\text{PM})^2 + 0.19(\text{TEMP}) \quad (R^2 = 0.88) \quad (5.9) \end{aligned}$$

Clay-silt level = 50%

$$\text{CBR} = -75.7 + 10.10(\text{PA}) + 1693.44(\text{PM}) \quad (R^2 = 0.85) \quad (5.10)$$

Clay-silt level = 60%

$$\begin{aligned} \text{CBR} = & 233.09 + 10.16(\text{PA}) - 1785.80 (\text{PM}) - 0.30(\text{PM})^2 \\ & (R^2 = 0.79) \quad (5.11) \end{aligned}$$

FIXED TEMPERATURE LEVEL

Temperature level = 40°F

$$\begin{aligned} \text{CBR} = & - 101.37 + 7.10(\text{PA}) + 1684.45 (\text{PM}) + 0.54(\text{CS}) \\ & (R^2 = 0.83) \quad (5.12) \end{aligned}$$

Temperature level = 65°F

$$\begin{aligned} \text{CBR} = & - 81.33 + 12.33(\text{PA}) + 1330.43(\text{PM}) + 0.48(\text{CS}) \\ & (R^2 = 0.81) \quad (5.13) \end{aligned}$$

Temperature level = 90°F

$$\text{CBR} = -74.60 + 14.37(\text{PA}) + 1683.76(\text{PM})$$

$$(R^2 = 0.76) \quad (5.14)$$

5.3.2 ADDITIVE TREATMENT STATISTICAL ANALYSIS (WITH INTERACTION EFFECTS)

As a means of obtaining the effects of interaction terms in the additive treatment regression modelling, cross terms in the additive, moisture and clay-silt variables were introduced. Temperature and dry density were excluded since the correlation matrix showed these were most poorly correlated with all the other first order and interaction terms entered into the correlation routine.

The results showed that the moisture and additive, and the moisture and clay-silt ratios are significant interaction terms at the 5% level, but are highly correlated with other independent first order variables.

The full model with all the interaction terms specified is

$$\begin{aligned} \text{CBR} = & 195.70 + 26.69(\text{PA}) - 10.48(\text{PM}) - 160.80(\text{CS}) \\ & + 0.19(\text{TEMP}) - 0.19(\text{DD}) - 0.68(\text{PA} \times \text{PM}) - 7.99(\text{PA} \times \text{CS}) \\ & + 11.34(\text{PM} \times \text{CS}) \end{aligned}$$

$$(R^2 = 0.76) \quad (5.15)$$

Clearly the interaction terms do not explain any more variations in the CBR values than the previously specified model of CBR performance with a coefficient of determination of 0.76. Consequently, this model is not as desirable for prediction because of its complexity, larger size, and computational inefficiency.

5.3.3 CONTROL CASE STATISTICAL ANALYSIS (NO ADDITIVE TREATMENT)

This analysis was effected on clay-silt mixtures that were untreated with any additive. A sample plot of the control test data points is shown in Figures 5.5, 5.6 and 5.7. The plots show in general that samples with a greater proportion by weight of clay ($C/S = 0.6$) can hold up resistance to deformation (as measured by the CBR) over a greater range of moisture content. At moisture contents in excess of 20%, all samples registered appreciably degraded CBR values. A statistical analysis of the 38 data points entered into the program incorporated CBR as the dependent variable. The other experimental variables are:

% Moisture	(PM)	} Independent Variables
Dry Density	(DD)	
Clay/Silt Ratio	(CS)	
Temperature	(TEMP)	
% Additive	(PA)	

For the control case, the percent additive did not feature in the modelling effort.

FIGURE 5.5 CBR vs. MOISTURE CONTENT BY CLAY-SILT RATIO AT 40°F
(UNSTABILIZED CLAY-SILT SYSTEM)

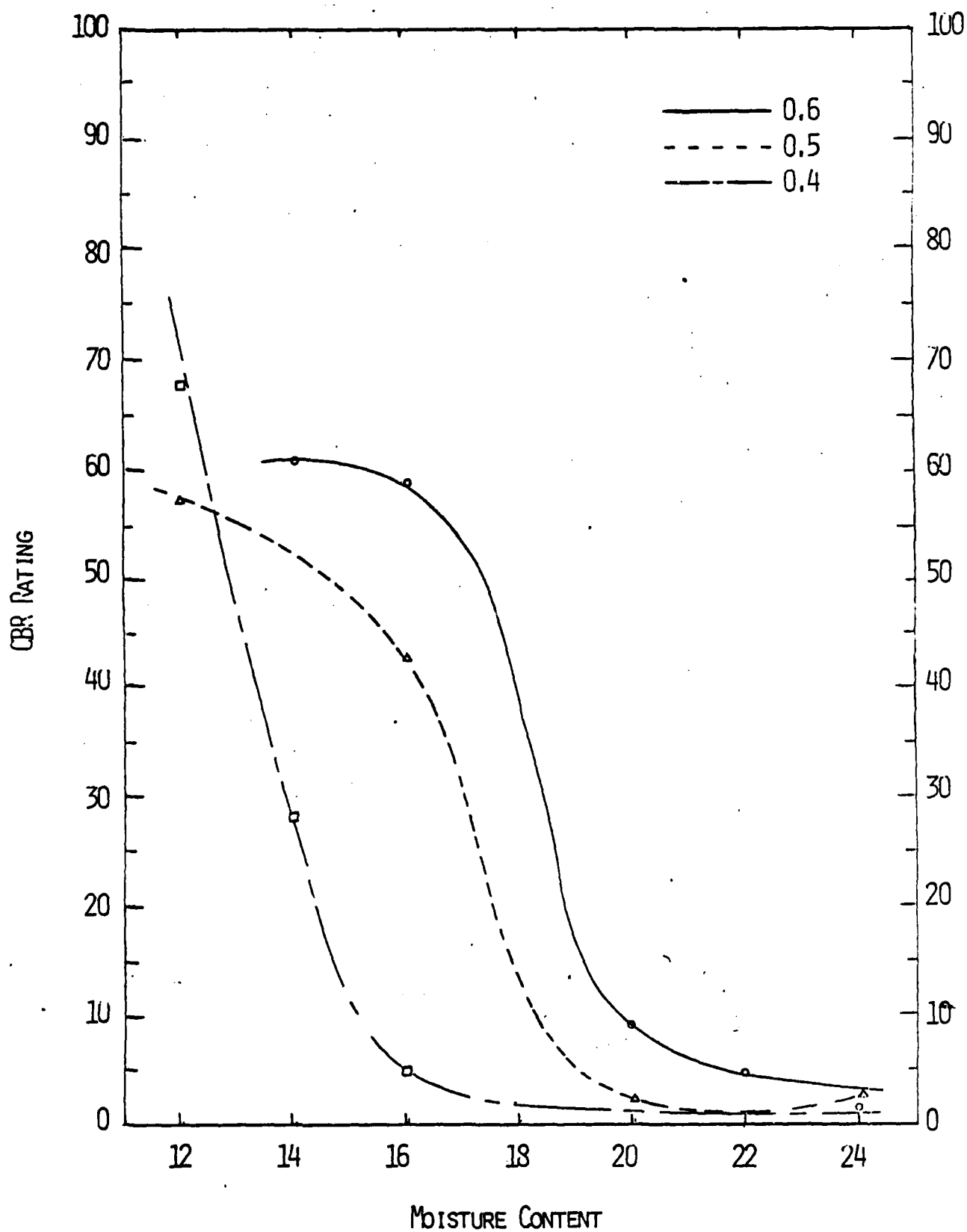


FIGURE 5.6 CBR vs. MOISTURE CONTENT BY CLAY-SILT RATIO AT 65°F
(UNSTABILIZED CLAY-SILT SYSTEM)

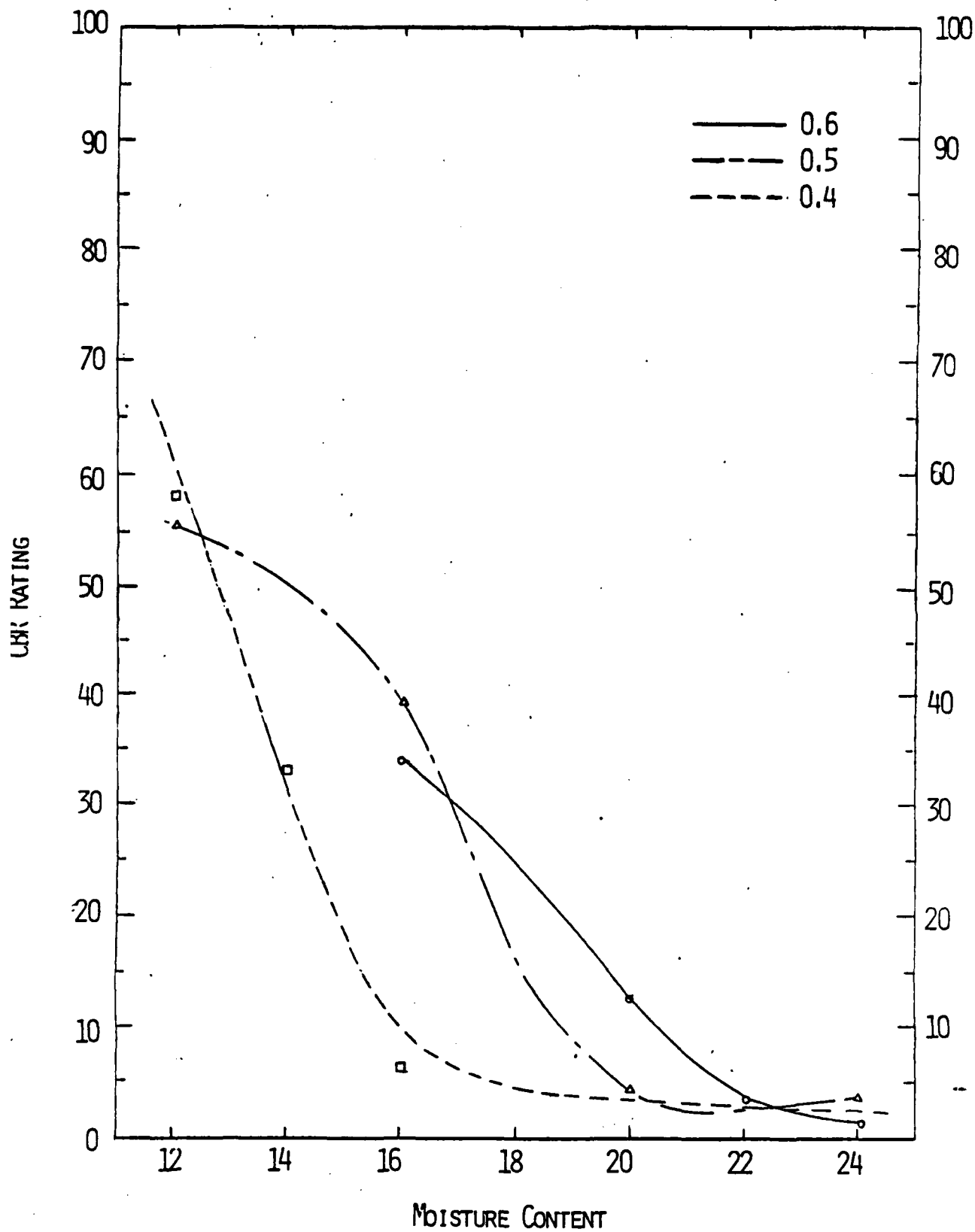
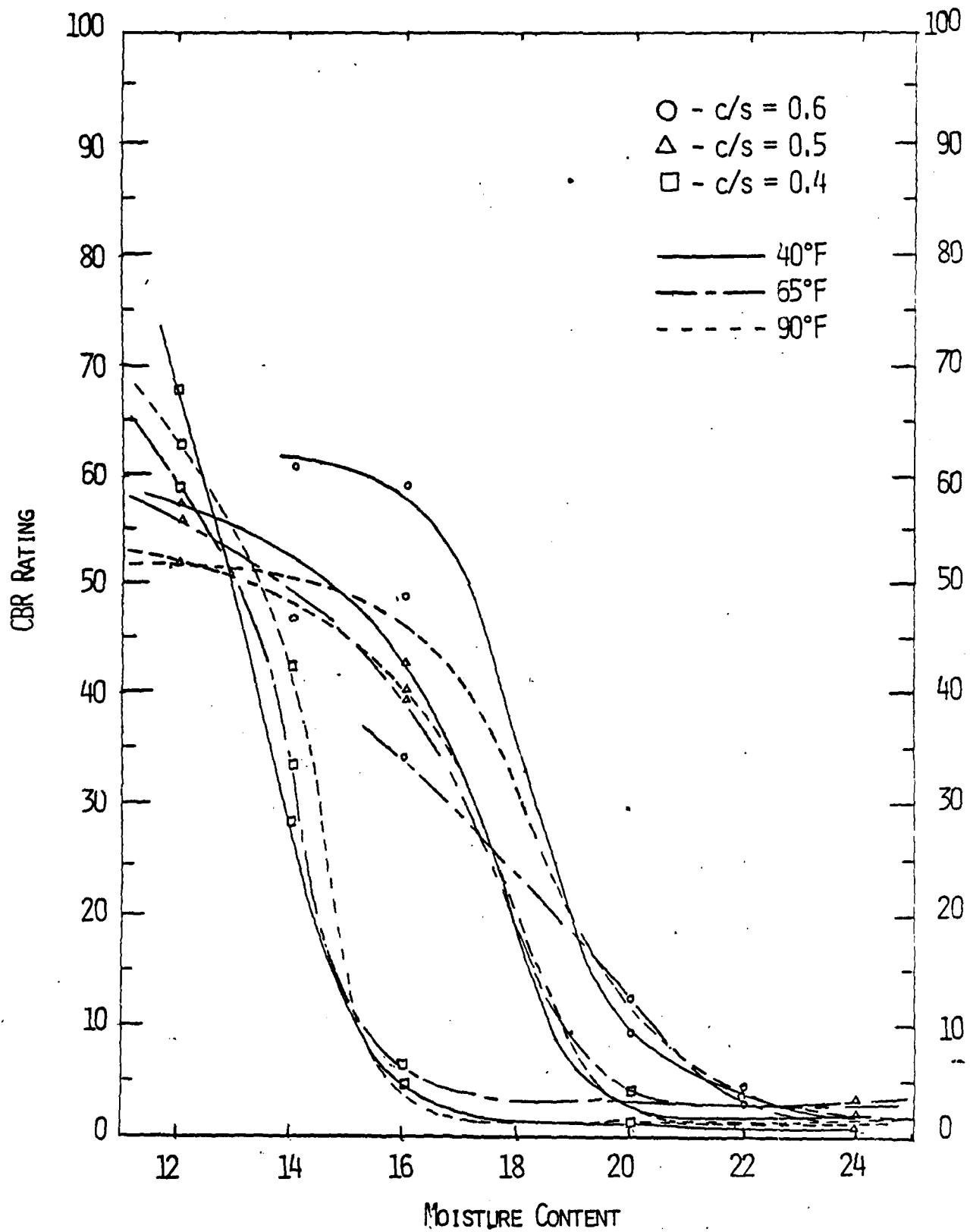


FIGURE 5.7 CBR vs. MOISTURE CONTENT BY CLAY-SILT RATIO AND TEMPERATURE
(UNSTABILIZED CLAY-SILT SYSTEM)



The analysis showed, in summary that:

- a) Stratified by increasing moisture content, an increase in clay-silt ratio is accompanied by a corresponding increase in CBR.
- b) CBR is highly correlated with moisture content (-0.855).
- c) Clay/silt ratio is correlated with dry density (-0.495).
- d) Percent moisture is correlated with clay/silt (0.4103) ratio.
- e) Temperature was not a significant variable and showed only a slight inverse correlation with dry density.
- f) For all samples tested, a significant break in mean CBR values occurred between a moisture content of 16% and 22% at a CBR of 5.5
- g) For a cross-tabulation of moisture content versus clay/silt ratio, no experimental data could be obtained for some points in the data matrix.

(This situation has been remedied by generation of additional data.) Some of the cells could not be filled due to practical test difficulties such as uncompactable powdery samples at the 12% moisture and 60% clay/silt combination, or the slushy, uncompactable sample for 24% moisture and 40% clay/silt combination.

- h) Scatter plots from the residuals had a representative bell shaped profile indicative of normality.

5.3.3.1 MODEL SPECIFICATIONS

The resulting regression model obtained using stepwise regression analysis including all significant variables is:

$$\text{CBR} = 79.49 - 5.71(\text{PM}) + 0.92 (\text{CS}) \quad (R^2=0.82) \quad (5.16)$$

where (PM) and (CS) are in percent.

For regression of data at fixed moisture content levels:

$$\text{CBR} = 168.84 - 1.224 (\text{DD}) \quad (R^2=0.84) \quad (5.17)$$

$$\text{PM} = 16\%$$

$$\text{CBR} = 75.24 + 2.12(\text{CS}) \quad (R^2=0.78) \quad (5.18)$$

$$\text{PM} = 16\%$$

$$\text{CBR} = 102.36 - 8.59(\text{PM}) + 1.31(\text{CS}) \quad (R^2=0.69) \quad (5.19)$$

$$\text{PM} = 16\%$$

For regression of data at fixed temperature levels:

$$\text{CBR} = 316.15 - 5.20 (\text{PM}) - 1.89(\text{DD}) \quad (R^2=0.87) \quad (5.20)$$

$$\text{TEMP} = 40^\circ\text{F}$$

$$\text{CBR} = 252.72 - 4.65(\text{PM}) - 1.41(\text{DD}) \quad (R^2=0.91) \quad (5.21)$$

$$\text{TEMP} = 65^\circ\text{F}$$

$$\text{CBR} = 83.34 + 0.78(\text{CS}) - 5.56(\text{DD}) \quad (R^2=0.83) \quad (5.22)$$

$$\text{TEMP} = 90^\circ\text{F}$$

For regression of data at fixed clay/silt ratio levels:

$$\text{CBR} = 141.66 - 7.45(\text{PM}) \quad (R^2=0.77) \quad (5.23)$$

$$\text{CS} = 40\%$$

$$\text{CBR} = 113.50 - 4.90(\text{PM}) \quad (R^2=0.89) \quad (5.24)$$

$$\text{CS} = 50\%$$

$$\text{CBR} = 136.15 - 5.86(\text{PM}) \quad (R^2=0.88) \quad (5.25)$$

$$\text{CS} = 60\%$$

5.3.3.2 MODEL REFINEMENT

A refinement of the preceding statistical models has been effected by the augmentation of available data, namely, those generated to cover the missing cells in the cross-tabulation matrix of moisture content versus clay/silt ratio. Ten such additional data points were incorporated.

The refined regression model for the control experimentation did not significantly improve or degrade the explanatory power of the model ($R^2 = 0.81$ vs $R^2 = 0.82$ previously).

The refined model is:

$$\text{CBR} = 77.79 - 5.53(\text{PM}) + 0.86(\text{CS}) \quad (R^2=0.81) \quad (5.26)$$

5.3.4 ADDITIVE TREATMENT EFFECTIVENESS ANALYSIS

The full factorial design experiment conducted at four additive levels PA = 4%, 1%, 1/4%, 0%, enabled, for the same design combination of moisture content, clay-silt ratio and temperature, a computation of the CBR increase over the control (no additive) case at each of the same and corresponding level of experimentation. The resulting difference in CBR (the CBR effectiveness differential) was subjected to regression analysis.

The k^{th} variable multiple linear regression model fitted was of the form:

$$Y_{eff} = \alpha_0 + \alpha_i \sum_{i=1}^k x_i \quad (i=1,2,\dots,k) \quad (5.27)$$

where:

$Y_{eff} = CBR_T - CBR_C$ = Calculated differential values of CBR associated with the treatment versus control data at the same experimental level of other independent variables.

α_0 = Multiple regression coefficient.

α_i = Regression coefficient for the i^{th} variable

x_i = set of independent variables ($i=1,\dots,k$).

The model developed from the data generated above is:

$$Y_{eff} = -10.03 + 10.91(PA) + 0.22(TEMP) \quad (R^2=0.65) \quad (5.28)$$

Figures 5.8 through 5.10 show a plot of the raw data underlying model 5.28. Moisture content and clay-silt ratio within the limits of the data points tested, did not significantly impact the improvement in soil strength due to additive application as compared to the corresponding strength under untreated conditions.

FIGURE 5.8 CBR DIFFERENTIAL VS. MOISTURE CONTENT BY ADDITIVE AT 3 LEVELS OF CLAY-SILT RATIO

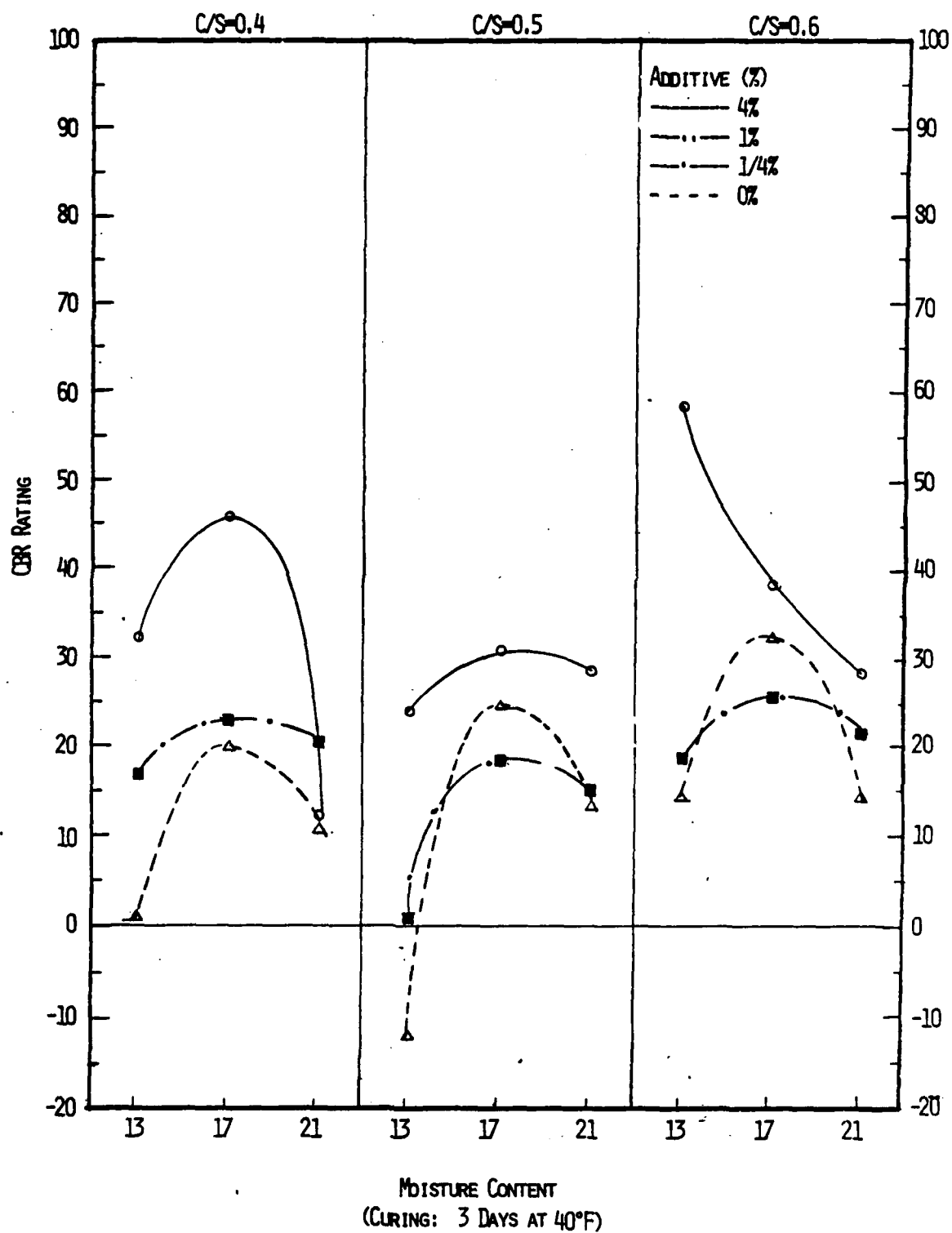


FIGURE 5.9 CBR DIFFERENTIAL VS. MOISTURE CONTENT BY ADDITIVE AT 3 LEVELS OF CLAY-SILT RATIO

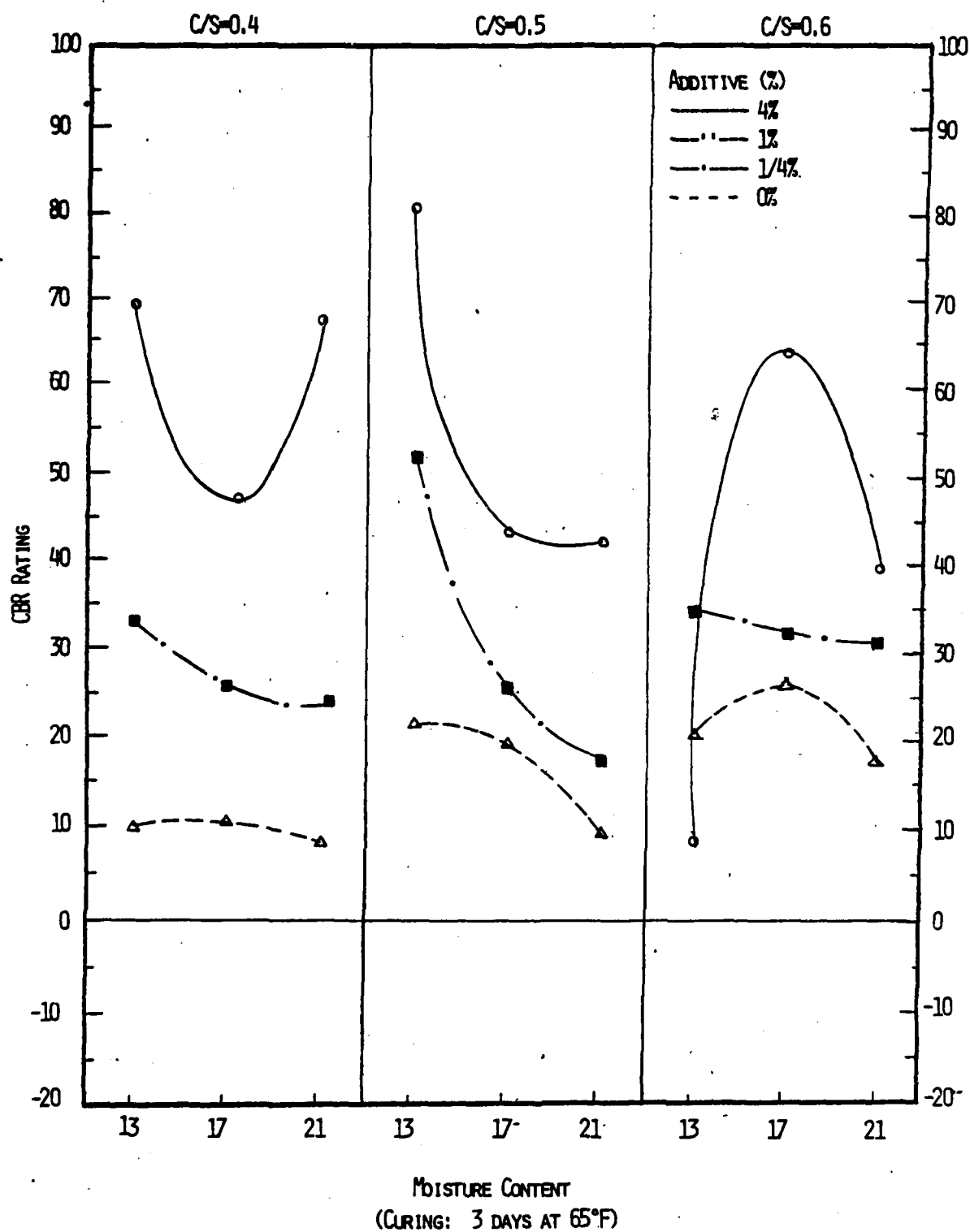
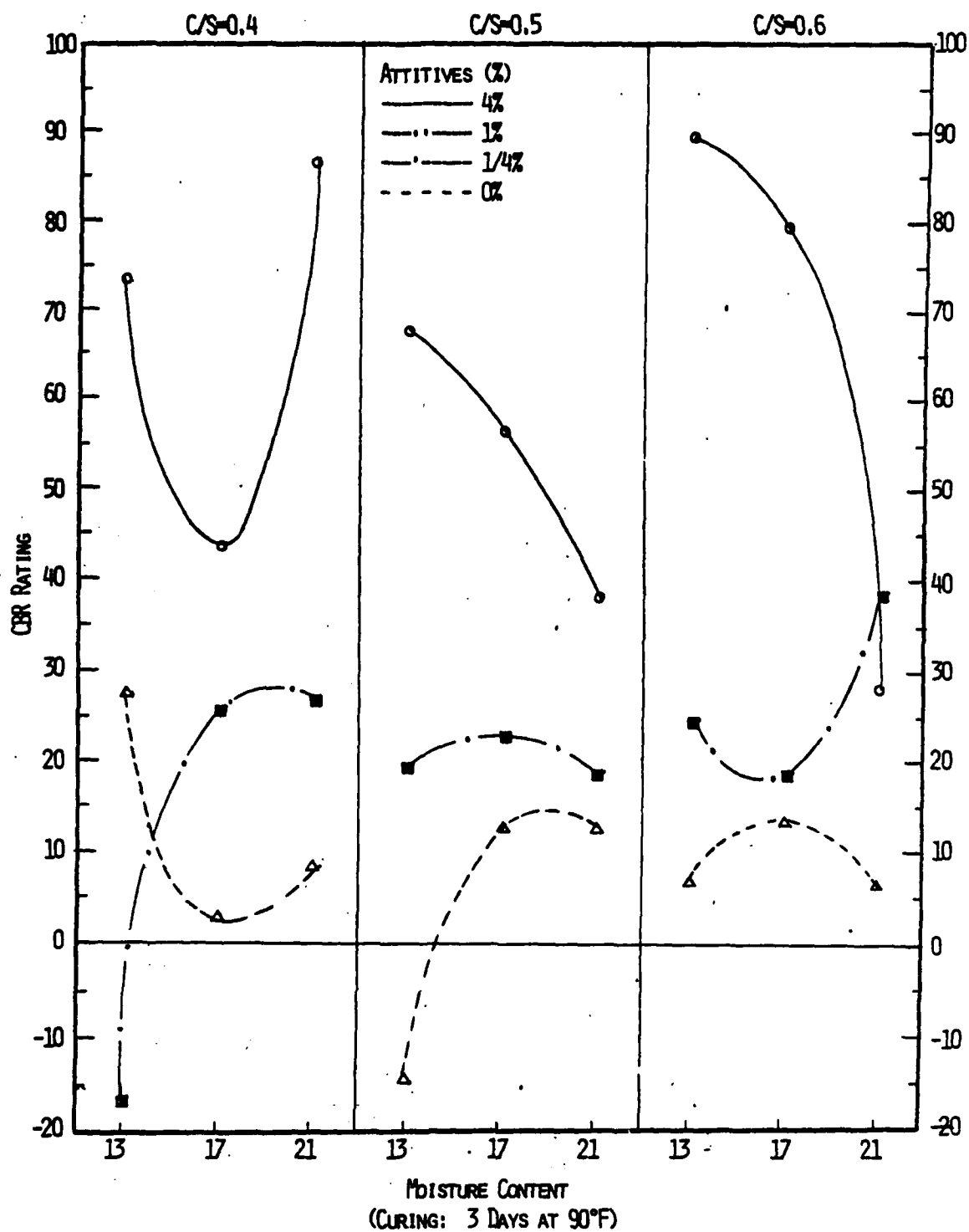


FIGURE 5.10 CBR DIFFERENTIAL VS. MOISTURE CONTENT BY ADDITIVE AT 3 LEVELS OF CLAY-SILT RATIO



5.4 MANOVA ANALYSIS

5.4.1 Four-Factor Full ($3^3 \times 4$) Factorial Model Analyses

To secure a more definitive understanding of the individual and joint effects of the four experimental independent variables, (which variables are appropriately referred to as treatments) the full factorial experimental design technique in conjunction with the Multivariate Analysis of Variance (MANOVA) routine contained within the SPSS^X library was used.

Such other statistical designs and analyses techniques as latin square, graeco latin square, hyper-graeco-latin square completely, randomized block designs, balanced incomplete block design, Youden Square, paired t-tests and others were not used for this multivariate phase of analysis since these are mainly concerned with the effect of one variable (referred to as "treatment"). In these tests usually the effect of extraneous variables on the treatment is accommodated and confounded by such classical statistical strategies as randomization, blocking, and replication. Other specialized methods include use of the rows and columns of latin squares or the other sophisticated designs such as the graeco-latin squares.

In order to obtain an estimate of the experimental error in the four-factor experiment, it is often necessary to repeat the entire set of 108 experimental conditions, say, a total of e times, where e is the number of replications, randomizing the order of applying the conditions in each replicate. If Y_{ijklm} is the CBR reading obtained at the i^{th} level of additive percentage (PA), the j^{th} level of moisture content (PM), the k^{th} level of

clay-silt ratio (CS), the l th level of temperature (TEMP) in the m th replicate, then a statistical model of the experimental phenomena can be expressed mathematically as:

$$\begin{aligned}
 Y_{ijklm} = & \mu + \alpha_i + \beta_j + \gamma_k + \delta_l + \\
 & (\alpha\beta)_{ij} + (\alpha\gamma)_{ik} + (\alpha\delta)_{il} + (\beta\gamma)_{jk} + \\
 & (\beta\delta)_{jl} + (\gamma\delta)_{kl} + (\alpha\beta\gamma)_{ijk} + (\alpha\beta\delta)_{ijl} + \\
 & (\alpha\gamma\delta)_{ikl} + (\beta\gamma\delta)_{jkl} + (\alpha\beta\gamma\delta)_{ijkl} + \\
 & \rho_m + \epsilon_{ijklm}
 \end{aligned} \tag{5.29}$$

for

$$i = 1, \dots, a = 4$$

$$j = 1, \dots, b = 3$$

$$k = 1, \dots, c = 3$$

$$l = 1, \dots, d = 3$$

$$m = 1, \dots, e = 1$$

In the above equation, μ is the grand mean, α_i is the effect of the i th level of additive percentage. β_j is the effect of the j th level of moisture percentage, $(\alpha\beta)_{ij}$ is the interaction, or joint effect of the i th level of additive and the j th level of moisture percentage and $(\alpha\beta\gamma\delta)_{ijkl}$ is the combined interaction or effect of all the experimental variables considered simultaneously. ρ_m is the effect of the m th replicate. In the absence of any replicates in this experimentation ($m=1$) the sums

of squares of the 4-way interaction term with $(3-1)^3(4-1)=24$ degrees of freedom was used as an estimate of the error mean square.

In parameterizing, the ϵ_{ijklm} terms are assumed to be values of independent random variables having normal distributions with zero means and a common variance σ^2 . It is further assumed that:

$$\sum_{i=1}^4 \alpha_i = \sum_{j=1}^3 \beta_j = \sum_{k=1}^3 \gamma_k = \sum_{l=1}^3 \delta_l = 0 \quad (5.30)$$

$$\sum_{i=1}^4 (\alpha\beta)_{ij} = \sum_{j=1}^3 (\alpha\beta)_{ij} = 0 \quad (5.31)$$

$$\sum_{i=1}^4 (\alpha\beta\gamma)_{ijk} = \sum_{j=1}^3 (\alpha\beta\gamma)_{ijk} = \sum_{k=1}^3 (\alpha\beta\gamma)_{ijk} = 0 \quad (5.32)$$

$$\sum_{j=1}^3 (\beta\gamma\delta)_{jkl} = \sum_{k=1}^3 (\beta\gamma\delta)_{jkl} = \sum_{l=1}^3 (\beta\gamma\delta)_{jkl} = 0 \quad (5.33)$$

$$\sum_{i=1}^4 (\alpha\beta\gamma\delta)_{ijkl} = \sum_{j=1}^3 (\alpha\beta\gamma\delta)_{ijkl} = \quad (5.34)$$

$$\sum_{k=1}^3 (\alpha\beta\gamma\delta)_{ijkl} = \sum_{l=1}^3 (\alpha\beta\gamma\delta)_{ijkl} = 0 \quad (5.35)$$

$$\sum_{m=1}^1 \rho_m = 0 \quad (\rho_1 = 0 \text{ and the term drops out}) \quad (5.36)$$

These restrictions will assure unique estimates for the parameters μ, α_i, β_j and other terms including ρ_m whenever it exists.

The analysis of the $3^3 \times 4$ factorial is based on the following breakdown of the total sum of squares (SST). First SST is subdivided into components attributable to treatment, replicates (or blocks), and error by means of the identity:

$$\begin{aligned}
 & \sum_{i=1}^a \sum_{j=1}^b \sum_{k=1}^c \sum_{l=1}^d \sum_{m=1}^e (\bar{y}_{ijklm} - \bar{y}_{\dots\dots})^2 = \\
 & r \sum_{i=1}^a \sum_{j=1}^b \sum_{k=1}^c \sum_{l=1}^d (\bar{y}_{ijkl.} - \bar{y}_{\dots\dots})^2 + \\
 & abcd \sum_{m=1}^e (\bar{y}_{\dots\dots m} - \bar{y}_{\dots\dots})^2 + \\
 & \sum_{i=1}^a \sum_{j=1}^b \sum_{k=1}^c \sum_{l=1}^d \sum_{m=1}^e (\bar{y}_{ijklm} - \bar{y}_{ijkl.} - \bar{y}_{\dots\dots m} + \bar{y}_{\dots\dots})^2 \quad (5.36)
 \end{aligned}$$

The total sum of squares on the left-hand side of the identity has $abcde-1$ degrees of freedom. The terms on the right are, respectively, the treatment sums of squares with $(abcd-1)$ degrees of freedom, the replicate (block) sum of squares with $(e-1)$ degrees of freedom and the error sum of squares with $(abdc-1)(e-1)$ degrees of freedom.

The following analysis of data which follows the two-way classification scheme for experimentation can be further

decomposed into components for the treatment sums of squares in view of the advantages offered by factorial experimentation. The subdivision for the four-factor experiment is therefore expressed as:

$$\begin{aligned}
 & r \sum_{i=1}^a \sum_{j=1}^b \sum_{k=1}^c \sum_{l=1}^d (\bar{y}_{ijkl.} - \bar{y}_{.....})^2 = \\
 & rbcd \sum_{i=1}^a (\bar{y}_{i.....} - \bar{y}_{.....})^2 + racd \sum_{j=1}^b (\bar{y}_{.j....} - \bar{y}_{.....})^2 + \\
 & rabd \sum_{k=1}^c (\bar{y}_{..k..} - \bar{y}_{.....})^2 + rabc \sum_{l=1}^d (\bar{y}_{...l.} - \bar{y}_{.....})^2 + \\
 & r \sum_{i=1}^a \sum_{j=1}^b \sum_{k=1}^c \sum_{l=1}^d (\bar{y}_{ijkl.} - \bar{y}_{i.....} - \bar{y}_{.j....} - \bar{y}_{..k..} - \bar{y}_{...l.} + \bar{y}_{.....})^2
 \end{aligned}
 \tag{5.37}$$

The first term in model 5.37 measures the variability of the means corresponding to different percentage levels of the epoxy-resin additive and it is the additive factor sum of squares, etc.

The $(abcd-1)$ degrees of freedom for the treatment are further subdivided into $(a-1)$ degrees of freedom for additive treatment, $(b-1)$ degrees of freedom for moisture content and $(abcd-1)-(a-1)-(b-1)-(c-1)-(d-1)$ or $(abcd-(a+b+c+d)+3)$ degrees of freedom for all the interaction terms in the design. The last 4 way interaction term has $(a-1)(b-1)(c-1)(d-1)$ degrees of freedom or $3(2)^3 = 24$. This last interaction term was chosen as an estimate of the error term in the model in the absence of replication.

5.4.2 MANOVA ANALYSIS RESULT:

5.4.2.1 Additive Treatment Case

Application of the MANOVA analysis to the factorial design data for the purpose of understanding the variations in the CBR for changes in the experimental variables rejected the null hypothesis that all the estimated parameters in engineering were zero and showed that the following variables were highly significant in influencing CBR values at the 5% level: (Table 5.1)

- Additive percentage
- Moisture percentage
- Clay-silt ratio
- Temperature

The following second order cross terms were highly significant at the 5% level:

- Additive and moisture jointly
- Additive and temperture jointly
- Moisture and clay-silt ratio jointly
- Moisture and temperature jointly

The only third order crossterm that was highly significant was:

- Additive by moisture by clay-silt ratio

The results obtained from the MANOVA analysis are as should

TABLE 5.1 MANOVA ANALYSIS OF MAIN INTERACTION EFFECTS FOR CBR DATA

12-MAY-87	STATISTICAL ANALYSIS OF SOIL DATA	DEC VAX-11/780 VMS V4.4		
19:39:15	CSU PARKER HALL COMPUTER			
***** ANALYSIS OF VARIANCE -- DESIGN 1*****				
TESTS OF SIGNIFICANCE FOR CBR USING UNIQUE SUMS OF SQUARES				
SOURCE OF VARIATION	SS	DF MS F SIG OF F		
RESIDUAL	1488.44	24	62.02	
PA	35951.18	3	11983.73	.000
PM	32031.18	2	19015.59	.000
CS	739.42	2	369.71	.008
TEMP	1707.95	2	853.98	.000
PA BY PM	2088.31	6	348.05	.001
PA BY CS	652.95	6	108.83	.151
PA BY TEMP	2854.28	6	475.71	.000
PM BY CS	11057.92	4	2764.48	.000
PM BY TEMP	1973.42	4	493.35	.014
CS BY TEMP	161.62	4	40.41	.631
PA BY PM BY CS	2563.28	12	213.61	.005
PA BY PM BY TEMP	1151.97	12	96.00	.175
PA BY CS BY TEMP	658.06	12	54.84	.573
PM BY CS BY TEMP	599.98	8	75.00	.335

NOTE: THE FIRST PARAMETER, CORRESPONDING TO THE CONSTANT, IS NO LONGER PRINTED BY DEFAULT. TO OBTAIN PARAMETER ESTIMATES, ETC. FOR THE CONSTANT, SPECIFY CCONSTANT IN THE DESIGN SUBCOMMAND.

ESTIMATES FOR CBR

PA --- INDIVIDUAL UNIVARIATE .9500 CONFIDENCE INTERVALS

PARAMETER	COEFF.	STD. ERR.	T-VALUE	SIG. T	LOWER -95%	CL- UPPER
2	-18.8734259259	1.31253	-14.37945	.00000	-21.58235	-16.16450
3	-10.4756481481	1.31253	-7.98128	.00000	-13.18457	-7.76672
4	-.0715740741	1.31253	-.05453	.95696	-2.78050	2.63735
PARAMETER	COEFF.	STD. ERR.	T-VALUE	SIG. T	LOWER -95%	CL- UPPER
5	24.0287962963	1.07167	22.42174	.00000	21.61697	26.24062
6	-2.2587037037	1.07167	-2.10764	.04569	-4.47053	-.04688
PARAMETER	COEFF.	STD. ERR.	T-VALUE	SIG. T	LOWER -95%	CL- UPPER
7	-2.8120370370	1.07167	-2.62397	.01487	-5.02386	1.60021
8	-.6770370370	1.07167	-.63176	.53352	-2.88886	1.53479

TABLE 5.2 MANOVA ANALYSIS OF MAIN AND INTERACTION EFFECTS FOR CRR DIFFERENTIAL DATA

13-MAY-87 STATISTICAL ANALYSIS OF SOIL DATA												
10:10:55 CSU BAKERER HALL COMPUTER DEC VAX-11/750 VMS V4.4												
***** ANALYSIS OF VARIANCE -- DESIGN 1*****												
TESTS OF SIGNIFICANCE FOR CBR USING UNIQUE SUMS OF SQUARES												
SOURCE OF VARIATION SS DF MS F SIG OF F												
RESIDUAL	3375.98	24	140.78	79.59	.000							
PA	3301.46	3	11204.82	.46	.637							
PM	129.20	2	64.60	.93	.408							
CS	262.26	2	131.13	8.72	.001							
TEMP	2450.01	2	1228.00	1.90	.512							
PA BY PM	758.62	6	126.44	1.08	.402							
PA BY CS	911.46	6	151.91	4.16	.005							
PA BY TEMP	3516.66	6	586.11	1.17	.349							
PM BY CS	658.98	4	164.74	.95	.451							
PM BY TEMP	536.77	4	134.19	.84	.511							
CS BY TEMP	475.62	4	118.90	1.46	.206							
PA BY PM BY CS	2472.25	12	206.02	1.46	.574							
PA BY PM BY TEMP	1492.30	12	124.36	.88	.769							
PA BY CS BY TEMP	1119.92	12	93.33	.66	.178							
PM BY CS BY TEMP	1798.05	8	224.76	1.60	.000							
CONSTANT	37267.02	1	37267.02	264.72								
ESTIMATES FOR CBR												
--- INDIVIDUAL UNIVARIATE .9500 CONFIDENCE INTERVALS												
PA												
PARAMETER	COEFF.	STD. ERR.	T-VALUE	SIG. T	LOWER -95%	CL- UPPER						
1	-18.5759259259	1.97750	-9.39363	.00000	-22.65729	-14.49456						
2	-9.9537037037	1.97750	-5.03347	.00004	-14.03507	-5.47234						
3	.2314814815	1.97750	.11706	.90779	-3.84988	4.31284						
PM												
PARAMETER	COEFF.	STD. ERR.	T-VALUE	SIG. T	LOWER -95%	CL- UPPER						
4	7.3981481481	1.61462	2.24659	.80732	-3.73057	2.93427						
5	1.4935185185	1.61462	.92500	.36418	-1.83890	4.82594						
CS												
PARAMETER	COEFF.	STD. ERR.	T-VALUE	SIG. T	LOWER -95%	CL- UPPER						
6	5601851852	1.61462	34694	.73166	-2.77223	3.89260						
7	-2.1259259259	1.61462	-1.31667	.20038	-5.45834	1.20619						
TEMP												
PARAMETER	COEFF.	STD. ERR.	T-VALUE	SIG. T	LOWER -95%	CL- UPPER						
8	-6.6370370370	1.61462	-4.11058	.00040	-9.96946	-3.30462						
9	2.2824074074	1.61462	1.41359	.17032	-1.05001	5.61483						

be expected. The effects of the identified variables or their interactions as specified will lead to statistically significant changes in CBR at the 5% level within the ranges of experimental conditions tested. The observation that the interaction of additive and clay-silt ratio does not affect the observed variations in CBR does not come as a surprise in view of the particle size distribution similarity between clay and silt leading to similar patterns of strength development. Therefore, the additive has a very similar interactive effect for varying compositions of the clay-silt mixture.

It is hypothesized that the interactive effect of moisture and clay-silt variables is statistically significant because moisture reduces the cohesive strength of a soil system due to the development of pore water pressure and also due to the moisture film that lubricates the relatively larger surface area of clay minerals.

5.4.2.2 ADDITIVE EFFECTIVENESS CASE:

Application of the MANOVA analysis to the data was obtained by calculating for each experimental point, the improvement in CBR obtained over the corresponding control case. This resulted in the test results displayed in Table 5.2. The data rejected the null hypothesis that all the parameters of the fitted model (Equation 5.29) were all zeros. The usefulness of this analysis lies in its being the most unbiased estimate of the improvement in CBR that can be made possible over the base (untreated) case. Further, using this technique, the marginal increases in soil

strength, else known as main and interaction effects, that are attributable to various factors, can be estimated as shown in equation 5.29.

The main factors that affect additive effectiveness, as measured on the CBR scale at the 5% significance level, are shown in order of descending significance:

- Additive percentage
- Temperature

The following second order interaction effects were highly significant at the 5% level:

- Additive and temperature jointly

All other terms were insignificant at the 5% level. The importance of this result lies in the suggestion that the only avenues for strength improvement over the natural CBR of the clay-silt material in its untreated state is through additive application or temperature increases or both, between the ranges of experimental conditions tested.

That moisture percent and clay-silt ratio do not feature in this statistical analysis is not without explanation though not obvious on the first impression. At the two levels considered, treated and untreated (control) for the clay-silt system, the effects of moisture and clay-silt composition are on the average the same. Therefore, the effects of these factors are cancelled

out. In other words, the reduction in CBR due to a specified moisture content is the same whether the sample is treated or untreated, whereas additive treatment and temperature treatment show different effects at the two levels tested, as supported by a comparison across all three Figures 5.8 through 5.10.

5.5 COMPLEMENTARY REGRESSION MODELLING

To capture more fully the perceived behavior of the full factorial experimental data, a dichotomization of the plots in Figures 5.1, 5.2, and 5.3 into a quadratic and inverse model form relative to moisture content was postulated. Regression modelling was effected cognizant of the observed inverse and quadratic trends.

5.5.1 COMPOSITE REGRESSION MODELLING (NO STRATIFICATION)

Stepwise regression analysis with all the independent variables specified was executed including also quadratic and inverse terms in moisture content. The regression modelling effort rejected the linear and quadratic terms in moisture content to yield the model:-

$$\text{CBR} = -99.97 + 11.3(\text{PA}) + 1575 (1/\text{PM}) + 0.44(\text{CS}) + 0.13(\text{TEMP})$$
$$(R^2 = 0.76) \quad (5.38)$$

Figures 5.11 through 5.14 show the predicted values of CBR as a function of moisture content and additive concentration for selected combinations of temperature and clay-silt ratio. The

FIGURE 5.11 CBR vs. % Moisture (a TP = 40 DEG; CS = 40%)

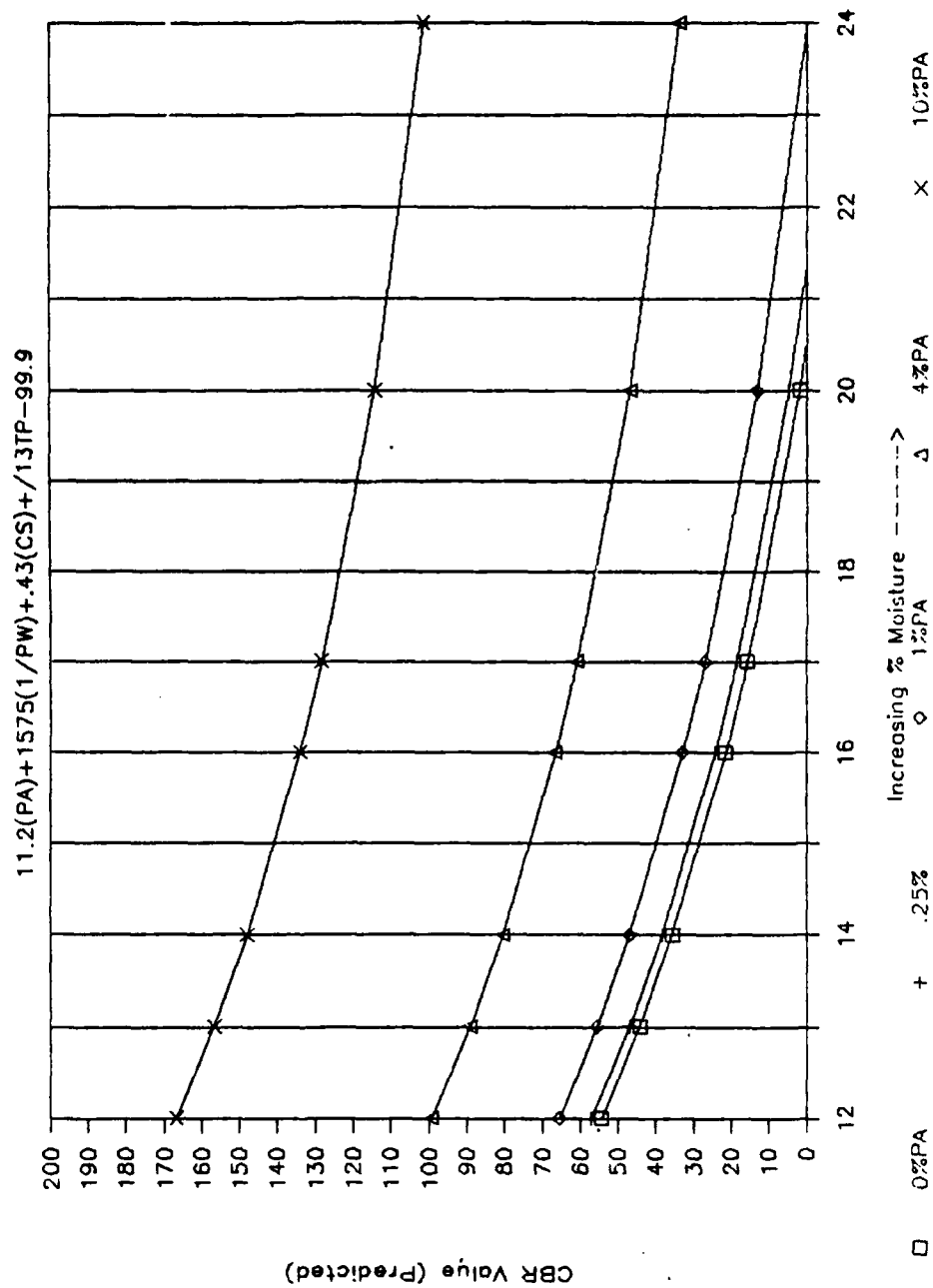


FIGURE 5.12 CBR vs. % Moisture (a CS = 40%, TP = 65 Deg)

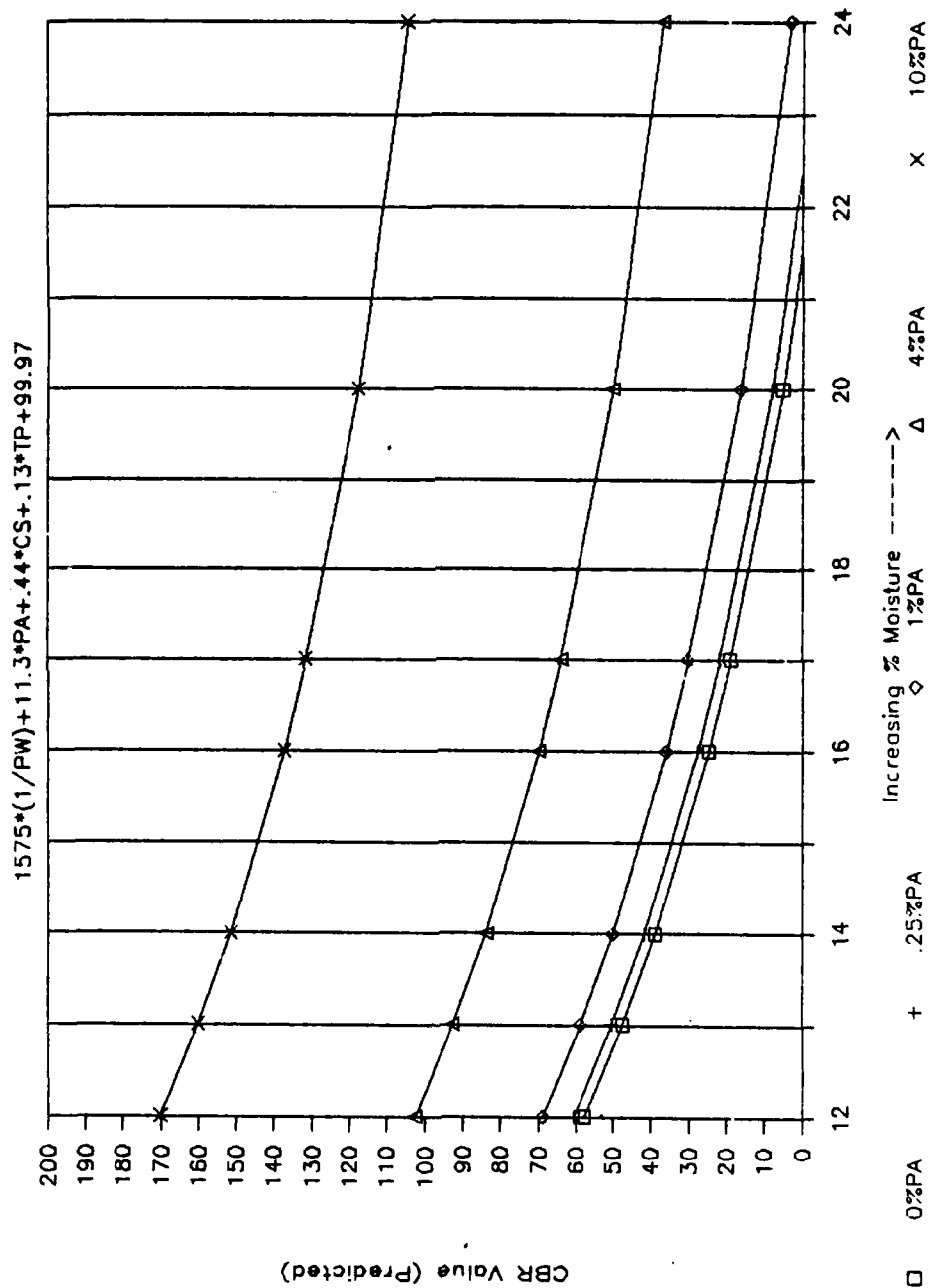


FIGURE 5.13 CBR vs. % MOISTURE (TP = 65 DEG; CS = 50%)

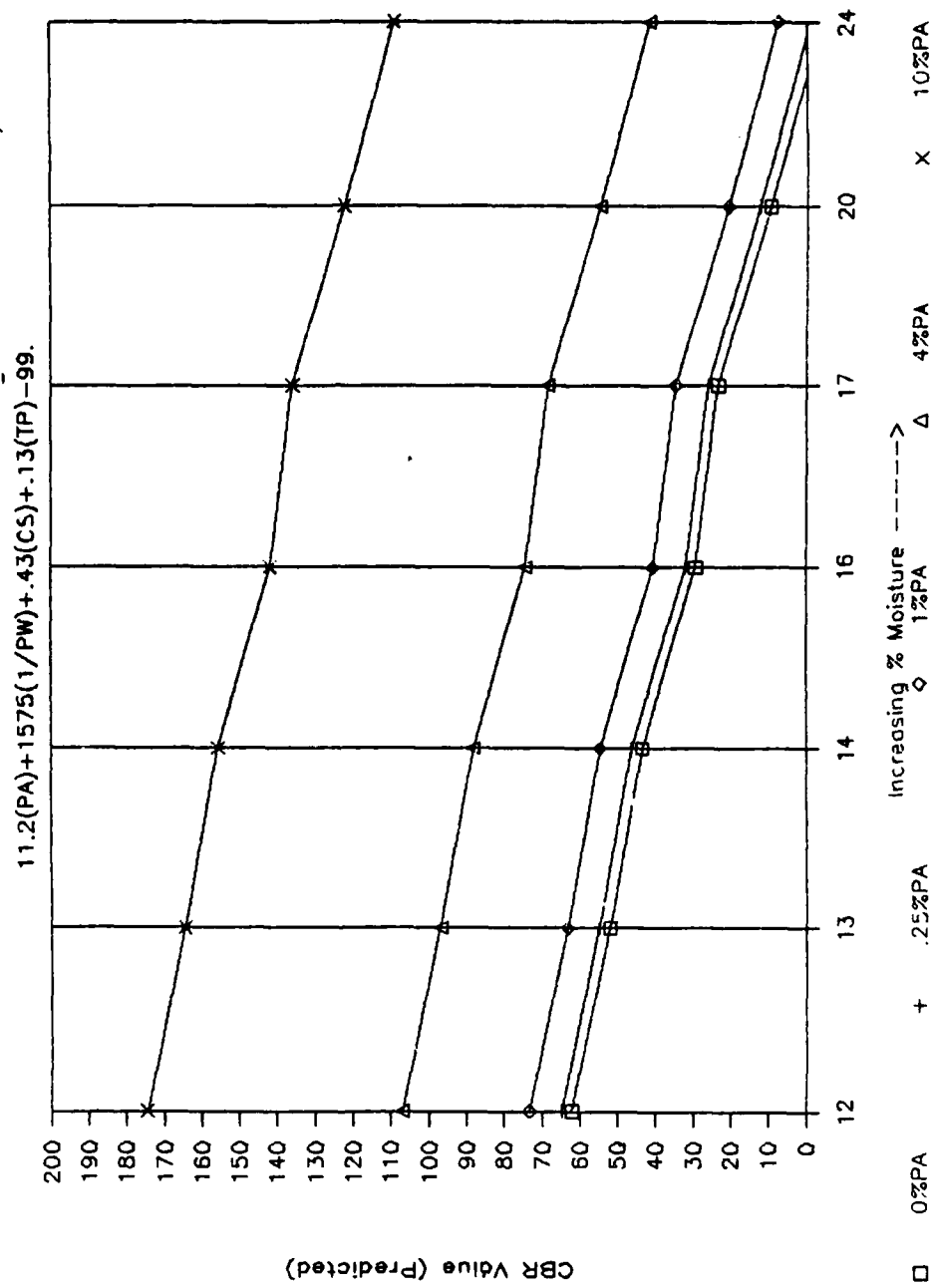
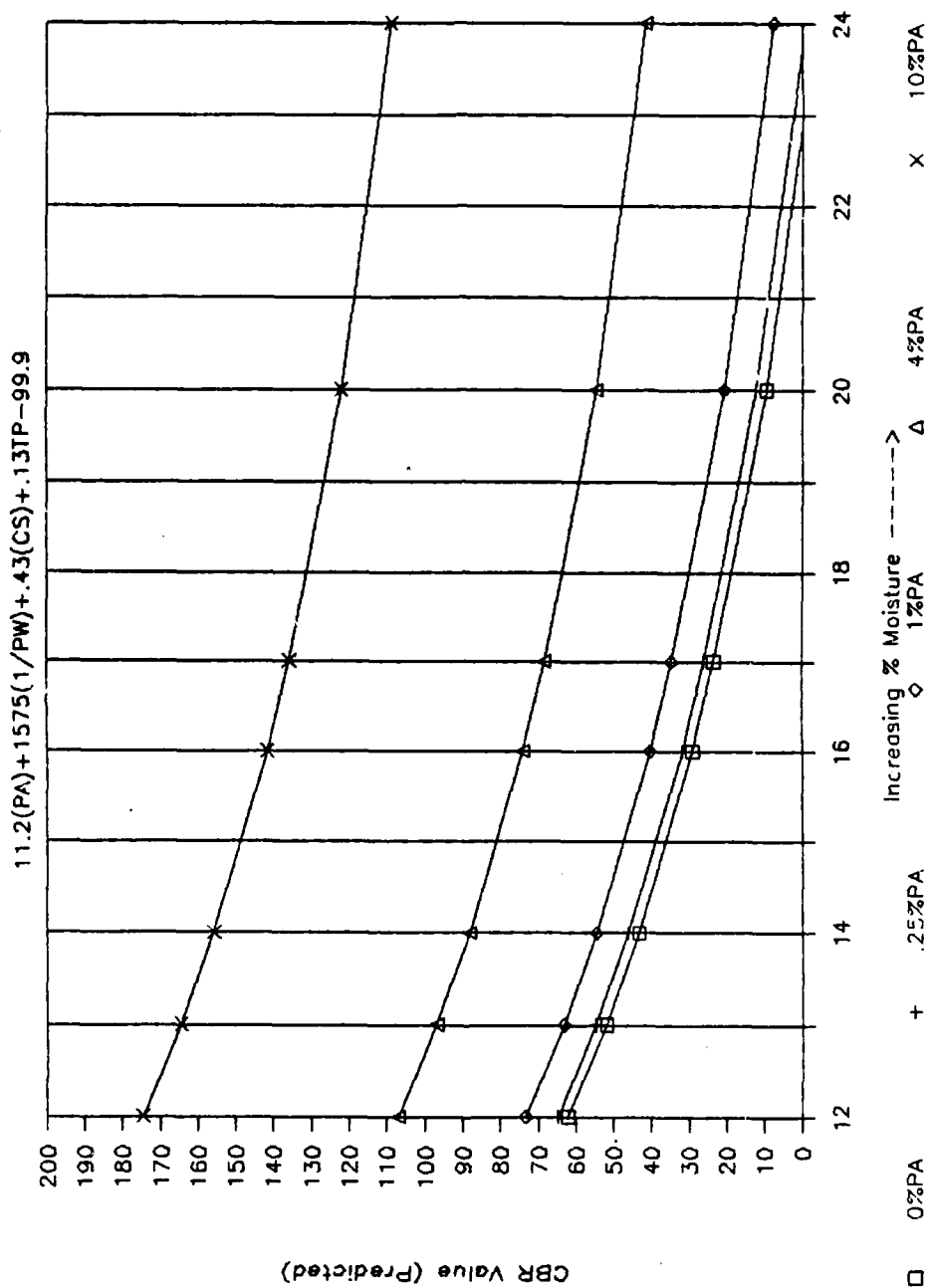


FIGURE 5.14 CBR vs. % Moisture (IP = 90 Deg; CS = 60%)



curves in general emphasize the degradation of CBR with increasing moisture content and the increasing marginal effect of additive concentration on predicted CBR. Table 5.3 quantifies expected CBR values for various levels of the four selected independent variables.

5.5.2 STRATIFIED REGRESSION MODELLING. (BY TEMPERATURE)

A stratification of the data by temperature was effected yielding the following models through use of stepwise regression analysis. Layered plots of these models are provided in Figures 5.15 through 5.19 and Table 5.4:

Model for Temperature = 40°F

$$\text{CBR} = -101.4 + 7.1(\text{PA}) + 1684 (1/\text{PM}) + 0.54(\text{CS})$$

$$(R^2 = 0.82) \quad (5.39)$$

Model for Temperature = 65°F

$$\text{CBR} = -54.6 + 12.3(\text{PA}) + 1288(1/\text{PM}) \quad (R^2 = 0.83) \quad (5.40)$$

Model for Temperature = 90°F

$$\text{CBR} = -74.6 + 14.37(\text{PA}) + 1683(1/\text{PM}) \quad (R^2 = 0.76) \quad (5.41)$$

**TABLE 5.3 PREDICTED CBR VALUES FOR SPECIFIED LEVELS OF
INDEPENDENT VARIABLES**

MODEL 3T-1: CS = 40% ; TP = 40 deg

		%ADDITIVE						
	54	0	0.25	1	4	5	10	20
%MOISTURE								
12	54	54	57	65	99	110	167	279
13	44	44	47	55	89	100	157	269
14	35	35	38	47	80	92	148	260
16	21	21	24	33	66	78	134	246
17	16	16	18	27	61	72	128	241
20	2	2	5	13	47	58	114	227
24	-11	-11	-9	6	34	45	101	214

MODEL 3T-2: CS = 40% TP = 65 deg

		%ADDITIVE						
	58	0	0.25	1	4	5	10	20
%MOISTURE								
12	58	58	60	69	103	114	170	283
13	47	47	50	59	92	104	160	272
14	39	39	42	50	84	95	151	264
16	25	25	28	36	70	81	137	250
17	19	19	22	30	64	75	131	244
20	5	5	8	16	50	61	118	230
24	-8	-8	-5	3	37	48	104	217

MODEL 3T-5: CS = 50%; TP = 65 deg

		%ADDITIVE						
	70	0	0.25	1	4	5	10	20
%MOISTURE								
12	62	62	65	73	107	118	174	287
13	52	52	55	63	97	108	164	277
14	43	43	46	54	88	99	156	268
16	29	29	32	40	74	85	142	254
17	23	23	26	35	68	80	136	248
20	9	9	12	21	54	66	122	234
24	-4	-4	-1	8	41	53	109	221

MODEL 3T-9: CS = 60%; TP = 90 deg

		%ADDITIVE						
	62	0	0.25	1	4	5	10	20
%MOISTURE								
12	62	62	65	73	107	118	174	287
13	52	52	55	63	97	108	164	277
14	43	43	46	54	88	99	156	268
16	29	29	32	40	74	85	142	254
17	23	23	26	35	68	80	136	248
20	9	9	12	21	54	66	122	234
24	-4	-4	-1	8	41	53	109	221

		%ADDITIVE						
	62	0	0.25	1	4	5	10	20
%MOISTURE								
12	62	62	65	73	107	118	174	287
13	52	52	55	63	97	108	164	277
14	43	43	46	54	88	99	156	268
16	29	29	32	40	74	85	142	254
17	23	23	26	35	68	80	136	248
20	9	9	12	21	54	66	122	234
24	-4	-4	-1	8	41	53	109	221

TABLE 5.4 PREDICTED CBR VALUES FOR SPECIFIED LEVELS
OF INDEPENDENT VARIABLES STRATIFIED BY
TEMPERATURE

MODEL 2T-1: TEMPERATURE = 40 DEGREES; CS = 40%

%MOISTURE	%ADDITIVE						
	0	0.25	1	4	5	10	20
12	60	62	68	89	96	132	203
13	50	51	57	78	85	121	192
14	40	42	48	69	76	111	183
16	25	27	33	54	61	96	167
17	19	21	26	48	55	90	161
20	4	6	11	33	40	75	146
24	-10	-8	-3	19	26	61	132

MODEL 2T-2: TEMPERATURE = 40 DEGREES; CS = 50%

%MOISTURE	%ADDITIVE						
	0	0.25	1	4	5	10	20
12	66	68	73	94	101	137	208
13	55	57	62	83	91	126	197
14	46	48	53	74	81	117	188
16	31	33	38	59	66	102	173
17	25	26	32	53	60	96	167
20	10	12	17	38	45	81	152
24	-4	-3	3	24	31	67	138

MODEL 2T-3: TEMPERATURE = 40 DEGREES; CS = 60%

%MOISTURE	%ADDITIVE						
	0	0.25	1	4	5	10	20
12	71	73	78	100	107	142	213
13	60	62	68	89	96	131	203
14	51	53	59	80	87	122	193
16	36	38	43	65	72	107	178
17	30	32	37	58	65	101	171
20	15	17	22	44	51	86	157
24	1	3	8	29	37	72	143

MODEL 2T-4: TEMPERATURE = 65 deg; (CS NOT IN MODEL)

%MOISTURE	%ADDITIVE						
	0	0.25	1	4	5	10	20
12	53	56	65	102	114	176	299
13	44	48	57	94	106	168	291
14	37	40	50	87	99	161	284
16	26	29	38	75	88	149	273
17	21	24	34	71	83	145	268
20	10	13	22	59	71	133	257
24	-1	2	11	48	61	122	246

MODEL 2T-5: TEMPERATURE = 90 deg (CS NOT IN MODEL)

%MOISTURE	%ADDITIVE						
	0	0.25	1	4	5	10	20
12	66	69	80	123	138	209	353
13	55	59	69	112	127	199	342
14	46	49	60	103	118	189	333
16	31	34	45	88	102	174	310
17	24	28	39	82	96	160	311
20	10	13	24	67	81	153	297
24	-4	-1	10	53	67	139	283

FIGURE 5.15 CBR VS. MOISTURE (a TP = 40 DEG; CS= 40%)

$$CBR = 7.1(PA) + 1684(1/PW) + .54(CS) - 101.4$$

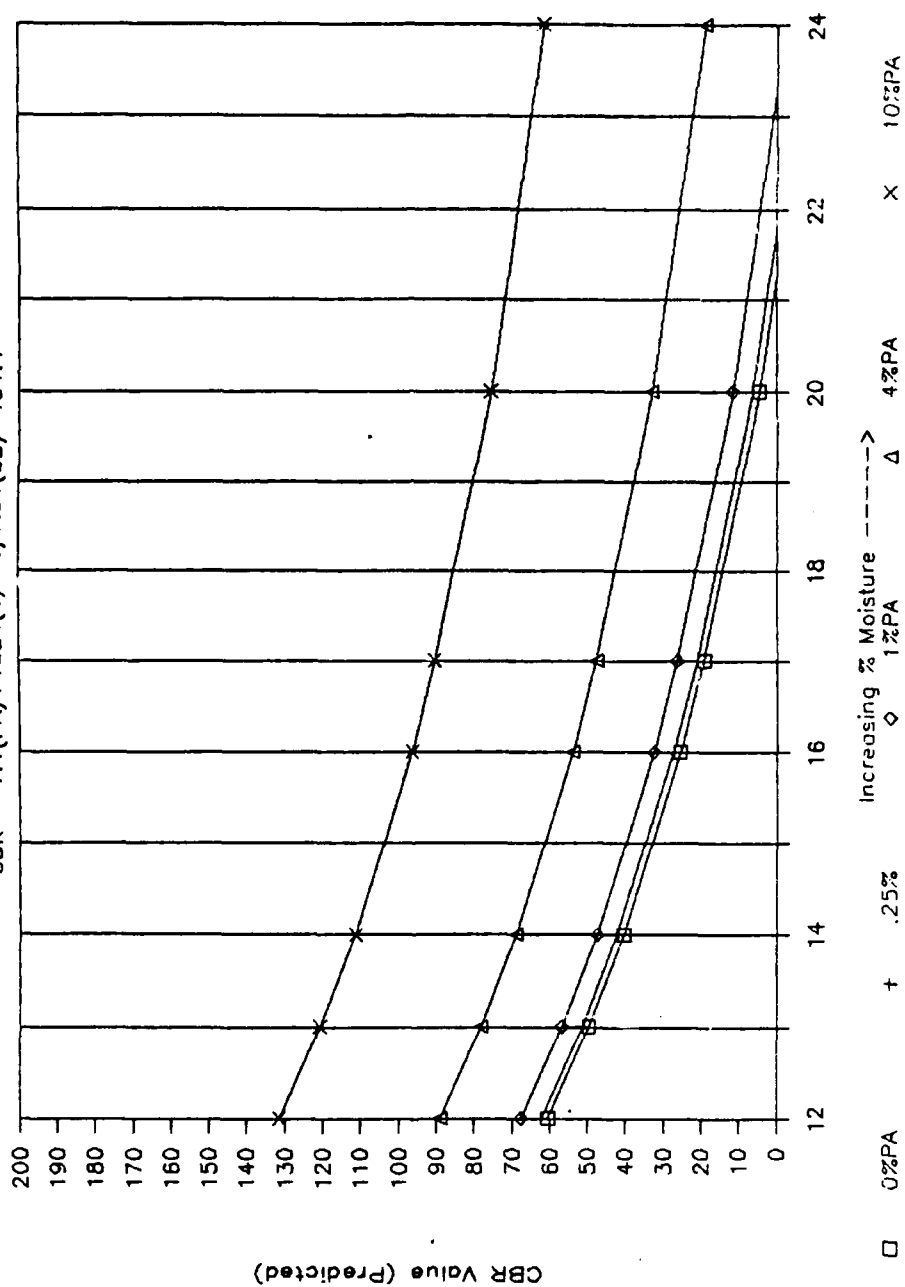


FIGURE 5.16 CBR vs. Moisture (a TP = 40 DEG; CS = 50%)

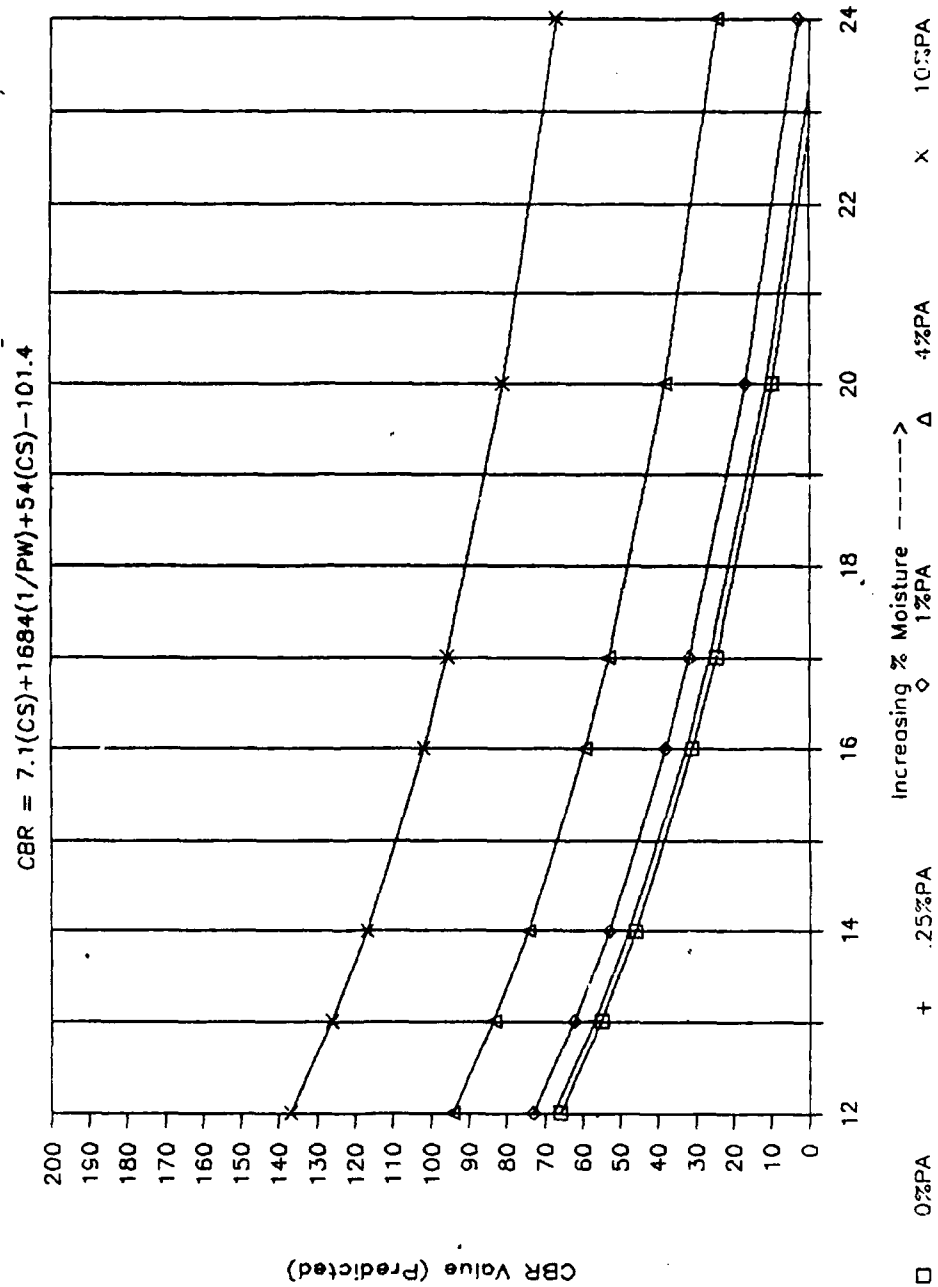


FIGURE 5.17 CBR vs. MOISTURE (a TP = 40 DEG; CS = 60%)

$$CBR = 7.1(PA) + 1684(1/PW) + .54(CS) - 101.4$$

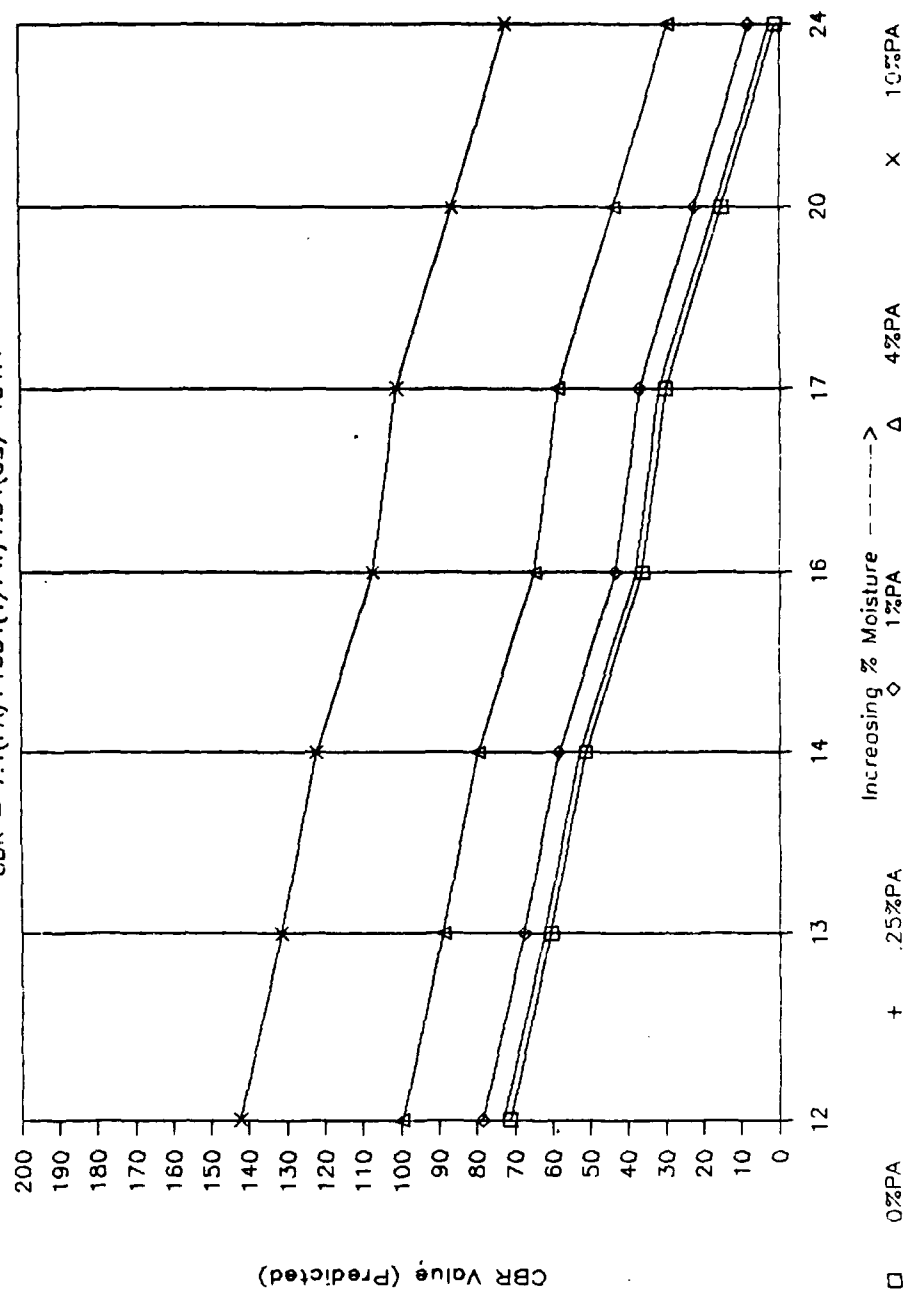


FIGURE 5.18 CBR VS. MOISTURE (@ TP = 65 DEG; CS = N/A)

$$\text{CBR} = 12.3(\text{PA}) + 1288(1/\text{PW}) - 54.6$$

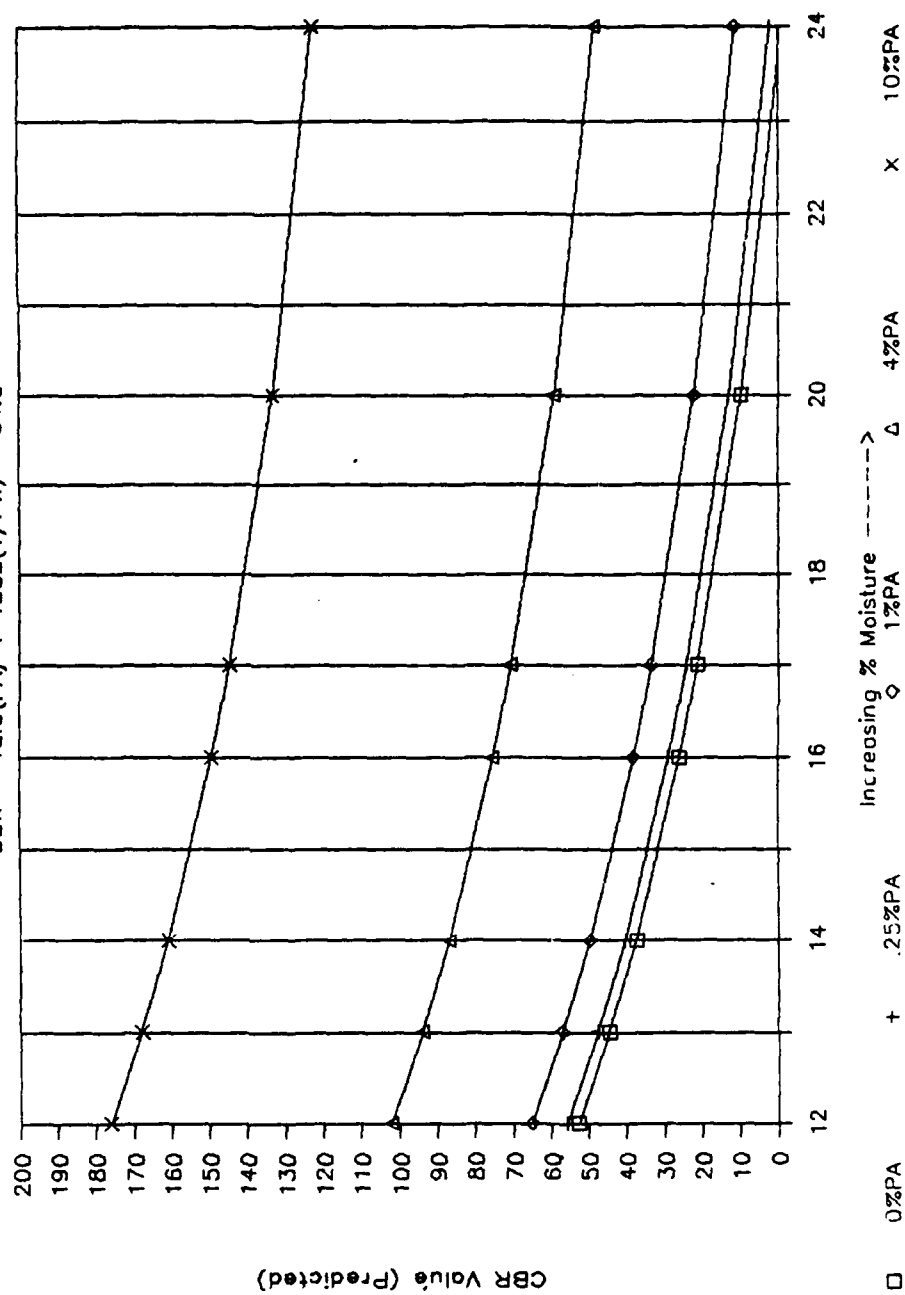
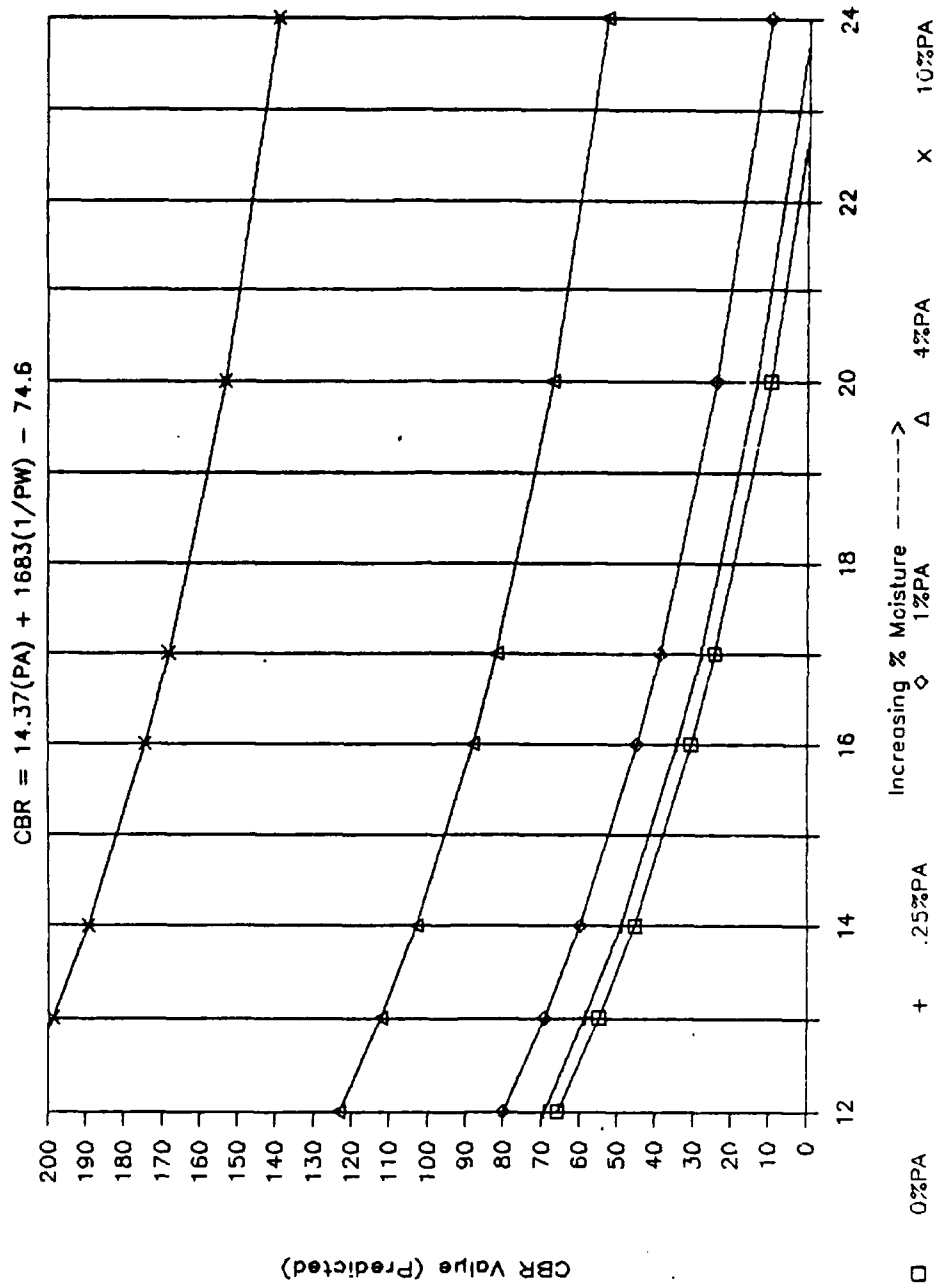


FIGURE 5.19 CBR vs. Moisture (@ TP = 90 Deg; CS = N/A)



5.5.3 STRATIFIED REGRESSION MODELLING (BY CLAY-SILT RATIO)

In consonance with the behavior of the clay-silt system for various levels of moisture content, a stratification by clay-silt ratio shows in Figures 5.1, 5.2, and 5.3 that at a clay-silt ratio (C/S) of 0.4 an inverse and quadratic concave upward moisture trend exists, at C/S = 0.5, a purely inverse moisture trend predominates, while at C/S = 0.6, an inverse and quadratic concave downward trend are both represented.

Guided by these observations, the regression modelling by clay-silt ratio stratification was effected. The stepwise regression modelling at a clay-silt ratio of 0.4 and 0.6 supported the hypothesis that both an inverse and quadratic trend exist, at the 5% significance level. At C/S = 0.5 only an inverse moisture content term was admitted. The temperature term was not significant at the 5% level. The resulting models, illustrated in Figures 5.20 to 5.22 and Table 5.5, are shown below:

Model for Clay-Silt Ratio = 0.4

$$\text{CBR} = -411 + 13.4(\text{PA}) + 5164(1/\text{PM}) + 0.39(\text{PM}^2) \quad (R^2 = 0.88) \quad (5.42)$$

Model for Clay-Silt Ratio = 0.5

$$\text{CBR} = -75.65 + 10.1(\text{PA}) + 1693(1/\text{PM}) \quad (R^2 = 0.85) \quad (5.43)$$

FIGURE 5.20 CBR vs. MOISTURE (CS = 40%; TP = N/A)

$$\text{CBR} = 5164(1/\text{PW}) + 13.4(\text{PA}) + .39(\text{PW})^2 - 411$$

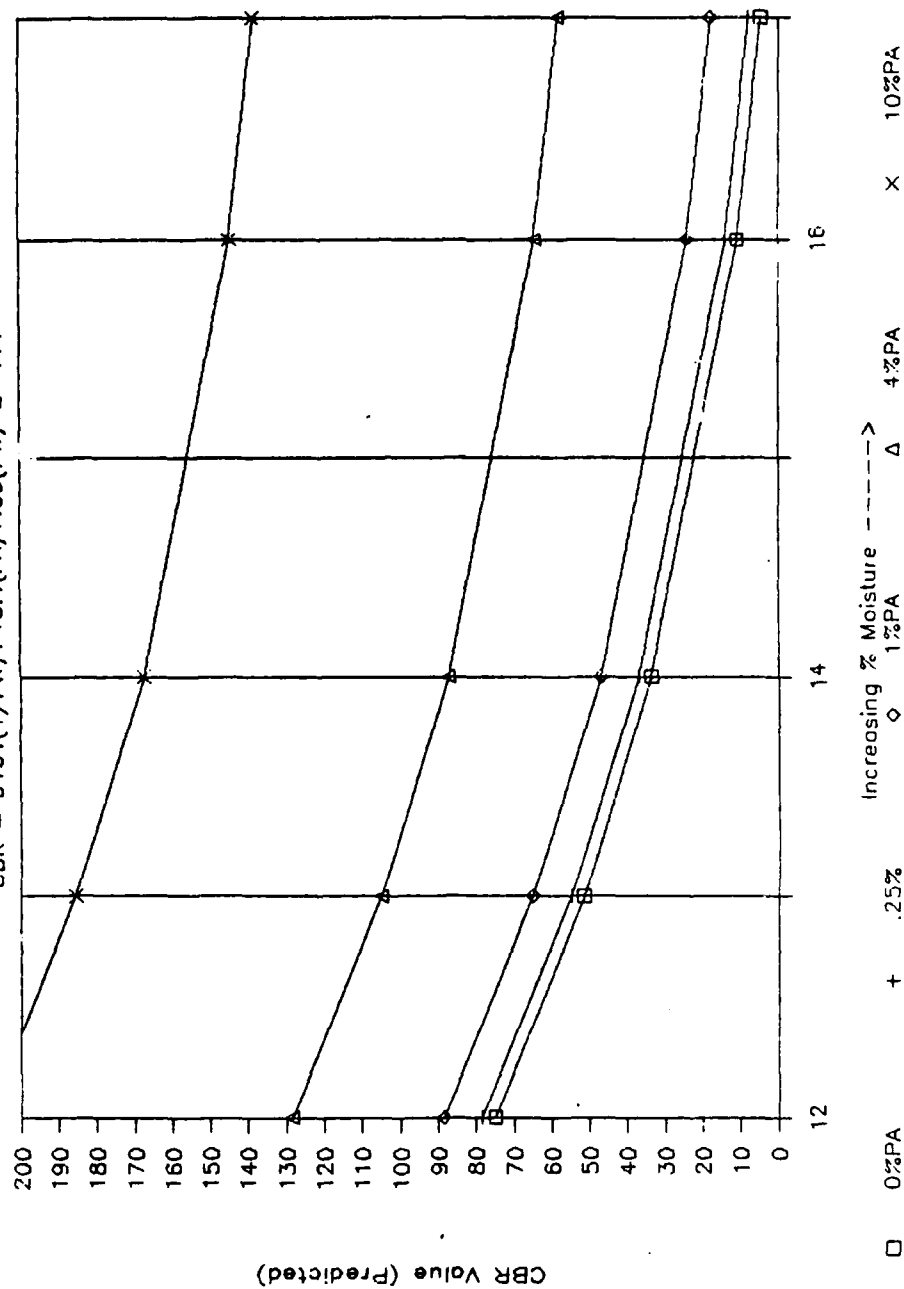


FIGURE 5.21 CBR vs. Moisture (CS = 50%; TP = N/A)

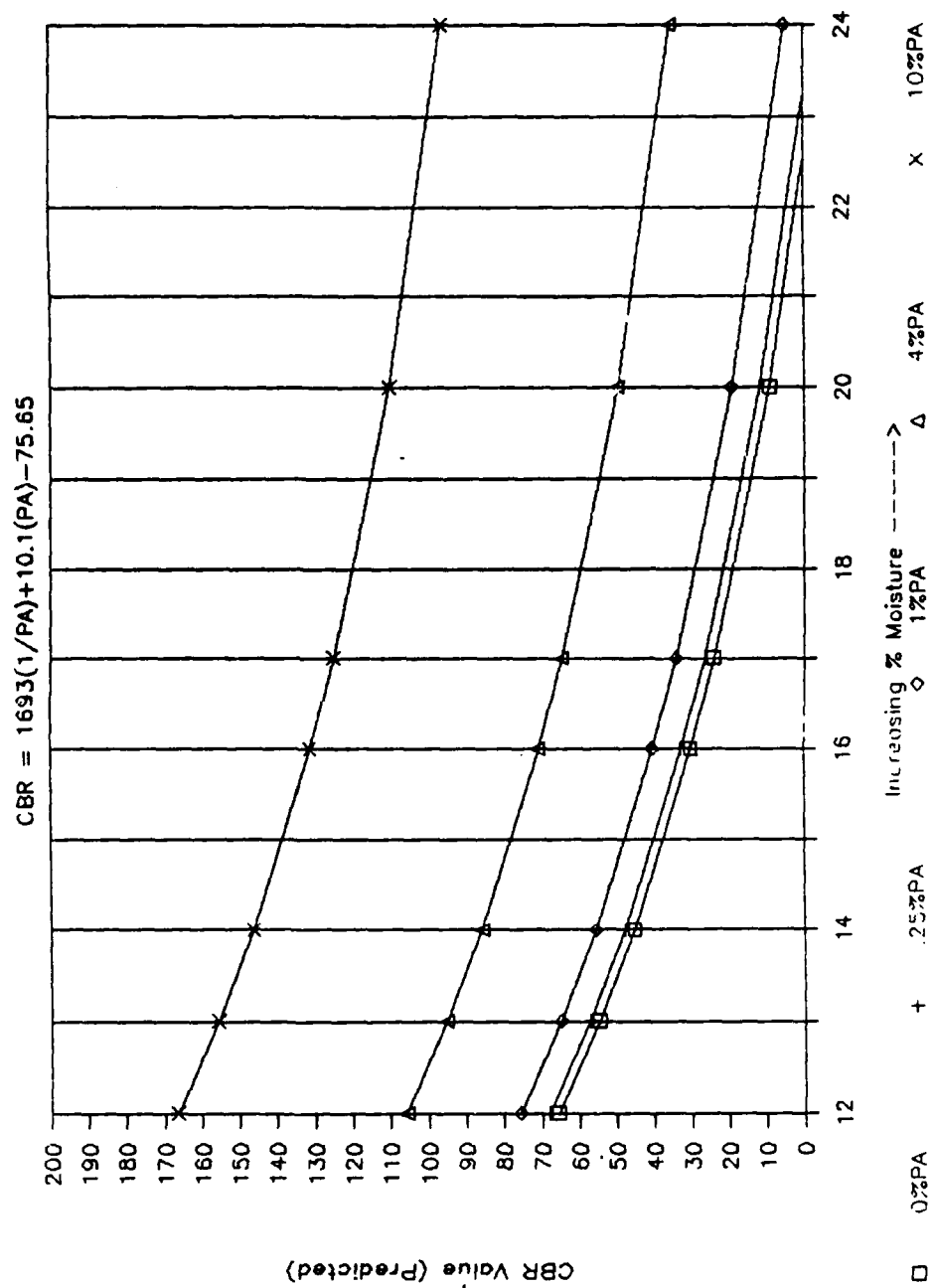


FIGURE 5.22 CBR vs. MOISTURE (CS = 60%; TP = N/A)

$$\text{CBR} = -1785(1/\text{PW}) + 10.2(\text{PA}) - .21(\text{PW})^2 + 233$$

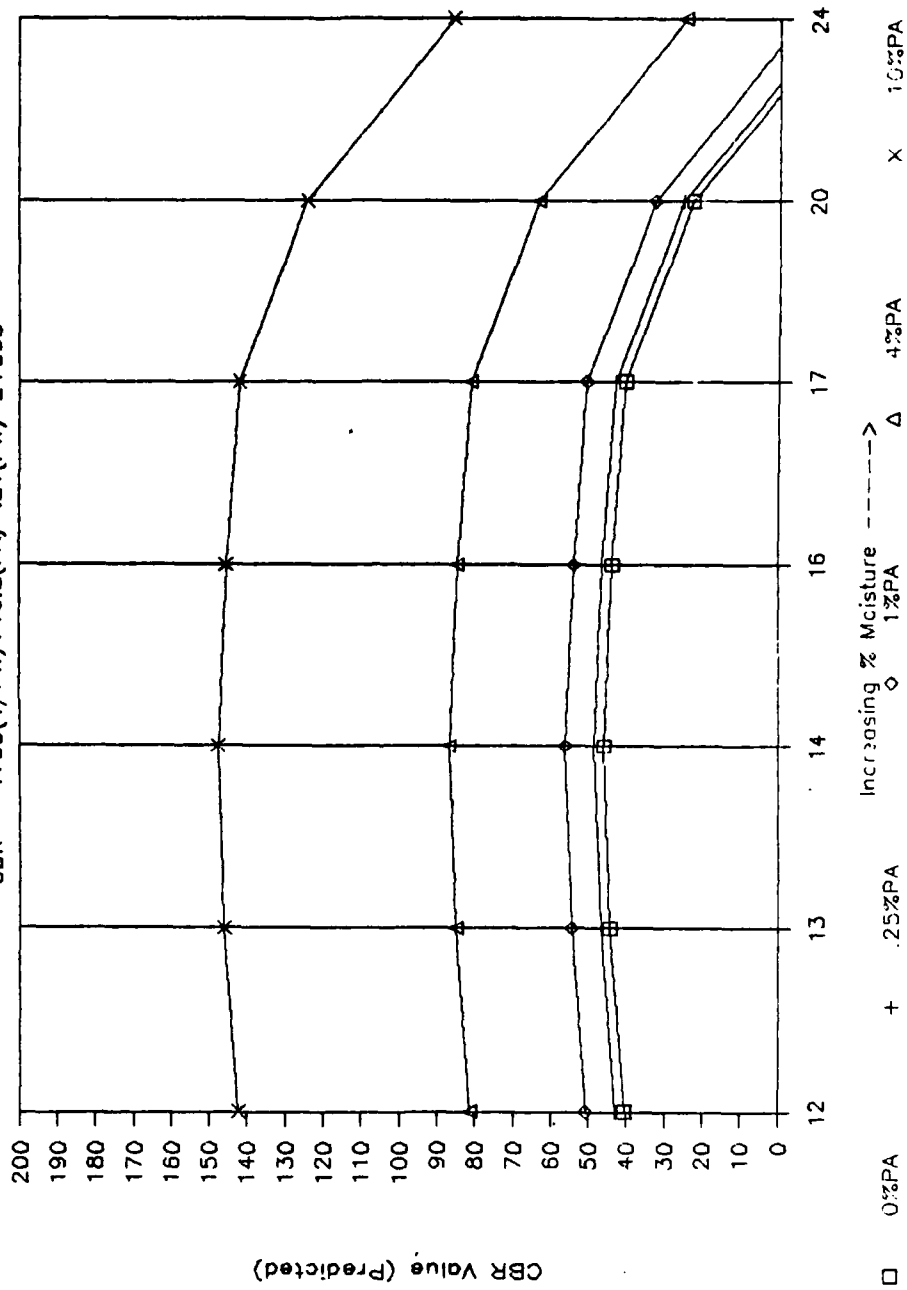


TABLE 5.5 PREDICTED CBR VALUES FOR SPECIFIED LEVELS OF INDEPENDENT VARIABLES (STRATIFIED BY C/S RATIO)

MODEL 4T-1: CS = 40% (TP NOT IN MODEL)

		%ADDITIVE						
	75	0	0.25	1	4	5	10	20
%MOISTURE								
12	75	75	78	88	128	142	209	343
13	52	52	55	65	105	118	185	319
14	34	34	37	47	87	101	167	301
16	11	11	14	24	64	78	145	278
17	4	4	8	18	58	71	138	272
20	2	2	5	15	55	69	136	270
24	27	27	30	40	80	94	161	295

MODEL 4T-2: CS = 50% (TP NOT IN MODEL)

		%ADDITIVE						
	65	0	0.25	1	4	5	10	20
%MOISTURE								
12	65	65	68	76	106	116	166	268
13	55	55	57	65	95	105	156	257
14	45	45	48	55	86	96	146	247
16	30	30	33	40	71	81	131	237
17	24	24	26	34	64	74	125	226
20	9	9	12	19	49	60	110	211
24	-5	-5	-3	5	35	45	96	197

MODEL 4T-5: CS = 60% (TP NOT IN MODEL)

		%ADDITIVE						
	41	0	0.25	1	4	5	10	20
%MOISTURE								
12	41	41	43	51	81	91	142	244
13	44	44	47	55	85	95	146	248
14	46	46	49	56	87	97	148	249
16	44	44	46	54	84	95	145	247
17	40	40	43	51	81	91	142	244
20	22	22	25	33	63	73	124	226
24	-16	-16	-13	-6	25	35	86	187

Model for Clay-Silt Ratio = 0.6

$$\text{CBR} = 233 + 10.2(\text{PA}) - 785(1/\text{PM}) - 0.21(\text{PM})^2$$

($R^2 = 0.79$) (5.44)

5.6 SOAKED TEST CBR ANALYSIS

5.6.1 General Discussion:

A limited number of soaked test data (22 points) were generated and analyzed using regression analysis. The soaked test data were obtained at a constant bath curing temperature of 63°F. The curing period was between three and five days. The initial sample moisture contents of molding were either at 13%, 17% or 21%. The final saturated moisture content obtained varied with the level of other variables for the particular experimental point but was between 17% and 33%, 17% being associated with the highest level of additive used and 33% the case of no epoxy additive. The highest CBR obtained was 77.7 under soaked condition at 4% additive level, 17% and 19% molding and final moisture contents respectively, C/S ratio = 0.6, bulk and dry density 119/102 lb/cu ft respectively, with cylindrical crack patterns on testing.

5.6.2 SOAKED CBR MODEL (Molding Moisture Content Specification)

Using the molding moisture content as input into the model, the regression model obtained is:

$$\text{CBR} = -127.84 + 16.13(\text{PA}) + 1.23(\text{DD}) \quad (R^2 = 0.92)$$

where: (5.45)

DD is the dry density (lbs/cu ft)

CBR and PA are as specified previously.

Incorporating interaction terms into the stepwise regression procedure, at 5% level of significance, the model obtained is:

$$\text{CBR} = -6.88 + 1.0.6(\text{PM} \times \text{PA}) \quad (R^2 = 0.91)$$

where : (5.46)

PM is molding moisture content

Other terms as previously defined.

5.6.3 SOAKED CBR MODEL (Final Saturated Moisture Content Specification)

Using the final soaked moisture content as input into the model, the regression model obtained is:

$$\text{CBR} = -7.54 + 16.63(\text{PA}) \quad (R^2 = 0.89)$$

where: (5.47)

CBR = California bearing ratio

PA = Additive percentage.

Incorporating interaction terms into the stepwise regression procedure at the 5% level of significance, the model obtained is:

$$\text{CBR} = 13.23 + 15.77(\text{PA}) - 1.37(\text{PM} \times \text{CS}) \quad (R^2 = 0.91)$$

where: (5.48)

PM = final saturated moisture content

Other terms as defined previously.

In general, the CBR values obtained under the soaked condition were lower than under the dry conditions. The degradation of CBR, compared to the corresponding dry test cases, was pronounced for samples with 1% additive with molding moisture content of 24% or greater. At the 4% level, the degradation of CBR was comparatively less pronounced for a wide range of final soaked moisture content, i.e. 17-33%. The lowest CBR value obtained was 36.2 and the highest 77.7.

This observation suggests the possible use of hydrophilic epoxy hardeners such as in the amino-amine category for securing of possibly greater strength and enhanced performance in the presence of moisture.

DISCUSSION/CONCLUSIONS:

6.1 General Discussion

In problem airport sites where an exclusive preponderance of clay and silt exists, the use of epoxy resin as a stabilizing agent is a viable method of improving the bearing strength of clay/silt mixtures. This assertion is based on the analysis of experimental data obtained through the stabilization of silt-clay systems using a two part epoxy system. The first is a Bisphenol A/Epichlorohydrin resin and the other a Polyamide hardener.

The CBR values obtained from the experimental test runs were either at one or three days after thermal soaking in a test chamber regulated to either 40°F, 65°F or 90°F. A limited number of soaked tests were also made.

6.2 CONTROL CLAY-SILT SYSTEM RESULTS:

For the control case analysis involving experimentation at zero additive level, the moisture content levels established were guided by the compactability of the clay-silt mixture. The lower threshold of moisture content, below which the sample was so powdery that it could not be compacted, was 12%. The higher limit of moisture content, above which the sample was too plastic for compaction was 24%.

The influence of moisture was found to be profound in affecting variations in CBR values. For moisture contents less than 13%, all tested samples produced CBR values greater than 50, if properly compacted. For samples with a lower clay-silt ratio, the drop off of CBR with increasing moisture was very rapid. At

moisture content of 16%, the CBR value was approximately 5 representing a CBR drop off of 15 per unit increase in moisture content over 13%. Samples with a greater percentage of clay held up CBR values better, dropping off to a CBR of 5 at moisture contents in excess of 19% for a C/S of 0.5 and 21% for C/S of 0.6. At moisture contents in excess of 20%, all the samples were in the vicinity of CBR values of 5. In excess of 24%, the CBR values were essentially zero.

In the study by Carpenter and Lytton (6) on the influence of clay particles in affecting the strength behavior of clay-silt systems, it was observed that clay particles maintain an intimate relation with the available moisture that surrounds them, and the affinity with which this moisture is held by the clay particles leads to the existence of clay pore water pressure. The clay-moisture attraction depends on the size of the clay particles, the ions in the moisture and on the surface of the clay mineral. Furthermore, when clay is mixed with silt, electron micrography shows that the clay minerals combine to form a clay skin around the larger silt particles.

Decreases in temperature and moisture especially through freezing causes a reorientation of the clay minerals and larger silt particles leading to marginally increased compressive strength and volumetric contraction due to the enhanced interlocking of the particles. This phenomenon is controlled by the ion concentration and specific surface under freezing conditions. Increase in moisture content increases the clay pore water pressure and reduces the interlocking strength between the

clay and silt explaining the loss in CBR strength.

The attractive potential which can be described as an absorptive force-field effect resulting from Vander Waal's forces is accentuated by low moisture contents. Increasing moisture contents reduce inter-particle spacing and leads to reduced attractive potential and soil strength.

Increases in the clay-silt ratio as shown in Figures 5.5 through 5.7 at fixed and appropriate moisture content levels leads to increasing CBR confirming the work of Carpenter and Lytton (6). At some level of clay-silt ratio greater than 0.4, marginal increases in the CBR value due to increasing moisture content was obtained. In this case the clay skin surrounding the silt particles had reached a state of saturation for all the silt surfaces and no appreciable increases in interlocking strength could be secured.

Dry density values for the unstabilized clay-silt mixture ranged from 91 to 115 lb/cu ft for a moisture content varying from 12% - 24%. The maximum dry density for this range of moisture content varied with the clay-silt ratio and temperature but was within the 13% - 21% moisture band (Figure 6.1). This band gave the rationale for specifying the optimum moisture content parameter at three levels 13%, 17%, and 21% (Figures 6.1 and 6.2).

The dry density values of clay-silt systems are generally smaller than for well graded gravel (133 - 140 lb/cu ft) essentially because gravel has a lower optimum moisture content (about 7%), retains less water and is more amenable to compaction

FIGURE 6.1 DRY DENSITY VS. MOISTURE CONTENT BY CLAY-SILT RATIO BY TEMPERATURE

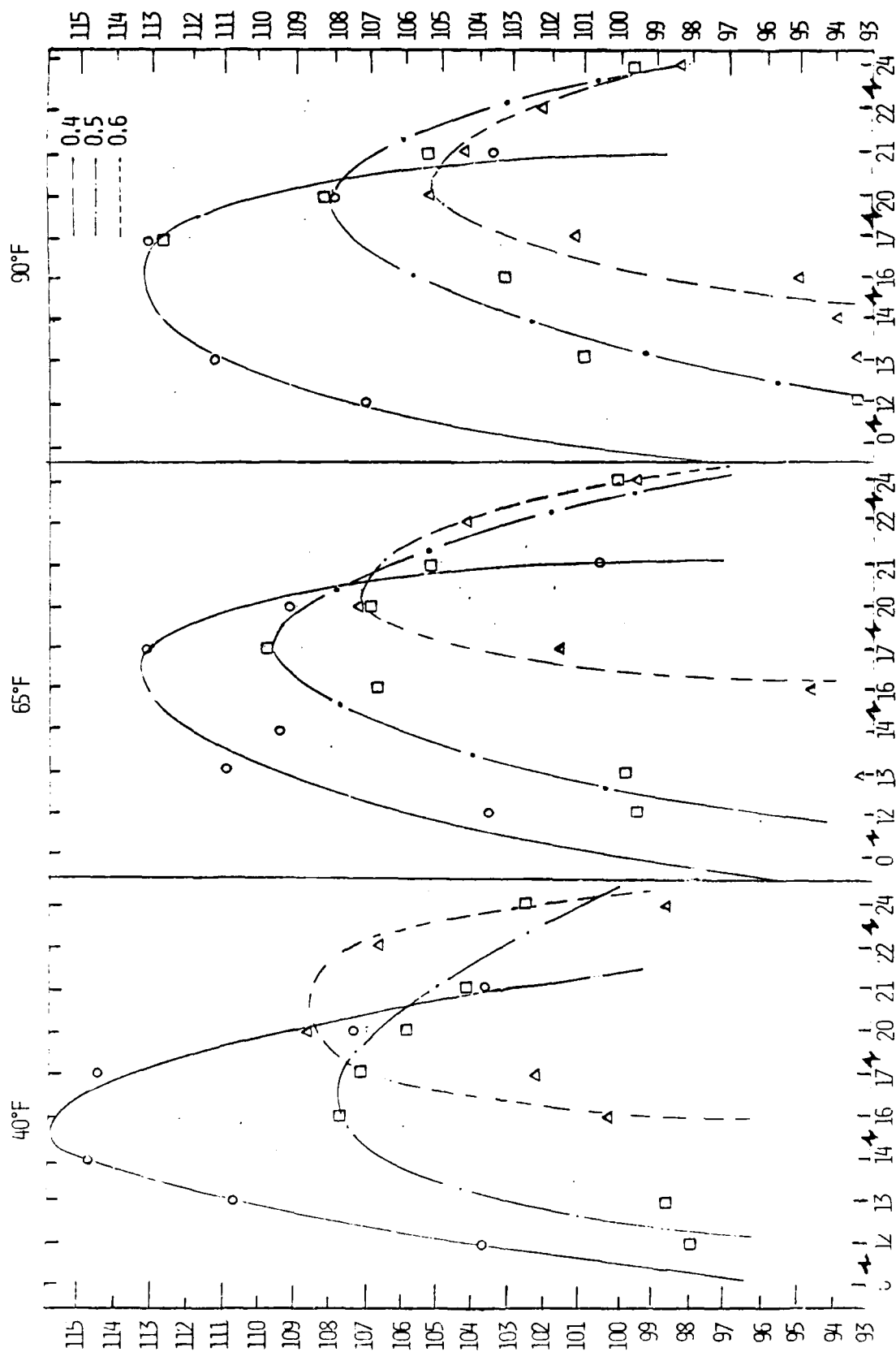
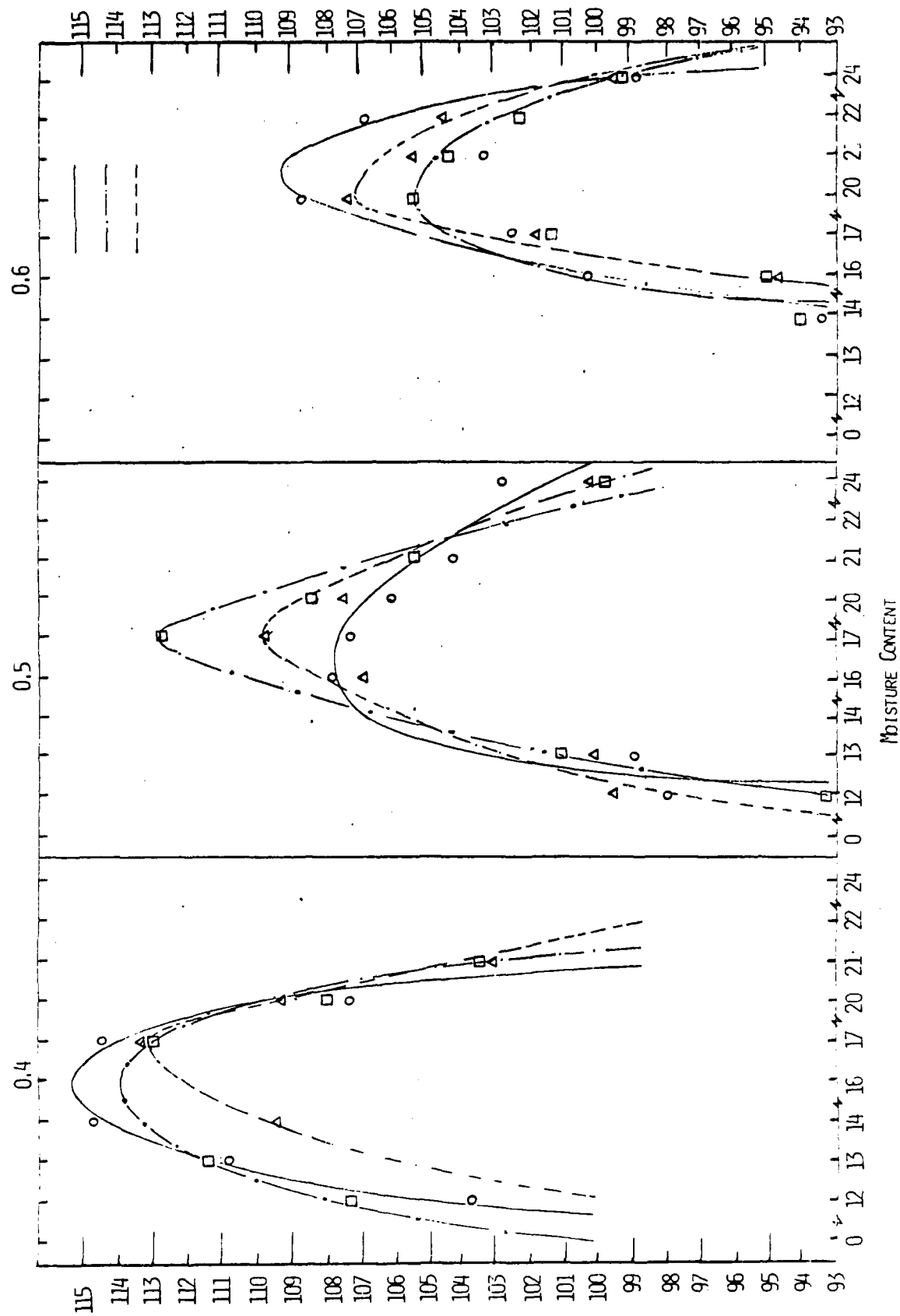


FIGURE 6.2 LAY DENSITY VS. MOISTURE CONTENT BY TEMPERATURE BY CLAY-SILT RATIO



according to Yoder, et al., (14). Some silty clay mixtures hold up a dry density of 120 lb/cu.ft at optimum moisture content of 16%. Yoder, et al., (14) observed a non-linear relationship between CBR and dry density. The CBR dropped off at increasing levels of moisture content. In this research the relationship between CBR and dry density was not as clear cut though similar trends are discernable.

The variations in dry density values for changes in temperature shown in Figure 6.2, are marginally small, but lend credence to the hypothesis that clay minerals under different but progressively smaller temperature regimes undergo a limited amount of reorientation leading to volumetric contraction resulting in marginally higher dry density values.

A limited number of soaked tests were carried out on the unstabilized clay-silt system, and they all registered zero CBR, elucidating the significance of the control of moisture in the stabilization of clay-silt systems.

Though no swell data were obtained, the typical short-term swell for the clay-silt system tested is less than 5% (14). It is expected that the sample swell is correlated both with the development of pore water pressure in the saturated clay-silt system and loss of strength beyond the optimum moisture content. The instability of clay-silt systems finds explanation also in the fact that pore water is called upon to share in the load carrying ability of the system, leading to relative sliding and early failure of the plate-like clay minerals.

Statistical tests performed on the control analysis data show

the existence of highly significant relationships between the variables tested. The regression of the CBR on the experimental variables provided coefficients of determination in excess of 0.8 in most of the cases. These data pertain to dry-CBR testing conditions and suggest that moisture and compaction control are important for the achievement of adequate strength in untreated clay-silt subgrades.

6.3 ADDITIVE CASE CLAY-SILT SYSTEM RESULTS

The design of airport pavements depends on several important inputs one of which is the strength of the subgrade. This parameter, in turn, depends on both the native moisture content and soil density, and in cases involving chemical stabilization, the additive properties. Usually the soaked CBR test is employed in determining the subgrade strength. This represents the worst possible field condition; however, in cases where factors such as ambient moisture content and compaction characteristics are known with certainty, use of the unsoaked CBR strength is justified.

The result of the $3^3 \times 4$ full factorial experiment with the additive variable at 4 levels, 4%, 1%, 1/4%, and 0% has provided previously unknown insight into the effect of changes in such variables as temperature, moisture content and clay-silt ratio on the CBR strength of clay-silt systems.

A confirmation of the results of the control case experimentation has been provided by a subset of the full factorial experimental design corresponding to the 0% additive level. The shapes of the CBR vs. moisture content plots in both

experiments are similar and portray the degradation of CBR that occurs with moisture content. An exception to this trend is the behavior of CBR with increasing moisture content at clay-silt ratios of 0.6 where the concave downward shape of the curve at all temperature levels seems to suggest an increase in CBR with increasing moisture content until about 17% after which a rapid drop in CBR occurs with subsequent increases in moisture content. The research by Yoder, et al., (14) suggests that the optimum moisture content for a soil system with clay-silt ratio of 0.6 lies to the right of the point of maximum CBR and is about 21%.

The plot of CBR vs. moisture content by clay-silt ratio stratification is shown in Figure 6.3 for all tested temperatures.

The general similarity of the plots attests to the internal validity of the generated data. The variations in the graphs index the effect on the CBR of the variable whose change is being studied. In particular, comparison of the plots in Figure 6.3 shows that in the presence of epoxy resin as clay-silt system additive, CBR increases with temperature. Furthermore, the plots demonstrate the positive creep of CBR as temperature changes from 40°F to 90°F.

The gain in CBR with temperature is explained partly by the increased physical bonding between the clay-silt particles made possible by the epoxy resin. The strength gain is also explained by the accelerated curing of the stabilized clay-silt mixture in response to increased curing temperatures.

An examination of Figure 6.4 shows that for a 4% epoxy resin

FIGURE 6.3 CBR vs. MOISTURE CONTENT AT VARIOUS LEVELS OF ALL INDEPENDENT VARIABLES

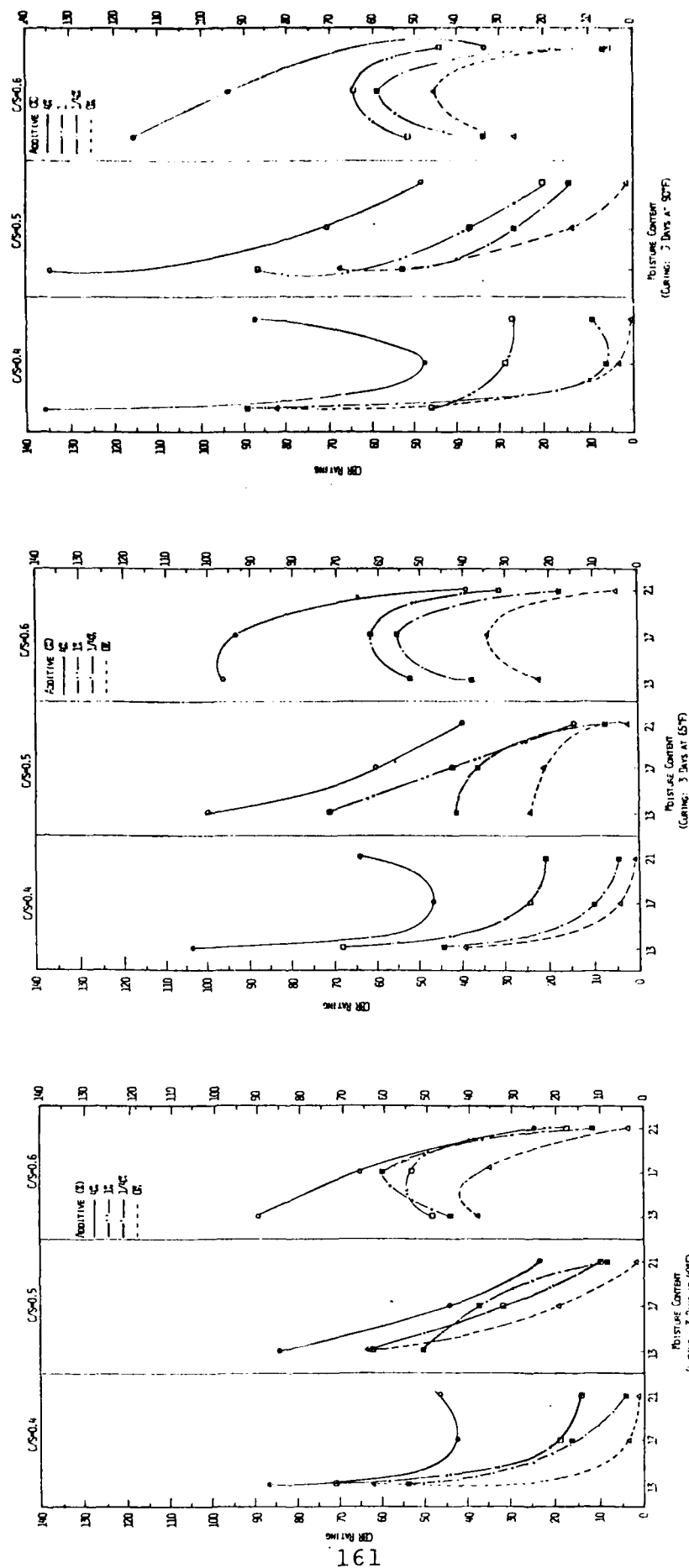
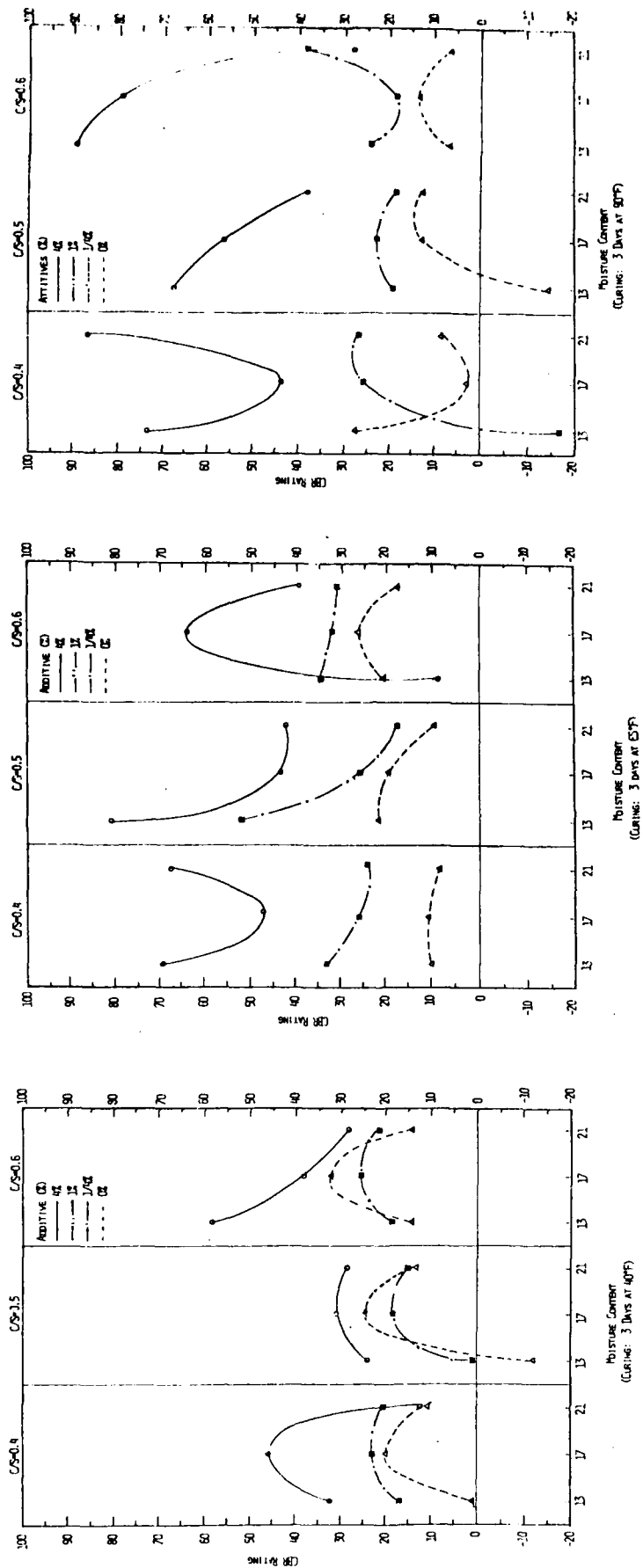


FIGURE 6.4 DIFFERENTIAL VS. MOISTURE CONTENT AT VARIOUS LEVELS OF ALL INDEPENDENT VARIABLES



application at 40°F, the range of CBR improvement varies approximately from 10 to 60 units. At 90°F the CBR increase obtained over the control case due to application of 4% epoxy varies from approximately 27 to 90 CBR units. At lower percentages of epoxy, proportionately lower CBR increases are obtained.

The plot of CBR values in Figures 5.1, 5.2, and 6.3 reveals that at lower clay-silt ratios, the greater relative improvements in CBR are generally possible at higher moisture contents while at higher clay-silt ratios greater relative improvements occur at lower moisture content ranges. Explanation for the relatively better performance of CBR at lower clay-silt ratio (0.4) is that since increases in clay content increases the clay skin around the larger silt particles leading to increased specific surface of the mixture, avenues for effective bonding between the silt particles and epoxy resin additive become increasingly limited in favor of the clay-silt physical bond enhanced by compaction. The relatively weaker clay-silt physical bond fails quickly under shearing forces imposed by the CBR plunger. This leads to lower CBR test results compared to the situation in which a lower clay-silt ratio allows for the formation of only a lower degree of clay-silt bonds in favor of stronger bonds that lead to higher CBR values.

Superimposing the effect of pore water pressure due to increased moisture content on the preceding hypothesis explains the effectiveness of the epoxy resin at higher moisture contents for low clay-silt ratios and at lower moisture content for the

higher clay-silt ratios. The adsorption of water by the flat, high surface area clay particles is smaller for samples with lower clay-silt ratios. Consequently, the effect of pore water pressures in the molded samples is smaller and relatively higher CBR improvements are possible. For samples with higher clay-silt ratios (0.6), the pronounced effect of pore water pressure leads to a further degradation of CBR over and above that resulting from the de-emphasizing of the stronger resin-silt particle bonds due to increased proportion of clay particles. The clay-silt ratio of 0.5 represents roughly the onset of the indifference threshold of CBR improvement due to varying levels of clay particles in the stabilized clay-silt mixture.

The effectiveness of additive treatment in producing CBR values over and above the control case for identical experimental points is calculated and plotted in Figures 5.8, 5.9, 5.10 and 6.4. The increases are generally smaller at 40°F and higher at 90°F. Consistent with the hypothesis enunciated in this research, the greatest CBR increases of 86 and 90 CBR units occur at 90°F and correspond to either low clay-silt ratios of 0.4 and high moisture contents of 21% or high clay-silt ratios of 0.6 and low moisture contents of 13% respectively. At lower moisture contents (13%) application of low additive percentage (1/4%) is not effective in increasing the bearing strength of clay-silt systems. This result, however, may be impacted by clay-silt soil and additive mixing quality.

The use of multivariate analysis of variance technique (MANOVA) on the full factorial data in Table 4.7 supports the

hypothesis that increases in CBR values over and above the untreated soil CBR are significantly affected by additive percentage and temperature and their interactions only.

One of the statistical models developed using regression theory has enabled the development of quick estimates of expected CBR values in the form of the nomograph for clay-silt system CBR prediction in Figure 6.5. The chart is used by first connecting the molding temperature and clay-silt ratio scale values with a straight line that cuts the auxiliary line F1. The intersection with F1 is next connected by a straightline to the molding (optimum) moisture content scale values to yield an intersection on F2 which is finally connected to the additive percentage scale value to yield the predicted CBR.

Regression modelling using the results of soaked CBR tests was effected and showed that additive percentage and the interaction of moisture content and clay-silt ratios were significant in explaining the variations in soaked CBR readings. The highest soaked CBR reading obtained was 77.7 and the lowest 36.2 at the 4% additive level.

6.4 VALIDATION/CORRELATION FOLLOW-UP STUDY

A field correlation study and check on the laboratory values of the data obtained in this research constitutes the second phase of this research effort.

Previous field studies by Yoder, et al., (14) suggest that in some cases, especially for granular materials, the correlations

NOMOGRAPH FOR CLAY-SILT SYSTEM CBR PREDICTION

(STABILIZING AGENT - EPOXY RESIN)

$$CBR = 91.69 + 11.07(PA) - 5.62(PM) + 44.97(CS) + 0.14(TEMP) \quad (R^2=0.78)$$

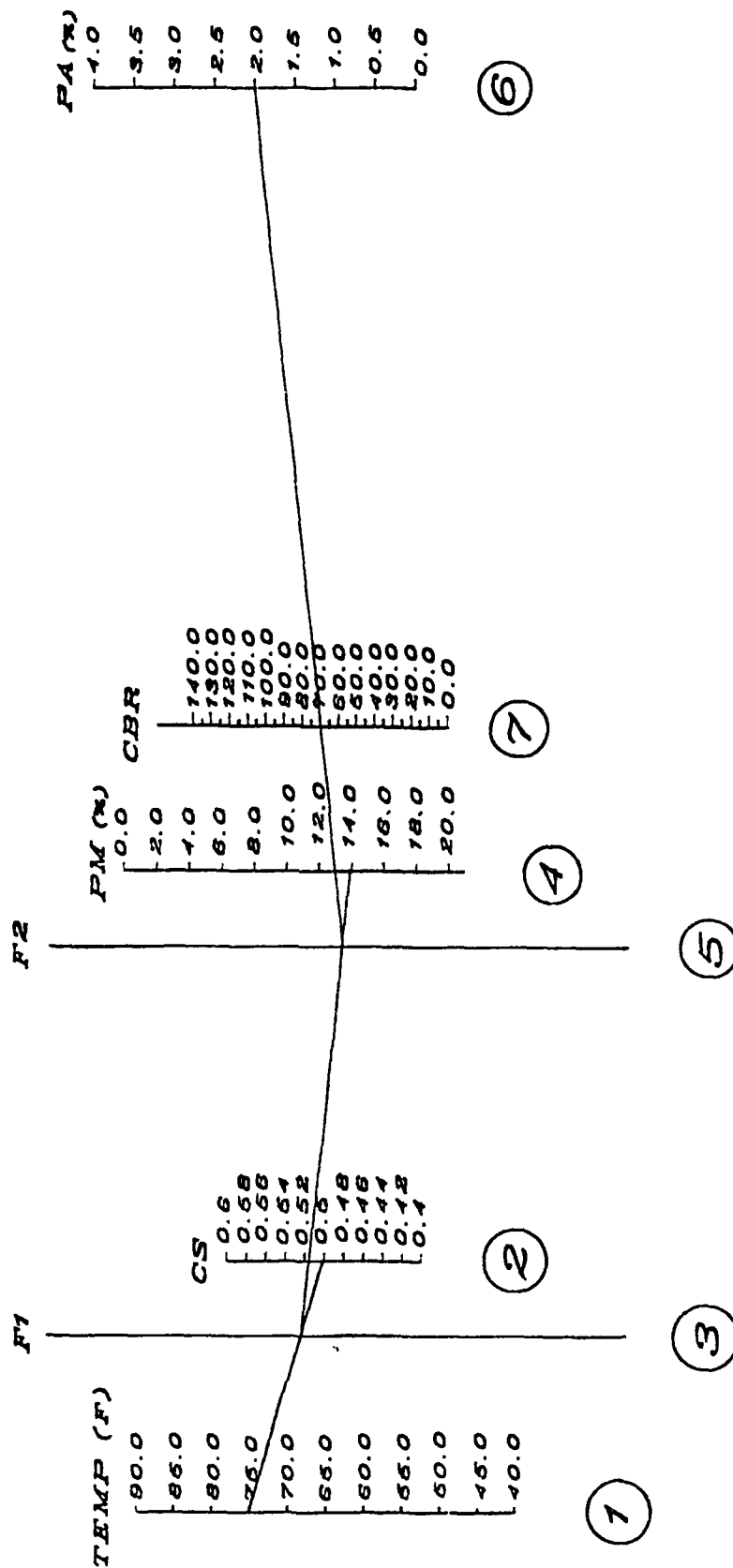


FIGURE 6.5

between field and laboratory CBR test values are erratic, but in most cases for clay-silt systems under identical moisture and density conditions, the two tests will give the same result practically.

Since obtaining identical materials such as silt and clay in the field in the form that duplicates laboratory conditions could prove difficult, the possibility of correlating the laboratory results with a rutting test is considered as an appropriate and viable follow-up validation study for Phase II.

6.5 CONCLUSIONS

In conclusion, the following findings are highlighted:

1. The effectiveness of a two-part epoxy system, Bisphenol A/Epidiloroxyhydrin resin plus a Polyamide hardener in enhancing the soil bearing strength of clay-silt systems, has been demonstrated. This finding is significant considering the poor particle size gradation of clay-silt systems and the inability of most conventional additives to achieve sizeable increases in CBR's such as obtained in this study.
2. Within the ranges of the experimental variables and data tested in this research, the two-part epoxy system studied is effective for additive applications between 1/4% and 4%. The largest CBR's obtained under unsoaked and soaked conditions are 135 and 77 at 4% level of epoxy application respectively.

3. The nomograph for CBR prediction developed from this research effort allows a quick estimate of the expected CBR for specified levels of soil testing variables incorporated in the model. The marginal increase in CBR values due to a percent increase in epoxy resin application is 11.1, the marginal increase due to a percent increase in clay-silt ratio is 0.45 and due to a degree Fahrenheit increase in temperature is 0.14, the marginal degradation of CBR due to a percent increase in moisture level is 5.6.
4. In this study, the influence of moisture content in degrading the CBR has been found to depend on the curing condition, the ratio of clay to silt, and curing temperature. Under unsoaked testing conditions, the onset of CBR degradation occurs at moisture levels of about 14%, 17%, and 18% for clay-silt ratios of 0.4, 0.5, and 0.6 respectively based on a cutoff CBR value of 40. This suggests that moisture control, wherever possible, holds a very important key for the stabilization of clay-silt systems. In addition, the combined effects of clay-silt ratio and temperature were found to be significant in influencing dry density and consequently CBR values. This result is confirmed by the work of Carpenter and Lytton (6) that explains the internal forces at work in clay-silt systems and the contraction and heave behavior of such samples under different temperature regimes.

5. The cost of Epoxy Resin chemical stabilization may be three times the cost of construction (material, labor, overhead) on an unstabilized terrain per cubic yard of clay/silt material stabilized. This cost factor does not take into account the pavement failure costs associated with construction on an unstabilized terrain. The threefold cost factor would vary and probably be lower as the labor content of the construction cost increases other factors remaining constant. Other factors that could conceivably affect this numeric include the prevailing clay/silt soil condition, equipment sophistication, labor efficiency, volume or scale of epoxy resin stabilization, epoxy resin demand and production economics, and other market forces.

6. The impact of high technology Epoxy Resin application techniques could lead to a greater usage of Epoxy Resin for chemical stabilization. The advantages secured using epoxy resins include, i) improved consistency and quality leading to savings in terms of reduced deterioration, ii) accelerated strength attainment resulting in the rapid formation of a dense solid mass capable of withstanding unfavorable weather, chemical attack, and deleterious heavy traffic effects, iii) high technology induced direct cost reduction, iv) reduction in such indirect cost as runway downtime due to repairs, airport closure and costly delays. This partial list of

attributes for the two-part epoxy resin system attests to the significant engineering properties and potential of epoxy resin based applications.

7. This study reinforces and upholds the need for stringent compaction standards, sustained mixing quality, and moisture control for prospective airport pavements constructed on clay-silt terrains. Compaction of the subgrade to specifications is very important, especially for areas subject to rutting due to channelized aircraft traffic. Increased density and reduced moisture content resulting from effective (100%) compaction to specification and provision of effective and adequate drainage will result in higher performance clay-silt subgrades capable of sustaining imposed aircraft loads when treated with such additives as Epoxy Resin.

FIELD VALIDATION
PHASE II
RUTTING TEST

INTRODUCTION

7.1 BACKGROUND

When flexible airport pavements are exposed to various traffic and environmental conditions, their performance and serviceability degrade over their service life in proportion to the severity of the imposed conditions. Two paramount factors generally accepted as responsible for the deterioration of an airport pavement are rutting and fatigue cracking.

When a visco-elastic material, such as asphalt concrete, or a visco-plastic material such as a clay-silt soil is relieved of the superimposed load the deformation response consists of a recoverable and non-recoverable portion which is responsible for the rutting. In the case of a visco-plastic material such as a clay-silt mixture, almost all the imposed strain is non-recoverable.

To be able to ensure such desirable attributes as : 1) comfort, 2) acceptable ride quality both during takeoff and landing, 3) safety, 4) satisfactory performance over service life, and 5) reduced aircraft wear and tear, adequate understanding and control of rutting and fatigue cracking is essential.

7.2 SCOPE

This study examines the rutting response of a stabilized clay-silt system under a selected combination of pavement

conditions and environmental factors. The instantaneous rutting of pavement in response to repetitively applied load was studied. It is assumed or expected that an elastic recovery composed of the rutting exists but is relatively negligible. The mechanism of fatigue cracking is outside the purview of this study.

7.3 DEFINITION

Rutting or permanent deformation, is the progressive accumulation of plastic strain in a pavement system under repetitive load application. The rutting of pavements which typically occur near regions of channelized traffic results from intensive load applications that lead to differential surface deformation under a moving or dynamic wheel load.

7.4 OBJECTIVES

The following objectives were set forth in executing this research:

a) Verification of the effectiveness of the chemical stabilization agent, Bisphenol A/Epichlorohydrin used in conjunction with a polyamide hardener obtained by reacting dimerized linoleic acid with di-ethylene triamine. This stabilization agent was tested on a clay-silt mixture through a field rutting test.

b) Establishment of the relationship between resistance to permanent deformation of a stabilized clay-silt subgrade (rutting) and the level of application of chemical stabilization.

c) Examination of the relationship between field CBR and rutting indices for a prescribed aircraft wheel load for various levels of chemical stabilization of a clay-silt mixture.

d) Determination of the influence of aircraft tire type passes on rut-depth for various levels of application of a clay-silt soil chemical stabilizer.

REVIEW OF LITERATURE

8.1 INTRODUCTION

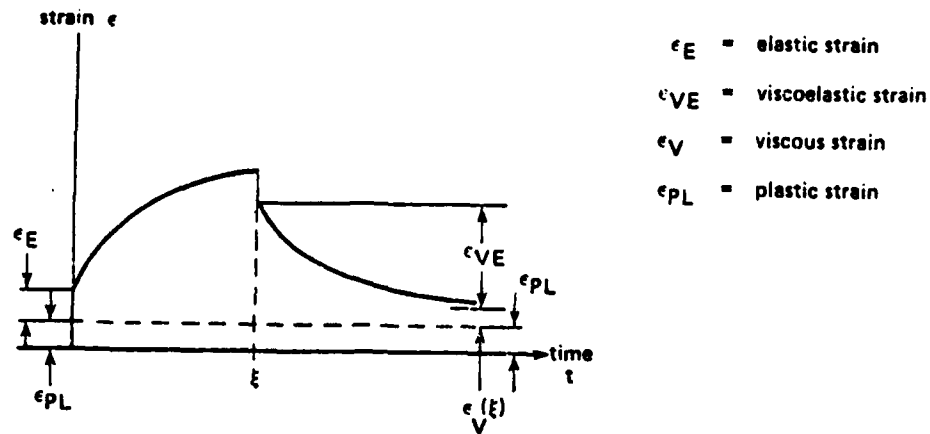
Subgrade rutting resulting in pavement surface distortion can be caused by consolidation of the underlying soil under repetitively applied load. This process may be precipitated either by the superposition of loads much in excess of the design stipulation, by inadequately stabilized subgrades or inadequate design thickness. Pavements under the influence of rutting conditions may require a pavement overlay of thickness determined by standard methods.

Review of literature on rutting indicates that considerable research has been carried out to study the rutting behavior of pavements over time under varying loading and environmental conditions. Generally the deformation of materials in a pavement system under imposed aircraft wheel load is resolvable into three components:

- 1) Elastic strain recovered immediately
- 2) Delayed elastic strain recovered with time.
- 3) Plastic and viscous non-recoverable strain.

Rutting is generally construed as the accumulation of non-recoverable strain (Figure 8.1).

Figure 8.1 Strain versus Time Dependency



Research on prediction of pavement rutting hypothesize two broad types of pavement systems.:

- a) The elastic layer representation of a pavement system with material properties characterized by either the repeated dynamic load test, or the creep test or both.
- b) The visco-elastic layer representation of a pavement system with material properties characterized by means of creep tests.

8.2 PAVEMENT SIMULATION ANALYSIS

The use of these tests recognize the fact that three broad variables affect the rutting response of an aircraft pavement: load application variables, environmental variables, and mix-design variables.

Ullidtz (15) provides a framework for a systems approach to the design, construction and maintenance task of providing transportation at the lowest overall cost to society. An analytical (or mechanistic) method of pavement analysis and also more advanced methods of computer simulation of pavement performance are presented. However the specific problems related to pavements with a gravel or silt surface is not addressed. A design curve is presented incorporating the US Corps of Engineers CBR design method for airfields (Equation 8.1). The curve (Figure 8.2) considers a thickness adjustment factor which accounts for traffic repetition (Equation 8.2).

$$T = P * (1 / (8 * CBR) - 1 / (\pi * P)) \quad (8.1)$$

Where :

T = Thickness of pavement in inches

P = Equivalent single wheel load in pounds

P_r = Tire pressure in psi

$$T_d = K_1 * \log (N) + K_2 \quad (8.2)$$

Where :

N = the number of repetitions and,

K_1 = 0.231 for flexible pavements

K_2 = 0.144 for flexible pavements

FIGURE 8.2 Perm. stress/CBR versus number of loads

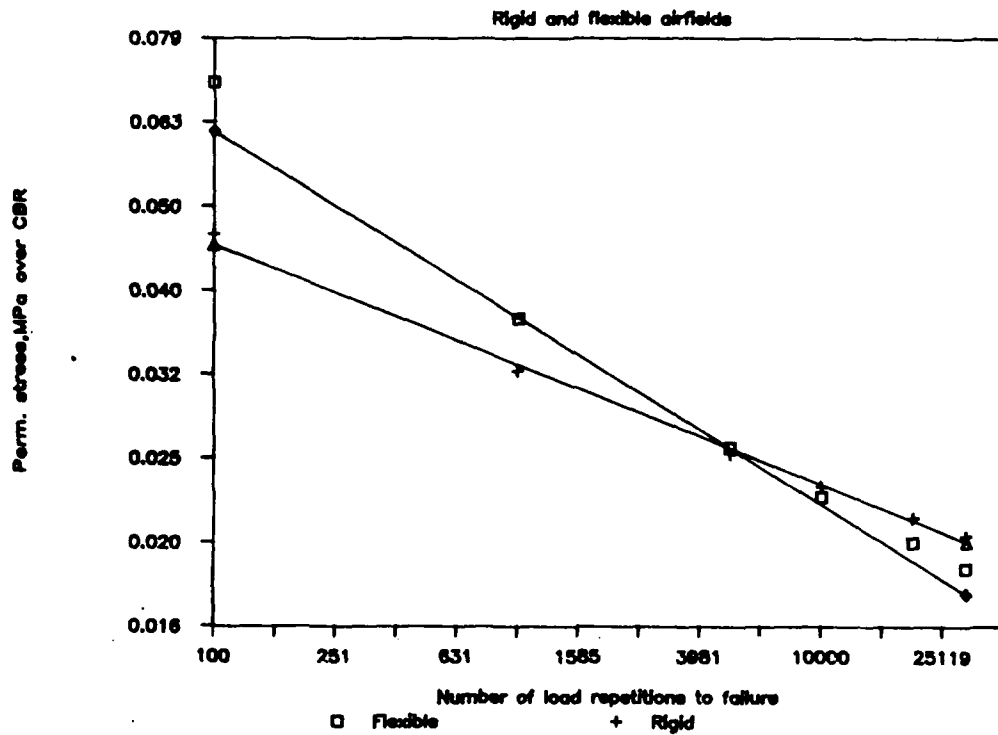


FIGURE 8.2 Ratio of permissible stress (in MPa) over CBR of material versus number of loads to failure, obtained by using Boussinesq's equations on US Army Corps of Engineers design method for airfield pavements (equations (8.1) and (8.2)).

8.3 CLAY SOIL RHEOLOGY

Keedwell (16) in discussing the rheology of clay minerals submits that the mechanical properties of cohesive soils are very much influenced by the atomic and electrical forces which exist between the very small and mainly plate-like clay mineral particles. The level of these forces is determined by the type of clay minerals present and the nature of any dissolved salts in the pore water. Figures 8.3 and 8.4 illustrate the typical card house structure of clay particles and arrangement of atoms in these types of clay mineral, namely Kaolinite, Illite and Montmorillonite. These are made up of predominantly two units, the silica sheet and the gibbsite sheet. The arrangement of these sheets distinguishes one mineral from another though there exists some variation in the nature of the atoms present in the sheets. The net repulsive force between the basal planes tend to open up the structure, causing the soil to swell, while compressive stresses applied to the soil element boundaries have the opposite effect. The normal component of force transmitted across a particle contact zone is the sum of an electrical force of attraction and a force due to the boundary stress. The atoms in any of the clay minerals are constantly oscillating between a mean position with the frequency increasing with temperature. When a particular set of atoms detach themselves from a particular set of neighbors, bond rupture occurs increasing in frequency with temperature, and in the case of a viscous material, this

FIGURE 8.3 ARRANGEMENT OF ATOMS IN CLAY MINERALS

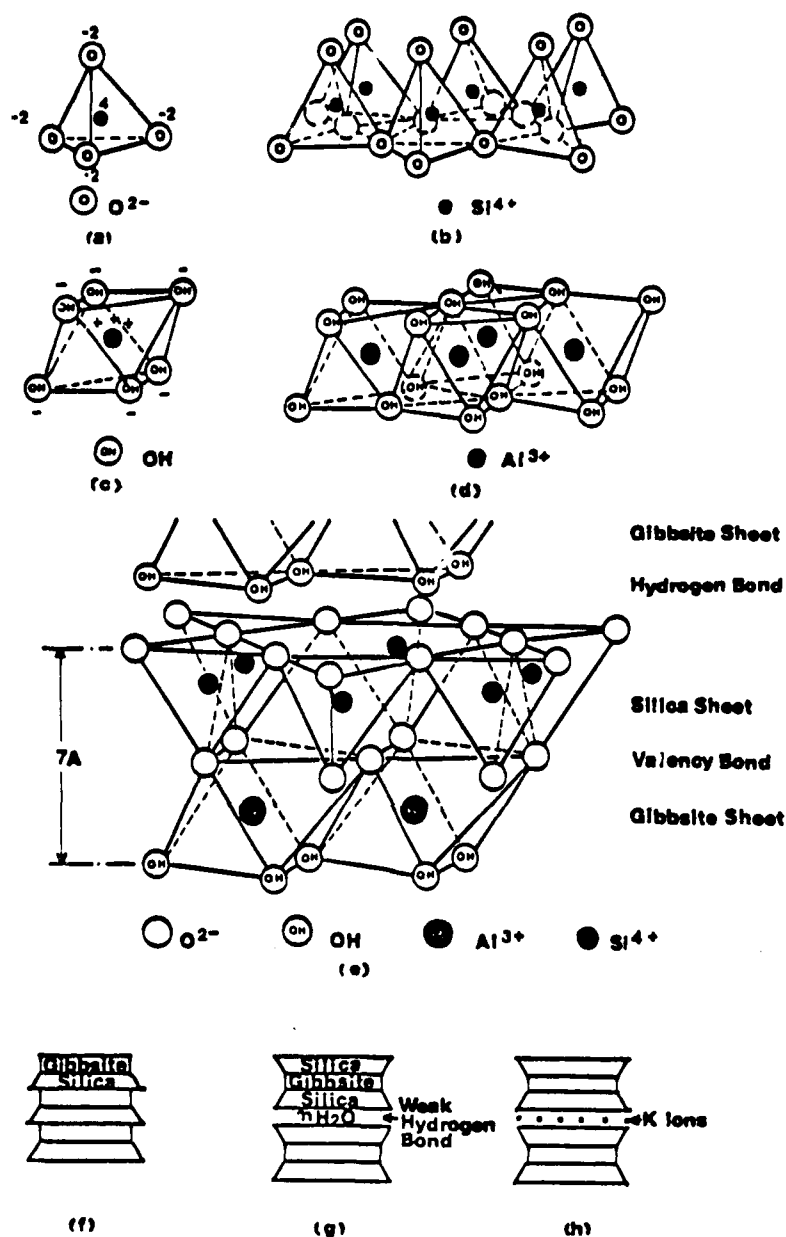
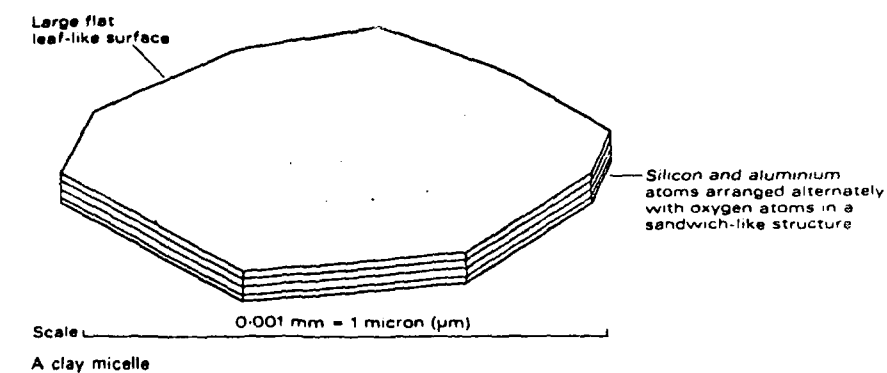
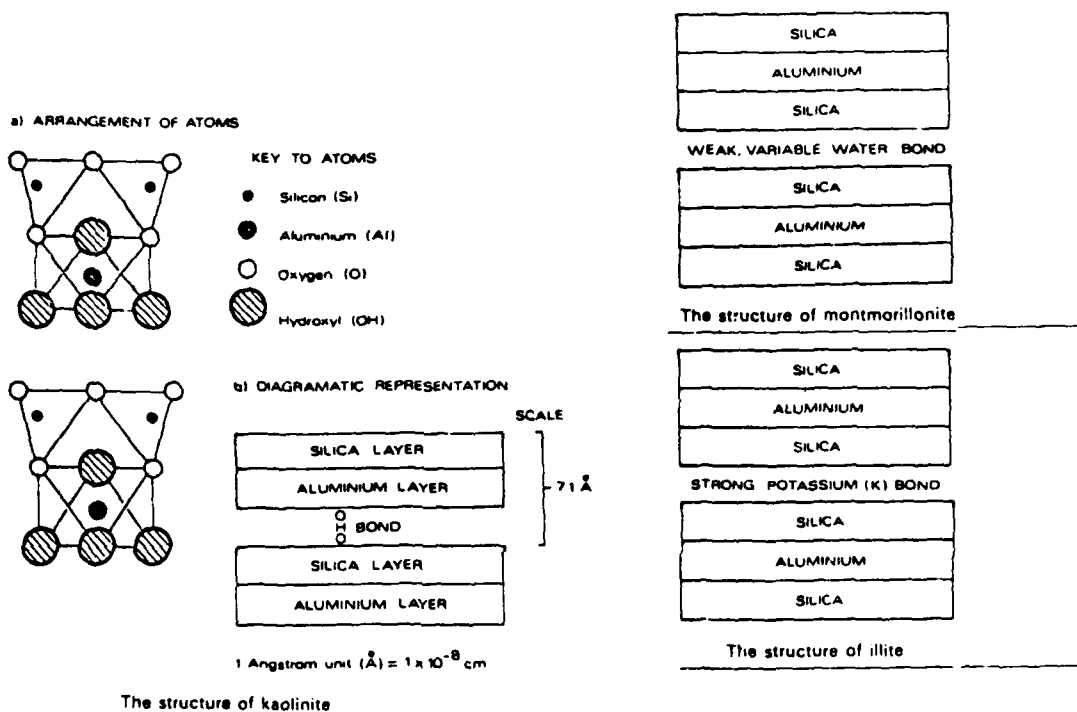


FIGURE 8.3 Typical arrangements of atoms in clay minerals (after Grim, 1953). (a) Fundamental silica molecule. (b) Combination of tetrahedral silica units to form silica sheet. (c) Fundamental hydrous aluminium oxide molecule. (d) Combination of octahedral aluminium hydroxyl units to form gibbsite sheet. (e) Elemental silica-gibbsite sheet. (f) Arrangement of silica-gibbsite sheets in kaolin. (g) Arrangement of silica-gibbsite sheets in montmorillonite. (h) Arrangement of silica-gibbsite sheets in illite.

FIGURE 8.4 STRUCTURE OF CLAY MINERALS



determines the rate of strain at a given level of stress application.

Courtney (17) in discussing the electrical nature of clay particles indicates that they have a negative electrical charge (or anions) at their surface and to balance this electrically, a layer of positive ions (or cations) coat the clay particles. These cations attached to the clay surface are referred to as the adsorbed ions. They are not absorbed (incorporated in) but are adsorbed (stuck) to the clay. According to Courtney (17), Guoy first observed and described the double layer of negative and positive charges. Consequently this layer is referred to as the electric double layer or the Guoy layer. The amount of cations in the soil water next to the clay increases toward the clay surface and the amount of negative ions (anions) decrease toward the clay surface. The cations are usually the plant nutrients and include calcium (Ca^{++}), Magnesium (Mg^{++}), potassium (K^{+}) and sodium (Na^{+})

8.4 MODELS PREDICTING PERMANENT STRAIN

The method of using repeated triaxial load compression tests with elastic stress-strain theory has been used by Brown et al. and Monismith et al. (18) on subgrade type materials. The results of repeated load testing can be expressed in equations of the form:

$$\epsilon^P = A N^b \quad (8.3)$$

and

$$= \epsilon^P / (1 + m \epsilon^P) \quad (8.4)$$

where

ϵ^P = permanent strain

$\Delta\sigma$ = applied stress, and,

N = number of stress applications.

A, b, l, and m = experimentally determined coefficients.

8.5 RUTTING PREDICTION MODELS

Barber, et al., (19), developed a combined procedure for the prediction of deterioration and assessment of the reliability of pavements. The approach provides a framework for lifecycle management of pavements. The method utilized the result of full scale field and prototype laboratory testing to develop a methodology for pavement deterioration prediction and assessment of the reliability of pavements. To do this, deterministic equations were developed to predict deterioration in terms of rutting. The extensive data utilized were accumulated over four decades of research and represent a wide variety of pavement types and wheel loads. The reliability assessment models developed provide a method of determining the probability that a pavement will give support and desired service for time period or number of vehicle operations. The overall research is useful for maintenance and repair prediction as well as prediction of future serviceability.

Barker (20), developed a simplified procedure for considering roughness in pavement design. The method utilizes statistical techniques and parameters to generate stochastic pavement profiles and material properties. Incorporating the results of the rutting prediction model into the generated surface profile allows a determination of pavement roughness. The rutting model developed (Figure 8.5) provides a mechanistic evaluation of the rut depth and consists of the permanent strain model and the stress distribution model.

When the dynamic load test is applied to a stabilized soil sample or pavement system, the permanent deformation per cycle is relatively large initially, but decreases as the test progresses. A plot of the accumulated permanent strain versus the number of load applications shows a typically concave downward shape (Figures 11.35 and 11.36). Log-log transformation enables the permanent deformation characteristics of the material to be obtained using the relation :

$$\epsilon_a = I N^S \quad (8.5)$$

where I = Strain axes intercept value

S = Slope of line

N = Number of loading cycles

FIGURE 8.5 PROCEDURE FOR COMPUTING PERMANENT DEFORMATION OF SUBGRADE

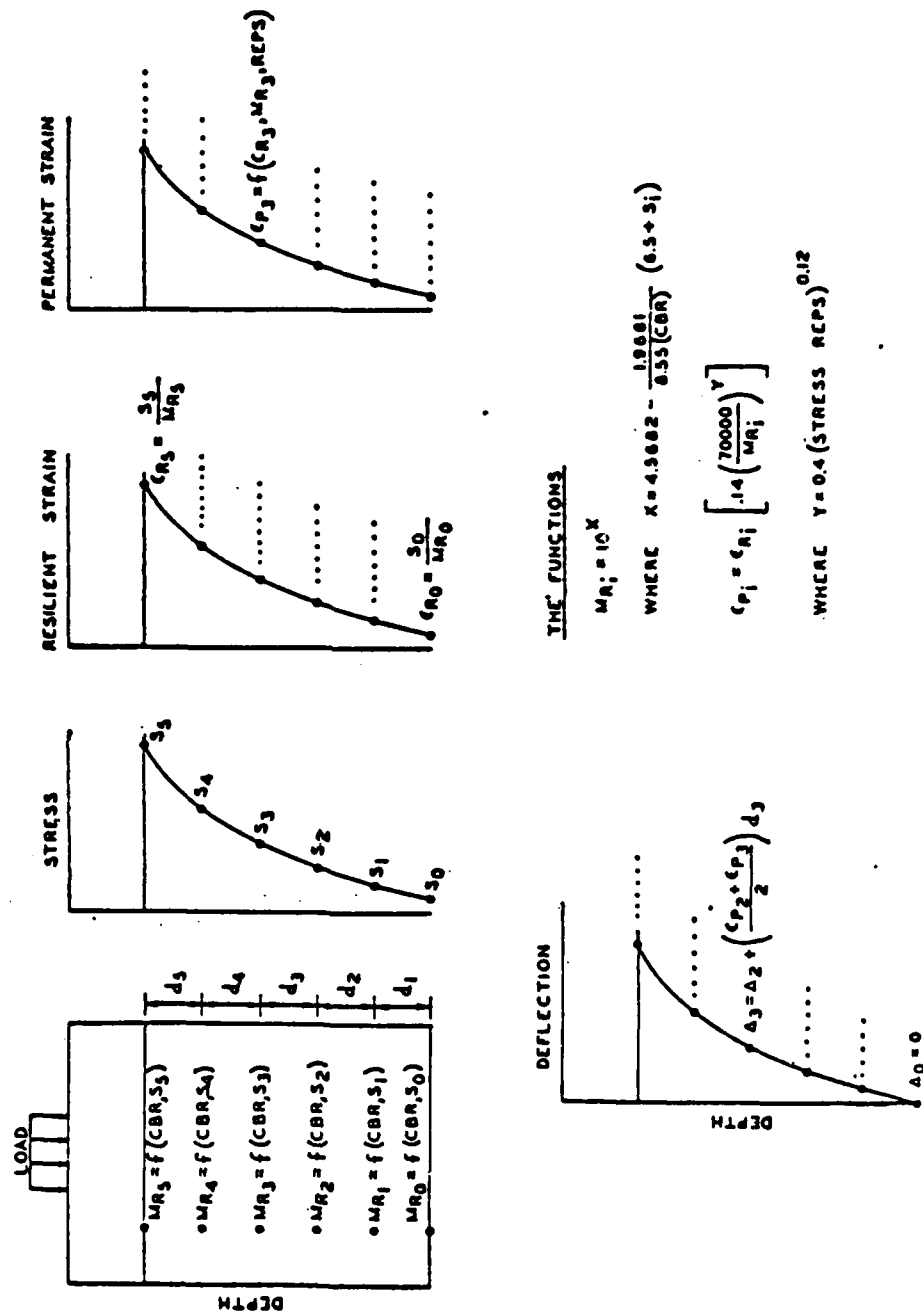


Illustration of rutting model

In the FHWA method, two other parameters were introduced, alpha (α) and gnu (μ), where

$$\alpha = 1 - S \quad (8.6)$$

$$\mu = IS/\epsilon^r \quad (8.7)$$

ϵ^r = Elastic strain of the 200th cycle

I and S, or alpha and gnu, are material parameters which are influenced by stress, temperature and material properties.

A regression of thirty-three experimental observations of alpha and gnu yielded the following relations :

$$\alpha = 1.218 - 0.0047 \sigma_d - 0.06 AC \quad (8.8)$$

$$\mu = 1.985 - 0.1870 \sigma_d \quad (8.9)$$

where

σ_d = deviatoric stress in psi;

AC = asphalt content in percent.

A summary of the nature of alpha and gnu, is as follows:

"Alpha is primarily dependent on deviatoric stress level and secondarily dependent on temperature, mix, materials, air voids, etc. Gnu is heavily dependent on deviatoric stress but is a more complex function of interrelated variables and its relationships are less clear."

Ullidtz (21) provides a program for predicting the performance of a flexible pavement structure in terms of slope variance, rutting and cracking as a function of loads and climatic variations. The results obtained compared qualitatively well with published field data and gave to some extent, quantitatively correct results.

Morris (22) making use of the elastic theory, the dynamic test and some of the constitutive equations discussed previously, suggested the following procedure to predict rutting :

(1) Relationships between permanent strain and applied stress must be available for each of the pavement constituents, i.e., the constitutive equation for each layer should be known.

(2) The permanent deformation of the whole system is found by summing the products of the permanent strains and the corresponding depth at each layer:

$$\gamma_p = \sum_i \epsilon_{pi} * h_i \quad (8.10)$$

where

γ_p = rutting of the whole system,

ϵ_{pi} = average permanent strain of the ith layer,

h_i = thickness of the ith layer.

The rutting results using this procedure were compared with those measured in the field and reasonably good

agreement was obtained.

Monismith and Freeme (18) estimated the amount of rutting in a layered system. Saraf, et al. (23) presented a regression model for obtaining a correlation between seasonal rutting and primary response for an 18,000 lb-ft. single load. It is expressed in the form:

$$RR = f(\sigma, \epsilon, \Delta, N_{18}) \quad (8.11)$$

where RR = seasonal rate of rutting or permanent deformation per equivalent load application
 σ = stress in component layers;
 ϵ = strain in component layers;
 Δ = surface deflection;
 N_{18} = total equivalent number of 80 KN single axle load up to and including the season for which the rate of rutting is to be calculated.

Two equations are used to calculate rutting:

For pavements with 152 mm (6") or less concrete:

$$\log RR = -5.716 + 4.343 \log d - 0.167 \log (N_{18}) - 1.118 \sigma_c \quad (8.12)$$

For pavements with more than 152 mm (6") of asphalt concrete:

$$\log RR = -1.173 + 0.717 \log d - 0.658 \log (N_{18}) + 0.666 \sigma_c \quad (8.13)$$

where :

RR = rutting value

d = surface deflection = 25.4 mm (1 x 10⁻⁶ in)
per repetition;

σ_c = vertical compressive stress in asphalt
concrete (6.9 KPa, 1 lb/ft²)

Bock (24) compared the FHWA method with the Ohio State University (OSU) method of calculating pavement rutting by considering the whole pavement as a unit and using visco-elastic theory via creep compliance data. The OSU method uses the elastic method to account for permanent deformation of each layer, which is then summed up for all the layers. (Figures 8.6 to 8.9)

A summary of the results of the prediction of rutting using the visco-elastic theory and creep tests shows that the permanent deformations that were estimated using this procedure are substantially less than those computed using the elastic analysis for essentially the same conditions (Figures 8.2 to 8.4)

FIGURE 8.6

RUTTING PREDICTION
AT 80 F

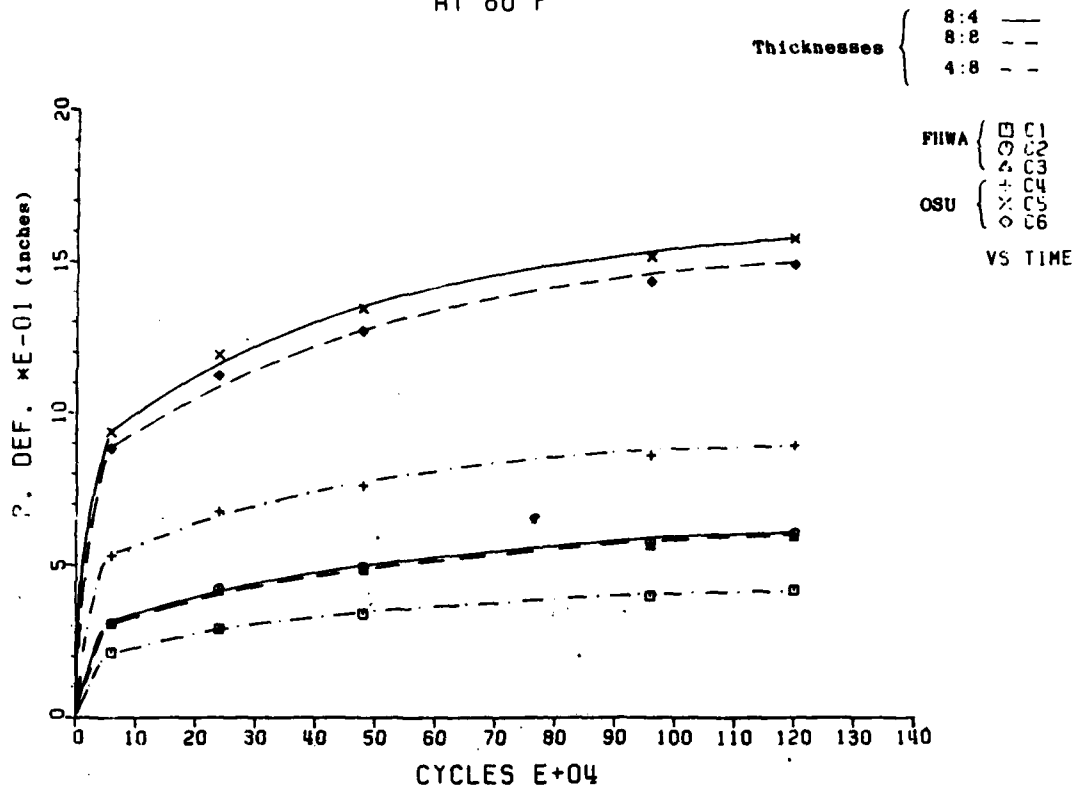


FIGURE 8.7

RUTTING PREDICTION
UNDER VARIED TEMPERATURE

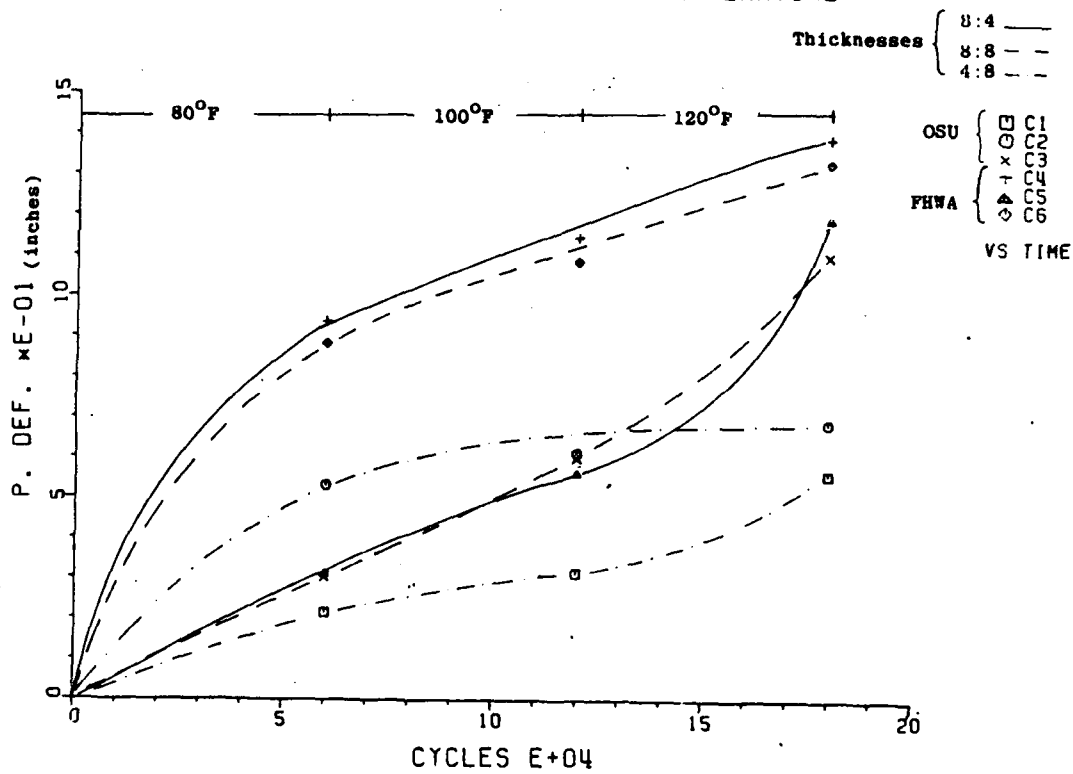


FIGURE 8.8 RUTTING COMPARISON
OSU-FHWA for Different Numbers
of Cycles

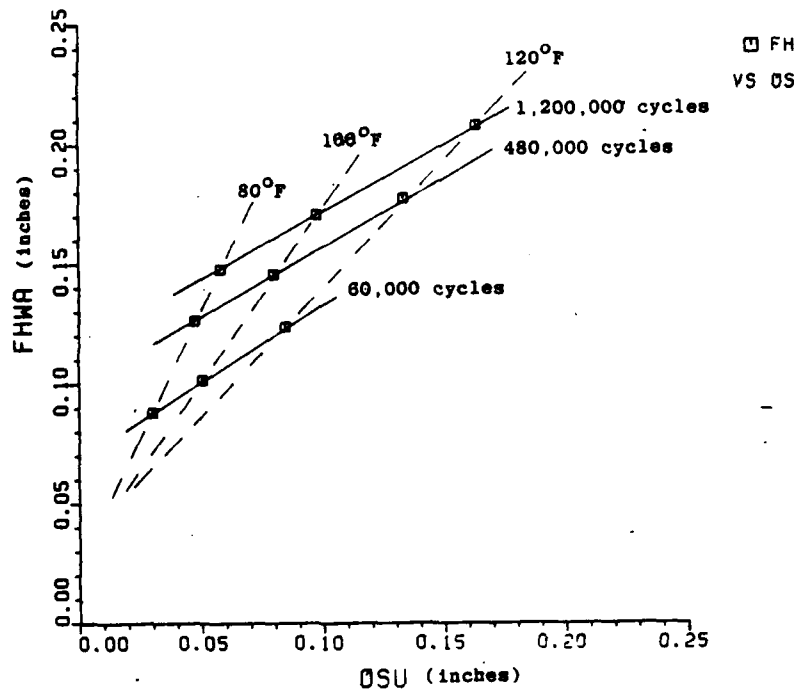
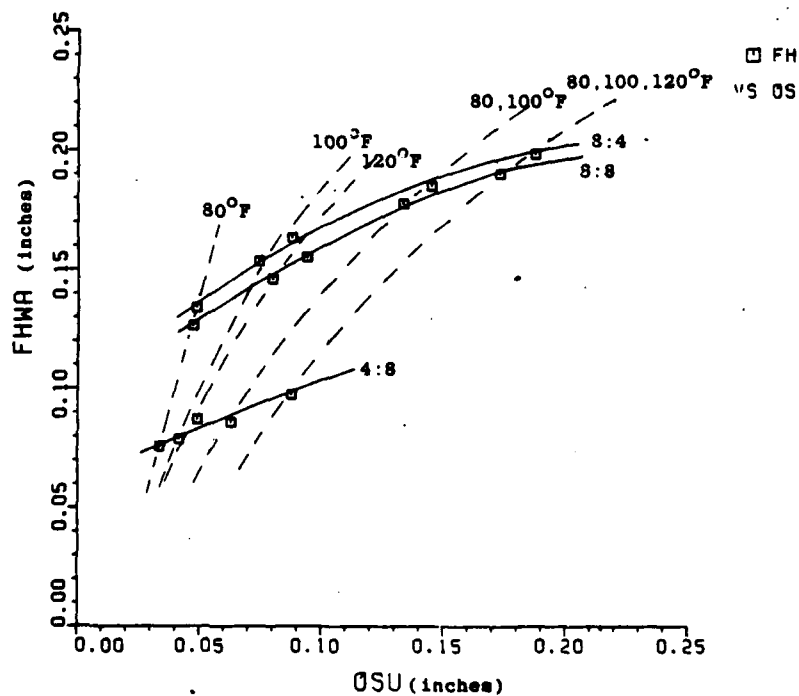


FIGURE 8.9 RUTTING COMPARISON
OSU-FHWA for Different Thicknesses



METHODOLOGY

9.1 RATIONALE

An experimental investigation of rutting behavior of a specially constructed and stabilized pavement was studied. This approach was considered appropriate for the verification and validation of the effectiveness of the two-part stabilizing agent Bisphenol A/Epichlorohydrin, and a Polyamide hardener obtained by reacting dimerized linoleic acid with di-ethylene triamine identified and used in Phase I for enhancing the strength of a clay-silt system.

The rutting indices of a pavement is dependent on several factors including pavement composition and type, loading characteristic and intensity, stress application level, elastic and plastic component of the pavement modulus, pavement height, poisson ratio of layer(s), and rate of change of the plastic modulus. These factors jointly determine the magnitude of rutting a pavement will experience, however for a constant specified load applied to a clay-silt pavement of identical materials and dimensions but different mixing specification, the differential rutting obtained during testing of samples could be related to soil parameters that specify the material state.

The approach used in this study involved an evaluation of the effectiveness of the two-part stabilizing agent Bisphenol A/Epichlorohydrin and the Polyamide hardener by comparison of

the rutting of stabilized and unstabilized pavement(s). This enabled the establishment of statistically significant differences in rutting response. A comparative evaluation of the actual rutting data obtained with predicted rutting response using the modified Waterways Experiment Station (WES) model was considered. The analysis incorporated the result of Phase I of this study in which a model for the prediction of CBR response of a stabilized subgrade was developed.

9.2 EXPERIMENTAL DESIGN

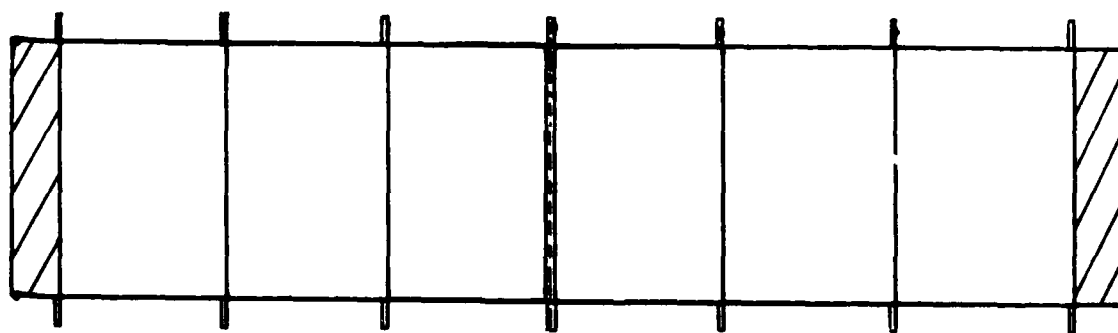
In developing a soil matrix for experimental investigation, a factorial design was chosen to enable an evaluation of the effects of the governing soil parameters. The variables and their associated levels of experimentation are : clay/silt ratio (1-level), moisture content (2-levels), and additive content (3-levels). Clay/silt ratio was fixed at 0.5, moisture content at 14% and 17% and additive percentage at 4%, 2% ,0%. The experimental points corresponding to 0% additive served as the control experiment and a baseline against which the effectiveness of the stabilizing agent could be measured. For each of the experimental points, the rutting of the prepared sample was measured at varying levels of the wheel load passes. The onset of failure is generally accepted as a wheel load rut depth of 1 (one) inch for general aviation purposes.

9.2.1 TEST-BED EXPERIMENTAL ARRANGEMENT

The goal of the arrangement was to minimize both the differences in clay-silt soil strengths and the expected rutting damage at contiguous clay-silt sample edges due to the superimposition of wheel load (Figure 9.1). This rutting damage can occur due to differential rutting of clay-silt samples at the test sample interface for two contiguous sections of differing strength. To ensure minimal experimental errors for each test-bed unit, the samples were positioned with the 4% sample closest to the loading platform, next was positioned the 2% sample, then the control (A = 0%) sample. The two separate control samples were adjacent to one another.

FIGURE 9.1 TEST-BED EXPERIMENTAL ARRANGEMENT

TEST-BED 1.....2.....3.....4.....5.....6.
SECTION



•%•A → 4%.....2%.....0%.....0%.....2%.....4%...

•%•M → 14%.....14%.....14%.....17%.....17%.....17%...

EXPERIMENTAL INVESTIGATION

10.1 THE TIRE FORCE MACHINE (TFM)

The tire force machine (Figures 10.1 to 10.4) located within the landing gear test facility at the Wright Patterson Air Force Base (WPAFB) is a sophisticated machine built by Systems Research Laboratory (SRL) about 25 years ago to determine a variety of tire and pavement characteristics such as dynamic and static tire mechanical properties, pavement coefficient of friction of aircraft tires exposed to various runway surfaces, tire footprint under varying tire pressures, and wheel stresses. It is however a very versatile machine and is amenable to such tests as the permanent deformation of aircraft pavements subjected to normal or tangential loads.

The TFM (Figures 10.1, 10.2) consists of two large subsystems, a static load delivery subsystem and a linear or rotational motion pavement subsystem. In combination, these motion subsystems have four independent lines of motion. The load delivery subsystem consists of a semi-circular yoke supported by a ram made of a concentric steel mass at the top. A space truss is welded to the ram at the bottom which truss holds the semi-circular yoke at the bottom. The ram which has a maximum allowable vertical motion of 2 ft. is supported by four steel box columns braced at the bottom by steel gusset plates. The steel box columns support a superstructure surrounded by a walkway platform for ease of maintenance,

FLAT SURFACE TIRE FORCE MACHINE

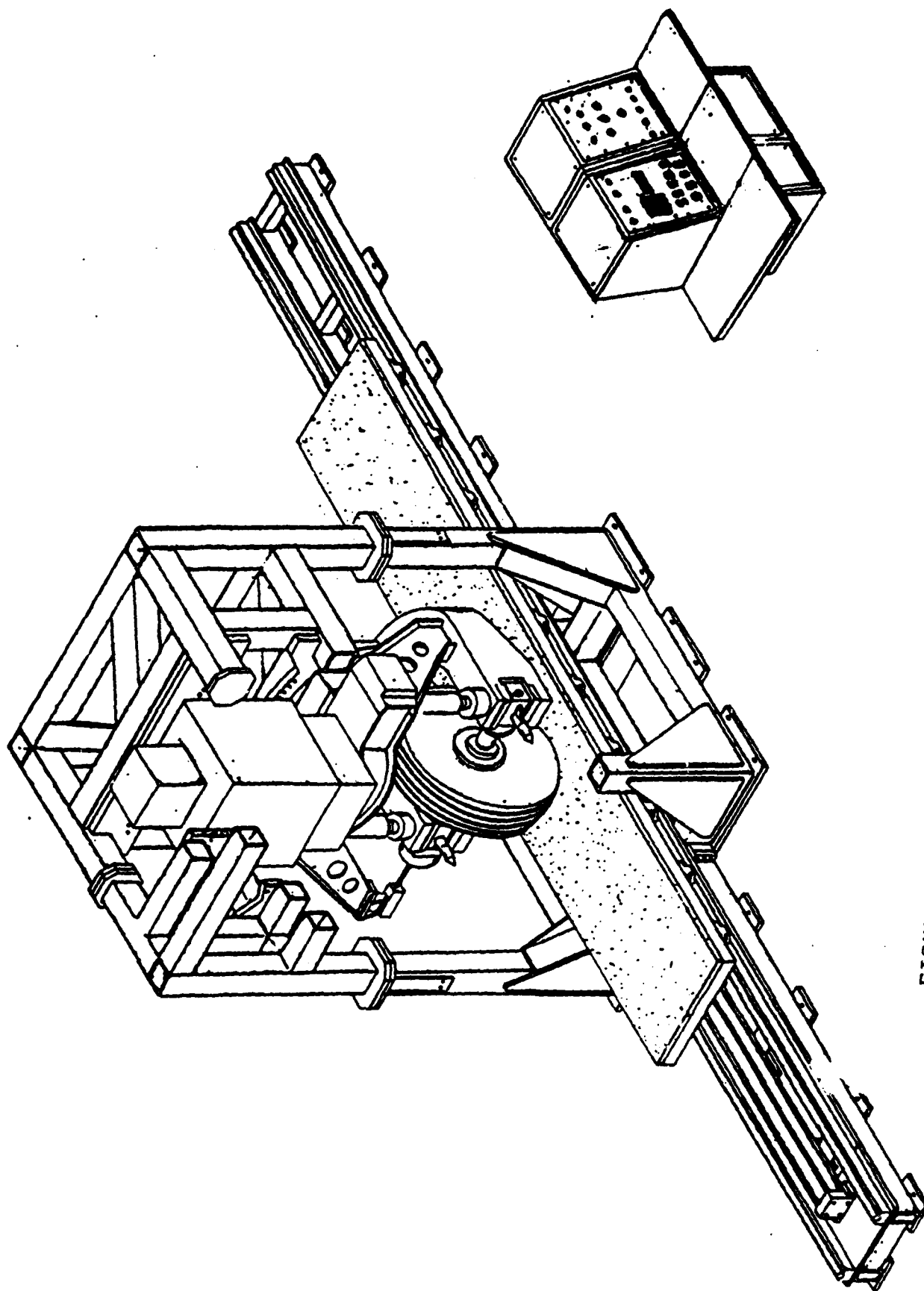


FIGURE 10.1 FLAT SURFACE TIRE-FORCE MACHINE (TFM).

FIGURE 10.2 SCHEMATIC REPRESENTATION OF VECTOR FORCES AND MOMENTS ACTING ON TEST TIRE.

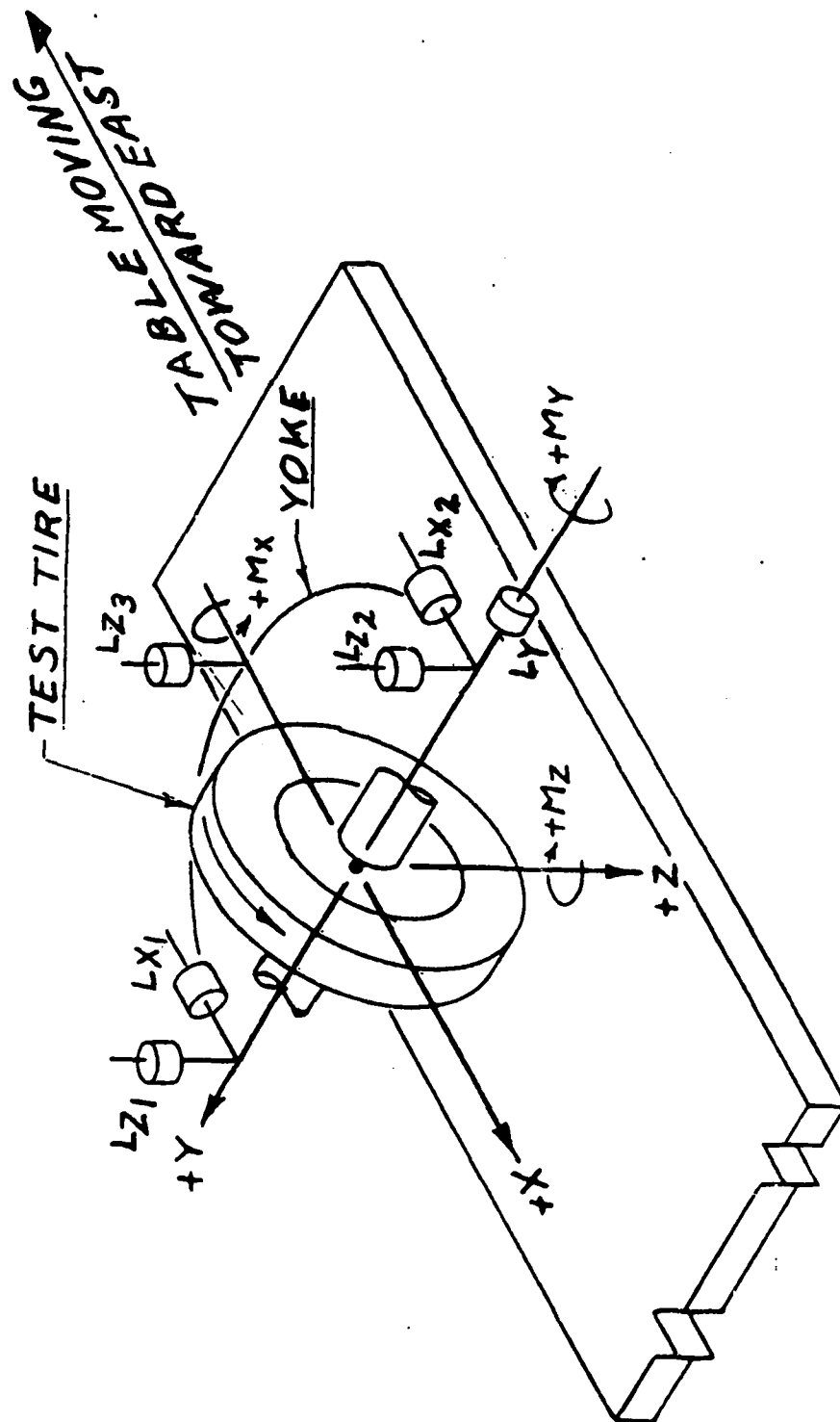


FIGURE 10.3 FRONT VIEW OF UNLOADED TIRE-FORCE MACHINE (TFM).

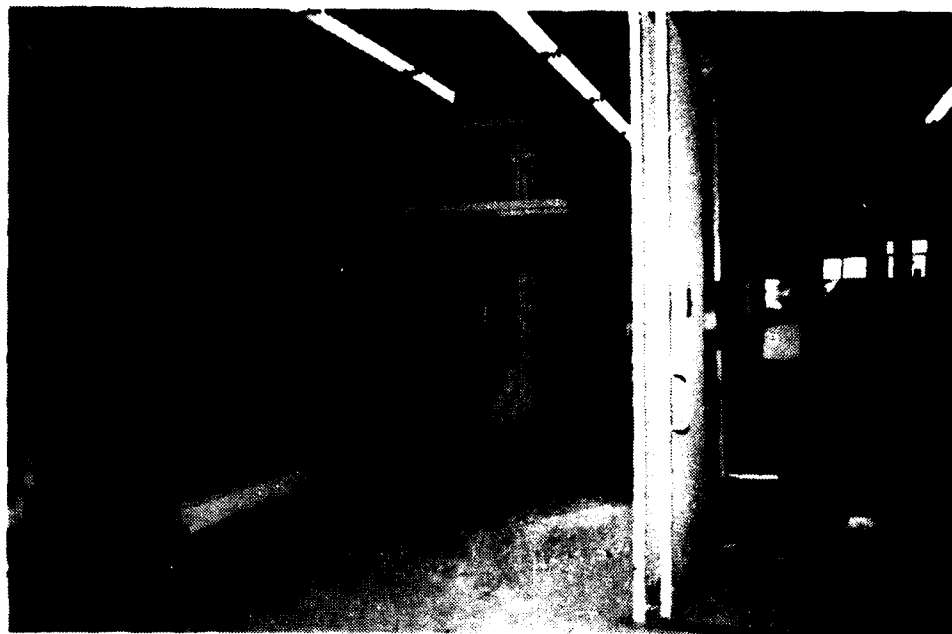
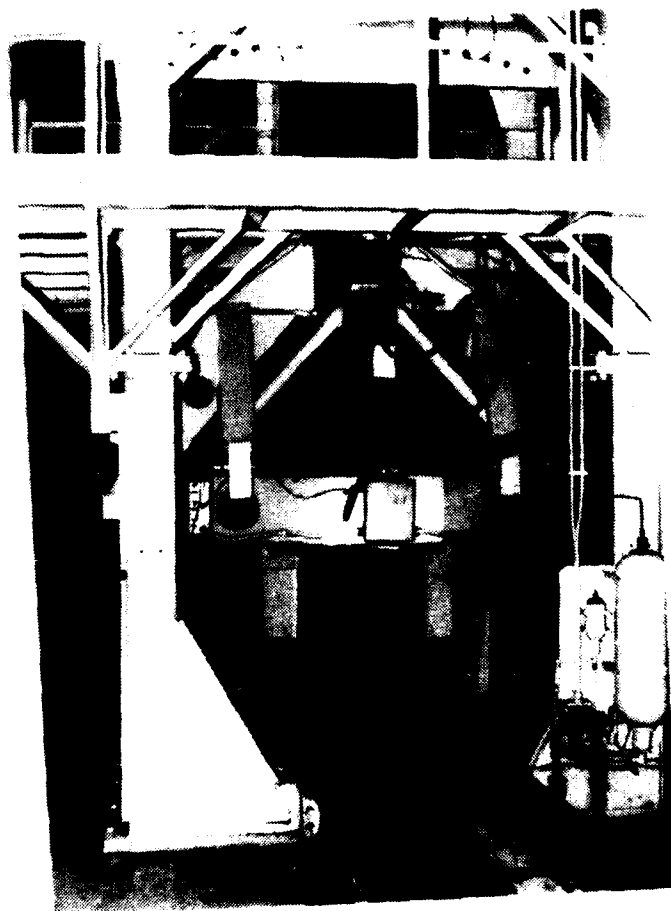


FIGURE 10.4 REAR VIEW OF TIRE FORCE MACHINE (TFM) SHOWING UNBALANCED HYDRAULIC SYSTEM.



repair and equipment calibration. (Figures 10.3, 10.4). The semi-circular yoke receives test tires mounted on interchangeable tire/wheel mandrels. The tires can range in size (diameter and width) from 6" x 6" to 56" x 10". The linear motion pavement subsystem consists of two interchangeable horizontal tables 20' long by 3' 4" wide. One of the tables, the linear motion table, has the option of several surfaces - smooth aluminum, brushed concrete, asphalt or carrier deck epoxy surfaces. The table is propelled by a hydraulic power unit with a hydraulic system rating of 40 horsepower and 3000 psi pressure. The table travel range is 18 feet and the table speed ranges from 0 to 3-1/2 inches per second in one direction. It is a little slower in the opposite direction due to the use of an unbalanced hydraulic propulsion system. The other table allows up to 70 degrees of rotary motion on a smooth steel surface. The overall length of the tire force machine is 38 feet, the maximum load capacities are 75,000 lbs. vertical, 30,000 lbs. in both direction of table travel (x-direction), 25,000 lbs. sideways, and 25,000 ft-lb of braking torque can be delivered by the machine (Figure 10.2). Tire yaw and camber position are independent and manually adjustable.

For the testing, a vertical load of 5000 lbs. was applied as measured by load cells Lz1 and Lz2 and the vertical displacement profile of the ram after each pass was used in computing the rutting indices per pass. Figures 10.3 and 10.4 respectively show the front and rear view of the tire force

machine. The bearing assembly responsible for the smooth motion of the TFM test-bed platform is shown in Figures 10.5 and 10.6. The V-shaped assembly rides on a cylindrical rod securely mounted on a rail assembly bolted firmly to the floor. Figure 10.6 shows a close-up view of the bearings supporting each of the two 3730 lb. test-beds. The two units were secured to the TFM platform by giant G-clamps and bolts.

10.2 TEST-BED DESIGN AND CONSTRUCTION

The two test beds (Figures 10.7, 10.8), designed and constructed by the Manufacturing Engineering Department at Central State University consists of two long beds 3'4" x 8'6" weighing about 1000 lbs. of steel each. The test-bed base of dimension 40" x 102" is of 1/2" steel thickness to which is welded along the horizontal axis, two steel C-channels 12" high by 102" long weighing 25 lbs./ft. The C-channel has a tapered flange of length 3" and a web thickness of 3/8".

At one end of each test-bed is an aircraft tire startup platform designed to absorb the inertial wrap up forces associated with the onset of linear motion. The remainder of the test bed is divided equally by three partitions into three steel sections of dimension 2'6" (L) by 2'6" (W) by 1'0" (H) that are designed to receive the test materials. A cut-out 6"(H) by 10"(W) was removed from each of the 1/2" thick partitions to avoid tire interference with the partitions,

FIGURE 10.5 REAR VIEW OF TFM SHOWING V-SHAPED BEARING ASSEMBLY ON WHICH THE TEST PLATFORM MOVES.

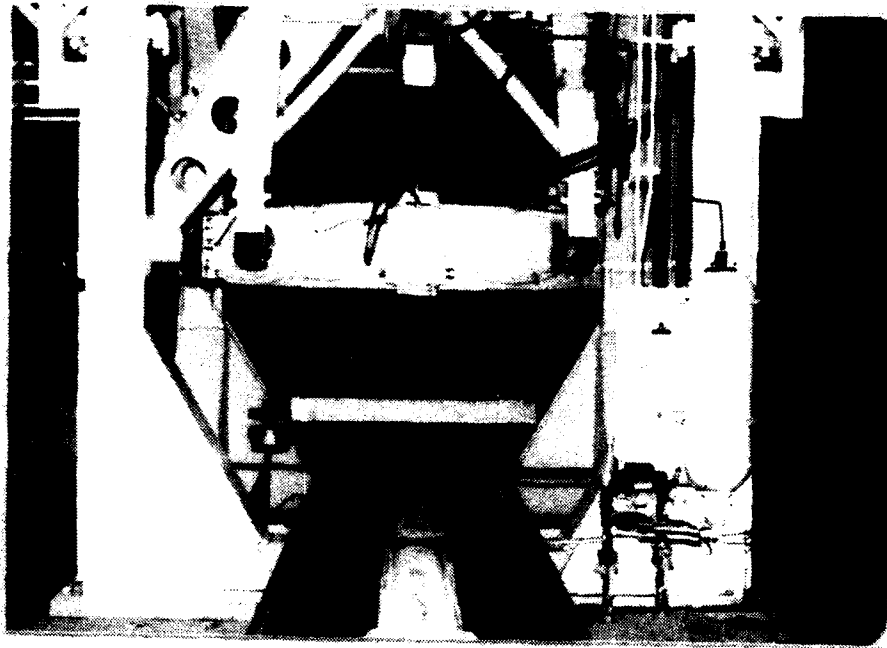


FIGURE 10.6 CLOSE-UP VIEW OF TFM BEARING ASSEMBLY SUPPORTING TESTBED.

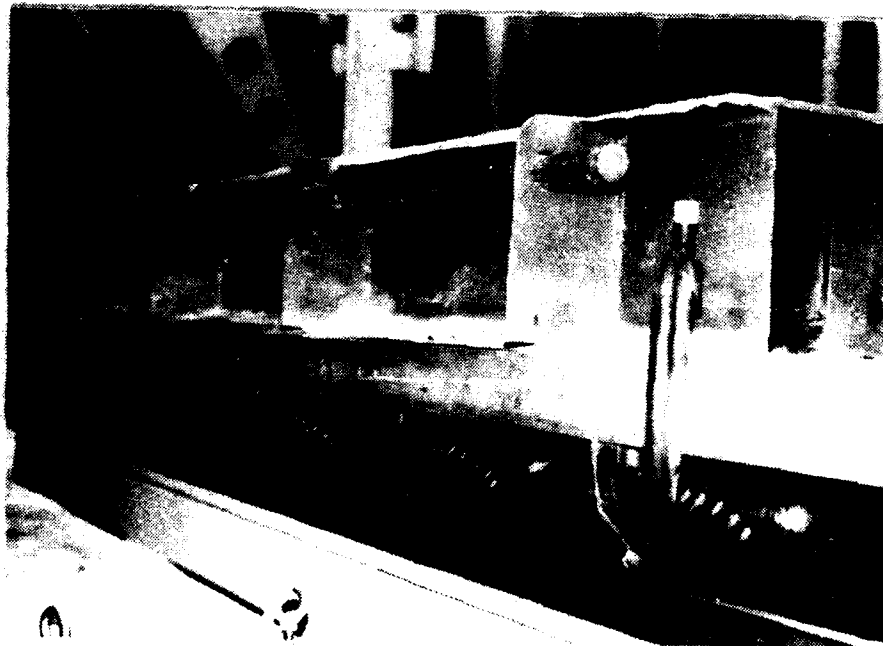
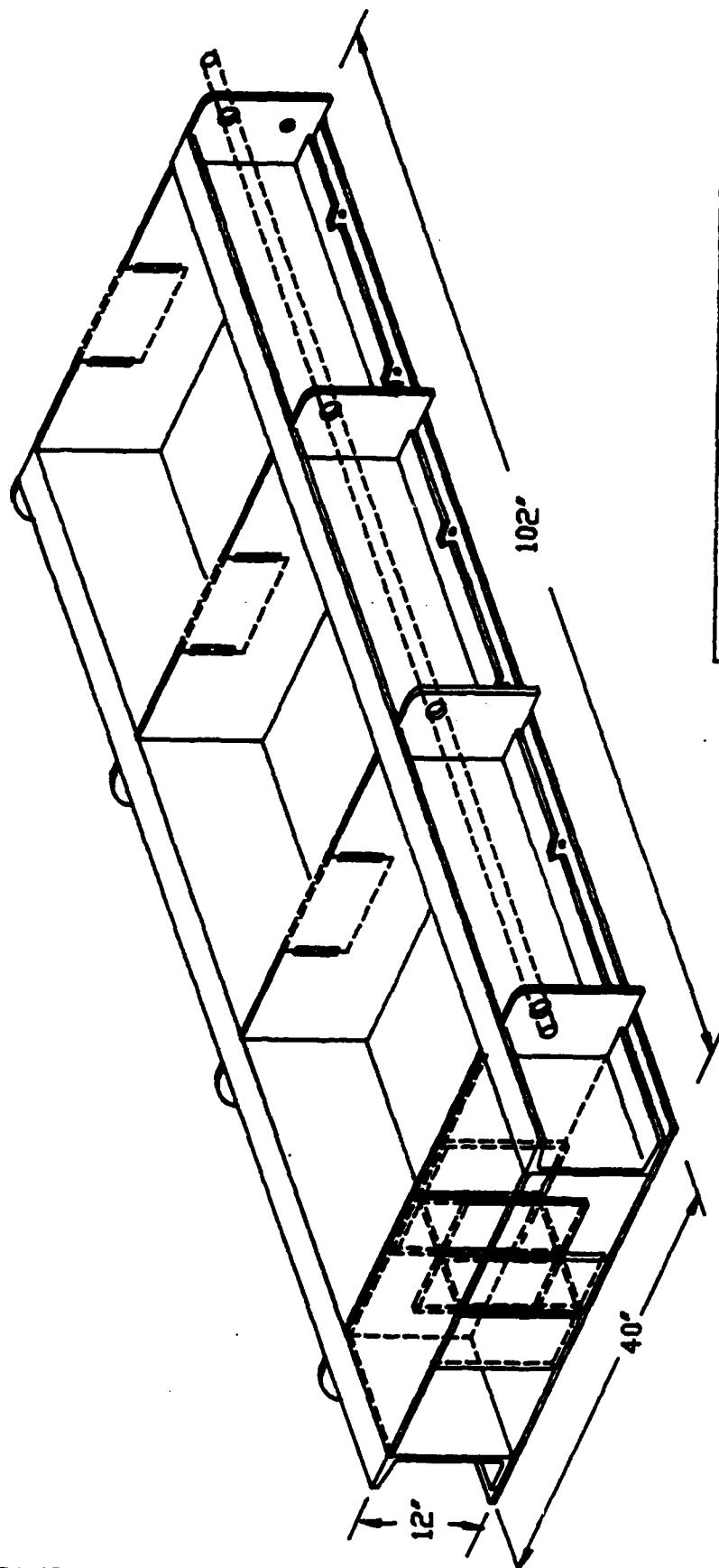


FIGURE 10.7 3-D VIEW OF TWO (2) IDENTICAL TEST BEDS CONSTRUCTED AT CSU.



TEST BED FOR FAA SOIL STABILIZATION RESEARCH			
SCALE 1/16.41	CO-PRINCIPAL INVESTIGATOR A. AJAYI-MAJEJI		AUTOCAD DRAWING L.A. WEIR
DATE: 4-5-88			
CENTRAL STATE U. MFG. ENG. DEPT.			
PRINCIPAL INVESTIGATOR V.A. GRISSOM			

test-bed walls and the six samples. The overall weight of a single fully loaded unit of dimension 40" x 102" was approximately 3800 lbs.

The test-bed was placed in position on the TFM using a 1-7/8" diameter rod of length 8' for load transfer. The rod runs through 2" diameter holes in the end plates and side plates welded to the C-channel.

Using beam theory and plate theory to calculate the structural deflections on the fully loaded test-bed, a value of 1.5×10^{-2} inch in the long direction was obtained. The test-bed however was lifted as a continuously supported beam at quarter points on each side and not as a simply supported beam; therefore the actual maximum deflection is much smaller than the indicated value.

An important construction detail is the linearly aligned and equidistant 6" high by 9" wide metal cut out from each of the six partitions that separate the test-bed into six (6) chambers. These cut-outs were necessary to allow the aircraft wheel load to move smoothly from one test section to another while preserving test-bed geometry and integrity and eliminating sample disturbances.

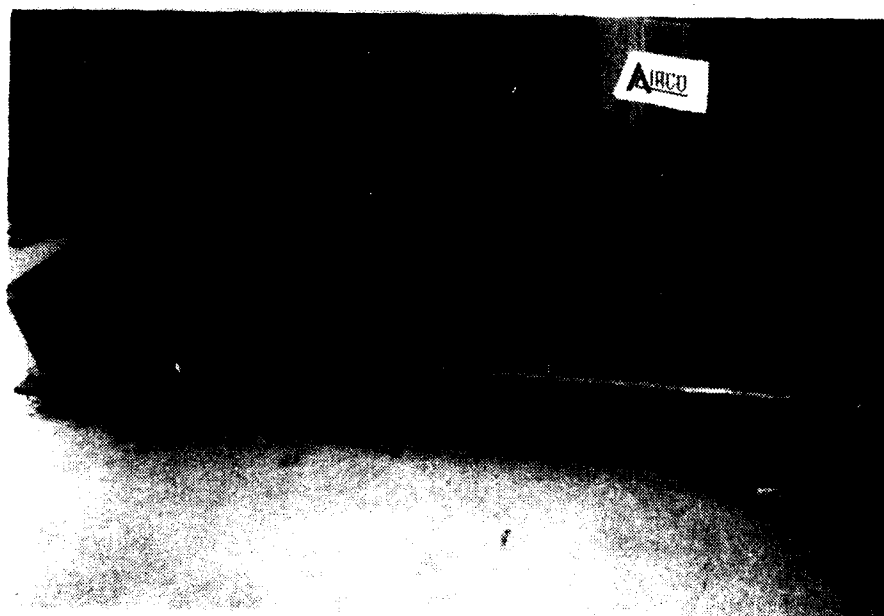
The choice of a 9" width of the cut-out was dictated by the width of the YF-16 aircraft tire which was about 7 1/4". A clearance of approximately one inch between the tire and the side partition wall was therefore available.

Figure 10.8 shows a stage of the test bed construction. The steel plates and cut-outs were fabricated, assembled and clamped in place for subsequent manufacturing operations. The clamped structures were next drilled and notched using a magnetic- base drill. Other construction tasks were executed: oxy-acetylene cutting of open U-shapes in the C-channels for the facilitation of bolted connections to the platform was completed; L-shaped connectors were welded to the test-bed partition and the connectors were subsequently bolted to the walls of the C-channel. This was done to ensure flexibility of the test-bed design and ease of adaptation to other possible future usage of the test-bed. The shear connectors receiving the horizontal $1\frac{7}{8}$ " diameter rods were welded to the C-channel with the rods positioned in place for concentricity. The two C-channels were finally welded to the 40" x 102" flat $\frac{1}{2}$ " thick steel sheet using a combination of $\frac{1}{4}$ ", $\frac{3}{8}$ ", $\frac{1}{2}$ ", and $\frac{5}{8}$ " welding electrodes of appropriate specification. Standard welding practices were adhered to. The completed welded steel assembly was degreased, caulked to prevent moisture loss and rust-o-leum paint was applied to give the final product in Figure 10.9. Two identical units were manufactured at Central State University.

FIGURE 10.8 TWO (2) IDENTICAL TEST BED CONSTRUCTION IN PROGRESS
SHOWING MAGNETIC BASE DRILL, CLAMPS, etc.



FIGURE 10.9 ONE (1) TEST BED UNIT AFTER CONSTRUCTION AND
FINISHING



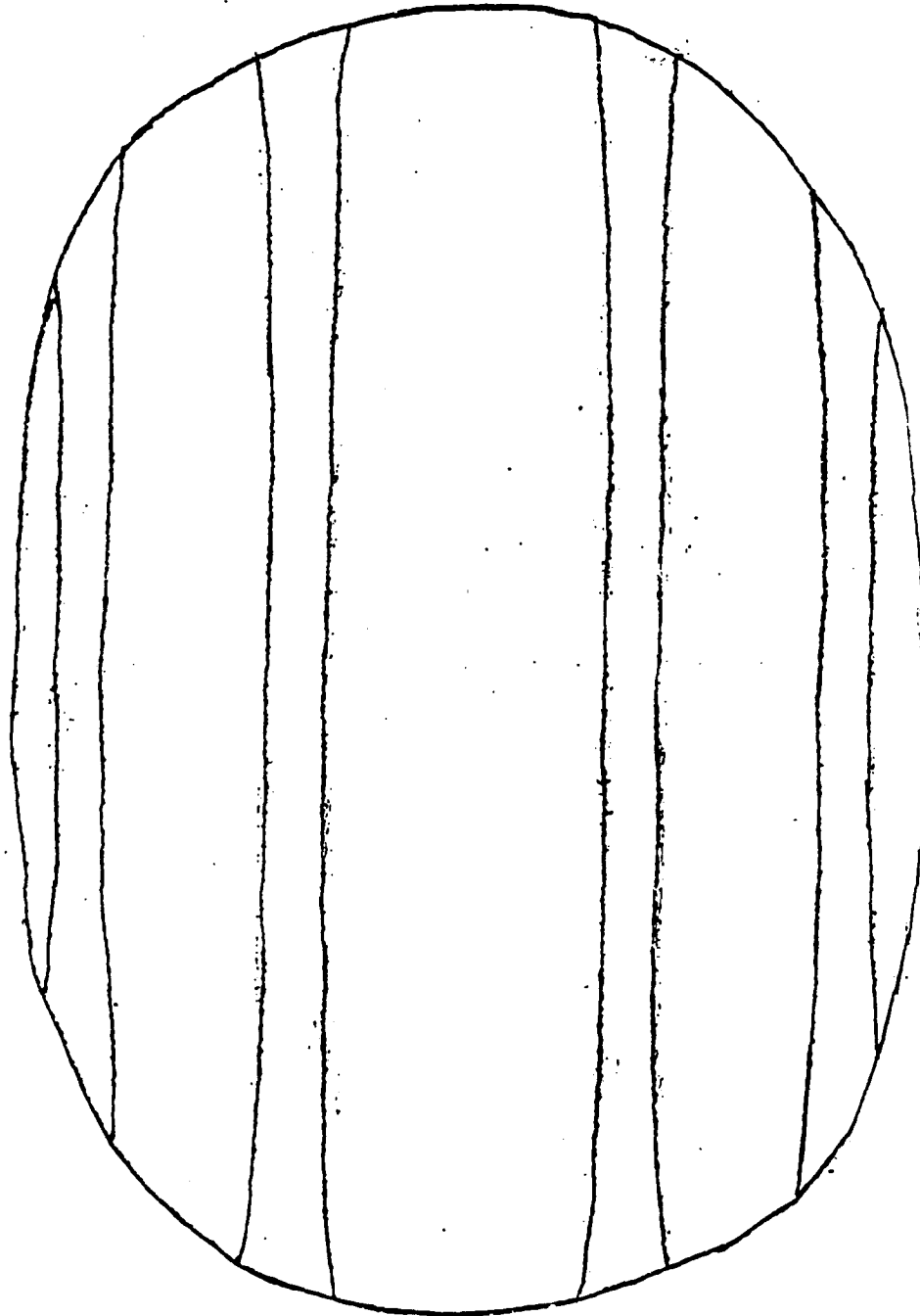
10.3 TIRE FOOTPRINT / JUSTIFICATION OF TEST-BED STRUCTURAL DIMENSIONS

The actual tire foot print obtained prior to the onset of testing is shown in Figure 10.10. The gross area of 25.67 sq.inches, exclusive of the tire groove non-contact space, reduces to a net area of 20.85 sq. inches at a pressure of 200 psi. The maximum tire footprint length of 6.8 inches and width of 4.7 inches are of particular significance.

The configuration of the tire footprint especially the maximum dimension of 6.8 inches has an important bearing on the stress distribution in the clay silt medium and consequently the adequacy of the test-bed dimension. From the centerline of the footprint to an extreme spherical envelope of radius 3.4 inches requires approximately a depth of 10 inches to ensure a stress dissipation less than 10% of the maximum stress value under the point of load application. From symmetry considerations a test-bed of width at least twice this value is needed, i.e. 20 inches. The test-bed dimension of 30" (L) x 30" (W) x 12" (H) is therefore satisfactory for construction and was adopted.

----- RATED LOAD 5000 ----- LBS. DATE 30 Jun 88 OPERATOR -----
S/O NO. 88-16 TIRE SIZE 25.5" x 8.0" MFR. Goodyear
CODE NO. ----- SERIAL NO. ----- RETR'D MGR. Airtreads
RATED INFLATION 200 ----- PSI. ----- % DEFLECTION
MAX. LENGTH 6.844 ----- IN. MAX. WIDTH 4.6875 ----- IN.
GROSS CONTACT AREA 25.67 IN² NET CONTACT AREA 20.85 IN²

FIGURE 10.10 YF-16 TIRE FOOTPRINT FOR 5000 LBS RATED LOAD
(Actual Imprint)



10.4 SOIL SAMPLE PREPARATION

10.4.1 GENERAL

The materials prepared for placement in the test-bed consisted of clay, silt, water and the identified stabilization agent. Specifically the transported materials were composed of:

- 1) 2400 lbs (Approx.) of clay measured in 50lb bags,
- 2) 2000 lbs of silt transported in seven 30 gallon drums,
- 3) Two-part resin system-Epoxy resin and the V-40 hardener transported in separate 55 gallon drums,
- 4) CBR test molds,
- 5) Modified AASHTO compaction rammer,
- 6) Mixing troughs, wheeled carts,
- 7) Six (6) cu. ft. mortar mixer on wheels,
- 8) BOMAG soil compactor,
- 9) Clay-silt mixture finishing trowels,
- 10) Sturdy tent for abatement of dust environmental pollution,
- 11) Asphalt surfacing material in 55 gallon containers,
- 12) 250 lb water-fillable manual roller,
- 13) Thermometer, stopwatch, and other miscellaneous items.

These were transported from Central State University to the

Wright Patterson Air Force Base (WPAFB) in Dayton, Ohio.

The adsorbed moisture in the clay was 1.5% and in the silt 0.5%. This adsorbed moisture, in addition to the water introduced during mixing, brought the sample to the moisture content level specified for testing, i.e. 14% and 17%.

The two rigid test beds constructed at Central State University with a self weight of about 1000 lbs. each were transported to WPAFB on firm wooden supports. After unloading they were placed on a flat reinforced concrete floor to prevent the development of test bed distortions. These distortions could lead to bending and shear stresses capable of affecting the result of the rutting test. The six compartments in the two units were filled and compacted to specification while ensuring necessary moisture control. The samples were cured in preparation for the rutting test.

Limitations on the mechanical strength or delivered torque of the mortar mixer made it necessary to mix 1.1 cubic feet of material about 5 or 6 times to fill each of the 6 compartments of the test-bed to a volume of 11" (H) x 2.5' (L) x 2.5' (W). The batching specification for moisture contents at 14% and 17% for the two-levels of additive application and the control case was deciphered using a computer program that takes into account the adsorbed moisture in the clay and silt.

10.4.2 MIXING SPECIFICATION

The two identical steel test beds were each caulked and sealed to prevent moisture loss at seam locations. The test beds were prepared to moisture contents of 14% and 17%. Each test-bed had three compartments two of which were treated with 4% and 2% of the Bisphenol A/Epichlorohydrin resin and the V-40 polyamide hardener at the indicated levels. Equal weights (1.3 lbs) of resin and hardener were each mixed to yield the required weight of additive at the 2 % level. A double portion by weight of the two-part resin system yielded the 4 % additive concentration required. The two-part epoxy system was mixed separately until its flow increased substantially and a uniform texture was obtained. The third test bed sample had no additive. Clay and silt weighing 65 lbs and 64 lbs respectively were poured into a mortar mixer that was shielded partially by a tent (Figure 10.11) to reduce the dust pollution of the environment that results from open air soil mixing and to minimize moisture loss due to the evaporative effect of sunlight and windy weather. After a few seconds of churning the mortar mixer, 17 lbs or 20.3 lbs of water (for 14% and 17% samples respectively) was uniformly introduced into the clay/silt mixture and the mixing progressed until a uniform texture of moisture soaked clay and silt was obtained. The resin mixture was next uniformly applied to the moisturized clay/silt mixture as the mortar mixer churned the samples to a uniform consistency. The final mixture was carted to the test

FIGURE 10.11 SAMPLE PREPARATION UNDER TENT USING 6 CU.FT. MORTAR MIXER.



FIGURE 10.12 TEST BED SAMPLES COMPACTED TO AASHTO SPECIFICATION USING THE BCMAG COMPACTOR



bed location on wheel barrows covered with polythene bags for moisture retention. A gas powered compactor was used to compact the sample to modified AASHTO specification (Figure 10.12).

10.4.3 COMPACTION SPECIFICATION

The compaction was delivered using the 150 lb gas powered BOMAG compactor with a jump height of 2.4" (Figures 10.13, 10.14). Compaction to AASHTO specification was achieved by determining the time it would take to deliver an equivalent energy per unit volume referenced to the modified AASHTO specification. Compaction to modified AASHTO requires the impartation of compactive energy to a sample such that each of the five layers receive 25 blows of a 10 lb rammer dropped from a height of 18". Equating the total energy (potential and kinetic) of the BOMAG compactor to that of the CBR rammer, a total time of 413 seconds of compaction was needed. Each layer therefore received 83 seconds of compaction.

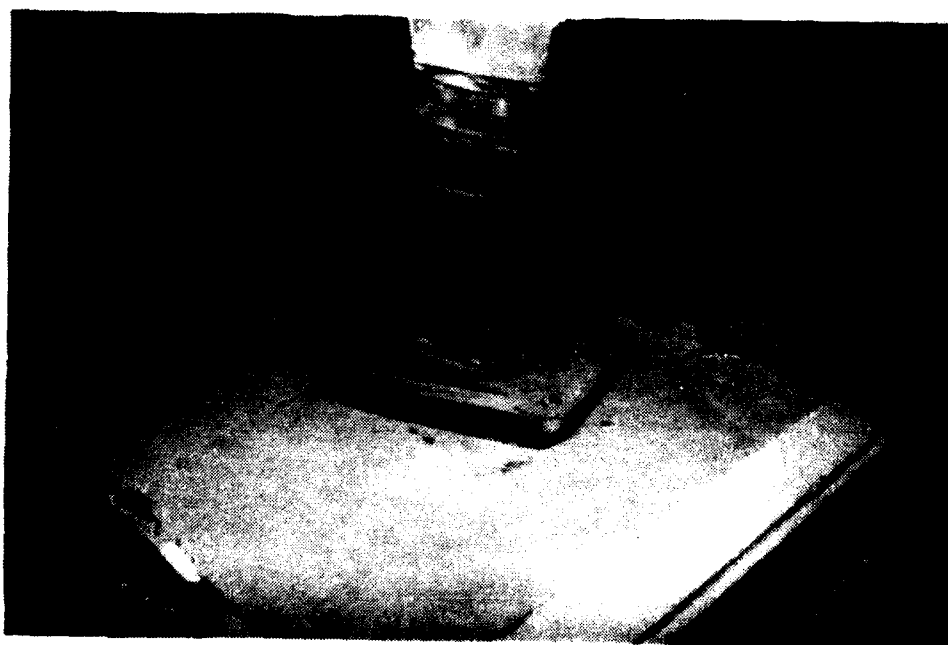
10.4.4 ASPHALT SURFACING

A one inch protective coat of M502 Asphalt based top surfacing material was applied to bring the sample to a depth of 12 inches. It was compacted relatively lightly with a 250 lb roller to provide increased wear resistance for the clay and silt surface and to provide a smooth riding surface.

FIGURE 10.13 CLOSE-UP VIEW OF RESONATING BOMAG COMPACTOR



FIGURE 10.14 BOMAG COMPACTOR IN ACTION



Figures 10.15 to 10.18 show the soil preparation procedures leading to asphalt topping and the commencement of the rutting test. The three metal cutouts removed from each of the partitions in each test-bed unit to ensure smooth wheel load traverse are displayed in Figure 10.18. Some of the cutouts are also shown in Figures 10.15 and 10.16.

10.5 ENVIRONMENTAL CONDITION OF TESTING:

A warm and dry weather devoid of any rain prevailed during the week the soil specimens were prepared and compacted. Clear skies with no cloud covers existed for much of the preparation period. A gentle wind of about 1 knot was experienced at intervals during the mixing. The mixing was conducted outdoors under a tent while the soil sample placement and compaction was executed indoors in the high bay area of the Landing Gear Development Facility (LGDF). The mean recorded temperature and

shown below: Table 10.1 Mean Daily Temperature and Humidity.

WEEK OF JUNE '88	MON 6/20	TUE 6/21	WED 6/22	THUR 6/23	FRID 6/24
TEMP (°F)	91	92	92	84	87
HUMIDITY (%) (DRY BULB)	63	63	59	61	55

Figure 10.19 shows the operator controlled rutting experiment in progress with the 5000 lb load applied to the

FIGURE 10.15 11" THICKNESS OF COMPACTED SOIL SAMPLE SHOWING 10" WIDE CUTOUT PLATES REMOVED FROM TRANSVERSE PARTITION.

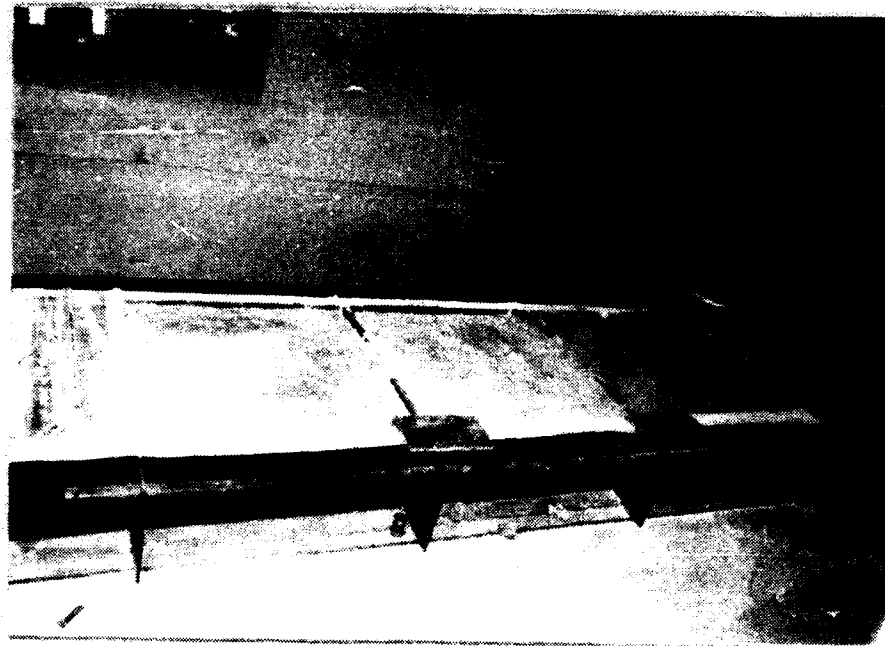


FIGURE 10.16 CLOSE-UP VIEW OF A SINGLE TESTBED SECTION SHOWING LOADING PLATFORM IN REAR.



FIGURE 10.17 COMPACTION OF ASPHALT SURFACING USING A 250 LB ROLLER.

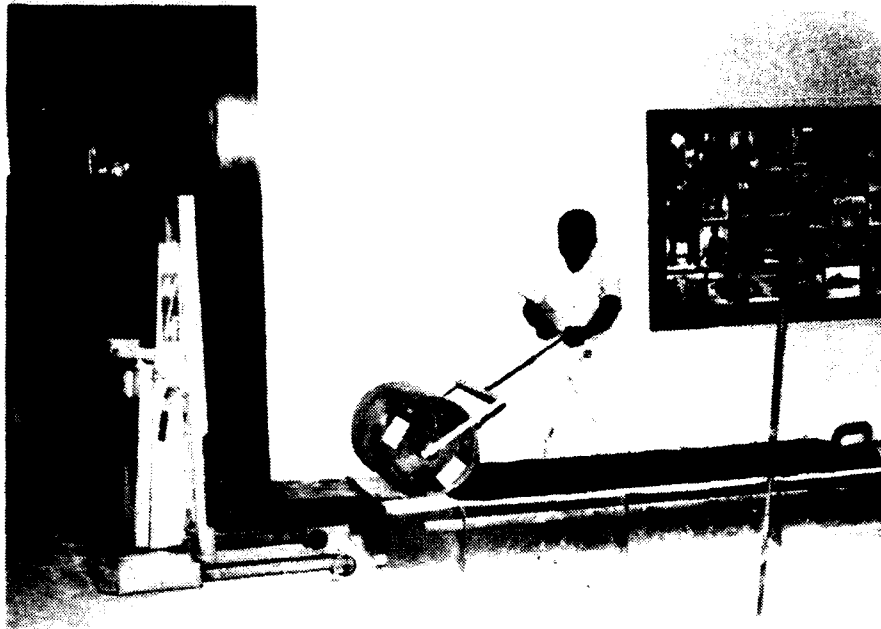


FIGURE 10.18 TWO TESTBED UNITS TREATED WITH 1" ASPHALT SURFACING

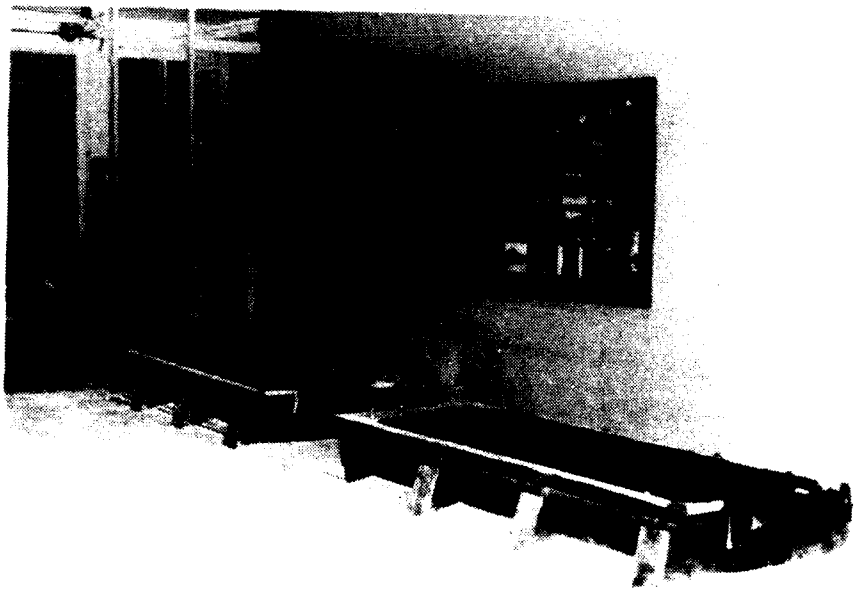


FIGURE 10.19 SIDE VIEW OF THE TIRE FORCE MACHINE WITH TIRE AT START POSITION; IN FOREGROUND, CONTROL STATION WITH OPERATOR.

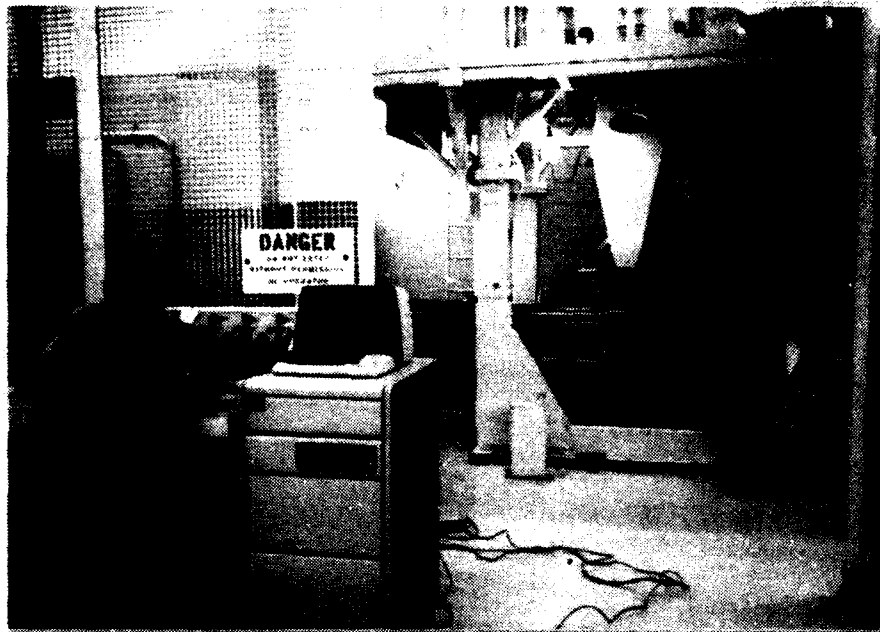
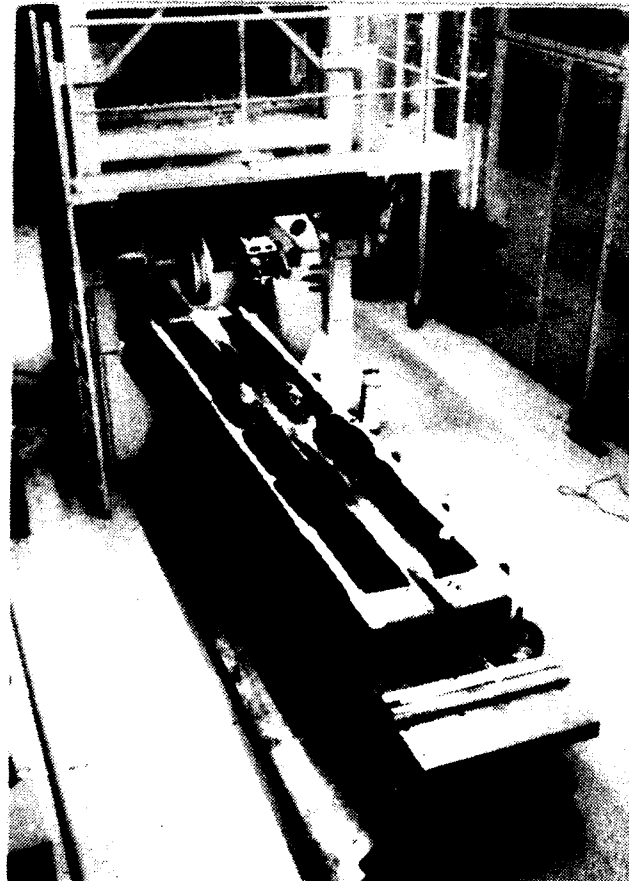


FIGURE 10.20 BIRD'S EYE VIEW OF TEST SETUP SHOWING TEST PAVEMENT CHANNELIZATION AND RUTTING.



full length of the clay-silt test-bed. The platform is at rest position and about to begin another traverse. It is noteworthy that the tire is stationary while the platform moves at 0.17 knots (0.20 mph). Figure 10.20 provides a bird's eye view of the experimental arrangement and rutting profile. The YF-16 tire and the ram are shown in an elevated parked position.

RUT TEST RESULT AND ANALYSIS

11.1 TEST INFORMATION SPECIFICATION

11.1.1 EXPERIMENTAL TESTING PROGRESS PHOTOGRAPHS

At regular intervals during the experimental testing, photographs were taken for technical and historical records. They aid in documenting and corroborating the experimentation and rutting data collected. A video-tape of the rutting test was prepared for a limited portion of the experimentation.

Figures 11.1 to 11.2 show the stabilized clay-silt soil test-bed with asphalt surfacing and the YF-16 tire as loaded on to the horizontal yoke via a mandrel. The aircraft tire is shown at start position, resting on the edge platform constructed to absorb startup inertial forces. These forces occur at the start and finish of a particular pass and were not disruptive to the rutting or damaging to the test sample in view of the rigidity of the end platform and test-bed unit. Figures 11.3 and 11.4 show visual and videotape observations being made of the rutting test progress. The tire imprint on the testbed end platform is vividly displayed in Figure 11.3 and represents the resultant footprint produced by cumulative wheel load passes.

Figures 11.5 and 11.6 indicate that for the 4% level of stabilizer application at the 17% moisture content level, the

FIGURE 11.1 TIRE FORCE MACHINE (TFM) LOADED WITH TEST-BEDS READY FOR RUTTING TEST.



FIGURE 11.2 YF-16 AIRCRAFT TIRE 25.5" x 8.0" AT 200 PSI TIRE PRESSURE.



FIGURE 11.3 RUTTING TEST IN PROGRESS SHOWING TIRE IMPRINT ON
LOADING PLATFORM.

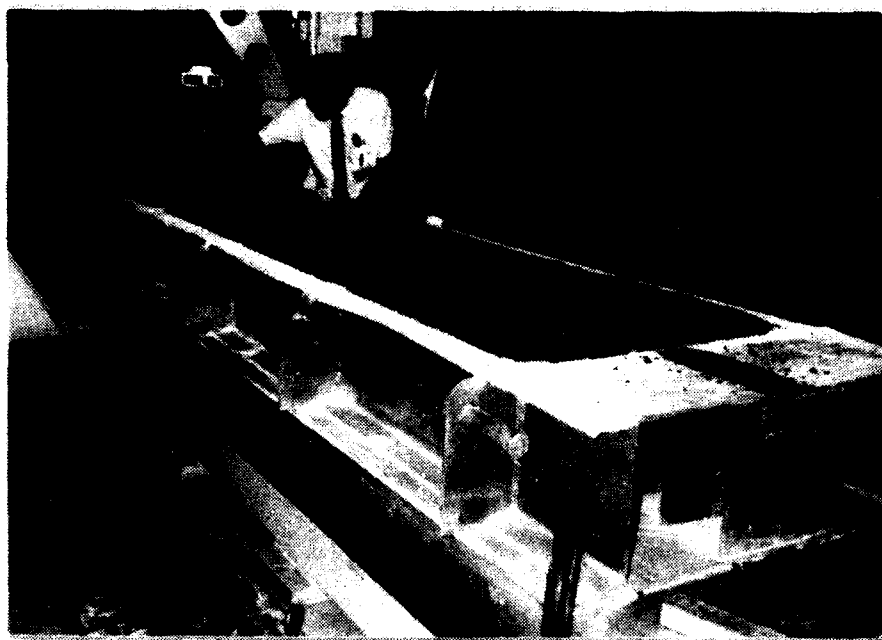


FIGURE 11.4 RUTTING TEST SHOWING VIDEO-TAPE OF TESTING DURING
FORWARD MOTION OF TABLE AT SPEED OF 0.17 KNOTS.

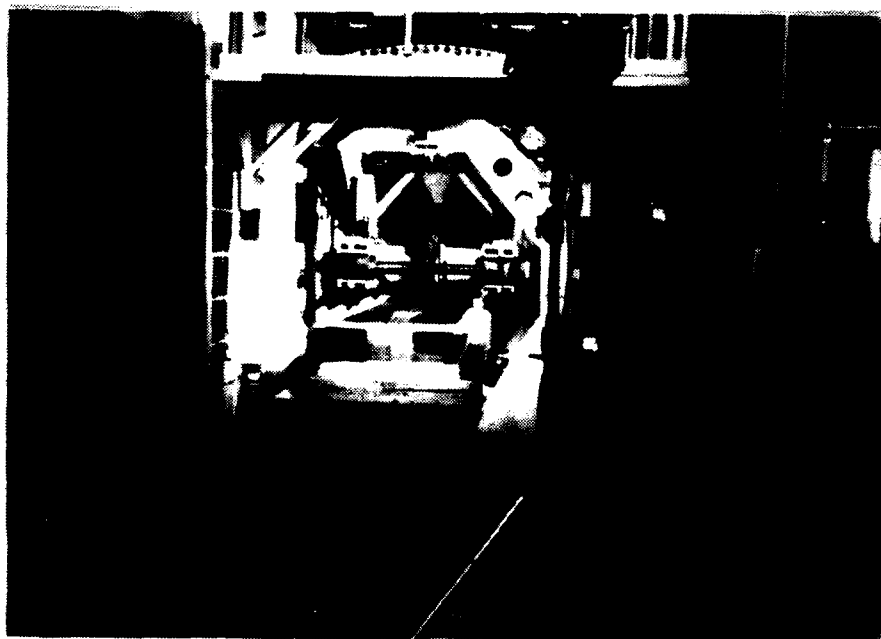


FIGURE 11.5 RUT DEPTH INDICATION FOR $A=4\%$, $M=17\%$ EXPERIMENTAL POINT AFTER 10 PASSES.

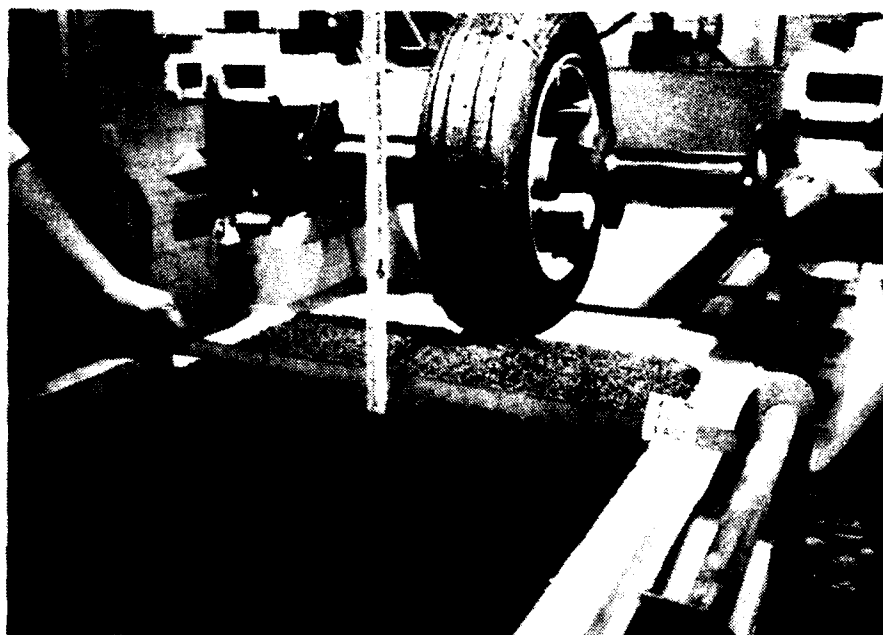


FIGURE 11.6 RUT DEPTH INDICATION FOR $A=4\%$, $M=17\%$ EXPERIMENTAL POINT AFTER 100 PASSES.



magnitude of the rutting for ten wheel load passes and one hundred wheel load passes are 0.56 and 0.72 inch respectively, reflecting a difference in rutting of 0.16 inch. The readings indicated by the vertical linear scale are inflated by the heave value of the shoulder associated with the rut channel at the point of measurement. The amount of heave indexed by the horizontal ruler and the rut measured is taken at the midpoint of the channel created by the rutting.

In Figures 11.7 and 11.8, the rut depth indication for the sample with additive level (A) of 4%, and moisture content level (M) of 14% sample was 0.34 and 0.42 inch at 20 and 100 passes respectively indicating a difference of 0.08 inch.

Figures 11.9 and 11.10 are very significant because they reveal the catastrophic failure that could result from not stabilizing a clay-silt soil in this state. Rutting values of 3.72 inches and 5.20 inches were obtained for this control case after 40 and 150 passes respectively. These values are absolutely unacceptable for airport pavements.

Figures 11.11 to 11.16 display the rut depth profiles at various wheel load passes. In Figure 11.14 (top right quadrant) the dip in the test sample due to the failure of the control clay-silt pavement is clearly visible. This is amplified in Figure 11.15 and the foreground of Figure 11.16.

FIGURE 11.7 RUT DEPTH INDICATION FOR $A=4\%$, $M=14\%$ EXPERIMENTAL POINT AFTER 20 PASSES.

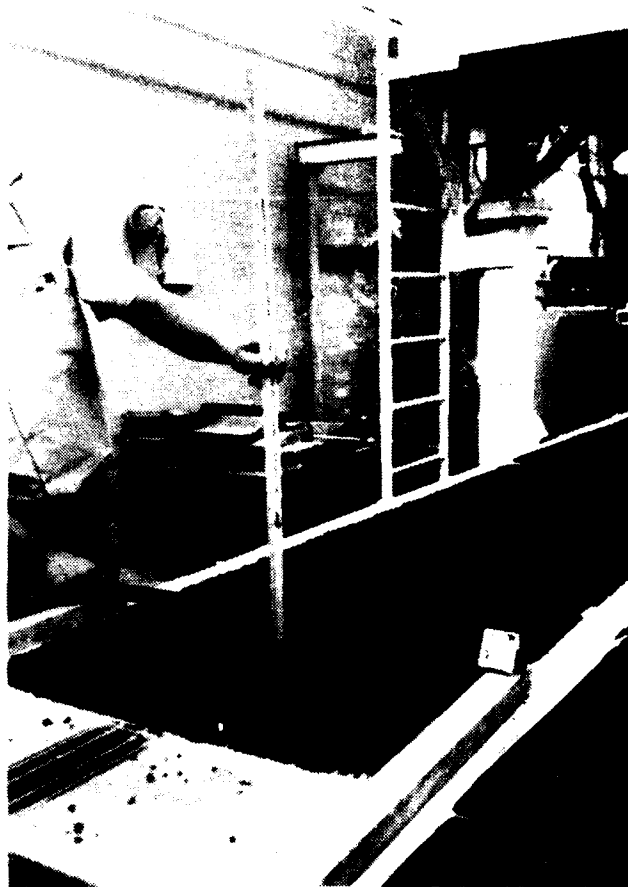


FIGURE 11.8 RUT DEPTH INDICATION FOR $A=4\%$, $M=14\%$ EXPERIMENTAL POINT AFTER 100 PASSES.



FIGURE 11.9 RUT DEPTH INDICATION (7" INCLUDING HEAVE) AFTER 40 PASSES (A=0%, M=17%, CONTROL).



FIGURE 11.10 RUT DEPTH INDICATION (8" INCLUDING HEAVE) AFTER 150 PASSES (A=0%, M=17%, CONTROL).



FIGURE 11.11 RUT DEPTH PROFILE AFTER 300 PASSES

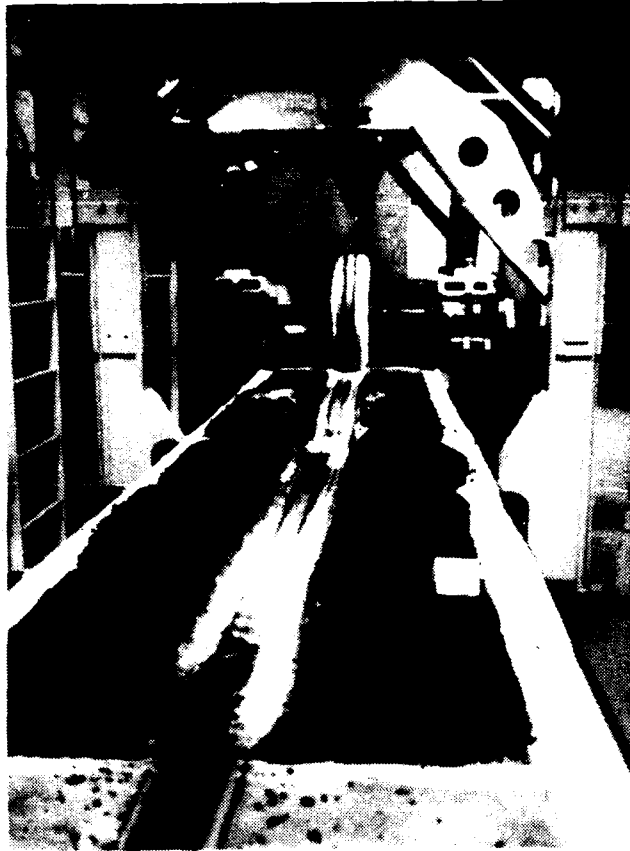


FIGURE 11.12 RUT DEPTH INDICATION AFTER 250 PASSES (A=4%, M=14%)

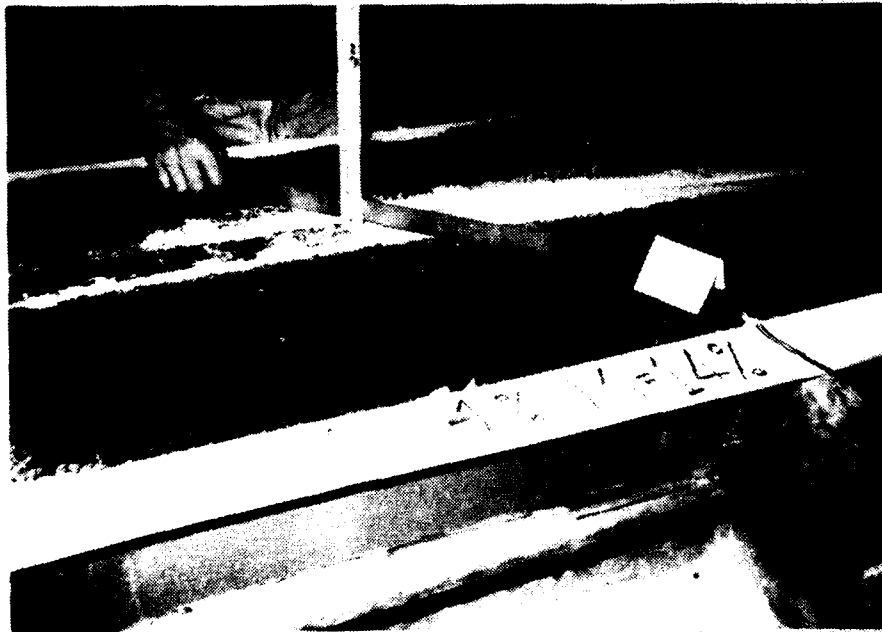


FIGURE 11.13 RUT DEPTH INDICATION AFTER 450 PASSES ($A=4\%$, $M=14\%$)



FIGURE 11.14 RUT DEPTH INDICATION AFTER 450 PASSES ($A=2\%$, $M=14\%$)

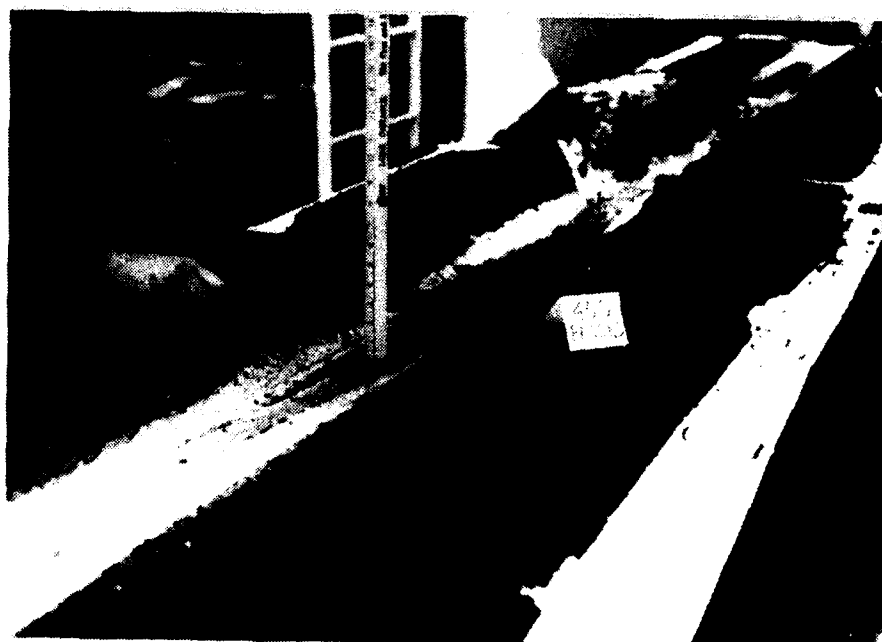


FIGURE 11.15 RUT DEPTH INDICATION AFTER 450 PASSES ($A=0\%$, $M=14\%$)



FIGURE 11.16 RUT DEPTH INDICATION AFTER 450 PASSES ($A=2\%$, $M=17\%$)



Figure 11.17 shows the automated data acquisition interface with the load cell calibration plugs, signal conditioners, motion and load control panels and the PDP-11 computers for data acquisition. The acquired data are transferred to a mainframe computer for analysis and graphical display via a Tektronix plotting device.

Figure 11.18 shows the vertical rutting and the lateral flow of the visco-plastic clay-silt sample after 650 wheel load passes.

11.1.2 RUTTING DATA

The rutting data in Table 11.1 represent the progressive accumulation of permanent deformation of the stabilized clay-silt soil under a 5000 lb. load applied by the YF-16 aircraft tire. The YF-16 tire is geometrically similar to the tire of a B707-320B, DC-8-63 or a 747A aircraft. A total of 1000 wheel load passes were applied to the pavement. Table 11.1 indicates that the control groups within the two test-beds failed rapidly, while the stabilized soil groups were more effective in resisting permanent deformation. The curing period was approximately 7 days.

The minimum recorded rut depth after 1000 passes for the most effective test sample was 0.5". The next effective stabilized soil sample had a rut depth of 0.91" while the soil

TABLE 11-1(i) RESULT OF RUTTING TEST USING FACTORIAL EXPERIMENTAL DESIGN
WITH WHEEL LOAD PASSES AS A CORRELATED VARIABLE

CLAY/ SILT RATIO	MOISTURE CONTENT	ADDITIVE CONTENT	RUTTING DATA (inches)*											
			YF -16 AIRCRAFT WHEEL LOAD PASSES											
			0	10	20	30	40	50	75	100	150	200		
0.5	14%	%												
		4%	0.00	0.28	0.34	0.35	0.38	0.39	0.40	0.42	0.44	0.44		
		2%	0.00	0.38	0.56	0.63	0.63	0.64	0.69	0.94	1.03	1.28		
	17%	0%	0.00	0.75	0.94	1.06	1.09	1.10	1.44	1.66	1.88	2.08		
		0%	0.00	2.38	3.00	3.47	3.72	3.80	4.13	4.50	5.20	5.80		
		2%	0.00	0.72	0.91	1.16	1.03	1.10	1.09	1.19	1.22	1.28		
	4%	0.00	0.56	0.66	0.66	0.72	0.72	0.72	0.72	0.84	0.84			

*CURING PERIOD (7-14 DAYS @ 88°F), TIRE LOAD - 5000 LBS

TABLE 11-1:(ii)RESULT OF RUTTING TEST USING FACTORIAL EXPERIMENTAL DESIGN
WITH WHEEL LOAD PASSES AS A CORRELATED VARIABLE

CLAY/ SILT RATIO	MOISTURE CONTENT %	MOISTURE CONTENT %	R U T T I N G D A T A (i n c h e s) *									
			YF-16 AIRCRAFT WHEEL LOAD PASSES									
			250**	300	350	400	450	500	550	600	650	700
0.5	14%		0.47	0.47	0.47	0.47	0.47	0.47	0.47	0.47	0.47	0.49
		4%										
		2%	1.28	1.44	1.46	1.48	1.51	1.69	1.88	1.93	2.00	2.31
	17%		2.16	2.25	2.27	2.29	2.31	2.47	2.66	2.90	3.19	3.34
		0%										
		0%	6.10	6.40	6.50	6.60	6.70	7.00	7.30	7.40	7.60	7.90
		2%	1.31	1.31	1.33	1.35	1.37	1.38	1.34	1.38	1.41	1.44
		4%	0.84	0.84	0.84	0.85	0.85	0.87	0.87	0.89	0.91	0.91

*CURING PERIOD (7-14 DAYS @ 88°F), TIRE LOAD - 5000LBS.

**START OF EXTRAPOLATED RUTTING VALUES

TABLE 11-1:(iii)RESULT OF RUTTING TEST USING FACTORIAL EXPERIMENTAL DESIGN
WITH WHEEL LOAD PASSES AS A CORRELATED VARIABLE

CLAY/ SILT RATIO	MOISTURE CONTENT %	MOISTURE CONTENT %	R U T T I N G D A T A (i n c h e s) *							
			YF-16 AIRCRAFT WHEEL LOAD PASSES							
			750	800	850	900	950	1000		
0.5	14%	4%	0.49	0.50	0.50	0.50	0.50	0.50		
		2%	2.50	2.63	2.78	2.78	2.84	2.90		
		0%	3.75	3.81	4.03	4.13	4.31	4.38		
	17%	0%	8.20	8.50	8.80	9.10	9.40	9.70		
		2%	1.41	1.42	1.42	1.44	1.44	1.44		
		4%	0.91	0.88	0.88	0.88	0.91	0.91		

*CURING PERIOD (7-14 DAYS @ 88°F), TIRE LOAD - 5000LBS.

FIGURE 11.17 AUTOMATED DATA ACQUISITION INTERFACE SHOWING: LOAD CELL CALIBRATION SWITCHES, SIGNAL CONDITIONERS, CONTROL PANEL AND PDP-11 COMPUTERS AND TERMINALS.

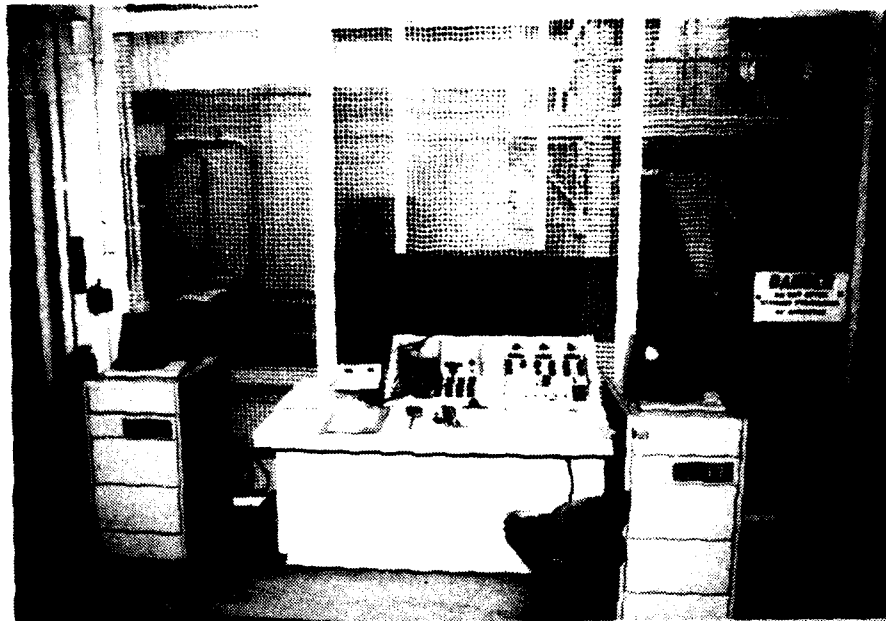
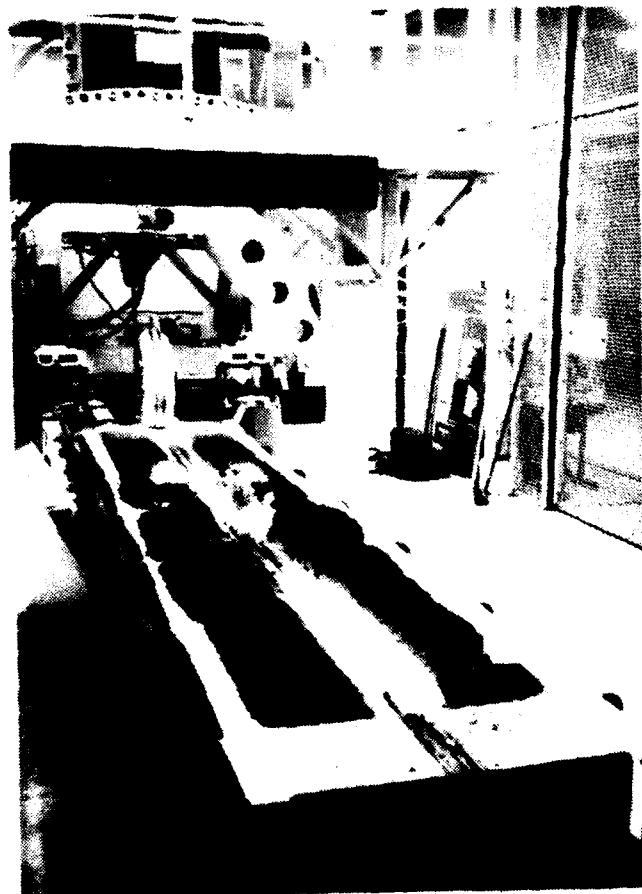


FIGURE 11.18 RUT DEPTH PROFILE AFTER 650 PASSES



samples stabilized at the 2% additive level for moisture contents of 17% and 14% had 1.44" and 2.90" of rutting respectively. Extrapolated rutting of the control samples indicate a 4.38" and 9.70" of rutting for the 14% and 17% moisture content samples respectively.

Compared to the control case, the difference in the rutting values for the 4% additive mixture was very significant. This difference increased with the increase in the number of wheel load passes. A small amount of soil sample rebound was observed to have occurred after overnight relief of sample from load application.

11.1.3 CBR TEST / CONE PENETROMETER TEST RESULTS

The cone penetrometer shown in Figure 11.19 was used to provide a quick estimate of the stabilized soil strength. The stabilized samples were however so highly resistant to deformation or shearing stress that the graduated scale limit of 300 psi was exceeded for all samples except the control samples.

A more reliable index of soil strength, the CBR test was performed; the CBR values obtained fell within the range of the provisions in phase I. The maximum stabilized soil dry CBR test was 105 and the minimum 75. During the CBR testing almost all the samples developed hair line cracks in response to the level of stress application (Table 11.2).

FIGURE 11.19 CONE PENETROMETER (MAXIMUM GAGE - 300 PSI)

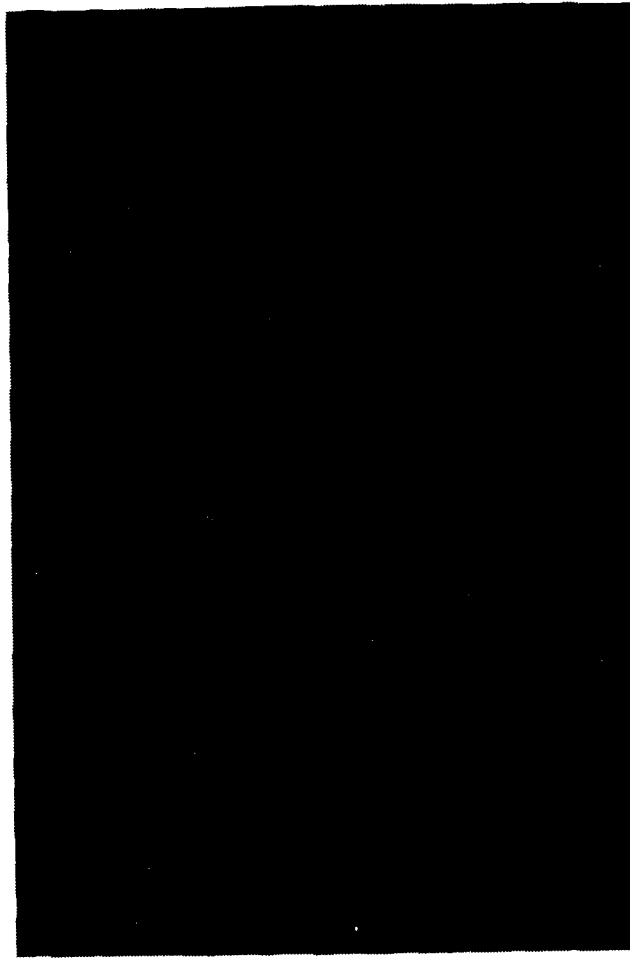


TABLE 11-2

CBR VALUES FOR CLAY-SILT SPECIMENS SAMPLED FROM TEST BEDS

(C/S = 0.5, Temp. 89°F, 3-Days Curing Period)

Additive (%)	Moisture Content	CBR Values (Dry)	Cone Base Reading	Remarks (CBR Test Observations)
4	14	105	> 300	Radial cracks in progress
4	17	80	> 300	Visible radial cracks observed
2	14	85	> 300	No cracks observed
2	17	75	> 300	Numerous radial cracks
0	14	40	250	Few radial cracks observed
0	17	15	200	Incipient radial crack appearing at late stage

11.1.4 RUTTING PROFILE OF CLAY-SILT STABILIZED SOIL VS WHEEL LOAD PASSES

The linear forward and backward motion of the tire force machine (TFM) table was constantly being recorded by a shaft position encoder. Figure 11.20 shows a plot of the table position (in feet) versus the time base (seconds) of the testing. Figure 11.21 shows the six test-bed positions during the first pass from left to right. It indicates that position control was inadvertently enforced through the first three test beds. A restoration to normalcy and relaxation of control kicked in toward the end of the fourth bed.

Figure 11.22 shows the excessive dip of the 17% control sample after just two passes of the 5000 lb wheel load. The trends in the surface profile of the rut test are internally consistent. The relative difference between successive profiles with respect to the original no load profiles gives the rutting value for the accumulated number of passes. The 4% additive samples can be seen to remain highly resistant to the imposed 5000 lb. load; it experienced very little changes in the test profile. (Figures 11.23 to 11.30) Most of the deflection and load signatures were filtered to average out the large oscillations and noise in the data. Figure 11.31 shows a signal that was not filtered. Figure 11.32 shows an overlay plot of the deflection profiles for various wheel load passes ranging from 1 to 20.

Figure 11.20: Plot of Horizontal Table Position (Inches) vs. Time

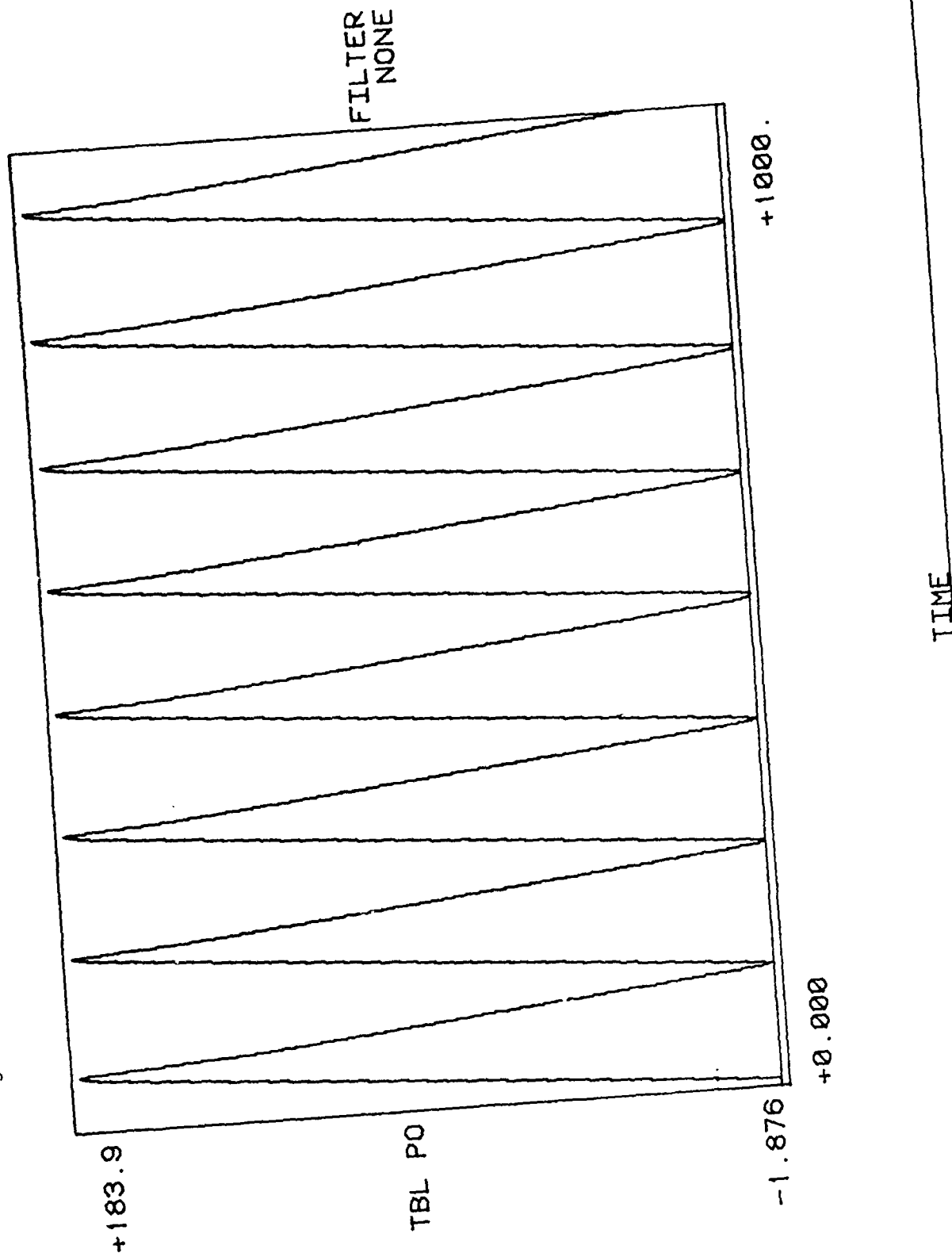


FIGURE 11.21, 11.22: PLOTS OF VERTICAL RAM POSITION (CLAY-SILT SURFACE PROFILE) FOR SIX SAMPLES, BY PASSES

Figure 11.21 (PASS 1) DEFLECTION VS. TABLE POSITION

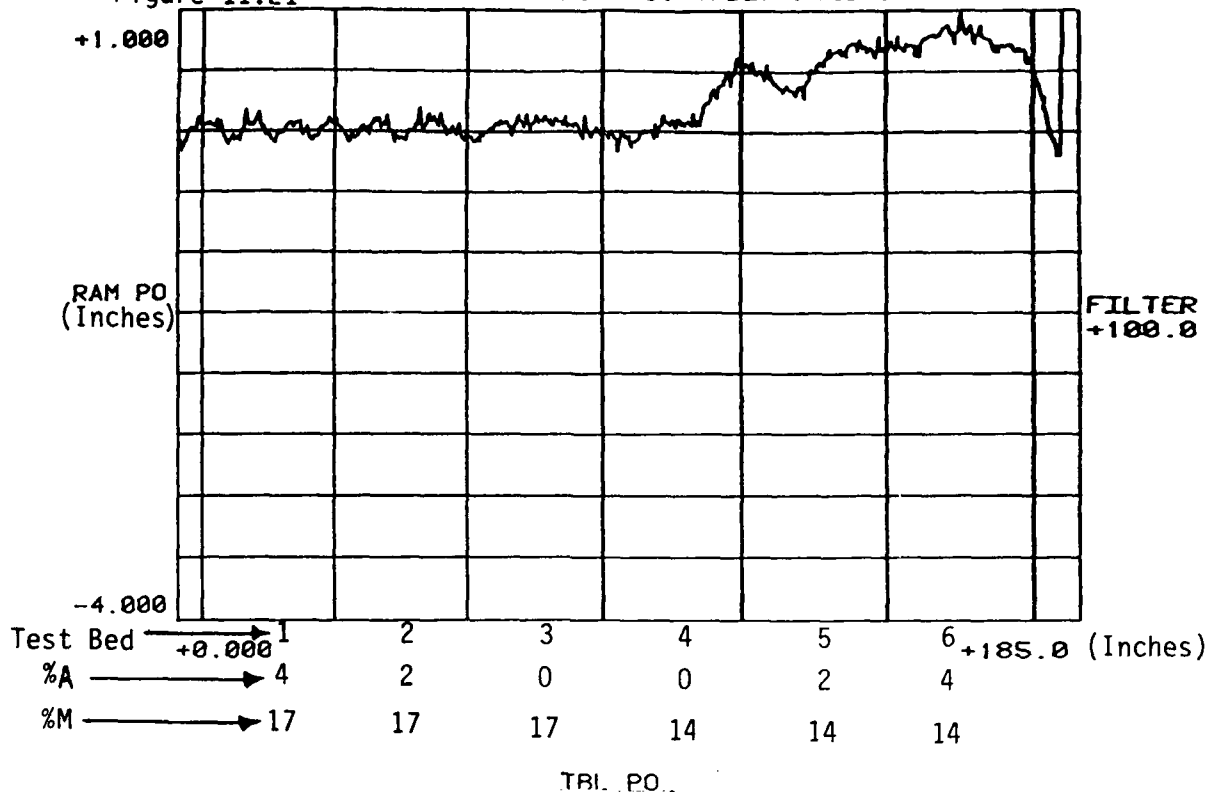
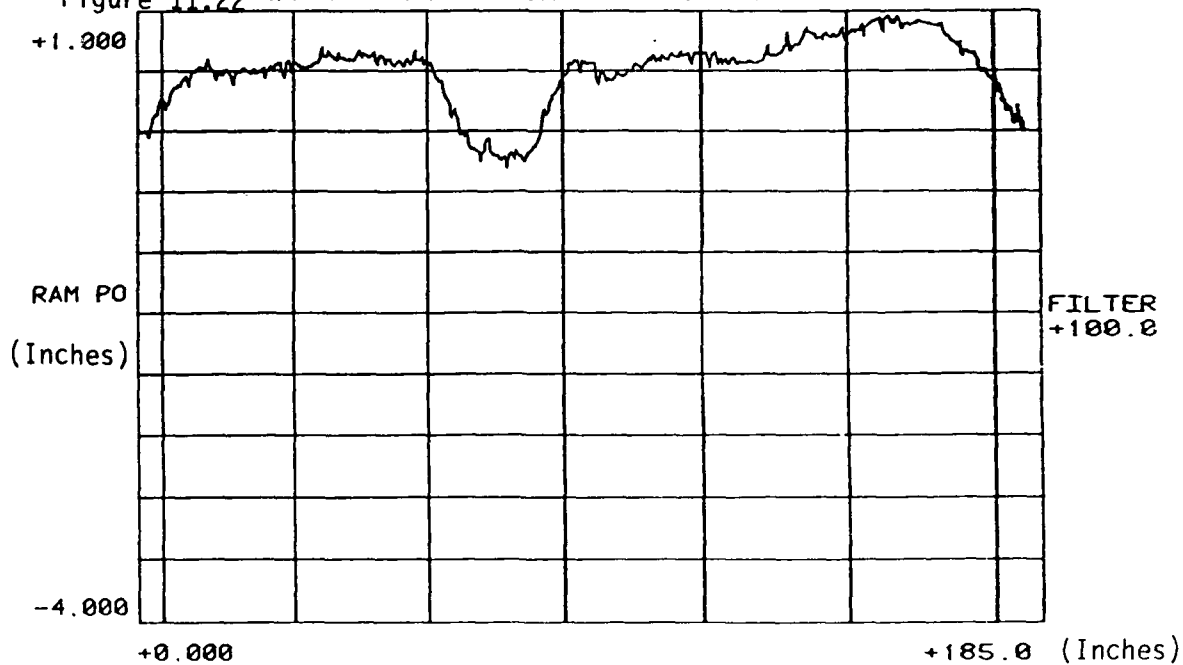


Figure 11.22 (PASS 2) DEFLECTION VS. TABLE POSITION



TBL PO

Figure 11.23 (PASS 50) DEFLECTION VS. TABLE POSITION

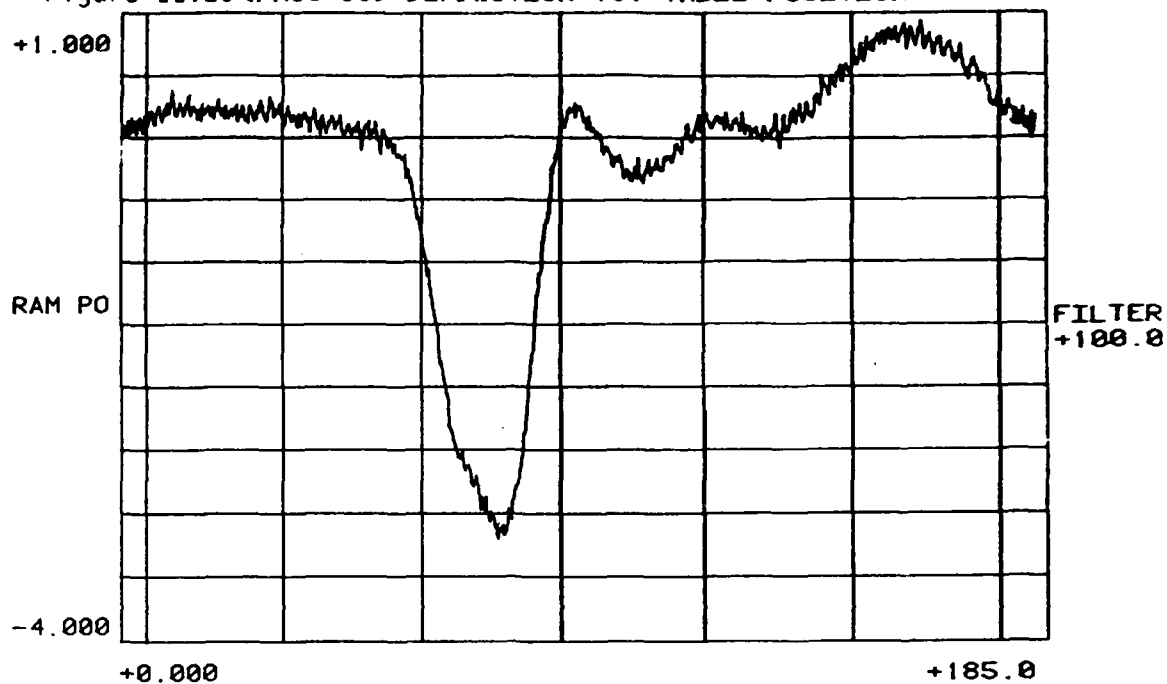


Figure 11.24 (PASS 100) DEFLECTION VS. TABLE POSITION

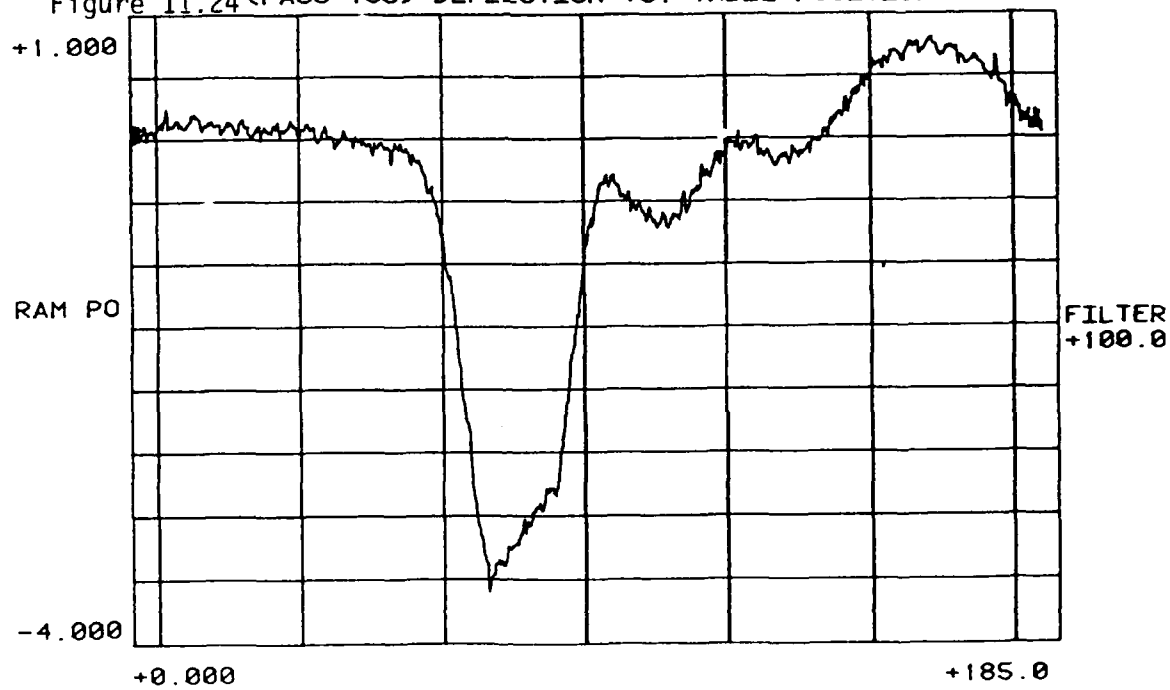


Figure 11.25(PASS 200) DEFLECTION VS. TABLE POSITION

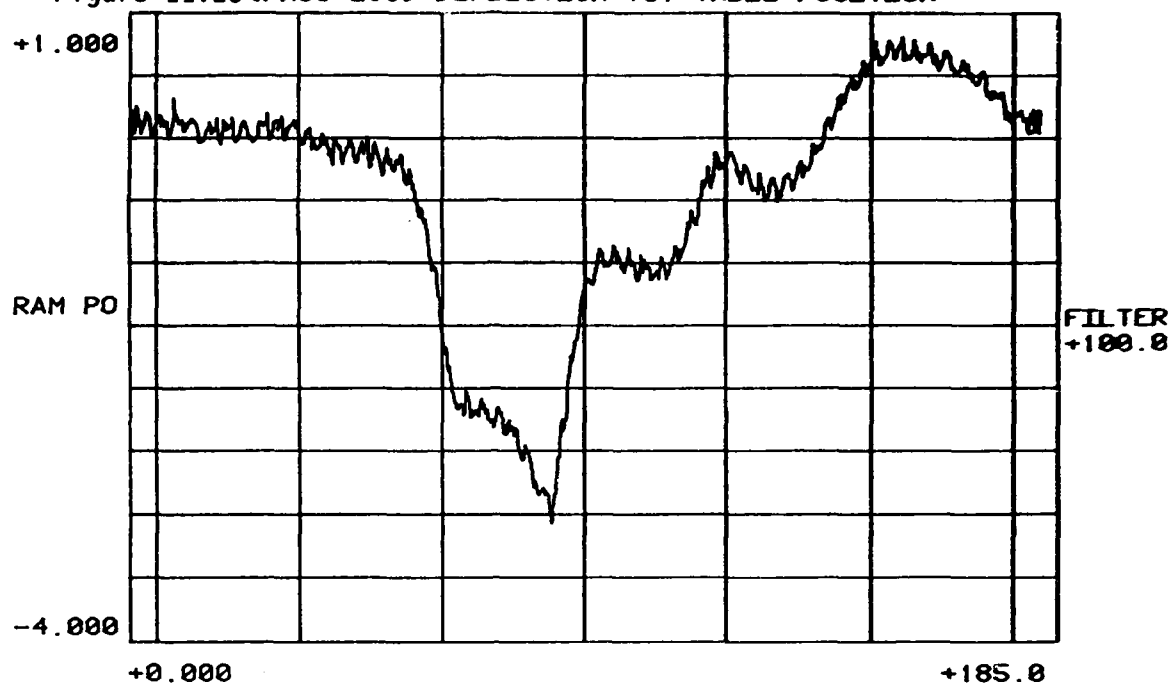


Figure 11.26(PASS 400) DEFLECTION VS. TABLE POSITION

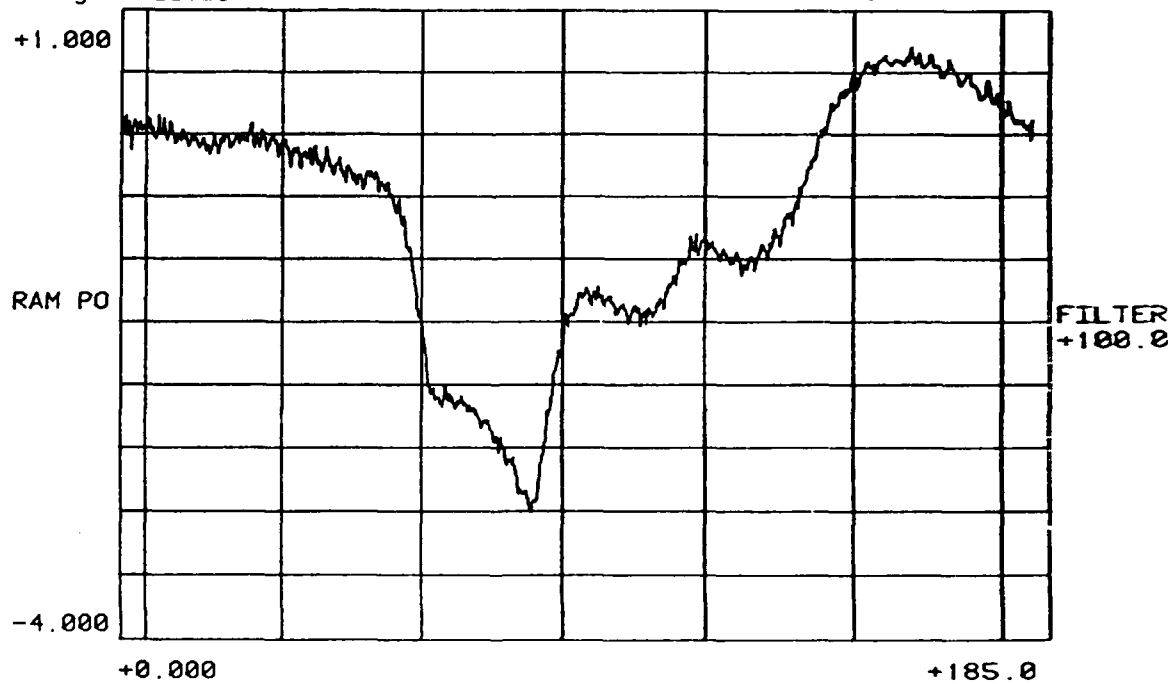


Figure 11.27(PASS 450) DEFLECTION VS. TABLE POSITION

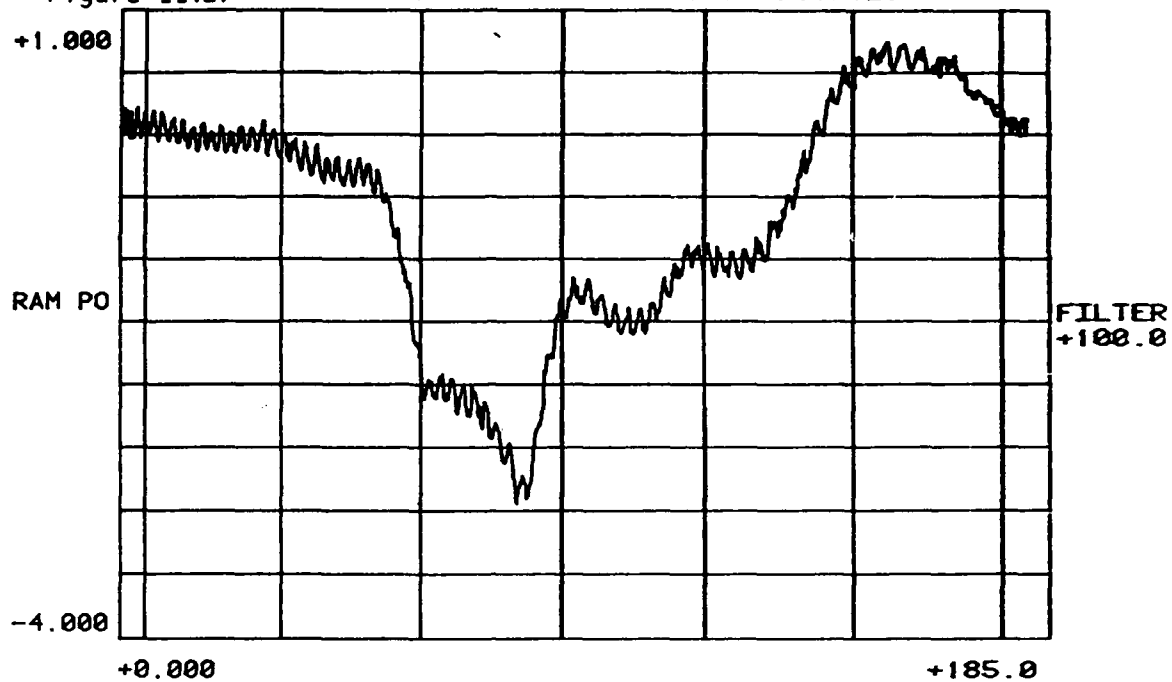
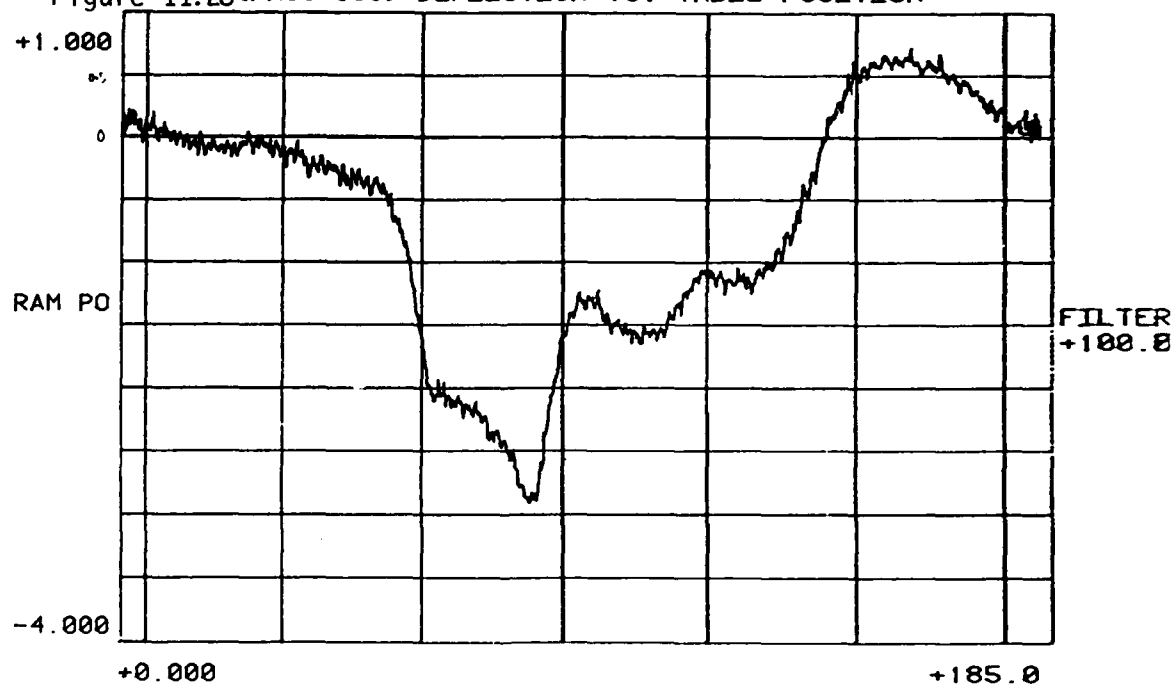


Figure 11.28(PASS 500) DEFLECTION VS. TABLE POSITION



TBL PO

Figure 11.29(PASS 600) DEFLECTION VS. TABLE POSITION

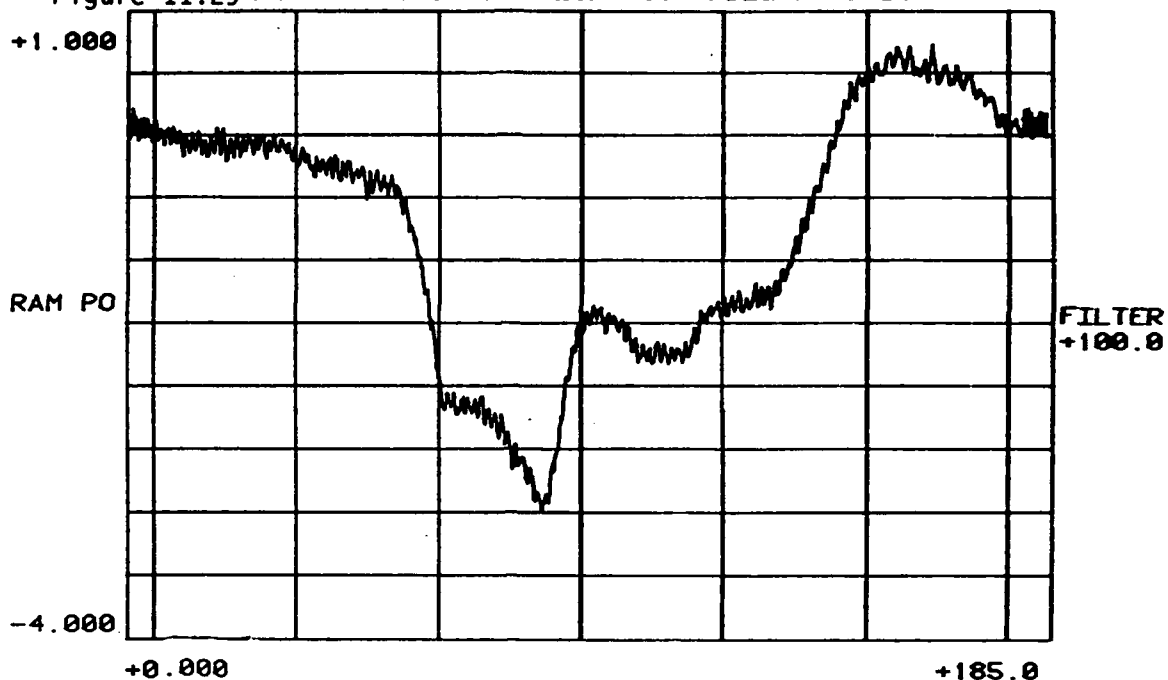


Figure 11.30(PASS 750) DEFLECTION VS. TABLE POSITION

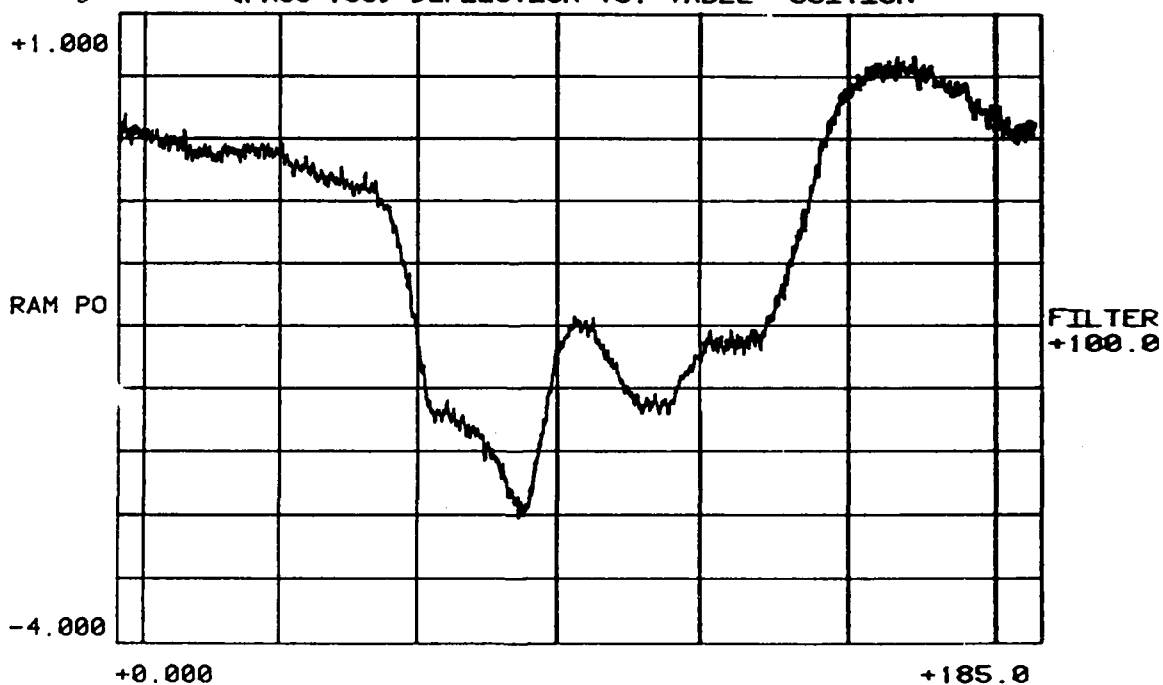
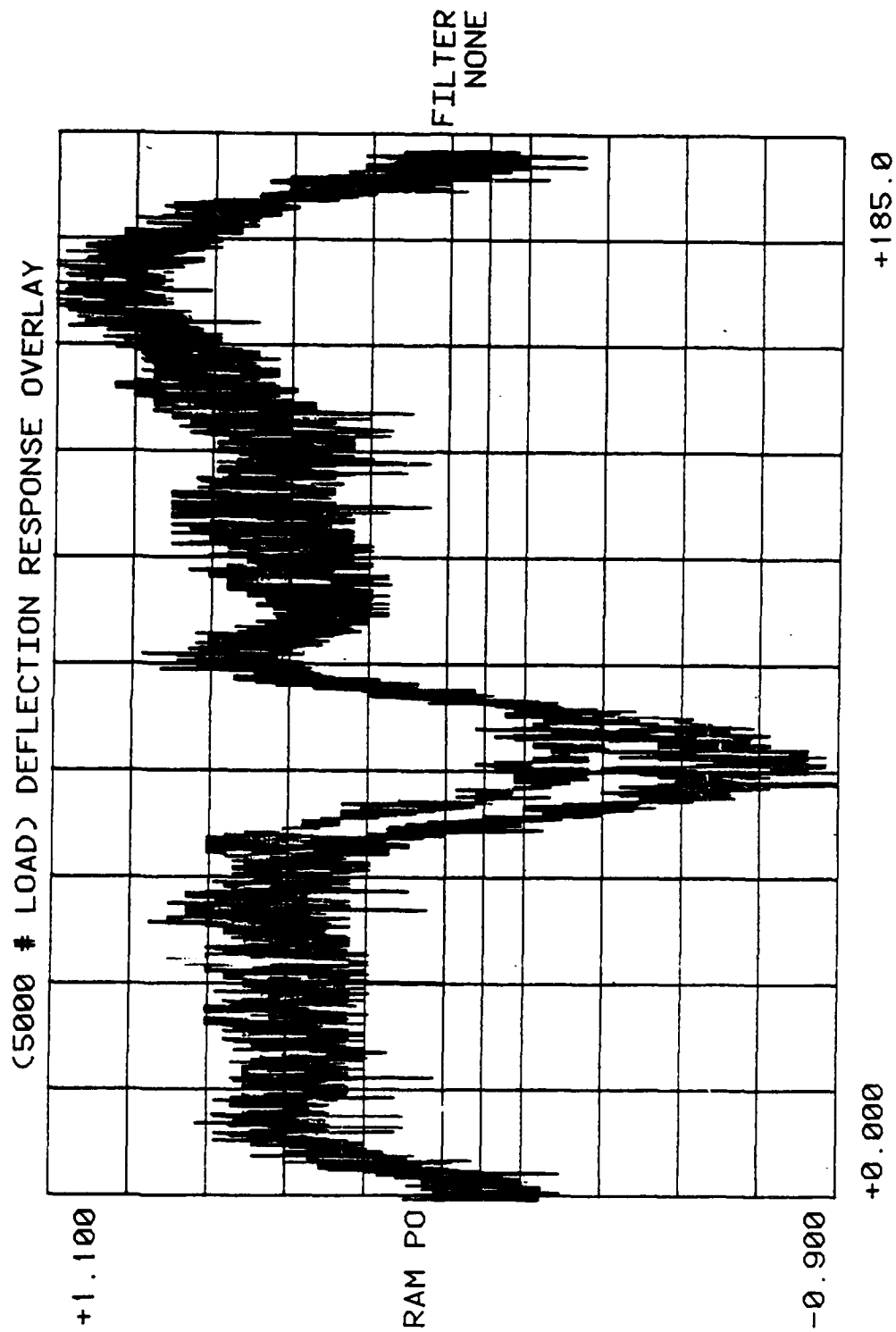
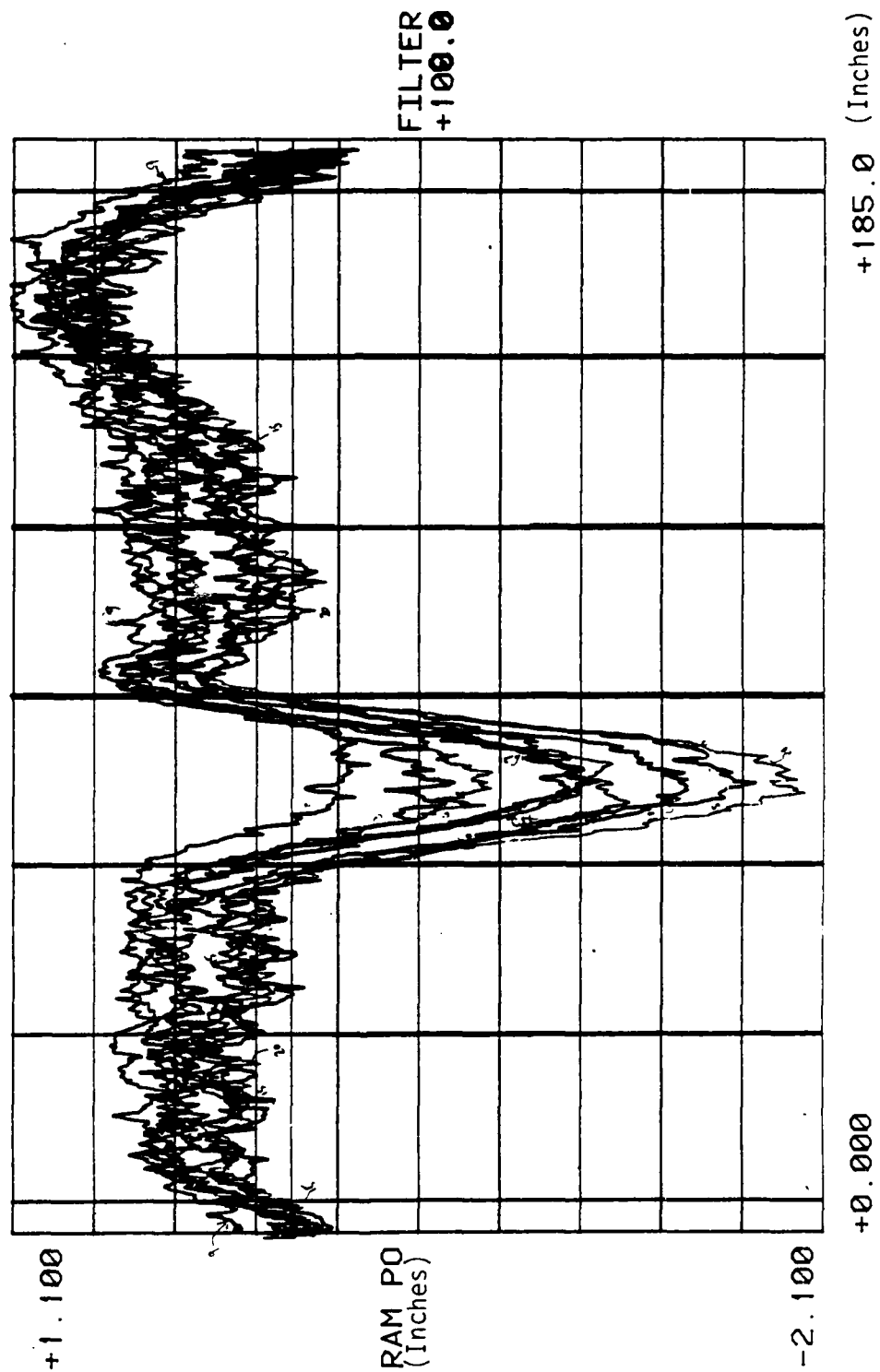


FIGURE 11.31 UNFILTERED SURFACE PROFILE READING VS TESTING POSITION FOR PASSES = 2,3,4



TBL PO

FIGURE 11.32: SURFACE PROFILE VS TEST-BED POSITION FOR PASSES = 2,3,6,7,9,10,15,20



IBL PO

FIGURE 11.33: APPLIED WHEEL LOAD VARIATION VS TIME (MEAN LOAD 5000 LBS)

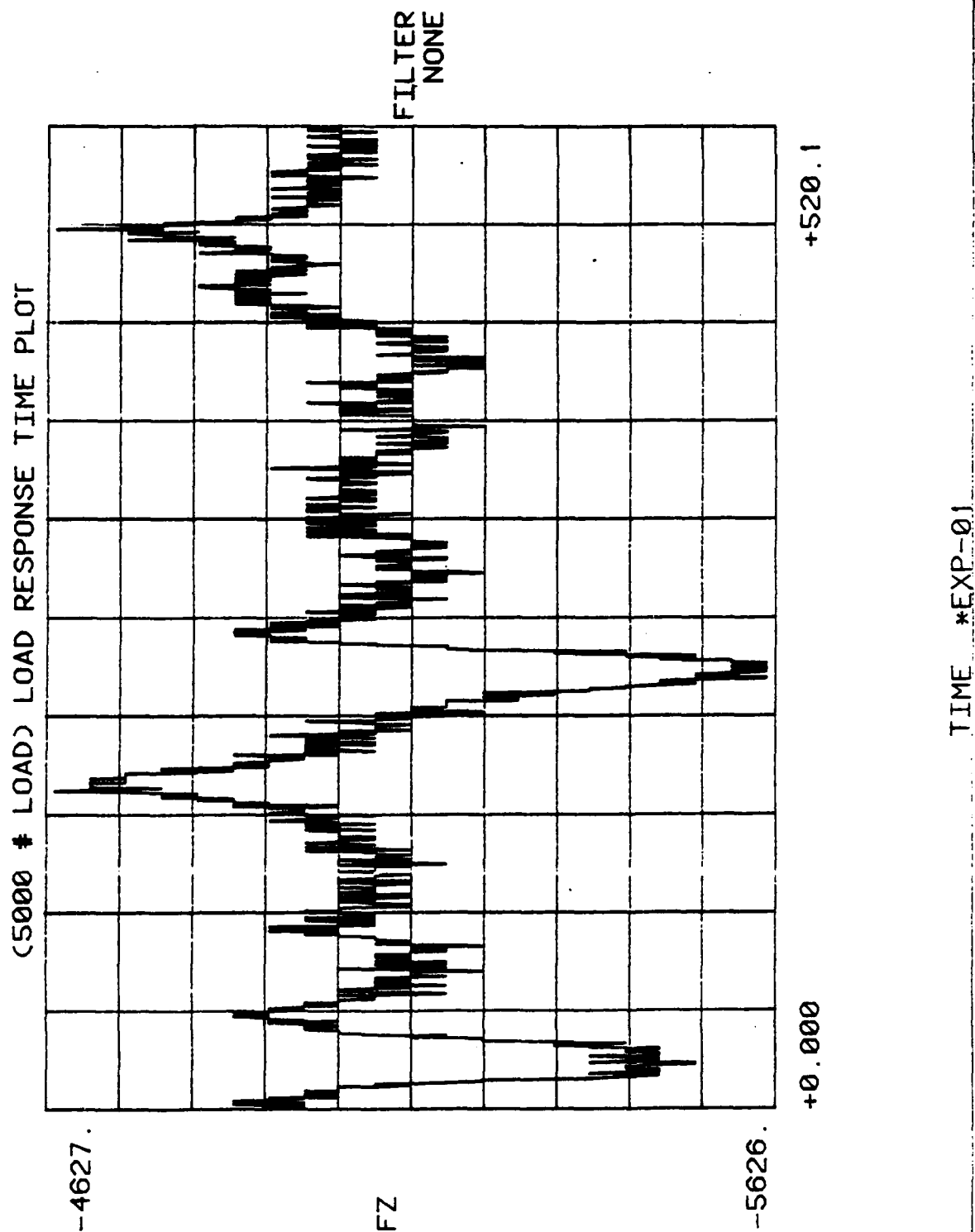
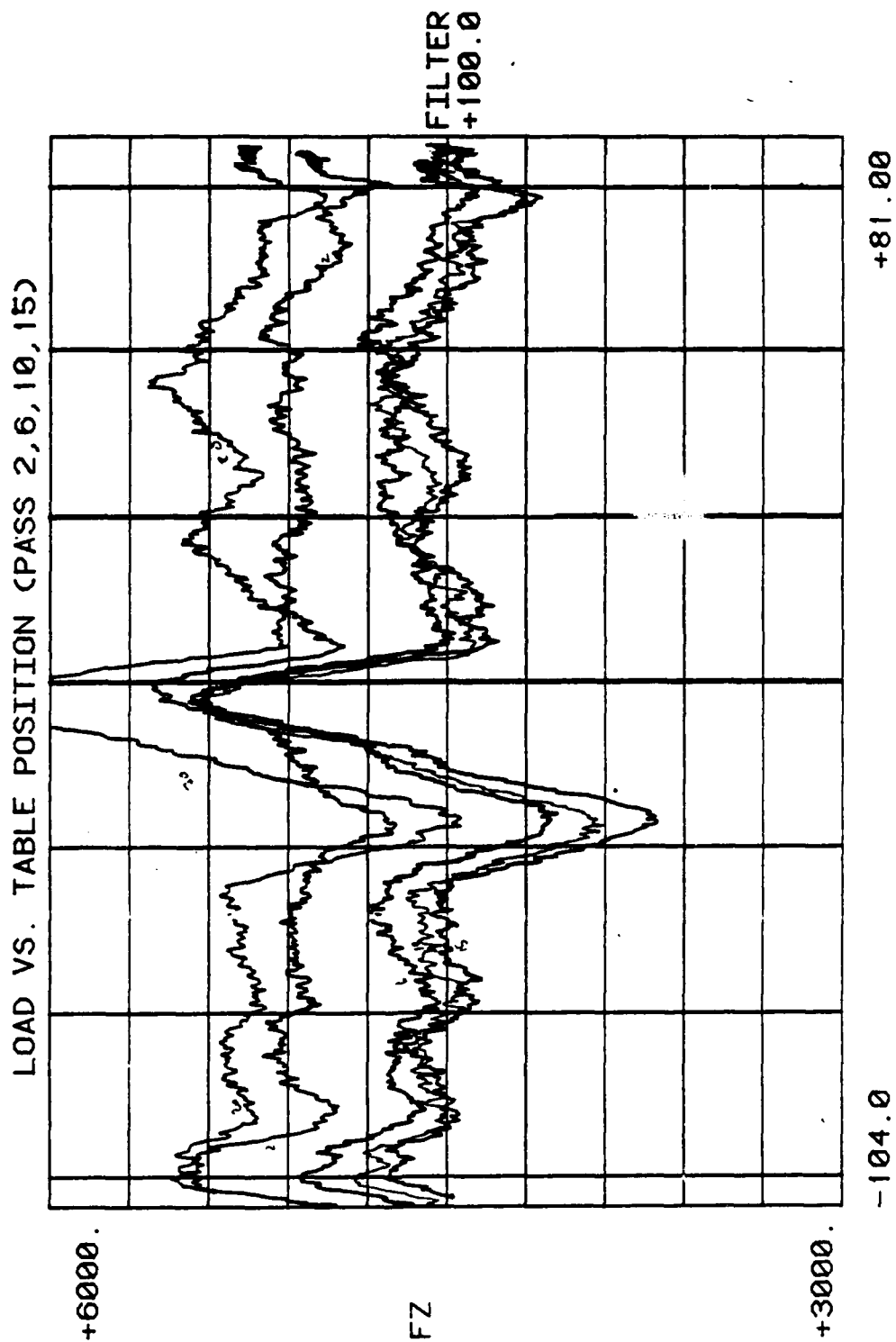


FIGURE 11.34: APPLIED WHEEL LOAD PROFILE (FILTERED) VS TIME FOR PASSES = 2,6,10,15,20



TBL PO

11.1.5 TIRE LOAD RESPONSE PROFILE

Although the load was set at 5000 lbs. during the experimentation, load fluctuations occurred resulting in tire load variations of +8% about the mean load of 5000 lbs. Figure 11.33 shows an unfiltered load response signature. The greatest variation occurred as the sample passed the midpoint of the test-bed when it started to climb up the trough created by the weak (M=17%) control sample.

Figure 11.34 shows the load signatures for various wheel load passes. A horizontal line can be drawn for the 5000 lb. load to indicate that the line is reasonably positioned at the mean of the various wheel load signatures.

11.1.6 RUTTING RESPONSE SURFACE ANALYSIS

A three dimensional plot of the experimental data in rut depth, additive and wheel load passes is shown in Figures 11.35 and 11.36. The two surfaces illustrate graphically the effectiveness of the stabilizing agent at the 4% level of application in reducing significantly the incidence of rutting.

At the 17% moisture level, the additive at the 2% and 4% level is more effective in reducing rutting when compared to the control case. For the dryer (M=14%) sample the progression of rutting seems to increase as wheel load application increases, however for the M=17% case the rut depth leveled out for the 2% and 4% additive application after about 150 passes.

FIGURE 11.35

(MOISTURE CONTENT = 14%, C/S = 0.5)

SURFACE PLOT OF RUT DEPTH VS PASSES & ADDITIVE

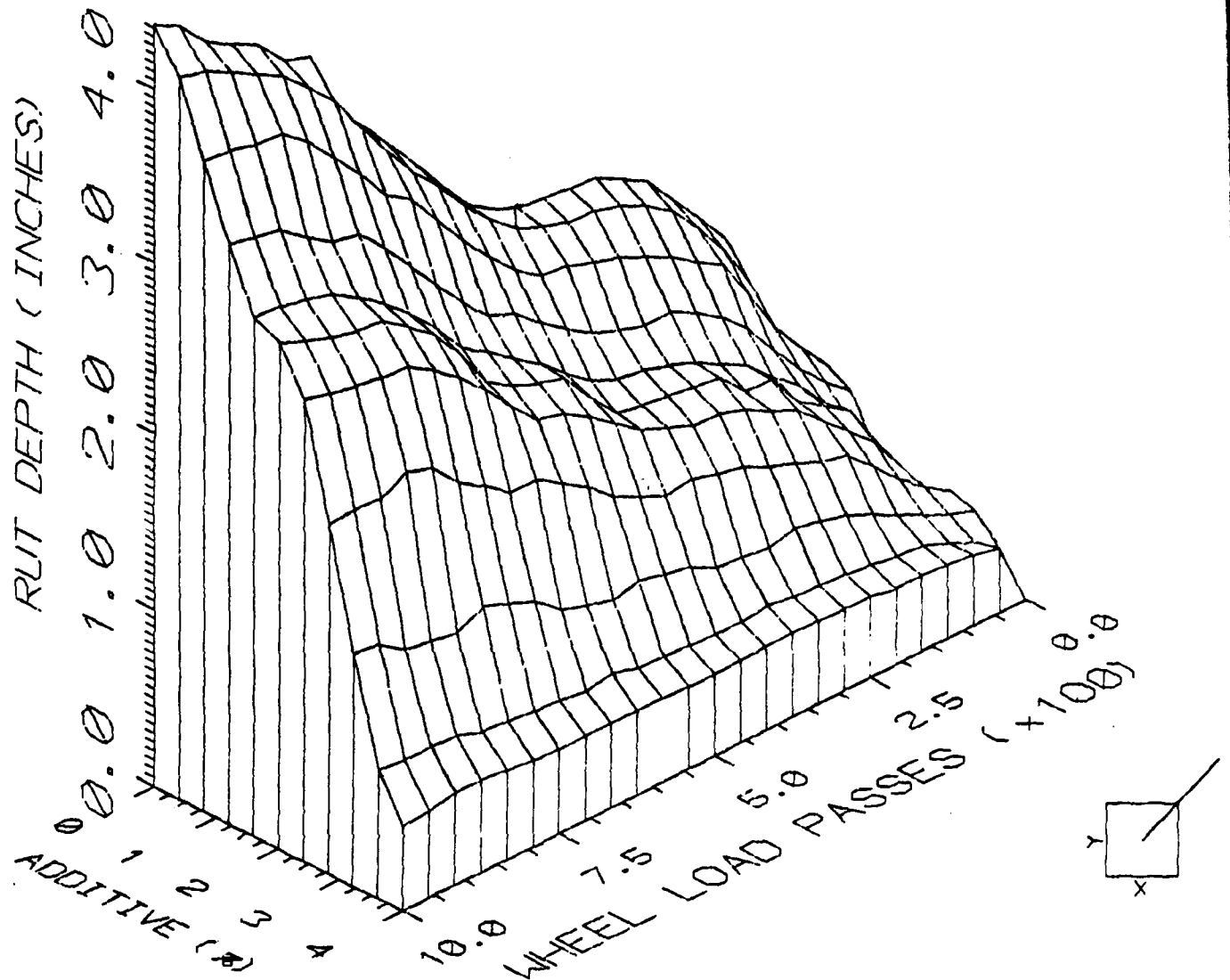
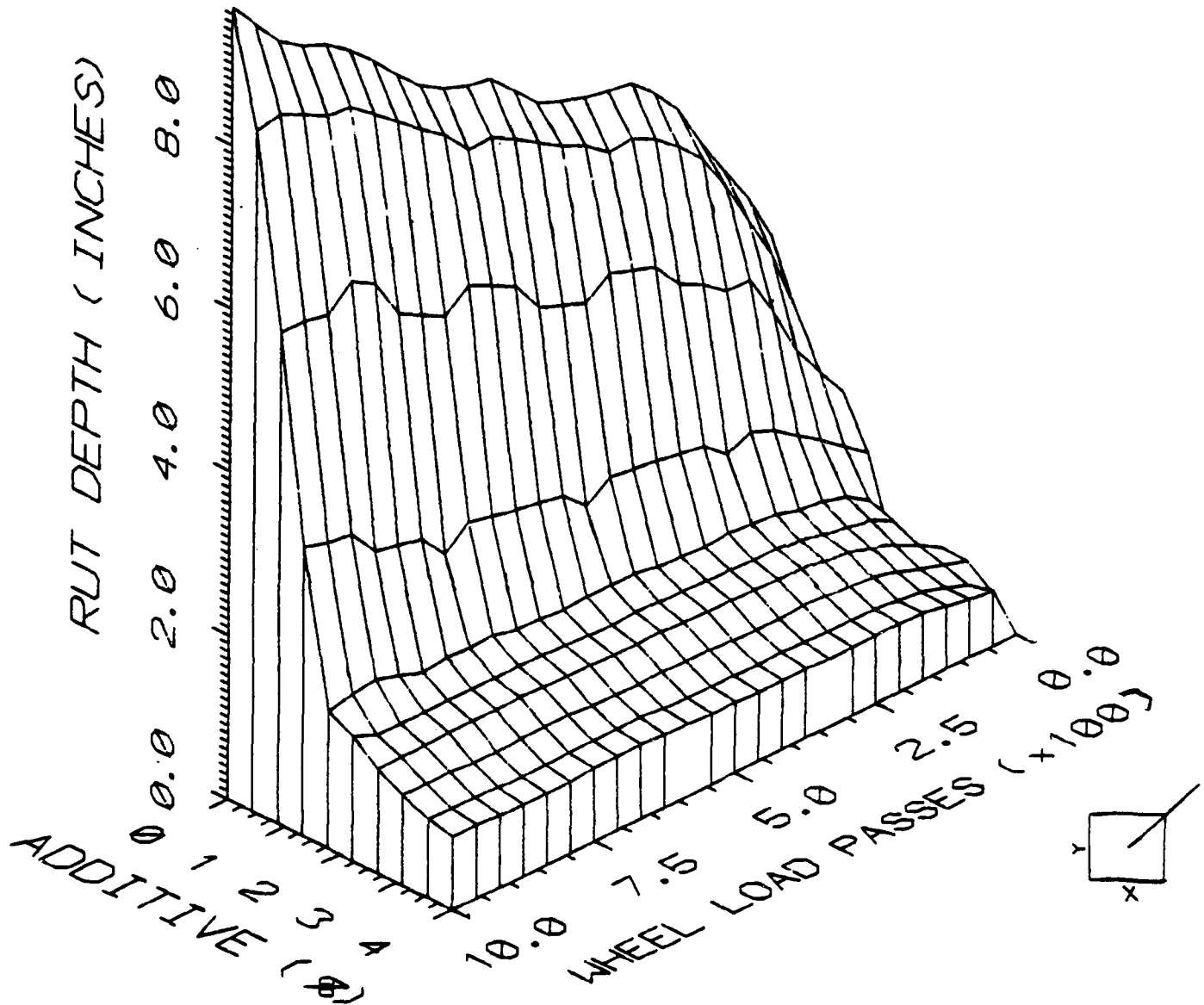


FIGURE 11.36

(MOISTURE CONTENT = 17%, C/S = 0.5)

SURFACE PLOT OF RUT DEPTH VS PASSES & ADDITIVE



COMPUTER MODELING FOR RUT DEPTH PREDICTION

12.1 THE WES RUT DEPTH MODEL

The assessment of the degree of pavement deterioration using actual historic data has been examined by Barber, V. C. et al. (19) using statistical techniques. The study analyzed the deterioration of pavements using a two step constrained stepwise regression of rutting data. Historically, pavement rutting has constituted a failure criteria for flexible pavements.

The database used was the result of two man-years of effort that reviewed all existing data on pavement rutting at the Waterways Experiment Station (WES) and screened the data for overall applicability prior to the data analysis. The result provided a large quantity of high-quality rutting data applicable to two and three layer flexible pavements as well as gravel-surfaced and unsurfaced facilities. The variables in the model are :

- RD = Rut depth in inches
- P = Equivalent Single Wheel Load (ESWL)
- t_p = Tire Pressure, psi
- R = No. of wheel load passes
- t_i = Thickness of ith pavement layer, inches
- c_i = CBR of ith pavement layer

These variables were used to develop relationships for rut-depth through a three-step procedure of :

- 1) Determining rut depth as a function of traffic variables, which are equivalent single-wheel load, tire pressure, and number of wheel repetitions.
- 2) Normalization of rut-depth to reduce the effect of loading
- 3) Correction for non-linearities that may have been produced in the first two steps. This exercise resulted in higher coefficient of correlation, r , and lower error, SE_3 , than other well known regression analysis procedures.

The two pavements selected for the purpose of rutting prediction in this research are 1) Gravel surfaced stabilized airport pavement, and 2) A flexible two-layer pavement system.

A gravel surfaced facility usually has the subgrade protected by gravel and is characterized by a protective gravel surface CBR that is higher than that of the subgrade.

The expression developed for the gravel surface facility was derived from an original 299 data points and is specified as follows :

$$RD = \left(\frac{0.8705 * P_k^{0.4707} * T_p^{0.5695} * R^{0.2476}}{(\log t)^{2.0020} * C_1^{0.9335}} \right) \quad (12.1)$$

Where P_k is the load in (thousand pounds) and other variables retain their earlier defined meanings, with the additional specification that C_1 , C_2 imply the CBR of the top

and bottom layers respectively, and t = thickness of top layer. For the two-layer flexible pavement system, a regression model was developed from 337 data points. The system is identified by a pavement that has no subbase directly above the subgrade. The expression developed is:

$$RD = \left(\frac{29.1465 * P_k^{1.3127} * t_p^{0.0499} * R^{0.3240}}{(\log(1.25 * t_1 + t_2))^{3.4204} * C_1^{1.6877} * C_2^{0.1156}} \right) \quad (12.2)$$

Where the variables t_1 , t_2 represent the thickness of the asphalt cement and the base, while C_1 , C_2 represent the CBR of the base and subgrade respectively.

12.2 CSU MODIFIED RUT DEPTH PREDICTION MODEL

Using the available rutting data generated from testing on the tire force machine (TFM), a calibration of the relationship developed relating CBR to rutting for both models has been executed. The results are shown in Tables 12.1 and 12.2. The clay-silt system CBR values were obtained by use of the model developed in phase I relating clay-silt CBR to the soil system parameters.

TABLE 12.1

COMPARISON OF ACTUAL VS PREDICTED RUT-DEPTH FOR STABILIZED
CLAY SILT SOIL (MOISTURE LEVEL = 14%)

WHEEL LOAD PASSES	R U T T I N G (Inches)					
	% A = 4		CBR = 92.3		% A = 2	
	Actual	Predicted	Actual	Predicted	Actual	Predicted
5	0.22	0.13	0.28	0.21	0.47	0.40
20	0.34	0.22	0.56	0.36	0.94	0.68
50	0.39	0.30	0.64	0.48	1.10	0.92
100	0.42	0.38	0.94	0.60	1.66	1.15
150	0.44	0.43	1.03	0.68	1.88	1.31
200	0.44	0.47	1.28	0.75	2.08	1.44
250	0.47	0.51	1.28	0.81	2.16	1.55
500	0.44	0.63	1.69	1.01	2.47	1.94
750	0.49	0.74	2.47	1.17	3.75	2.24
1000	0.50	0.81	2.90	1.28	4.38	2.44

11" Stabilized Layer, CBR = 48.10; 1" Asphalt Surfacing, Tire Load = 5000 lbs.

TABLE 12.2

COMPARISON OF ACTUAL VS PREDICTED RUT-DEPTH FOR STABILIZED
CLAY SILT SOIL (MOISTURE LEVEL = 17%)

WHEEL LOAD PASSES	R U T T I N G (Inches)					
	% A = 4		CBR = 92.3		% A = 2	
					CBR = 70.2	
	Actual	Predicted	Actual	Predicted	Actual	Predicted
5	0.45	0.18	0.59	0.33	1.66	0.86
20	0.66	0.31	0.91	0.57	3.00	1.46
50	0.72	0.42	1.10	0.77	3.80	1.96
100	0.72	0.53	1.19	0.96	4.50	2.46
150	0.84	0.60	1.22	1.09	5.20	2.80
200	0.84	0.66	1.28	1.20	5.80	3.10
250	0.84	0.71	1.31	1.29	6.10	3.31
500	0.85	0.89	1.38	1.62	7.00	4.14
750	0.91	1.04	1.41	1.87	8.20	4.74
1000	0.91	1.13	1.44	2.04	9.70	5.19

11" Stabilized Layer, CBR = 15.0, 1" Asphalt Surfacing, Tire Load = 5000 lbs.

12.3 COMPARISON OF ACTUAL VS PREDICTED RUT DEPTH

The values of the permanent deformation of the clay-silt pavement due to a constant 5000 lb superimposed moving load exhibit a generally consistent trend with increasing wheel load passes. As the additive content of the stabilized layer decrease, the rutting values correspondingly increase. Increased moisture content further leads to increased rutting.

The predicted rutting values are consistent across moisture content and additive variations for progressively increased wheel load passes. The computer program developed is capable of predicting the rutting values for conditions within the range of the predefined experimental values. A comparison of the actual rutting (experimental data) versus the predicted rutting (model results) indicates a consistency in trend and a mean absolute relative error of 35% of the actual rut depth values obtained.

The greatest discrepancy in the rutting values in Tables 12.1 and 12.2 occur for the control (i.e. no additive case). Explanation for this include the inherent weakness and instability of the fine uniformly graded clay-silt sample as evidenced by markedly decreased resistance to shear deformation. The predicted rutting values were generally lower than the actual values except in a few situations in which the incidence of higher wheel load passes induced a higher predicted rutting value.

DISCUSSION AND SUMMARY

The engineering problems created by unsuitable soils located on potential airport runway sites have received some attention in the literature; however considerably less research effort has been targeted at the specific problem imposed by clay and silt soil mixtures. The study in phase I of this research quantified the stabilization using the two part organic stabilizer - Bisphenol A/Epichlorhydrin resin plus a polyamide hardener obtained by reacting dimerized linoleic acid with di-ethylene triamine.

Substantial soil strength improvement has been obtained using the identified additive based on the phase I results of the CBR test run conducted using a full factorial experimental design. The phase I data and results gave impetus to the need for a follow-on validation study to verify the test results using a generally accepted test of pavement resistance to superimposed traffic load.

For the phase II studies, the rutting test was considered more suitable than other alternative tests; literature review and data exist correlating pavement rutting with CBR test data such as conducted in phase I. The rutting test has a physical similarity to the mode of progressive pavement distress; furthermore criteria for pavement failure based on the rutting test exist and are easily implementable.

The test bed for the rutting test was prepared to a 3 x 2 x 1 factorial design specification in additive (3-levels), moisture content (2-levels) and clay-silt ratio (1-level). These chosen variables were identified as the most significant from the phase I study.

The rigid all-steel test bed 102" (L) by 40" (W) (Figures 10.7 to 10.9) has a deflection when fully loaded, of less than one-hundredth of an inch when lifted from the ends in a simply supported fashion. It was however lifted at quarter points approximating a continuous beam with a much smaller deflection.

It was lifted onto a Tire Force Machine (TFM) at four equally spaced locations to minimize stress distortion on the sample after a curing period ranging from seven days for the newest sample to ten days for the oldest sample prepared. The samples which were mixed using a motorized 6 cu. ft. mortar mixer to ensure sample homogeneity were each compacted to modified AASHTO specification using the BOMAG impulse/vibratory compactor to a depth of 11".

Curing was preceded by wrapping the samples with polythene protective covers to prevent the evaporative losses of the sample moisture. Further moisture loss prevention was guaranteed by a protective M502 asphalt based top surfacing material that was applied and compacted with a 250 lb. roller

to provide a smooth riding surface for the aircraft tire. The asphalt topping also prevented premature onset of the progressive and incipient wear of the stabilized clay/silt soil surface.

The TFM table speed of 0.17 knot was considered low and insignificant to cause alteration of compacted clay-silt soil sample structure and strength properties. Furthermore, end platforms 12" long and 40" wide were included in the test bed design to absorb the inertial wrapup forces associated with table direction reversals after each pass. The automated data collection equipment affixed to the TFM yoke and ram provided experimental data that were analyzed and displayed in Table 11.1. Manual data collected supplemented and corroborated the automated data collected and close agreements were obtained.

A total of approximately 40 hours of rutting test data were obtained and the maximum rutting value obtained for the strongest sample (A=4%, M=14%) was a half inch (1/2"). The maximum equivalent rut depth of the weakest sample (A=0%, M=17%) was 9.7" after extrapolation. The extrapolation was necessary because a four-inch position control on the allowable depth of sinkage was in effect. It is submitted, that the rut depth values obtained are conservative. They are generally larger than would have been the case because of such factors as the inadequate compaction of the asphalt surfacing. This leads to an inflated value of the rutting of the asphaltic layer

which would not have resulted, using standard field compaction of the asphalt layer.

Application of the first pass of a 5000 lb tire load resulted in a visible compaction of the asphalt overlaying the stronger samples to depths ranging from 1/4" to 3/4". The weaker sample, it is hypothesized, had a 2" deformation the bulk of which is attributable to permanent deformation of the clay-silt soil sample. Allowing for the inadequate pre-load compaction of the asphalt topping on the clay-silt soil sample would indicate a rutting depth after 1000 wheel load applications of less than 1/2" for the 4% additive treatment case at the 14% level of moisture. A rutting value in excess of 1/2 inch is considered unacceptable for commercial aviation purposes.

The rutting prediction model developed by Central State University based on the earlier work at the Waterways Experiment Station (WES) of the Army Corps of Engineers showed good agreement both in terms of relative values and the trend of rutting data with passage of wheel loads up to 1000 passes. Also, the comparative evaluation of the actual versus the predicted rutting of the clay-silt sample is not statistically different based on non-parametric statistical tests (Tables 12.1 and 12.2).

CONCLUSIONS / RECOMMENDATIONS

The following conclusions and recommendations are made based on the results of the rutting studies performed:

- 1) An effective epoxy based organic additive capable of significantly increasing the resistance to deformation of a clay-silt soil sample has been identified and tested. Effectiveness at the 2% and 4% level of application has been demonstrated based on the results of the California bearing ratio tests (Phase I) and rutting tests (Phase II) conducted.
- 2) The close agreement in terms of relative magnitude and trend obtained from the rutting data establishes the validity of the correlation claimed between CBR and pavement rutting; furthermore these results apply to a load threshold of 5000 lb of equivalent single wheel load on an aircraft tire.
- 3) Construction of an aircraft pavement on a clay-silt terrain for moisture conditions even as low as 14% without adequate stabilization could lead to unsatisfactory runway performance and excessive rut depths, such as 3-1/2 inches of rut after 1000 passes at the 14% moisture level.

- 4) The outer edges of the interface between a loaded aircraft tire and an effectively stabilized clay-silt soil pavement suffer little heave due to stress induced pavement distortions after 1000 passes. For samples having additive levels between 2% and 4% of the epoxy-based chemical stabilizer used in this study, this observation is particularly valid.
- 5) It is recommended that at locations where clay-silt soils predominate as pavement materials and soil importation is impractical, uneconomical, or not advisable, chemical stabilization of a pavement to depths of 12 inches at the 4% level of the additive tested is a viable alternative. The use of the stabilizer as specified will allow for the safe operation of a 10,000 lb aircraft load annually at locations where approximately three (3) average operations per day are performed, based on 1000 wheel load coverages in a 365-day period as simulated by the rutting test.
- 6) At low volume airports where the suggested stabilization is adopted, it is recommended that periodic pavement performance monitoring and maintenance activities be conducted.
- 7) Further studies are recommended to further isolate,

focus and quantify the magnitude of the clay-silt soil problem from an engineering standpoint. More tests are needed to develop generally accepted criteria for broader limits of application of this chemical stabilization method.

REFERENCES

1. Terrel, R. L., Epps, J. S., Barenberg, E. J., Mitchell J. K., and Thompson, M. R., "Mixture Design Considerations," Soil Stabilization in Pavement Structures, A User's Manual, U.S. Department of Transportation, Vol. 2., October 1979,
2. Horonjeff, R. "Airport Design & Operations," McGraw-Hill Book Co., 1975.
3. McLaughlin, A. L., "The Performance of Civil Airport Pavements with Lime-Cement-Fly Ash Base Course," Report No. DDT/FAA/PM-84/10, US Department of Transportation, April 1984.
4. Kinter, E. B., "Development and Evaluation of Chemical Soil Stabilizer," Report No. FHWA-RD-75-17, U.S. Dept of Transportation, March 1975.
5. Fohs, D. G., "A Laboratory Evaluation of Two Proprietary Materials As Compaction Aids and Soil Stabilizers," Report No. FHWA-RD-75-32, U. S. Dept. of Transportation, March 1975.
6. Carpenter, S. H., Lytton, R. L., "Physio-chemical Considerations in Thermal Susceptibility of a Base-Course Material," Transportation Research Record, No. 642, pp. 36-38, 1977.
7. McKeen, R. G., Nielson, J. P., "Characterization of Expansive Soils for Airport Pavement Design," Interim Report, Report No. FAA-RD-78-59, US Dept. of Transportation, August 1976.
8. McKeen, R. G., "Design of Airport Pavements for Expansive Soils," Report No. DOT/FAA/RD-81-25, US Dept of Transportation, January 1981.
9. Edris, E. V., Jr. and Lytton, R. L., "Climatic Materials Characterization of Fine-grained Soils," Texas A & M University, Transportation Research Records, No. 642, pp. 39-44, 1977.
10. Chou Y. T., "Probabilistic and Reliability Analysis of the California Bearing Ratio (CBR) Design Method for Flexible Airfield Pavements," Technical Report GL-86-15, U. S. Army Engineers, Waterways Experiment Station, Corps of Engineers, Vicksburg, Mississippi.

11. Brabston, W. N., "Investigation of Compaction Criteria for Airport Pavement Subgrade Soils," US. Army Engineer Waterways Experiment Station, Geotechnical Lab., Report No. DOT/FAA/RD.-81/48, U.S. Dept. of Transportation, October 1981.
12. "Specifications for Subsurface Investigations," State of Ohio, Dept. of Transportation, February 1984.
13. Lamb, J. H., Ritchie, J. M., "Sampling a Glacial Silty Clay," Transportation Research Record, No. 642, pp. 53-56, 1977.
14. Yoder, E. J., Witczak, M. W., "Principles of Pavement Design," John Wiley & Sons, Inc., NY, 2nd Edition 1975.
15. Ullidtz, P., "Pavement Analysis," Institute of Roads, Transport and Town Planning, The Technical University of Denmark, Lyngby, Denmark, Elsevier Publishers, 1987.
16. Keedwell, M. J., "Rheology and Soil Mechanics," Department of Civil Engineering and Building, Coventry Polytechnic, UK., Elsevier Science Publishing Co., Inc., New York, USA, 1984.
17. Courtney, F. M., Trudgill, S. T., "The Soil," 2nd Edition, Edward Arnold Publishers Ltd, London, UK, 1984.
18. Monismith, C. L., Ogama, N., Freeme, C. R., "Permanent Deformation Characteristics of Subgrade Soils in Repeated Loading," Transportation Research Record, No. 537, 1975.
19. Barber, V. C., Odam, E. C., Patrick, R. W., "The Deterioration and Reliability of Pavements," Final Report, Geotechnical Laboratory, U. S. Army Engineers, Waterways Experiment Station, Technical Report S-78-8, U. S. Department of the Army, Washington, D. C., July 1978.
20. Barker, W. R., "Prediction of Pavement Roughness," Final Report, Geotechnical Laboratory, U. S. Army Engineers, Waterways Experiment Station, Miscellaneous Paper GL-82-11, U.S. Department of the Army, Washington, D. C., September 1982.
21. Ullidtz, P., "Computer Simulation of Pavement Performance," Report No. 18, Institute of Roads, Transport and Town Planning, The Technical University of Denmark, January 1978.

22. Morris, J., Haas, R. C. G., Reilly P. and Hignell, E. T., "Permanent Deformation in Asphalt Pavement Can Be Predicted," Proc. AAPT, Vol. 43, 1974.
23. Saraf. C. L., Smith, W. S., Finn, F. H., "Rut Depth Prediction," Transportation Research Record, No. 616, 1976.
- 24 Lydia Vock, "Comparison Between the OSU and FHWA Methods for Asphalt Concrete Rutting Prediction," Thesis M. S., The Ohio State University, Columbus, Ohio, 1979.

APPENDIX A:

Clay-Silt Batching and Data Reduction Programs

APPENDIX A-1:

Formulae for Batching Clay-Silt Mixtures

S U M M A R Y

- ① Specifying & Additive
 GIVEN:
 $P_w, P_a, \delta_a, \delta_s, \delta_c$ C/S RATIO
 $r = \text{clay/aggregate ratio}$

Calculate:

$$W_s = \frac{10(1-r)}{1-\delta_s}$$

$$W_c = \frac{10r}{1-\delta_c}$$

$$W_T = \frac{10}{(1-P_w - P_a)}$$

$$W_A = \frac{P_a W_T}{1-\delta_a}$$

W_{WATER} IF W_{WATER} IS
 Negative, Go to ② & ③

- ② Specifying & Additive Only
 GIVEN:
 $P_a, \delta_a, \delta_s, \delta_c$ C/S RATIO
 $r = \text{clay/aggregate ratio}$

Calculate:

$$W_s = \frac{10r}{1-\delta_s}$$

$$W_c = \frac{10(1-r)}{1-\delta_c}$$

$$W_T = \left(\frac{1-\delta_a}{1-\delta_a - P_a} \right) [\delta_s W_s + \delta_c W_c + 10]$$

$$W_A = \frac{P_a W_T}{1-\delta_a}$$

$$P_w = \frac{\delta_a W_a + \delta_s W_s + \delta_c W_c}{W_T}$$

- ③ Specifying & Water Only
 GIVEN:
 $P_w, \delta_a, \delta_s, \delta_c$ C/S RATIO
 $r = \text{clay/aggregate ratio}$

Calculate:

$$W_s = \frac{10r}{1-\delta_s}$$

$$W_c = \frac{10(1-r)}{1-\delta_c}$$

$$W_a = \frac{(\delta_s W_s + \delta_c W_c)(1-P_w) - 1}{P_w - \delta_a}$$

$$W_T = \frac{(1-\delta_a)W_a + 10}{1-P_w}$$

$$P_a = \frac{(1-\delta_a)W_a}{W_T}$$

APPENDIX A-2:

**Computer Program for Batching
Clay-Silt Mixture**

```

10 CLEAR : CLS
20 SCREEN 2
30 DIM PW(15),PA(15),WS(15),WC(15),WT(15),WA(15),WW(15)
40 DIM EPW(15),EPA(15),EWS(15),EWC(15),EWT(15),EWA(15),EWW(15)
50 DIM MOIST(70),MSYS(70),CATALY(70),HADCOR(70),HARD(70)
60 LPRINT "INPUT DATA FOR PW,PA,DA,DS,DC,R,S,C"
70 LPRINT TAB(1); "PERCENT"; TAB(9); "PERCENT"; TAB(18); "ADDITIVE"; TAB(27); "SILT";
80 LPRINT TAB(36); "CLAY"; TAB(45); "C/S"; TAB(54); "WEIGHT"; TAB(63); "WEIGHT";
90 LPRINT TAB(1); "MOISTURE"; TAB(9); "ADDITIVE"; TAB(18); "MOISTURE"; TAB(27); "MOISTURE";
100 LPRINT TAB(36); "MOISTURE"; TAB(45); "AG RATIO"; TAB(54); "CLAY"; TAB(63); "SILT";
110 LPRINT TAB(72); "W/SIL FAC"
120 I=1
130 READ PW(I),PA(I),DA,DS,DC,R,S,C
140 IF PW(I) > 11 THEN 1180
150 NAIL$ = "GENERIC EPOXY "
160 WEIGHT=101
170 MIXFAC = 11
180 PW(I) =.1
190 PA(I) =.08
200 ACCEL=PA(I)
210 HADCOR=PA(I)
220 DA =.01
230 DS =.005
240 DC =.015
250 R =.6
260 C =WEIGHT*R
270 S =WEIGHT*(1-R)
280 LPRINT USING "###.### " PW(I),PA(I),DA,DS,DC,R,C,S,MIXFAC
290 LPRINT
300 LPRINT
310 LPRINT
320 LPRINT "oooooooooooooooooooooooooooooooooooooooooooooooooooooooooooooooooooooooooooo"
330 LPRINT USING " COMPUTED DESIGN COMBINATIONS FOR \ " NAIL$
340 LPRINT "oooooooooooooooooooooooooooooooooooooooooooooooooooooooooooooooooooooooooooo"
350 LPRINT
360 LPRINT
370 LPRINT
380 LPRINT
390 LPRINT
400 FOR K=1 TO 4
410 LPRINT "oooooooooooooooooooooooooooooooooooooooooooooooooooooooooooooooooooooooooooo"
420 NEXT K
430 LPRINT
440 LPRINT
450 LPRINT
460 LPRINT TAB(1); "PERCENT"; TAB(13); "PERCENT"; TAB(25); "TOTAL"; TAB(37); "WEIGHT";
470 LPRINT TAB(49); "WEIGHT"; TAB(61); "WEIGHT"; TAB(72); "WEIGHT"
480 LPRINT TAB(1); "MOISTURE"; TAB(13); "ADDITIVE"; TAB(25); "WEIGHT"; TAB(37); "WATER"
490 LPRINT TAB(48); "ADDITIVE"; TAB(62); "CLAY"; TAB(73); "SILT"
500 REM *SPECIFYING ZADDITIVE & WATER*
510 EPW(I)=PW(I)
520 Z=EPW(I)
530 K=0
540 FOR I= 1 TO 15
550 WS(I)= (C+S)*(1-R)/(1-DS)
560 K=K+1
570 WC(I) = (C+S)*R/(1-DC)
580 WT(I)= (C+S)*(1+PW(I)+PA(I))
590 WA(I) = PA(I)*(S+C)
600 WW(I) = (PW(I)*(S+C)-DA*WA(I)-DS*S-DC*C)
610 EWS(I) = WS(I)*454
620 EWC(I) = WC(I)*454
630 EWT(I) = WT(I)*454
640 EWA(I) = WA(I)*454
650 EWW(I) = WW(I)*454

```

```

660 EPW(I) = PW(I)*100
670 EPA(I) = EWA(I)/((S+C)*454)*100
680 PA(I) = WA(I)/(S+C)
690 WT(I) = (C+S)*(1+PW(I)+PA(I))
700 EWT(I) = WT(I)*454
710 WW(I) = (PW(I)*(S+C)-DA*WA(I)-DS*S-DC*C)
720 WSYS(K) = WT(I)*454
730 MOIST(K) = PW(I)*100
740 CATALY(K) = ACCELK*WSYS(K)
750 HARD(K) = HADCON(K)*WSYS(K)
760 A1$ = "WATER CONTENT"
770 A2$ = "TOTAL WEIGHT"
780 A3$ = "ACCELERATOR"
790 A4$ = "V40 HARDENER"
800 Z=EPW(I)
810 LPRINT USING "####.##" ;EPW(I),EPA(I),WT(I),WW(I),WA(I),WC(I),WS(I)
820 LPRINT USING "(#####.##)" ;Z,EPA(I),ENT(I),EWW(I),EWA(I),EWC(I),EWS(I)
830 LPRINT
840 TEST = PW(I) + PA(I)
850 IF PW(I) > .22 THEN 1180
860 IF TEST < 1 THEN 900
870 LPRINT "THIS CONDITION IS IMPOSSIBLE >> TEST > 1"
880 GOTO 120
890 END IF
900 IF WW(I)<0 THEN
910 PW(I)=PW(I) + .01
920 GOTO 550
930 ELSE
940 GOTO 960
950 END IF
960 PW(I+1) = PW(I) + .02
970 PA(I+1) = PA(I)
980 IF PW(I) > .3 THEN 1180
990 NEXT I
1000 A1=" SPECIFYING PERCENTAGE WATER & ADDITIVE (PW&PA)
1010 A2=" PERCENT ADDITIVE(PA) = ##
1020 A3="Z MOISTURE(PW)
1030 REM **
1040 REM * SPECIFYING Z ADDITIVE ONLY*
1050 WC = (C+S)*(1-R)/(1-DC)
1060 WS = (C+S)*R/(1-DS)
1070 WA = ((DS*WS+DC*WC)*(1-PW)-(C+S)*PW)/(PW-DA)
1080 WT = ((1-DA)*WA+(C+S))/(1-PW)
1090 PA = ((1-DA)*WA)/WT
1090 PRINT PW(X),PA(X),WT(X),WW(X),WA(X),WC(X),WS(X)
1100 DATA 0.06,0.15,0.06,0.005,0.02,0.6,6.0,4.0
1110 DATA 1.06,0.15,0.06,0.005,0.02,0.6,6.0,4.0
1120 DATA 10.0,0.15,0.06,0.005,0.02,0.6,6.0,4.0
1130 IF EKR = 24 THEN RESUME
1140 FOR L=1 TO 7
1150 LPRINT
1160 NEXT L
1170 LPRINT TAB(1);A1$;TAB(18);A2$;TAB(35);A3$;TAB(52);A4$
1180 FOR L=1 TO 7
1190 LPRINT
1200 NEXT L
1210 LPRINT TAB(1);A1$;TAB(18);A2$;TAB(35);A3$;TAB(52);A4$
1220 FOR M=1 TO K
1230 LPRINT USING " ####.#### " ;MOIST(M),WSYS(M),CATALY(M),HADCON(M)
1240 NEXT M
1250 END

```

APPENDIX A-3:

**Computer Program Output for
Batching Clay-Silt Mixture
Treated with Epoxy-Resin**

INPUT DATA FOR PW,PA,DA,DS,DC,R,S,C

PERCENT MOISTR	PERCENT ADDITIVE	ADDITIVE MOISTR	SILT MOISTR	CLAY MOISTR	C/S AG RATIO	WEIGHT CLAY	WEIGHT SILT	WEIGHT S/C
0.100	0.080	0.000	0.005	0.015	0.600	6.000	4.000	1.000

 (COMPUTED DESIGN COMBINATIONS FOR GENERIC EPOXY
 #####

 #####
 #####
 #####

PERCENT MOISTR	PERCENT ADDITIVE	TOTAL WEIGHT	WEIGHT WATER	WEIGHT ADDITIVE	WEIGHT CLAY	WEIGHT SILT
10.00	8.00	11.80	0.89	0.80	6.09	4.02
(10.)	(8.)	(5357.)	(404.)	(363.)	(2765.)	(1825.)
11.00	8.00	11.90	0.99	0.80	6.09	4.02
(11.)	(8.)	(5403.)	(449.)	(363.)	(2765.)	(1825.)
12.00	8.00	12.00	1.09	0.80	6.09	4.02
(12.)	(8.)	(5448.)	(495.)	(363.)	(2765.)	(1825.)
13.00	8.00	12.10	1.19	0.80	6.09	4.02
(13.)	(8.)	(5493.)	(540.)	(363.)	(2765.)	(1825.)
14.00	8.00	12.20	1.29	0.80	6.09	4.02
(14.)	(8.)	(5539.)	(586.)	(363.)	(2765.)	(1825.)
15.00	8.00	12.30	1.39	0.80	6.09	4.02
(15.)	(8.)	(5584.)	(631.)	(363.)	(2765.)	(1825.)
16.00	8.00	12.40	1.49	0.80	6.09	4.02
(16.)	(8.)	(5630.)	(676.)	(363.)	(2765.)	(1825.)
17.00	8.00	12.50	1.59	0.80	6.09	4.02
(17.)	(8.)	(5675.)	(722.)	(363.)	(2765.)	(1825.)
18.00	8.00	12.60	1.69	0.80	6.09	4.02
(18.)	(8.)	(5720.)	(767.)	(363.)	(2765.)	(1825.)

INPUT DATA FOR PW,PA,DA,DI,DC,R,SV,C
 PERCENT PERCENT ADDITIVE SILL CLAY C/S WEIGHT WEIGHT
 MOISTURE ADDITIVE MOISTURE MOISTURE MOISTURE AG RATIO CLAY SILL 9.500 1.000
 0.100 0.080 0.000 0.005 0.015 0.600 6.000 6.000

 COMPUTED DESIGN COMBINATIONS FOR GENERIC EPOXY
 #####

 #####
 #####
 #####

PERCENT MOISTURE	PERCENT ADDITIVE	TOTAL WEIGHT	WEIGHT WATER	WEIGHT ADDITIVE	WEIGHT CLAY	WEIGHT SILL
10.00	8.00	11.80	0.89	0.80	6.09	4.02
(10.)	(8.)	(5357.)	(404.)	(363.)	(2765.)	(1825.)
11.00	8.00	11.90	0.99	0.80	6.09	4.02
(11.)	(8.)	(5403.)	(449.)	(363.)	(2765.)	(1825.)
12.00	8.00	12.00	1.09	0.80	6.09	4.02
(12.)	(8.)	(5444.)	(495.)	(363.)	(2765.)	(1825.)
13.00	8.00	12.10	1.19	0.80	6.09	4.02
(13.)	(8.)	(5493.)	(540.)	(363.)	(2765.)	(1825.)
14.00	8.00	12.20	1.29	0.80	6.09	4.02
(14.)	(8.)	(5539.)	(586.)	(363.)	(2765.)	(1825.)
15.00	8.00	12.30	1.39	0.80	6.09	4.02
(15.)	(8.)	(5584.)	(631.)	(363.)	(2765.)	(1825.)
16.00	8.00	12.40	1.49	0.80	6.09	4.02
(16.)	(8.)	(5630.)	(676.)	(363.)	(2765.)	(1825.)
17.00	8.00	12.50	1.59	0.80	6.09	4.02
(17.)	(8.)	(5675.)	(722.)	(363.)	(2765.)	(1825.)
18.00	8.00	12.60	1.69	0.80	6.09	4.02
(18.)	(8.)	(5720.)	(767.)	(363.)	(2765.)	(1825.)

19.00	8.00	12.70	1.79	0.80	6.09	4.02
(19.)	(8.)	(5765.)	(813.)	(363.)	(2765.)	(1825.)
20.00	8.00	12.80	1.89	0.80	6.09	4.02
(20.)	(8.)	(5811.)	(858.)	(363.)	(2765.)	(1825.)
21.00	8.00	12.90	1.99	0.80	6.09	4.02
(21.)	(8.)	(5857.)	(903.)	(363.)	(2765.)	(1825.)
22.00	8.00	13.00	2.09	0.80	6.09	4.02
(22.)	(8.)	(5902.)	(949.)	(363.)	(2765.)	(1825.)

WATER CONTENT	TOTAL WEIGHT	ACCELERATOR	940 HARDENER
10.0000	5357.2010	428.5761	0.0000
11.0000	5402.6000	432.2080	0.0000
12.0000	5448.0000	435.8400	0.0000
13.0000	5493.4010	439.4720	0.0000
14.0000	5538.8010	443.1040	0.0000
15.0000	5584.2000	446.7360	0.0000
16.0000	5629.6000	450.3680	0.0000
17.0000	5675.0010	454.0001	0.0000
18.0000	5720.4010	457.6320	0.0000
19.0000	5765.8010	461.2640	0.0000
20.0000	5811.2010	464.8961	0.0000
21.0000	5856.6000	468.5280	0.0000
22.0000	5902.0010	472.1601	0.0000

APPENDIX A-4:

**Computer Program Code and Output
for Transforming Load, Penetration
and Mold Indices into CBR and
Dry Density Values**


```

10 FOR I = 1 TO 200
20 READ TESTNO, WT1, WT2, NC, CSR, PA, PEN1, PEN2
30 WT = WT2 - WT1
40 BDEM = WT/H/3.1416*(D^2)*1728/454
50 DDEM = BDEM/(1+OC)
60 VOL = 3.1416*(D^2)/4*H
70 CRR1 = (PEN1*10.125426+21.373785)/3000*100
80 CRR2 = (PEN2*10.125426+21.373785)/4500*100
90 IF I = 1 THEN L30
100 IF (IZ*10 * 10) (= IZ THEN 160
110 LPRINT
120 LPRINT
130 LPRINT TAB(1); "TESTNO"; TAB(8); "ADDITIVE"; TAB(17); "MOISTURE"; TAB(26); "CRR1";
TAB(33); "WEIGHT"; TAB(41); "VOLUME"; TAB(49); "PULKDEN";
140 LPRINT TAB(57); "DRYDEN"; TAB(64); "CRR(0.1)"; TAB(72); "CRR(0.2)"
150 LPRINT
160 LPRINT USING " *****"; TESTNO, PA, NC, CSR, WT, VOL, BDEM, DDEM, CRR1, CRR2
170 LPRINT
180 NEXT I
190 DATA 1,5.965,4.67,6566,10916,.13,.4,4,260,430
200 DATA 2,5.965,4.67,6566,10916,.13,0.4,4,252,394
210 DATA 3,5.955,4.72,6551,10635,.13,0.5,4,245,366
220 DATA 4,5.97,4.65,6515,10640,.17,.4,4,125,193
230 DATA 5,5.955,4.75,6531,10785,.17,.5,4,127,223
240 DATA 6,5.972,4.65,6531,10613,.17,.6,4,193,300
250 DATA 7,5.967,4.65,6567,10458,.13,0.6,4,268,391
260 DATA 8,5.975,4.38,3595,7376,.21,0.5,4,53,98
270 DATA 9,5.96,6.12,4279,9566,.21,0.6,4,97,136
280 DATA 10,5.97,5.02,4275,8650,.21,0.4,4,107,213
290 DATA 11,5.97,5.02,4275,8650,.21,0.4,4,136,206
300 DATA 12,5.975,4.38,3595,7376,.21,0.5,4,55,81
310 DATA 13,5.96,6.12,4279,9566,.21,0.6,4,74,126
320 DATA 14,5.97,4.72,6635,10924,.13,0.4,1,215,282
330 DATA 15,5.97,4.76,6561,10455,.13,0.5,1,189,0
340 DATA 16,5.97,4.76,6561,10455,.13,0.5,1,195,249
350 DATA 17,5.97,6.025,7276,11805,.13,0.6,1,140,181
360 DATA 18,5.95,5.04,4221,8508,.17,0.6,1,182,226
370 DATA 19,5.97,6.025,7276,11805,.13,0.6,1,159,156
380 DATA 20,5.96,5.0,4285,9037,.17,0.4,1,42,82
390 DATA 21,5.95,5.04,4221,8508,.17,0.6,1,165,207
400 DATA 22,5.95,4.25,3679,7630,0.17,0.5,1,95,145
410 DATA 23,5.95,4.06,3541,7230,0.21,0.4,1,30,50
420 DATA 24,5.95,4.06,3541,7230,0.21,0.4,1,195,258
430 DATA 25,5.99,5.82,4362,9625,0.21,0.50,1,32,51.5
440 DATA 26,5.99,4.1,3694,7481,0.21,0.6,1,55,84
450 DATA 27,5.95,5.02,4343,8095,0.13,0.6,0,90,110
460 DATA 28,5.95,5.15,4273,8980,0.13,0.40,0,211,260
470 DATA 29,5.95,5.15,4273,8980,0.13,0.40,0,168,221
480 DATA 30,5.95,5.02,4343,8095,0.13,0.60,0,125,125
490 DATA 31,5.95,5.10,4343,8507,0.13,0.50,0,214,213
500 DATA 32,5.960,5.00,4348,9263,0.17,0.40,0,12,23
510 DATA 33,5.97,5.2,4357,8925,0.21,0.60,0.25,33,60
520 DATA 34,5.97,4.70,6518,10852,0.17,0.50,0.60,118
530 DATA 35,5.97,4.71,6562,10472,0.17,0.60,0,159,195
540 DATA 36,5.97,4.6,6560,10805,0.21,0.40,0,1.5,2.5
550 DATA 37,5.97,4.70,6543,10860,0.21,0.60,0,14,23
560 DATA 38,5.95,5.15,6538,11277,0.21,0.50,0.4,5,6.7
570 DATA 39,6.01,5.12,2926,7243,0.13,0.40,0.25,159,187
580 DATA 40,6.0,7.0,4275,9700,0.13,0.50,0.25,149,174
590 DATA 41,5.97,6.00,3595,8124,0.13,0.60,0.25,141,169
600 DATA 42,5.96,4.64,2926,7231,.17,.5,1.0,125,175
610 DATA 43,5.97,4.58,2927,6740,0.13,0.50,0.25,194,239
620 DATA 44,5.95,4.98,4348,8833,0.13,0.40,0.25,231,276
630 DATA 45,6.0,5.08,4228,8776,0.21,0.40,4,179,286
640 DATA 46,6.0,5.02,4362,8751,0.21,0.50,4,109,167
650 DATA 47,6.0,6.0,3679,9142,0.21,0.40,1.0,56,82
660 DATA 48,6.02,4.99,7205,11407,0.17,0.60,0.25,177,220
670 DATA 49,6.02,5.01,7241,11939,0.21,0.40,0.25,11,21
680 DATA 50,6.01,5.00,6991,11821,0.17,0.40,0.25,50,96
690 DATA 51,6.01,5.00,4225,8100,0.13,0.60,0.25,159,185
700 DATA 52,5.98,5.00,7209,11349,0.17,0.50,0.25,124,155
710 DATA 53,6.00,4.66,6529,10735,0.21,0.60,0.25,36,68
720 DATA 54,5.96,5.30,2915,7806,0.00,0.21,0.50,0.25,22,36
730 DATA 55,6.01,4.59,2915,6472,0.00,0.13,0.50,0.00,146,150
740 DATA 56,6.02,4.59,2920,7272,0.17,0.60,0.0,53,29
750 DATA 57,6.00,4.68,2961,7312,0.17,0.50,0.0,66,101
760 GOTO
770 END

```

TESTING ADDITIVE MOISTURE CSRAT WEIGHT VOLUME BULK DEN DRY DEN CORCO.1 CORCO.2

1.00	4.00	0.13	0.40	4350.00	130.51	126.97	112.27	88.47	97.23
2.00	4.00	0.13	0.40	4350.00	130.51	126.97	112.27	89.77	99.13
3.00	4.00	0.13	0.50	4084.00	131.46	113.24	104.64	83.40	82.83
4.00	4.00	0.17	0.40	4125.00	130.16	120.62	103.09	42.90	43.90
5.00	4.00	0.17	0.50	4254.00	132.30	122.39	104.60	43.56	50.85
6.00	4.00	0.17	0.60	4082.00	130.25	119.28	101.95	64.85	67.98
7.00	4.00	0.13	0.60	3891.00	130.03	113.89	100.79	91.17	88.45
8.00	4.00	0.21	0.50	3781.00	122.81	117.18	95.84	18.60	22.53
9.00	4.00	0.21	0.60	5287.00	170.74	117.86	97.40	30.08	31.08
10.00	4.00	0.21	0.40	4375.00	140.52	118.50	97.93	36.83	45.40
11.00	4.00	0.21	0.40	4375.00	140.52	118.50	97.93	46.61	46.83
12.00	4.00	0.21	0.50	3781.00	122.81	117.18	95.84	19.28	19.70
13.00	4.00	0.21	0.60	5287.00	170.74	117.86	97.40	25.69	28.83
14.00	1.00	0.13	0.40	4289.00	132.12	123.56	109.34	73.28	63.93
15.00	1.00	0.13	0.50	3894.00	133.24	111.23	98.44	64.50	0.47
16.00	1.00	0.13	0.50	3894.00	133.24	111.23	98.44	66.53	56.50
17.00	1.00	0.13	0.60	4829.00	168.65	102.21	90.45	47.96	41.20
18.00	1.00	0.17	0.60	4287.00	140.14	116.44	99.52	62.14	51.33
19.00	1.00	0.13	0.60	4529.00	168.65	102.21	90.45	54.38	39.13
20.00	1.00	0.17	0.40	4752.00	139.49	129.66	110.82	14.89	18.93
21.00	1.00	0.17	0.60	4287.00	140.14	116.44	99.52	56.40	47.05
22.00	1.00	0.17	0.50	3951.00	119.37	125.98	107.68	32.78	33.10
23.00	1.00	0.21	0.40	3689.00	112.89	124.38	102.79	10.84	11.73
24.00	1.00	0.21	0.40	3689.00	112.89	124.38	102.79	66.53	58.53
25.00	1.00	0.21	0.50	5263.00	164.01	122.14	100.94	11.51	12.06
26.00	1.00	0.21	0.60	3787.00	115.54	124.25	103.10	19.28	19.38
27.00	0.00	0.13	0.60	3752.00	139.58	102.31	90.54	31.09	25.23
28.00	0.00	0.13	0.40	4707.00	143.20	125.11	110.72	71.93	58.93
29.00	0.00	0.13	0.40	4707.00	143.20	125.11	110.72	57.41	50.20
30.00	0.00	0.13	0.60	3752.00	139.58	112.31	90.54	42.90	28.60
31.00	0.00	0.13	0.50	4164.00	141.81	111.76	93.91	72.94	48.40
32.00	0.00	0.17	0.40	4915.00	139.49	114.11	114.62	4.76	5.65
33.00	0.00	0.17	0.60	4568.00	145.56	119.45	98.72	11.35	11.28
34.00	0.00	0.17	0.50	6334.00	131.56	115.13	102.12	20.95	22.03

35.00	0.00	0.17	0.60	3910.00	131.84	112.88	96.48	54.58	44.35
36.00	0.00	0.21	0.40	4245.00	128.76	125.43	103.70	1.22	1.01
37.00	0.00	0.21	0.60	4317.00	131.56	124.89	103.22	5.44	5.65
38.00	0.00	0.21	0.50	4739.00	143.20	125.93	104.40	1.23	1.98
39.00	0.25	0.13	0.40	4317.00	145.25	113.13	100.11	54.36	42.55
40.00	0.25	0.13	0.50	5425.00	197.92	101.33	99.32	51.90	39.33
41.00	0.25	0.13	0.60	4529.00	167.95	102.64	90.87	48.36	37.55
42.00	1.00	0.17	0.50	4305.00	129.45	125.58	108.19	42.95	39.85
43.00	0.25	0.13	0.50	3813.00	128.21	113.20	100.18	60.19	50.25
44.00	0.25	0.13	0.40	4435.00	139.37	122.05	108.01	24.62	61.53
45.00	4.00	0.21	0.40	4548.00	143.63	120.82	99.60	61.13	64.83
46.00	4.00	0.21	0.50	4389.00	141.94	117.69	97.27	37.50	38.05
47.00	1.00	0.21	0.40	5463.00	169.65	122.57	101.30	19.31	18.94
48.00	0.25	0.17	0.60	4202.00	142.03	112.61	96.24	60.55	47.98
49.00	0.25	0.21	0.40	4692.00	142.60	125.39	103.63	4.53	5.20
50.00	0.25	0.17	0.40	4830.00	141.84	129.61	110.77	1.59	21.08
51.00	0.25	0.13	0.60	3875.00	141.84	103.98	92.02	54.31	42.10
54.00	0.25	0.17	0.50	4640.00	140.43	125.76	107.49	42.58	39.60
55.00	0.25	0.21	0.60	4206.00	131.76	121.50	100.41	12.36	11.72
56.00	0.25	0.21	0.50	4891.00	147.86	125.90	104.05	8.15	1.58
57.00	0.00	0.13	0.60	3557.00	130.21	103.97	92.01	49.99	34.23
58.00	0.00	0.17	0.60	4352.00	130.65	126.79	100.37	20.29	13.75
59.00	0.00	0.17	0.50	4351.00	132.32	125.15	106.97	22.99	23.20

APPENDIX B

APPENDIX B:

Rut Depth Prediction Model (Four Pavement Types)

APPENDIX B-1:

**CSU Modified
Waterways Experiment Station Model
(CSU/WES Model)**

```

C*****
C234567    PROGRAM RUT - COMPUTES RUT DEPTH FOR FOUR
C          POSSIBLE PAVEMENT TYPES.
C
C          CODED BY: ABAYOMI AJAYI-MAJEBI
C                  DEPT. OF MANUFACTURING ENGINEERING
C                  CENTRAL STATE UNIVERSITY
C                  WILBERFORCE, OHIO
C*****
C          DIMENSION RD(300),P(300),TP(300),T1(300),C1(300)
C          DIMENSION C2(300),P(300),T2(300),T3(300),C3(300)
C          DIMENSION CASE(4),M(10),V(10),COMPUTE(10)
C          DIMENSION SKIP(300)
C          INTEGER TYPE,COMPUTE,CASE,START,STOP
C          REAL MRD,MP,MTP,MT1,MT2,MC1,MT3,MC2,MC3,MR
C          REAL M,K
C          CHARACTER CASE1(6)*2,CASE2(6)*2,CASE3(7)*2,CASE4(9)*2,TERM*8
C          DATA CASE/6,6,7,9/
C          DATA CASE1/'P','TP','R','T1','C1','C2'/
C          DATA CASE2/'P','TP','R','T1','C1','C2'/
C          DATA CASE3/'P','TP','R','T1','T2','C1','C3'/
C          DATA CASE4/'P','TP','R','T1','T2','C1','T3','C2','C3'/
C          DATA TERM/' 0,0,0,0 '/
C
C          FACTR1 = 5
C          FACTR2 = 1
C          FACTR3 = 15
C          FACTR4 = 1
C
C          I=0
C
C          1010    CONTINUE
C
C          LOOP BACK THROUGH FOR ANOTHER PROBLEM
C          WRITE(6,827)
C          WRITE(6,828)
C          828    FORMAT(3X,'TERMINATE PROGRAM BY TYPING O O O O AT DATA START')
C          WRITE(6,827)
C
C          ENTER CLAY/SILT SOIL SYSTEM PAVEMENT PARAMETERS
C
C          FOR STABILIZED SOIL LAYER
C
C          WRITE(6,899)
C          899    FORMAT(3X,' INPUT STABILIZED CLAY/SILT SOIL SYSTEM PARAMETERS')
C          WRITE(6,827)
C
C          WRITE(6,555)
C          READ(5,*)PA,PM,CS,TEMP
C
C          IF(PA.EQ.0 .AND. PM.EQ.0) GO TO 1090
C
C          COMPUTE STABILIZED CLAY/SILT SOIL SYSTEM CALIFORNIA BEARING RATIO (CBR)
C
C          CBR = 91.69 + 11.07*PA - 5.62*PM + 44.97*CS + 0.14*TEMP

```

```

      IF(CBR .LT. 0.001) CBR=0.001
C
555  FORMAT(//,3X,'ADDITIVE %',4X,'MOISTURE %',3X,'CLAY/SILT RATIO',
      &3X,'TEMPERATURE',///)
C
      WRITE(6,556) PA,PM,CS,TEMP
556  FORMAT(//,7X,'ADDITIVE % = ',F8.2,/,7X,'MOISTURE % = ',F8.2,/,
      &7X,'CLAY/SILT RATIO = ',F5.2,/,7X,'TEMPERATURE = ',F8.2,/)
C
C
C      READ INPUT DATA
      GO TO 20
1020  CONTINUE
C
C      PRINT MEAN AND VARIANCE RESULTS
      GO TO 30
1030  CONTINUE
C
C      SELECT AND SOLVE CORRECT RUT DEPTH EQUATION AND
C      OUTPUT RESULTS
      GO TO (41,42,43,44),TYPE
1040  CONTINUE
C      LOOP BACK THROUGH FOR ANOTHER PROBLEM
      WRITE(6,1917)
      WRITE(6,901)
901  FORMAT('1',3X,' COMPUTATIONS FOR ANOTHER PAVEMENT SYSTEM BEGINS')
      WRITE(6,827)
      GO TO 1010
1090  CONTINUE
C      END OF PROGRAM
      WRITE(6,1902)
1902  FORMAT(3X,' NORMAL TERMINATION')
      STOP
C
C*****-----END OF PAGE 1-----
C
C      READ INPUT DATA
20   CONTINUE
C
C
      I=I+1
      WRITE(6,827)
      WRITE(6,1903)
1903  FORMAT(3X,' ENTER CODE FOR TYPE OF PAVEMENT ANALYSIS :')
      WRITE(6,827)
      WRITE(6,*)
      WRITE(6,1904)
1904  FORMAT(3X,' STABILIZED AIRPORT PAVEMENT WITH CBR1 > CBR2 = 1')
      WRITE(6,1905)
1905  FORMAT(3X,' STABILIZED AIRPORT PAVEMENT WITH CBR1 < CBR2 = 2')
      WRITE(6,1906)
1906  FORMAT(3X,' STABILIZED ASPHALT PAVEMENT WO/SUBBASE (8 VBLS) = 3')
      WRITE(6,1907)
1907  FORMAT(3X,'STABILIZED ASPHALT PAVEMENT WITH SUBBASE (10 VBLS)=4')
C
      WRITE(6,827)
      WRITE(6,*)
      READ(5,*) TYPE
      WRITE(6,1908)TYPE

```



```

1908  FORMAT(8X,'TYPE = ',I2)
      WRITE(6,827)
      WRITE(6,*)
      WRITE(6,*)
C
      IF(TYPE.GT.4) GO TO 1090
      WRITE(6,1909)
1909  FORMAT(3X,' INPUT - ALLOWABLE RUT DEPTH. ')
      READ(5,*)ARD
C
C
      WRITE(6,1910)ARD
1910  FORMAT(6X,'ALLOWABLE RUT DEPTH = ', F8.3)
C
C
      WRITE(6,1911)
1911  FORMAT(3X,' INPUT MODE - KEYBOARD (1), OR FILE (2) ? ')
      READ(5,*)IO
C
C
      GO TO (13,13,13,13),IO
C
13  CONTINUE
      NVAR=CASE(TYPE)
      WRITE(6,1912)NVAR
1912  FORMAT(6X,'NO OF VARIABLES (NVAR) = ', I3)
C
C
      TYPE A 1 IF MEAN & VARIANCE WILL BE FURNISHED FROM
              KEYBOARD
C
C
      TYPE A 0 IF MEAN & VARIANCE COMPUTED IN SUBROUTINE
              STAT
C
C
      IF(TYPE.LT.3)WRITE(6,821)CASE1
      IF(TYPE.EQ.3)WRITE(6,823)CASE3
      IF(TYPE.EQ.4)WRITE(6,822)CASE4
      WRITE(6,827)
      WRITE(6,*)
      WRITE(6,*)
      WRITE(6,*)
      READ(5,*)(COMPUTE(I1),I1=1,NVAR)
C
C
      DO 199 L=1,NVAR
        L2=L
        IF(COMPUTE(L2).EQ.0)CALL STAT(M,V,L2)
        IF(IO.LT.3)GO TO 199
        IF(COMPUTE(L2).EQ.0)GO TO 199
        READ(5,*)LINENO,NONE
        START=1
C*****-----END OF PAGE 2-----
        STOP=8
25  CONTINUE
      IF(NONE-STOP)22,22,21
22  READ(5,*)LINENO,(SKIP(L3),L3=START,NONE)
      GO TO 199
21  READ(5,*)LINENO,(SKIP(L3),L3=START,STOP)
      START=STOP+1
      STOP=STOP+8
      GO TO 25

```

```

199  CONTINUE
800  FORMAT(3X,/)
C
C
C
821  FORMAT(3X,'INPUT - STAT CODE - COMPUTED(0),GIVEN(1)',
&      /,2X,6(A2,2X))
822  FORMAT(3X,'INPUT - STAT CODE -COMPUTED(0),GIVEN(1)',
&      /,2X,9(A2,2X))
823  FORMAT(3X,'INPUT - STAT CODE - COMPUTED(0),GIVEN(1)',
&      /,2X,7(A2,2X))
C
C
      DO 201 L=1,NVAR
          IF (COMPUTE(L).EQ.0) GO TO 201
          IF (TYPE.LT.3) WRITE(6,824) CASE1(L)
          IF (TYPE.EQ.3) WRITE(6,824) CASE3(L)
          IF (TYPE.EQ.4) WRITE(6,824) CASE4(L)
824   FORMAT(3X,' INPUT MEAN & VARIANCE FOR - ',A2)
          READ(5,*)M(L),V(L)
201  CONTINUE
      GO TO 1020
C
30  CONTINUE
C
C
      IF(TYPE.GE.3)GO TO 35
      MC1=CBR
      WRITE(6,1913)CBR
1913  FORMAT(3X,' PREDICTED CBR =',F7.2)
      WRITE(6,1914)M(5)
1914  FORMAT(3X,' SPECIFIED CBR =',F7.2)
      WRITE(6,827)
      M(5)=CBR
      GO TO 36
C
35  CONTINUE
C
      IF(TYPE.GT.2.AND.TYPE.LE.4)MC1=CBR
      WRITE(6,1915) CBR
1915  FORMAT(3X,' PREDICTED CBR =',F7.2)
      WRITE(6,1916) M(6)
1916  FORMAT(3X,' SPECIFIED CBR =',F7.2)
      M(6)=CBR
1917  FORMAT('1')
C
36  CONTINUE
C
C
      PRINT MEAN & VARIANCE RESULTS.
C
      WRITE(6,825)
825   FORMAT(/,29X,'STAT',/,3X,'VARIABLE      MEAN
& ,      VARIANCE',5X,'CODE')
      DO 204 L=1,NVAR
          IF(TYPE.LT.3)WRITE(6,826)CASE1(L),M(L),V(L),COMPUTE(L)
          IF(TYPE.EQ.3)WRITE(6,826)CASE3(L),M(L),V(L),COMPUTE(L)
          IF(TYPE.EQ.4)WRITE(6,826)CASE4(L),M(L),V(L),COMPUTE(L)
826   FORMAT(4X,A2,F14.2,F14.2,I8)
827   FORMAT(///)

```

204 CONTINUE

C

IF(TYPE.LT.3) M(5)=CBR
IF(TYPE.GT.2.AND.TYPE.LE.4)M(6)=CBR

C

GO TO 1030

C

C

CASE C1 > C2, 7 VARIABLES

C

C

41 CONTINUE

CONST=FACTR1
MP=M(1)
MP=MP/1000.
VP=V(1)
VP=VP/1000000.
MTP=M(2)
VTP=V(2)
MR=M(3)
VR=V(3)
MT1=M(4)
VT1=M(4)
M(5)=CBR
MC1=M(5)
VC1=V(5)
MC2=M(6)
VC2=V(6)
K=0.17410
A=0.4707
B=0.5695
C=0.2476
D=-2.0020
E=-0.9335
F=-0.2848
Q1=K*MP**A*MTP**B*MR**C
Q2=(ALOG10(MT1))**D
Q3=MC1**E*MC2**F
Q=Q1*Q2*Q3*CONST
P2=(A*(A-1)*VP)/MP**2
TP2=(B*(B-1)*VTP)/MTP**2
R2=(C*(C-1.)*VR)/MR**2
T12A=0.4343*D*VT1
T12B=MT1**2*ALOG10(MT1)
T12C=(0.4343*(D-1.))/ALOG10(MT1)
T12=T12A/T12B*(T12C-1.)
C12=(E*(E-1.)*VC1)/MC1**2
C22=(F*(F-1.)*VC2)/MC2**2
ERD=Q+(0.5*Q*(P2+TP2+R2+T12+C22))
P1=(A**2*VP)/MP**2
TP1=(B**2*VTP)/MTP**2
R1=(C**2*VR)/MR**2
T11A=(0.4343*D)**2*VT1
T11B=(MT1)**2*(ALOG10(MT1))**2
T11=T11A/T11B
C11=E**2*VC1/MC1**2
C21=(F**2*VC2)/MC2**2
VRD=Q*82*(P1+TP1+R1+T11+C11+C21)-(0.25*Q**2)*
(P2**2+TP2**2+R2**2+T12**2+C12**2+C22**2)
WRITE(6,904)Q

&

```

          WRITE(6,903)ERD
          WRITE(6,902)VRD
902      FORMAT(10X,'EXPECTED VARIANCE OF RUT DEPTH=',F16.6,/)
C      -----END OF PAGE 4-----
C
903      FORMAT(10X,'EXPECTED VALUE OF RUT DEPTH  =',F16.6,/)
904      FORMAT(//10X,'MEAN VALUE OF RUT DEPTH   =',F16.6,/)
          REL=(ARD-ERD)/VRD**0.5
          WRITE(6,919)REL
919      FORMAT(10X,'RELIABILITY STATISTIC      =',F16.6,/)
C
          GO TO 1040
C
C
C
C
C
C
C
42      CONTINUE
          CONST=FACTR2
          MP=M(1)
          VP=V(1)
          MTP=M(2)
          VTP=V(2)
          MR=M(3)
          VR=V(3)
          MT1=M(4)
          VT1=V(4)
          M(5)=CBR
          MC1=M(5)
          VC1=V(5)
          MC2=M(6)
          VC2=V(6)
          K=0.11009
          A=0.4925
          B=0.8548
          C=0.5018
          D=0.4293
          E=-1.9773
          F=-1.2015
          Q1=K*MP**A*MTP**B*MR**C
          Q2=(ALOG10(MT1))**D
          Q3=MC1**E*MC2**F
          Q=Q1*Q2*Q3*CONST
          P2=(A*(A-1)*VP)/MP**2
          TP2=(B*(B-1)*VTP)/MTP**2
          R2=(C*(C-1.)*VR)/MR**2
          T12A=0.4343*D*VT1
          T12B=MT1**2*ALOG10(MT1)
          T12C=(0.4343*(D-1.))/ALOG10(MT1)
          T12=T12A/T12B*(T12C-1.)
          C12=(E*(E-1.)*VC1)/MC1**2
          C22=(F*(F-1.)*VC2)/MC2**2
          ERD=Q+(0.5*Q*(P2+TP2+R2+T12+C12+C22))
C
C
C      -----END OF PAGE 5-----
C
          P1=(A**2*VP)/MP**2
          TP1=(B**2*VTP)/MTP**2
          R1=(C**2*VR)/MR**2

```

```

T11A=(0.4343*D)**2*VT1
T11B=(MT1)**2*(ALOG10(MT1))**2
T11=T11A/T11B
C11=E**2*VC1/MC1**2
C21=(F**2*VC2)/MC2**2
VRD=Q**2*(P1+TP1+R1+T11+C11+C21)-(0.25*Q**2)*
&      (P2**2+TP2**2+R2**2+T12**2+C12**2+C22**2)
WRITE(6,904)Q
WRITE(6,903)ERD
WRITE(6,902)VRD
REL=(ARD-ERD)/VRD**0.5
WRITE(6,919)REL

```

GO TO 1040

ASPHALTIC CONCRETE AIRPORT PAVEMENT WITHOUT SUBBASE, 8 VARIABLES.

43 CONTINUE

```

CONST=FACTR3
MP=M(1)
MP=MP/1000.
VP=V(1)
VP=VP/1000000.
MTP=M(2)
VTP=V(2)
MR=M(3)
VR=V(3)
MT1=M(4)
VT1=V(4)
MT2=M(5)
VT2=V(5)
M(6)=CBR
MC1=M(6)
VC1=V(6)
MC2=M(7)
VC2=V(7)
K=1.9431
A=1.3127
B=0.0499
C=0.3240
D=-3.4204
E=-1.6877
F=-0.1156
Q1=K*MP**A*MTP**B*MR**C
Q2=(ALOG10(1.25*MT1+MT2))**D
Q3=MC1**E*MC2**F
Q=Q1*Q2*Q3*CONST
P2=(A*(A-1)*VP)/MP**2
TP2=(B*(B-1)*VTP)/MTP**2
R2=(C*(C-1.)*VR)/MR**2
T12A=1.25**2*0.4343*D*VT1
T12B=(1.25*MT1+MT2)**2*ALOG10(1.25*MT1+MT2)
T12C=((0.4343*(D-1.))/ALOG10(1.25*MT1+MT2))
T12=T12A/T12B*(T12C-1.)
T22A=0.4343*D*VT2
T22=T22A/T12B*(T12C-1.)
C12=(E*(E-1.)*VC1)/MC1**2
C22=(F*(F-1.)*VC2)/MC2**2

```

```

ERD=Q+(0.5*Q*(P2+TP2+R2+T12+T22+C12+C22))
P1=(A**2*VF)/MP**2
TP1=(B**2*VTP)/MTP**2
R1=(C**2*VR)/MR**2
T11A=1.25**2*(0.4343*D)**2*VT1
T11B=(1.25*MT1+MT2)**2*(ALOG10(1.25*MT1+MT2))**2
T11=T11A/T11B
T21A=(0.4343*D)**2*VT2
T21=T21A/T11B
C11=E**2*VC1/MC1**2
C21=(F**2*VC2)/MC2**2
VRD=Q**2*(P1+TP1+R1+T11+T21+C11+C21)-(0.25*Q**2)*
&      (P2**2+TP2**2+R2**2+T12**2+T22**2+C12**2+C22**2)
WRITE(6,904)Q
WRITE(6,903)ERD
WRITE(6,902)VRD
REL=(ARD-ERD)/VRD**0.5
WRITE(6,919)REL

```

GO TO 1040

---END OF PAGE 43---

---PAGE 44---

ASPHALTIC CONCRETE WITH SUBBASE, 10 VARIABLES.

44 CONTINUE

```

CONST=FACTR4
MP=M(1)
MP=MP/1000.
VP=V(1)
VP=VP/1000000.
MTP=M(2)
VTP=V(2)
MR=M(3)
VR=V(3)
MT1=M(4)
VT1=V(4)
MT2=M(5)
VT2=V(5)
M(6)=CBR
MC1=M(6)
VC1=V(6)
MT3=M(7)
VT3=V(7)
MC2=M(8)
VC2=V(8)
MC3=M(9)
VC3=V(9)
K=0.031171
A=1.5255
B=0.0897
C=0.345
D=-0.8847
E=-0.7616
F=-1.1674
G=-0.5505
H=-0.3089

```

```

Q1=K*MP**A*MTP**B*MR**C
Q2=(ALOG10(1.25*MT1+MT2))**D
Q3=MC1**E*(ALOG10(MT3))**F*MC2**G*MC3**H
Q=Q1*Q2*Q3*CONST
P2=(A*(A-1)*VP)/MP**2
TP2=(B*(B-1)*VTP)/MTP**2
R2=(C*(C-1.)*VR)/MR**2
T12A=1.25**2*0.4343*D*VT1
T12B=(1.25*MT1+MT2)**2*ALOG10(1.25*MT1+MT2)
T12C=((0.4343*(D-1.))/ALOG10(1.25*MT1+MT2))
T12=T12A/T12B*(T12C-1.)
T22A=0.4343*D*VT2
T22=T22A/T12B*(T12C-1.)
C12=(E*(E-1.)*VC1)/MC1**2
T32A=0.4343*F*VT3
T32B=MT3**2*ALOG10(MT3)
T32C=0.4343*(F-1.)/ALOG10(MT3)
T32=T32A/T32B*(T32C-1.)
C22=(G*(G-1.)*VC2)/MC2**2
C32=(H*(H-1.)*VC3)/MC3**2
ERD=Q+(0.5*Q*(P2+TP2+R2+T12+T22+C12+T32+C22+C32))
P1=(A**2*VP)/MP**2
TP1=(B**2*VTP)/MTP**2
R1=(C**2*VR)/MR**2
T11A=1.25**2*(0.4343*D)**2*VT1
T11B=(1.25*MT1+MT2)**2*(ALOG10(1.25*MT1+MT2))**2
T11=T11A/T11B
T21A=(0.4343*D)**2*VT2
T21=T21A/T11B
C11=E**2*VC1/MC1**2
T31A=(0.4343*F)**2*VT3
T31B=MT3**2*ALOG10(MT3)**2
T31=T31A/T31B
C21=(G**2*VC2)/MC2**2
C31=(H**2*VC3)/MC3**2
VRD=Q**2*(P1+TP1+R1+T11+T21+C11+T31+C21+C31)-(0.25*Q**2)*
&      (P2**2+TP2**2+R2**2+T12**2+T22**2+C12**2+T32**2+C22
&      **2+C32**2)
WRITE(6,904)Q
WRITE(6,903)ERD
WRITE(6,902)VRD
REL=(ARD-ERD)/VRD**0.5
WRITE(6,919)REL

```

GO TO 1040

END

---END OF PAGE 44---

-----END OF PAGE 6-----

READ DATA FORM FILE. COMPUTED MEAN AND VARIANCE.

SUBROUTINE STAT(M,V,I)

READ FROM FILE. COMPUTES MEAN AND VARIANCE.

```

C      DIMENSION VALUE(300),M(10),V(10)
      INTEGER TO,GO
      REAL MEAN,M
C
C      INPUT SCHEME FOR DATA FILE.
C
      READ(10,*)LINENO,N
      GO=1
      TO=8
15  CONTINUE
      IF(N-TO)10,10,11
10      READ(10,*)LINENO,(VALUE(J),J=GO,N)
800    FORMAT(3X,/)
      GO TO 12
11      READ(10,*)LINENO,(VALUE(J),J=GO,TO)
      GO=TO+1
      TO=TO+8
      GO TO 15
12  CONTINUE
C
C      CALCULATE THE MEAN AND VARIANCE.
C
      SUM=0
      DO 180 J=1,N
          SUMM=VALUE(J)+SUMM
180  CONTINUE
      MEAN=SUMM/N
      SUMV=0.
      DO 190 J=1,N
          SUMV=(VALUE(J)-MEAN)**2+SUMV
190  CONTINUE
      IF(N.GT.30)N=N-1
      VAR=SUMV/N
      M(J)=MEAN
      V(J)=VAR
C
C      RETURN
      END

```


APPENDIX B-2:

Rutting Model Typical Input Data

```

$ SET VERIFY
$ FOR RUT.FOR/LIS
$ LINK RUT.OBJ
$ DEFINE/USER SYS$OUTPUT RUT.OUT
$ RUN RUT.EXE
0 17 0.5 90
1
1
1
1 1 1 1 1 1
5000 250000
200 100
4 2
11 0.25
20 25
15 10
0 17 0.5 90
1
1
1
1 1 1 1 1 1
5000 250000
200 100
20 4
11 0.25
20 25
15 10
0 17 0.5 90
1
1
1
1 1 1 1 1 1
5000 250000
200 100
50 9
11 0.25
20 25
15 10
0 17 0.5 90
1
1
1
1 1 1 1 1 1
5000 250000
200 100
100 25
11 0.25
20 25
15 10
0 17 0.5 90
1
1
1
1 1 1 1 1 1
5000 250000
200 100
150 25
11 0.25
20 25
15 10

```

```

1
1
1 1 1 1 1 1
5000 250000
200 100
100 25
11 0.25
20 25
15 10
4 14 0.5 90
1
1
1 1 1 1 1 1
5000 250000
200 100
150 25
11 0.25
20 25
15 10
4 14 0.5 90
1
1
1 1 1 1 1 1
5000 250000
200 100
200 25
11 0.25
20 25
15 10
4 14 0.5 90
1
1
1 1 1 1 1 1
5000 250000
200 100
250 25
11 0.25
20 25
15 10
4 14 0.5 90
1
1
1 1 1 1 1 1
5000 250000
200 100
500 25
11 0.25
20 25
15 10
4 14 0.5 90
3
1
1
1 1 1 1 1 1
5000 250000
200 100
500 25
11 0.25
20 25
15 10
4 14 0.5 90

```

```

15 10
2 14 0.5 90
3
1
1 1 1 1 1 1
5000 250000
200 100
250 100
1 0.25
11 0.25
50 25
15 10
2 14 0.5 90
3
1
1 1 1 1 1 1
5000 250000
200 100
500 100
1 0.25
11 0.25
50 25
15 10
4 14 0.5 90
1
1
1 1 1 1 1 1
5000 250000
200 100
4 2
11 0.25
20 25
15 10
4 14 0.5 90
1
1
1 1 1 1 1 1
5000 250000
200 100
20 4
11 0.25
20 25
15 10
4 14 0.5 90
1
1
1 1 1 1 1 1
5000 250000
200 100
20 4
11 0.25
20 25
15 10
4 14 0.5 90
1
1
1 1 1 1 1 1
5000 250000
200 100
50 9
11 0.25
20 25
15 10
4 14 0.5 90
1

```

1
 1 1 1 1 1 1 1
 5000 250000
 200 100
 150 25
 11 0.25
 20 25
 15 10
 4 17 0.5 90
 1
 1
 1
 1 1 1 1 1 1 1
 5000 250000
 200 100
 200 25
 11 0.25
 20 25
 15 10
 4 17 0.5 90
 1
 1
 1
 1 1 1 1 1 1 1
 5000 250000
 200 100
 250 25
 11 0.25
 20 25
 15 10
 4 17 0.5 90
 1
 1
 1
 1 1 1 1 1 1 1
 5000 250000
 200 100
 4 2
 1 0.25
 11 0.25
 20 25
 15 10
 4 17 0.5 90
 3
 1
 1
 1 1 1 1 1 1 1
 5000 250000
 200 100
 4 2
 1 0.25
 11 0.25
 20 25
 15 10
 4 17 0.5 90
 3
 1
 1
 1 1 1 1 1 1 1
 5000 250000
 200 100
 4 2
 1 0.25
 11 0.25
 20 25
 15 10
 4 17 0.5 90
 3
 1
 1
 1 1 1 1 1 1 1
 5000 250000
 200 100

20 9
 1 0.25
 11 0.25
 50 25
 15 10
 4 17 0.5 90
 3
 1
 1 1 1 1 1 1 1
 5000 250000
 200 100
 50 9
 1 0.25
 11 0.25
 50 25
 15 10
 4 17 0.5 90
 3
 1
 1 1 1 1 1 1 1
 5000 250000
 200 100
 100 25
 1 0.25
 11 0.25
 50 25
 15 10
 4 17 0.5 90
 3
 1
 1 1 1 1 1 1 1
 5000 250000
 200 100
 150 100
 1 0.25
 11 0.25
 50 25
 15 10
 4 17 0.5 90
 3
 1
 1 1 1 1 1 1 1
 5000 250000
 200 100
 200 100
 1 0.25
 11 0.25
 50 25
 15 10
 4 17 0.5 90
 3
 1
 1 1 1 1 1 1 1
 5000 250000
 200 100
 200 100
 1 0.25
 11 0.25
 50 25
 15 10
 4 17 0.5 90
 3
 1
 1 1 1 1 1 1 1
 5000 250000
 200 100

250 100
 1 0.25
 11 0.25
 50 25
 15 10
 4 17 0.5 90
 3
 1
 1 1 1 1 1 1 1
 5000 250000
 200 100
 500 100
 1 0.25
 11 0.25
 50 25
 15 10
 0 14 0.5 90
 1
 1
 1 1 1 1 1 1 1
 5000 250000
 200 100
 4 2
 11 0.25
 20 25
 15 10
 0 14 0.5 90
 1
 1
 1 1 1 1 1 1 1
 5000 250000
 200 100
 20 4
 11 0.25
 20 25
 15 10
 0 14 0.5 90
 1
 1
 1 1 1 1 1 1 1
 5000 250000
 200 100
 50 9
 11 0.25
 20 25
 15 10
 0 14 0.5 90
 1
 1
 1 1 1 1 1 1 1
 5000 250000
 200 100
 100 25
 11 0.25
 20 25

15 10
 0 14 0.5 90
 1
 1
 1 1 1 1 1 1 1
 5000 250000
 200 100
 150 25
 11 0.25
 20 25
 15 10
 0 14 0.5 90
 1
 1
 1 1 1 1 1 1 1
 5000 250000
 200 100
 200 25
 11 0.25
 20 25
 15 10
 0 14 0.5 90
 1
 1
 1 1 1 1 1 1 1
 5000 250000
 200 100
 250 25
 11 0.25
 20 25
 15 10
 0 14 0.5 90
 1
 1
 1 1 1 1 1 1 1
 5000 250000
 200 100
 500 25
 11 0.25
 20 25
 15 10
 0 14 0.5 90
 3
 1
 1 1 1 1 1 1 1
 5000 250000
 200 100
 4 2
 1 0.25
 11 0.25
 20 25
 15 10
 0 14 0.5 90
 3
 1

200 100
 100 25
 11 0.25
 20 25
 15 10
 2 14 0.5 90
 1
 1
 1 1 1 1 1 1 1
 5000 250000
 200 100
 150 25
 11 0.25
 20 25
 15 10
 2 14 0.5 90
 1
 1
 1 1 1 1 1 1 1
 5000 250000
 200 100
 200 25
 11 0.25
 20 25
 15 10
 2 14 0.5 90
 1
 1
 1 1 1 1 1 1 1
 5000 250000
 200 100
 250 25
 11 0.25
 20 25
 15 10
 2 14 0.5 90
 1
 1
 1 1 1 1 1 1 1
 5000 250000
 200 100
 500 25
 11 0.25
 20 25
 15 10
 2 14 0.5 90
 3
 1
 1
 1 1 1 1 1 1 1
 5000 250000
 200 100
 4 2
 1 0.25
 11 0.25
 20 25

15 10
 2 14 0.5 90
 3
 1
 1 1 1 1 1 1 1
 5000 250000
 200 100
 20 9
 1 0.25
 11 0.25
 50 25
 15 10
 2 14 0.5 90
 3
 1
 1 1 1 1 1 1 1
 5000 250000
 200 100
 50 9
 1 0.25
 11 0.25
 50 25
 15 10
 2 14 0.5 90
 3
 1
 1 1 1 1 1 1 1
 5000 250000
 200 100
 100 25
 1 0.25
 11 0.25
 50 25
 15 10
 2 14 0.5 90
 3
 1
 1 1 1 1 1 1 1
 5000 250000
 200 100
 150 100
 1 0.25
 11 0.25
 50 25
 15 10
 2 14 0.5 90
 3
 1
 1 1 1 1 1 1 1
 5000 250000
 200 100
 200 100
 1 0.25
 11 0.25
 50 25

4 2
 1 0.25
 11 0.25
 20 25
 15 10
 4 14 0.5 90
 3
 1
 1 1 1 1 1 1 1
 5000 250000
 200 100
 20 9
 1 0.25
 11 0.25
 50 25
 15 10
 4 14 0.5 90
 3
 1
 1 1 1 1 1 1 1
 5000 250000
 200 100
 50 9
 1 0.25
 11 0.25
 50 25
 15 10
 4 14 0.5 90
 3
 1
 1 1 1 1 1 1 1
 5000 250000
 200 100
 100 25
 1 0.25
 11 0.25
 50 25
 15 10
 4 14 0.5 90
 3
 1
 1 1 1 1 1 1 1
 5000 250000
 200 100
 150 100
 1 0.25
 11 0.25
 50 25
 15 10
 4 14 0.5 90
 3
 1
 1 1 1 1 1 1 1
 5000 250000
 200 100

200 100
 1 0.25
 11 0.25
 50 25
 15 10
 4 14 0.5 90
 3
 1
 1 1 1 1 1 1 1
 5000 250000
 200 100
 250 100
 1 0.25
 11 0.25
 50 25
 15 10
 4 14 0.5 90
 3
 1
 1 1 1 1 1 1 1
 5000 250000
 200 100
 500 100
 1 0.25
 11 0.25
 50 25
 15 10
 0 0 0 0
 9
 \$ DEASSIGN SYS\$OUTPUT
 \$! DEFINE/USER SYS\$OUTPUT RUT.RES
 \$! RUN RUTDEP.EXE
 \$! DEASSIGN SYS\$OUTPUT
 \$ PR RUT.FOR,RUT.LIS,RUT.OUT,RUT.COM
 \$ TY RUT.OUT
 \$ TY RUT.LIS
 \$ TY RUT.FOR
 \$! TY RUT.RES
 \$! PR RUT.RES
 \$ SET NOVERIFY

APPENDIX B-3:

Rutting Model Typical Output Data

INPUT STABILIZED CLAY/SILT SOIL SYSTEM PARAMETERS

ADDITIVE % MOISTURE % CLAY/SILT RATIO TEMPERATURE

ADDITIVE % = 2.00
MOISTURE % = 14.00
CLAY/SILT RATIO = 0.50
TEMPERATURE = 90.00

ENTER CODE FOR TYPE OF PAVEMENT ANALYSIS :

STABILIZED AIRPORT PAVEMENT WITH CBR1 > CBR2 = 1
STABILIZED AIRPORT PAVEMENT WITH CBR1 < CBR2 = 2
STABILIZED ASPHALT PAVEMENT W/O SUBBASE (8 VBLS) = 3
STABILIZED ASPHALT PAVEMENT WITH SUBBASE (10 VBLS) = 4

TYPE = 3

INPUT = ALLOWABLE RUT DEPTH.

ALLOWABLE RUT DEPTH = 1.000
INPUT MODE = KEYBOARD (1) OR FILE (2) ?
NO OF VARIABLES (NVAR) = 7
INPUT = STAT CODE = COMPUTED(0).GIVEN(1)
P TP R T1 T2 C1 C3

INPUT MEAN & VARIANCE FOR = P
INPUT MEAN & VARIANCE FOR = TP
INPUT MEAN & VARIANCE FOR = R
INPUT MEAN & VARIANCE FOR = T1
INPUT MEAN & VARIANCE FOR = T2
INPUT MEAN & VARIANCE FOR = C1
INPUT MEAN & VARIANCE FOR = C3
PREDICTED CBR = 48.10
SPECIFIED CBR = 20.00

VARIABLE	MEAN	STAT VARIANCE	CODE
P	5000.00	250000.00	1
TP	200.00	100.00	1
R	4.00	2.00	1
T1	1.00	0.25	1
T2	11.00	0.25	1
C1	48.10	25.00	1
C3	15.00	10.00	1

MEAN VALUE OF RUT DEPTH = 0.390576
EXPECTED VALUE OF RUT DEPTH = 0.399847
EXPECTED VARIANCE OF RUT DEPTH = 0.010505
RELIABILITY STATISTIC = 5.855628

INPUT STABILIZED CLAY/SILT SOIL SYSTEM PARAMETERS

ADDITIVE % MOISTURE % CLAY/SILT RATIO TEMPERATURE

ADDITIVE % = 0.00
MOISTURE % = 14.00
CLAY/SILT RATIO = 0.50
TEMPERATURE = 90.00

ENTER CODE FOR TYPE OF PAVEMENT ANALYSIS :

STABILIZED AIRPORT PAVEMENT WITH CBR1 > CBR2 = 1
STABILIZED AIRPORT PAVEMENT WITH CBR1 < CBR2 = 2
STABILIZED ASPHALT PAVEMENT W/O SUBBASE (8 VBLS) = 3
STABILIZED ASPHALT PAVEMENT WITH SUBBASE (10 VBLS) = 4

TYPE = 3

INPUT = ALLOWABLE RUT DEPTH.

ALLOWABLE RUT DEPTH = 1.000
INPUT MODE = KEYBOARD (1) OR FILE (2) ?
NO OF VARIABLES (NVAR) = 7
INPUT = STAT CODE = COMPUTED(0).GIVEN(1)
P TP R T1 T2 C1 C3

INPUT MEAN & VARIANCE FOR = P
INPUT MEAN & VARIANCE FOR = TP
INPUT MEAN & VARIANCE FOR = R
INPUT MEAN & VARIANCE FOR = T1
INPUT MEAN & VARIANCE FOR = T2
INPUT MEAN & VARIANCE FOR = C1
INPUT MEAN & VARIANCE FOR = C3
PREDICTED CBR = 70.24
SPECIFIED CBR = 20.00

VARIABLE	MEAN	STAT VARIANCE	CODE
P	5000.00	250000.00	1
TP	200.00	100.00	1
R	4.00	2.00	1
T1	1.00	0.25	1
T2	11.00	0.25	1
C1	70.24	25.00	1
C3	15.00	10.00	1

MEAN VALUE OF RUT DEPTH = 0.206138
EXPECTED VALUE OF RUT DEPTH = 0.208347
EXPECTED VARIANCE OF RUT DEPTH = 0.002251
RELIABILITY STATISTIC = 16.684927

INPUT STABILIZED CLAY/SILT SOIL SYSTEM PARAMETERS

ADDITIVE % MOISTURE % CLAY/SILT RATIO TEMPERATURE

ADDITIVE % = 0.00
MOISTURE % = 14.00
CLAY/SILT RATIO = 0.50
TEMPERATURE = 90.00

ENTER CODE FOR TYPE OF PAVEMENT ANALYSIS :

STABILIZED AIRPORT PAVEMENT WITH CBR1 > CBR2 = 1
STABILIZED AIRPORT PAVEMENT WITH CBR1 < CBR2 = 2
STABILIZED ASPHALT PAVEMENT WU/SUBBASE (8 VBLS) = 3
STABILIZED ASPHALT PAVEMENT WITH SUBBASE (10 VBLS)=4

TYPE = 3

INPUT - ALLOWABLE RUT DEPTH.

ALLOWABLE RUT DEPTH = 1.000
INPUT MODE - KEYBOARD (1), OR FILE (2) ?
NO OF VARIABLES (NVAR) = 7
INPUT - STAT CODE - COMPUTED(0), GIVEN(1)
P TP R T1 T2 C1 C3

INPUT MEAN & VARIANCE FOR = P
INPUT MEAN & VARIANCE FOR = TP
INPUT MEAN & VARIANCE FOR = R
INPUT MEAN & VARIANCE FOR = T1
INPUT MEAN & VARIANCE FOR = T2
INPUT MEAN & VARIANCE FOR = C1
INPUT MEAN & VARIANCE FOR = C3
PREDICTED CBR = 48.10
SPECIFIED CBR = 50.00

VARIABLE	MEAN	STAT VARIANCE	CODE
P	5000.00	250000.00	1
TP	200.00	100.00	1
R	20.00	9.00	1
T1	1.00	0.25	1
T2	11.00	0.25	1
C1	48.10	25.00	1
C3	15.00	10.00	1

MEAN VALUE OF RUT DEPTH = 0.657918
EXPECTED VALUE OF RUT DEPTH = 0.680921
EXPECTED VARIANCE OF RUT DEPTH= 0.025227
RELIABILITY STATISTIC = 2.008923

INPUT STABILIZED CLAY/SILT SOIL SYSTEM PARAMETERS

ADDITIVE % MOISTURE % CLAY/SILT RATIO TEMPERATURE

ADDITIVE % = 2.00
MOISTURE % = 17.00
CLAY/SILT RATIO = 0.50
TEMPERATURE = 90.00

ENTER CODE FOR TYPE OF PAVEMENT ANALYSIS :

STABILIZED AIRPORT PAVEMENT WITH CBR1 > CBR2 = 1
STABILIZED AIRPORT PAVEMENT WITH CBR1 < CBR2 = 2
STABILIZED ASPHALT PAVEMENT WU/SUBBASE (8 VBLS) = 3
STABILIZED ASPHALT PAVEMENT WITH SUBBASE (10 VBLS)=4

TYPE = 3

INPUT - ALLOWABLE RUT DEPTH.

ALLOWABLE RUT DEPTH = 1.000
INPUT MODE - KEYBOARD (1), OR FILE (2) ?
NO OF VARIABLES (NVAR) = 7
INPUT - STAT CODE - COMPUTED(0), GIVEN(1)
P TP R T1 T2 C1 C3

INPUT MEAN & VARIANCE FOR = P
INPUT MEAN & VARIANCE FOR = TP
INPUT MEAN & VARIANCE FOR = R
INPUT MEAN & VARIANCE FOR = T1
INPUT MEAN & VARIANCE FOR = T2
INPUT MEAN & VARIANCE FOR = C1
INPUT MEAN & VARIANCE FOR = C3
PREDICTED CBR = 53.38
SPECIFIED CBR = 50.00

VARIABLE	MEAN	STAT VARIANCE	CODE
P	5000.00	250000.00	1
TP	200.00	100.00	1
R	20.00	9.00	1
T1	1.00	0.25	1
T2	11.00	0.25	1
C1	53.38	25.00	1
C3	15.00	10.00	1

MEAN VALUE OF RUT DEPTH = 0.742602
EXPECTED VALUE OF RUT DEPTH = 0.766679
EXPECTED VARIANCE OF RUT DEPTH= 0.027969
RELIABILITY STATISTIC = 1.395128

INPUT STABILIZED CLAY/SILT SOIL SYSTEM PARAMETERS

INPUT STABILIZED CLAY/SILT SOIL SYSTEM PARAMETERS

ADDITIVE % MOISTURE % CLAY/SILT RATIO TEMPERATURE

ADDITIVE % MOISTURE % CLAY/SILT RATIO TEMPERATURE

ADDITIVE % = 4.00
MOISTURE % = 14.00
CLAY/SILT RATIO = 0.50
TEMPERATURE = 90.00

ADDITIVE % = 2.00
MOISTURE % = 14.00
CLAY/SILT RATIO = 0.50
TEMPERATURE = 90.00

ENTER CODE FOR TYPE OF PAVEMENT ANALYSIS :

ENTER CODE FOR TYPE OF PAVEMENT ANALYSIS :

STABILIZED AIRPORT PAVEMENT WITH CBR1 > CBR2 = 1
STABILIZED AIRPORT PAVEMENT WITH CBR1 < CBR2 = 2
STABILIZED ASPHALT PAVEMENT W/O SUBBASE (8 VBLS) = 3
STABILIZED ASPHALT PAVEMENT WITH SUBBASE (10 VBLS)=4

STABILIZED AIRPORT PAVEMENT WITH CBR1 > CBR2 = 1
STABILIZED AIRPORT PAVEMENT WITH CBR1 < CBR2 = 2
STABILIZED ASPHALT PAVEMENT W/O SUBBASE (8 VBLS) = 3
STABILIZED ASPHALT PAVEMENT WITH SUBBASE (10 VBLS)=4

TYPE = 3

TYPE = 3

INPUT - ALLOWABLE RUT DEPTH.

INPUT - ALLOWABLE RUT DEPTH.

ALLOWABLE RUT DEPTH = 1.000
INPUT MODE = KEYBOARD (1), OR FILE (2) ?
NO OF VARIABLES (NVAR) = 7
INPUT = STAT CODE = COMPUTED(0), GIVEN(1)
P TP R T1 T2 C1 C3

ALLOWABLE RUT DEPTH = 1.000
INPUT MODE = KEYBOARD (1), OR FILE (2) ?
NO OF VARIABLES (NVAR) = 7
INPUT = STAT CODE = COMPUTED(0), GIVEN(1)
P TP R T1 T2 C1 C3

INPUT MEAN & VARIANCE FOR = P
INPUT MEAN & VARIANCE FOR = TP
INPUT MEAN & VARIANCE FOR = R
INPUT MEAN & VARIANCE FOR = T1
INPUT MEAN & VARIANCE FOR = T2
INPUT MEAN & VARIANCE FOR = C1
INPUT MEAN & VARIANCE FOR = C3
PREDICTED CBR = 92.38
SPECIFIED CBR = 50.00

INPUT MEAN & VARIANCE FOR = P
INPUT MEAN & VARIANCE FOR = TP
INPUT MEAN & VARIANCE FOR = R
INPUT MEAN & VARIANCE FOR = T1
INPUT MEAN & VARIANCE FOR = T2
INPUT MEAN & VARIANCE FOR = C1
INPUT MEAN & VARIANCE FOR = C3
PREDICTED CBR = 70.24
SPECIFIED CBR = 50.00

VARIABLE	MEAN	STAT VARIANCE	CODE
P	5000.00	250000.00	1
TP	200.00	100.00	1
R	20.00	9.00	1
T1	1.00	0.25	1
T2	11.00	0.25	1
C1	92.38	25.00	1
C3	15.00	10.00	1

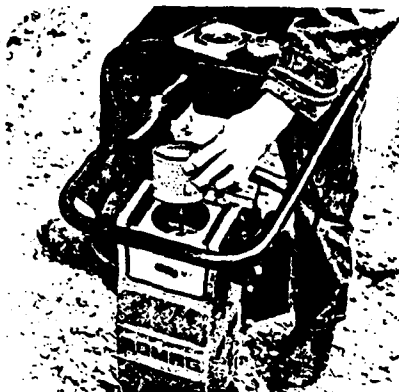
VARIABLE	MEAN	STAT VARIANCE	CODE
P	5000.00	250000.00	1
TP	200.00	100.00	1
R	100.00	25.00	1
T1	1.00	0.25	1
T2	11.00	0.25	1
C1	70.24	25.00	1
C3	15.00	10.00	1

MEAN VALUE OF RUT DEPTH = 0.218668
EXPECTED VALUE OF RUT DEPTH = 0.222406
EXPECTED VARIANCE OF RUT DEPTH= 0.001740
RELIABILITY STATISTIC = 18.639175

MEAN VALUE OF RUT DEPTH = 0.584911
EXPECTED VALUE OF RUT DEPTH = 0.599028
EXPECTED VARIANCE OF RUT DEPTH= 0.013790

APPENDIX C:

Technical Data for BOMAG Compactor Used for Test Sample Compaction (Phase II)



Description

The BOMAG BT 68 rammer is equipped with a BOMAG BM 30 engine. Power transmission is via a centrifugal clutch, a single stage spur gear and a crank gear to the piston. This operates between compression springs and transmits compaction energy via the guide rod to the tamper foot.

The tamper plate is of wooden construction covered with a steel plate.

Engagement of vibration and adjustment of the BT 68 variable vibration frequency is controlled by the throttle lever.

Advantages:

- Increased jump height giving better compaction
- Reduced noise levels
- Easier travel: the BT 68 is designed to resist any tendency for the foot to dig in

Areas of application

- Compaction of all soil types and bituminous materials
- Trench backfill and reinstatement
- Public Utility inspection openings
- Areas of restricted access

Reliability

Highly sophisticated production and testing methods such as endurance tests on all major components and strict quality control procedures ensure maximum reliability. Every machine is test run prior to delivery in BOMAG's Quality Control Department.

A flexible stop pin ensures that the tamper springs do not become coil-bound, thus preventing breakage.

All moving parts are oil lubricated.

The air filter is located in a recess of the crankcase housing for maximum protection against impact.

The BT 68 has been designed for easy strip down and re-assembly. Repairs can be made easily and quickly.

Maintenance on the BT 68 is reduced to engine air filter cleaning and oil changes every 250 hours.

Transportation

The compact size of the BT 68 together with its light weight makes transportation very straightforward.

Standard equipment

- Engine protection
- Centrifugal clutch
- Oil lubrication

Optional equipment

- Various tamper plates
- Transport wheels
- Special paint

Technical data

Weights

Basic weight	kg (lb)	68 (150)
Operating weight (CECE)	kg (lb)	71 (157)

Dimensions

Working width (tamper plate)	mm (in)	280 (11)
Tamper plate length	mm (in)	350 (13.8)
Overall length	mm (in)	670 (26.4)
Overall width	mm (in)	340 (13.4)
Overall height	mm (in)	980 (38.6)

Drive

Engine		BOMAG
Model		BM 30
Cooling		air
Number of cylinders		1
Stroke volume	cm ³ (in ³)	79 (4.8)
Performance DIN 6271 IFN	kW (hp)	2.2 (3.0)
Speed	min ⁻¹ /rpm	4600
Performance SAE	kW (bhp)	2.3 (3.1)
Speed	min ⁻¹ /rpm	4600
Fuel		mixture
Mixture ratio		50:1
Fuel consumption max.	l/h (gal/hr)	1.6 (0.4)
Fuel tank capacity	l (gal)	3.0 (0.8)
Starter		recoil starter

Vibration

Drive system		mechanical
Frequency	Hz (vpm)	10 - 13 (600 - 780)
Jumping height	mm (in)	up to 60 (2.4)
Working speed max. (depending on soil conditions)	m/min (ft/min)	up to 13 (42.7)
Area coverage max. (depending on soil conditions)	m ² /h (ft ² /hr)	up to 218 (2346)

Subject to technical alterations. Models shown may include optional equipment.



BOMAG USA
Springfield
Ohio
Tel: 513-3256723 Telex: 4984147

BOMAG CANADA
Mississauga
Ontario
Tel: 416-675-1111 Telex: 6961250

BOMAG GERMANY
Boppard/Rhein
Tel: 67 42-100-0 Telex: 426316

BOMAG AUSTRIA
Wien
Tel: 222-693617-0 Telex: 133-535

BOMAG FRANCE
Briatney Sur Orge
Tel: 6-0849530 Telex: 691370

BOMAG GREAT BRITAIN
Larkfield Kent Tel: 0622-766111 Telex: 945157

BOMAG NETHERLANDS
Barneveld Tel: 3420-91323-91639 Telex: 76352

303

BOMAG MIDDLE EAST
Jordan
Amman Tel: 661935 Telex: 21065

BOMAG ASIA PACIFIC
Singapore
Tel: 65-7346233 Telex: 33482

BOMAG JAPAN
Tokyo
Tel: 03-835/8765 Telex: 28519

BOMAG AUSTRALIA
Smithfield
Tel: 6049333 Telex: 121467

BOMAG, MENCK and TERRAMETER are Trademarks of BOMAG-MENCK GmbH